National Aeronautics and Space Administration

ICARTT Field Campaign Observation Assessment Report

Tropospheric Airborne Measurement Evaluation Panel

2008-2009

TAbMP

Acknowledgements

We would like to thank NASA headquarters for their support of this project through the Making Earth System data records for Use in Research Environments (MEaSUREs) program. In addition we would like to recognize the contributions and support of the National Oceanic and Atmospheric Administration (NOAA), the National Center for Atmospheric Research (NCAR), Deutsches Zentrum fuer Luft-und Raumfahrt (DLR) , Facility for Airborne Atmospheric Measurements (FAAM), the Unites States Environmental Protection Agency (EPA), and the United States Department of Energy (DOE).

Table of Contents

Tropospheric Airborne Measurement Evaluation Panel (TAbMEP)
Introduction to Analysis and ICARTT Field Study

1. Background

The primary objectives of TAbMEP are to provide an unbiased assessment of the measurement uncertainties and measurement consistency for historical airborne observations, and to establish systematic approaches for combining airborne data sets from multiple instruments/techniques and aircraft platforms. The TAbMEP assessment is part of larger effort sponsored by NASA MEaSUREs program to make the airborne databases suitable for the assessment of global and region models. In the case of ICARTT, four different aircraft conducted extensive intercomparisons during the summer 2004 field campaign [*Fehsenfeld et al.*, 2006, *Singh et al*., 2006]. This report is to recommend methods to combine these ICARTT data for any analysis based upon data collected on different aircraft, especially the analysis involving the comparisons and contrasts of the ICARTT data. Measurement biases between platforms can potentially confound such comparisons and contrasts. The current TAbMEP work is designed to put limits on the magnitude of possible biases and to provide objective uncertainty limits for the data collected from the instruments on all of the intercompared aircraft. The present analysis is limited to a few selected species: O_3, H_2O, CO, NO, NO_2, PAN, HNO_3, SO_2, few VOCs including CH_2O, temperature, wind, $j(NO_2)$, $j(O^1D)$, particle number density, volume density, and sulfate. The following chapters give the assessments of the measurements of each of these species.

2. Intercomparison Flights

This assessment is based primarily upon five intercomparison flights conducted during the field campaign. Each of the intercomparison flights involved two aircraft flying wingtip-to-wingtip at two or three different altitudes for 40 minutes to more than an hour. The flights were planned to encounter a range of conditions. Table 1 summarizes the five flights, and Figures 1(a)-1(e) illustrate the flight tracks.

Table 1. Summary of intercomparison flights

Date – Time (UTC)	Aircraft	Location
7/22/2004 - 14:45:50-15:32:14	DC-8/WP-3D	W. Atlantic – E. of Massachusetts, US
7/31/2004 - 22:52:50-23:32:10	DC-8/WP-3D	Eastern Maine, US
8/07/2004 - 21:35:10-22:19:10	DC-8/WP-3D	Bay of Fundy
7/28/2004 - 15:49:30-17:01:20	DC-8/BAe-146	Central N. Atlantic – W. of Azores
8/03/2004 - 15:08:45-16:31:00	BAe-146/DLR Falcon	French Atlantic coast

3. Analysis Techniques

Several different analysis techniques have been utilized in this assessment of instrument precision and bias. Summaries of these techniques are given in the following sections.

3.1. Precision Analysis

Internal Estimate of Instrument Precision (IEIP) is an objective and data-driven approach to assess absolute and/or relative instrument precisions. IEIP directly estimates, under a few assumptions, the instrument precision through the variance over a small time interval, Δt. For species x, the total variance can be expressed as:

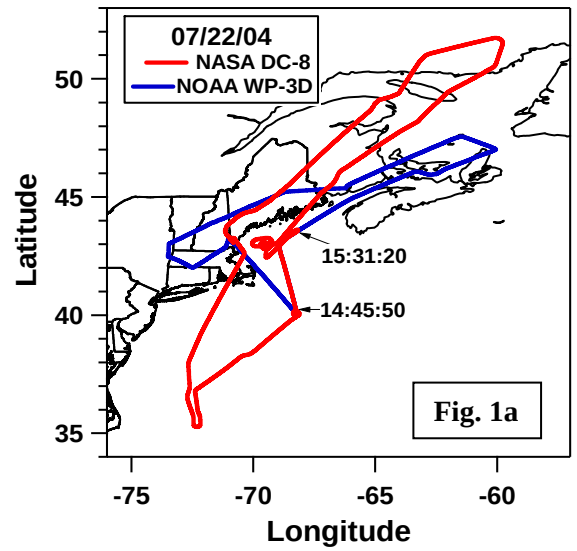

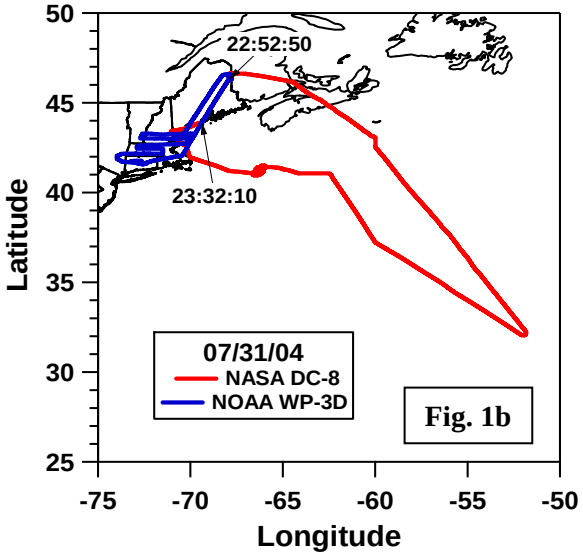

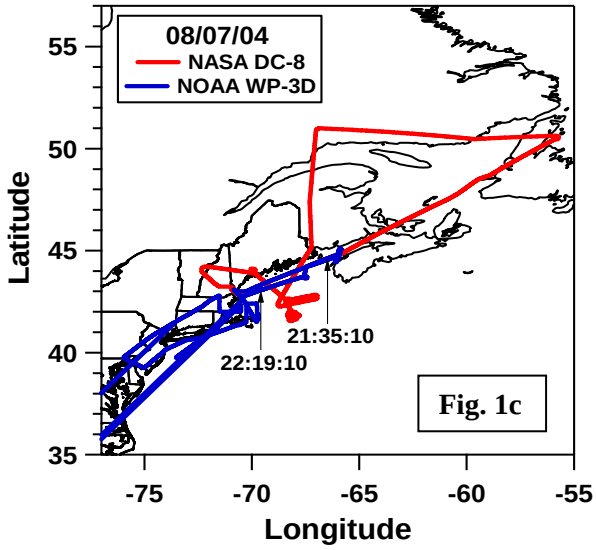

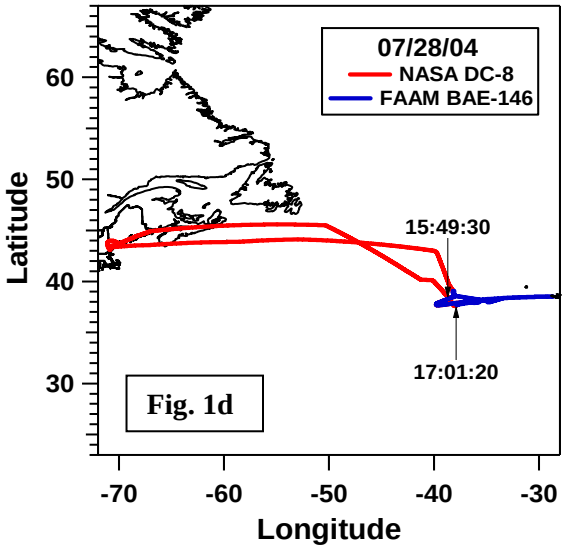

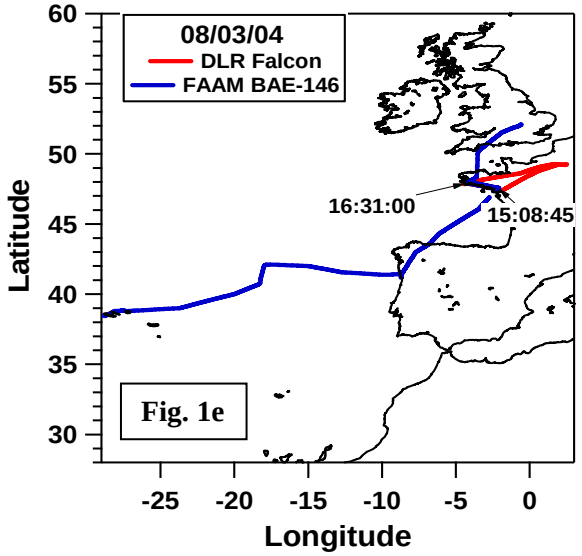

Figure 1(a), (b), (c). Flight tracks for the NASA DC-8 (red) and NOAA WP-3D (blue) intercomparison flights on (a) July 22, 2004, (b) July 31, 2004, (c) August 7, 2004.

Figure 1(d). Flight tracks for the NASA DC-8 (red) and FAAM BAE-146 (blue) intercomparison flights on July 28, 2004.

Figure 1(e). Flight tracks for the DLR Falcon (red) and FAAM BAE-146 (blue) intercomparison flights on August 3, 2004.

$$V(x) = \sigma_x^2 + \sigma_{\varepsilon-x}^2 \quad (1)$$

where $\sigma_{\varepsilon-x}^2$ is the random instrument variability (instrument precision) for measurement of species x and σ_x^2 represents the natural ambient variability.

$V(x)$ can be a reasonable estimate for $\sigma_{\varepsilon-x}^2$ if Δt is small enough such that σ_x^2 is negligible compared to $\sigma_{\varepsilon-x}^2$. At the same time, Δt must be large enough to minimize the effect of autocorrelation. $\sigma_{\varepsilon-x}^2$ can be assessed by following procedures listed below:

1. Compute standard deviation over Δt and generate frequency distribution or histograms.
2. Vary Δt and repeat the previous step, then look for the values of the modes, which are relatively constant over a limited range of Δt values.
3. How long should Δt be? In principle, it should be long enough to overcome any significant autocorrelation impact and short enough such that σ_x^2 is negligible.
   - Δt depends on temporal and spatial variability of the species or parameter of interest.
   - Δt depends on instrument sampling rate.
   - Δt determination requires expert judgment.

IEIP analysis is typically applied over an entire flight and/or a large segment of data with fairly constant values. It should be noted that this approach may or may not be feasible for measurements with long integration times and/or significant gaps between the data points. IEIP analysis may also be problematic when measurement precision is strongly dependent on the ambient values.

IEIP Example: O_3 instrument precision assessment

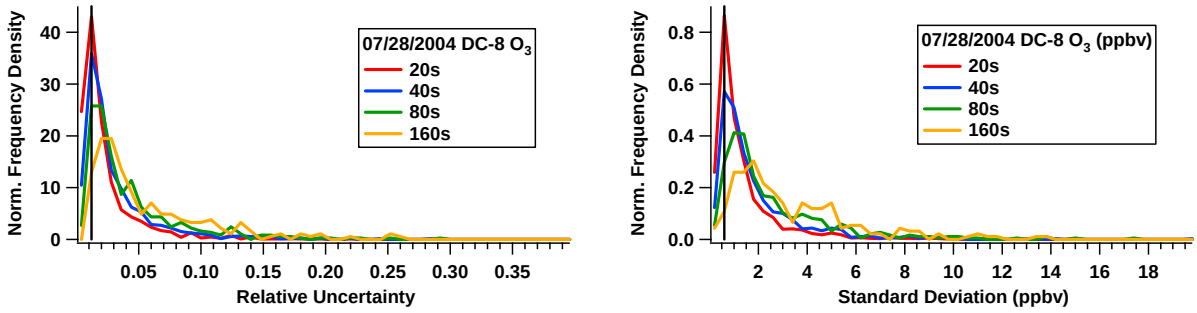

Figure 2. Example of IEIP analysis of NASA DC-8 O_3 observations during INTEX-A/ICARTT.

Figure 2 shows an example of IEIP assessment for O_3 for both relative and absolute uncertainties. Note that the modes of the distributions (i.e., the location of the peaks) are relatively constant over the range of Δt from 20-40 seconds. The standard deviation increases with longer Δt times, which is likely due to the O_3 natural variability. The resulting relative uncertainty for this DC-8 flight is about 1.2% and absolute uncertainty is 0.6 ppbv.

This procedure is an effective method to estimate so called "short-term" precision, which accounts for signal variation during a short period of assumed constant measurements. Because this assumption is not always valid, the IEIP estimate tends to provide an upper limit of the instrument short-term precision. Over longer time scales, however, some instruments are subject to lower precision (i.e. larger variability), which includes variability that arises from uncorrected

changes in the zero level or sensitivity of the instrument. These additional contributions to the variability are not likely reflected in the IEIP derived precision, but the intercomparison flights do provide a reasonable check on their influence. This effect was examined through the comparisons of the "expected variability" and "observed variability" in the individual species assessments. "Expected variability" is defined as the quadrature sum of the individual IEIP precisions for the paired instruments. "Observed variability" is derived from relative residual plots, an example of which is shown in Figure 3.

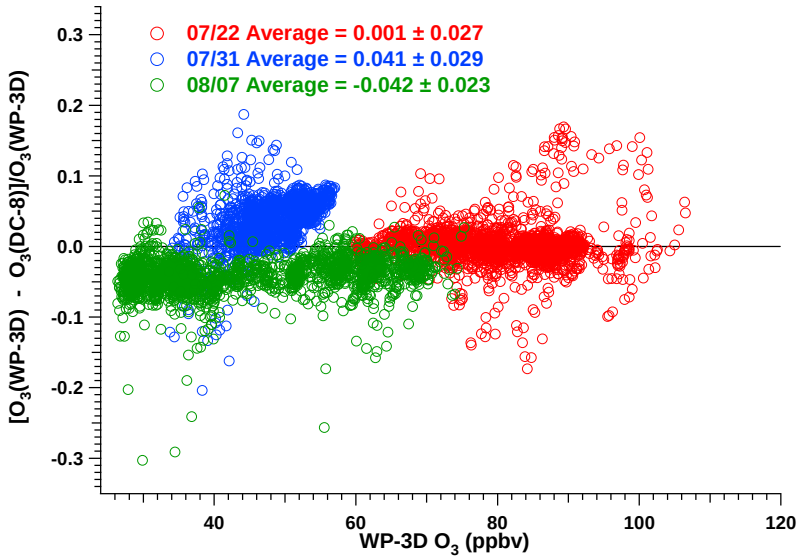

Figure 3. Relative residual for NOAA WP-3D and NASA DC-8 O_3 during the ICARTT campaign.

Table 2. Example of IEIP analysis results

Flight	Platform	IEIP Precision	Expected Variability	Observed Variability	Adjusted Precision
07/22	O_3 DC-8	1.2%	1.8%	2.7%	1.8%
	O_3WP-3D	1.4%			2.1%
07/31	CO DC-8 DACOM	0.8%	1.7%	1.6%	0.8%
	CO WP-3D VUVF	1.5%			1.5%

The "observed variability" (in percentage) equals 100 × standard deviation (or 2.7% on 7/22 in this example). Each standard deviation (or "observed variability" value) should equal the "expected variability". When the "observed variability" is larger than the "expected variability", the IEIP derived (short-term) precision needs to be adjusted to reflect the longer term fluctuations (see 07/22 O_3 example in Table 2). This "adjusted precision" is obtained by proportionally scaling the IEIP estimates so that the "expected variability" value equals the "observed variability." When the "observed variability" is smaller than the "expected variability", the "adjusted precision" is set equal to the "IEIP precision" (see 07/31 CO example in Table 2). Ambient variability should not pose a problem, since it should have been sampled by both instruments during the intercomparison period. A key assumption made here for the precision adjustment is that the long-term precision is proportionally scaled with the short-term precision. This assumption may not reflect the actual instrument performance and may lead to either an underestimate or an overestimate of the long-term precision for each of the given

instruments. The final adjusted precision estimates are required to be reviewed by TAbMEP measurement experts.

3.2. Linear Regression Techniques

The results of instrument intercomparisons are often reported as the linear regression of the measurements of one instrument as a function of the measurements of another, e.g. [*Hoell et al.*, 1985]. Orthogonal distance regression (ODR) is a regression technique similar to ordinary least squares (OLS) fit with the stipulation that both x and y are independent variables with errors. ODR minimizes sum of the squares of the orthogonal distances rather than the vertical distances (as in OLS). ODR is generally equivalent to

$$\min_{\boldsymbol{\beta},\boldsymbol{\delta},\boldsymbol{\varepsilon}} \frac{\mathbf{1}}{\mathbf{2}} \sum_{\boldsymbol{i}=\mathbf{1}}^{\boldsymbol{n}} (\boldsymbol{w}_{\boldsymbol{\varepsilon}_i} \boldsymbol{\varepsilon}_{\boldsymbol{i}}^{\mathbf{2}} + \boldsymbol{w}_{\boldsymbol{\delta}_i} \boldsymbol{\delta}_{\boldsymbol{i}}^{\mathbf{2}})$$

subject to $\boldsymbol{y_i} + \boldsymbol{\varepsilon_i} = \boldsymbol{f}(\boldsymbol{x_i} + \boldsymbol{\delta_i}; \boldsymbol{\beta})$ where $\boldsymbol{\varepsilon_i}$is the error in $\boldsymbol{y}$, $\boldsymbol{\delta_i}$ the error in $\boldsymbol{x}$, $\boldsymbol{w}_{\boldsymbol{\varepsilon}_i}$and $\boldsymbol{w}_{\boldsymbol{\delta}_i}$ weighting factors, and $\boldsymbol{\beta}$ a vector of parameters to be determined (i.e. slope and intercept in this case), [*Zwolak et al*., 2007]. Note that a weighted ODR ($\boldsymbol{w}_{\boldsymbol{\varepsilon}_i}$ and $\boldsymbol{w}_{\boldsymbol{\delta}_i} \neq \mathbf{1}$) is necessary when observations $\boldsymbol{x_i}$ and $\boldsymbol{y_i}$ are heteroscedastic (variance changes with $\boldsymbol{i}$, or observations have point by point uncertainties), [*Boggs et al.*, 1988].

It has been shown that ODR performs at least as well and in many cases significantly better than OLS, especially when $\boldsymbol{d} = \boldsymbol{\sigma_\varepsilon}/\boldsymbol{\sigma_\delta} \leq \mathbf{2}$, [*Boggs et al.*, 1988]. Boggs et al. have shown that ODR results in smaller bias, variance, and mean square error (mse) than OLS, except possibly when significant outliers are present in the data, [*Boggs et al.*, 1988]. For the bias of the parameter, ($\boldsymbol{\beta}$), and function estimates, $\boldsymbol{f}(\boldsymbol{x_i}; \boldsymbol{\beta})$, OLS is statistically better only 2% of the time while ODR is significantly better 50% of the time. Results for the variance and mse of the parameter and function estimates were similar; ODR variance and mse were smaller than that from OLS about 25% of the time. OLS results were significantly better than ODR only 2% of the time, [*Boggs et al.*, 1988].

For our application, the data from the instruments being compared is merged to the same time base then plotted and fit using ODR. Normally the observations are not heteroscedastic. In addition, an accurate estimate of measurement uncertainty is not often available on point by point basis. Therefore, in the interest of treating all the intercomparisons uniformly, we use $\boldsymbol{w}_{\boldsymbol{\varepsilon}_i}$and $\boldsymbol{w}_{\boldsymbol{\delta}_i} = \mathbf{1}$. The coefficient of determination, $\boldsymbol{R^2}$, is used to evaluate the robustness of the regression. Under some circumstances, we do not use ODR analysis. This occurs when the range of the data is small or there are very few data pairs (typically for some VOCs). The general rule to assess the range is when variability of the data set is less than 5 times the uncertainty, ODR is not used. In that case we present the data but do not subject it to additional analysis.

3.3. Bias Calculations

The Reference Standard for Comparison (RSC) is introduced to quantitatively evaluate the bias for each individual measurement. Conceptually, RSC can be derived through a weighted average of measurements from instruments on spatially and temporally co-located aircraft platforms. This can mathematically be expressed as

$$RSC(t, \overrightarrow{L}) = \sum_{i=1}^{n} m_i\,(t, \vec{L}) * \; w_i$$

where RSC is a function of a given time *t* and location $\vec{L}$, intercomparison data from the i^{th} instrument is given by m_i, there are n total number of instruments involved in a the field study, and the normalized weighting factor assigned to the i^{th} data set is w_i (i.e., $\sum_{i=1}^{n} w_i = 1$). The values of the w_i are determined by consensus of the TAbMEP measurement experts. It should be noted that the RSC is only used for measurement comparison purposes.

In practice, the RSC is difficult to find since each intercomparison was conducted between only two aircraft at a time. However, the field campaign measurement comparison strategy was designed to guarantee that each instrument could be related to any other instrument through paired intercomparisons. The approach prescribed below is an effective way to arrive at a reasonable approximation to the RSC.

Data from n instrument intercomparison flights will first be analyzed via pairwise orthogonal distance regressions (ODR) over intercomparison periods when pairs of planes were flown in wingtip-to-wingtip formations. The regressions will yield best-fit curves

$$m_i = a_{i,j} + \; b_{i,j} m_j \quad (1)$$

where m_i and m_j are data from instruments i and j, respectively. Once data from each instrument is related via best-fit line to at least one other instrument, the system of best-fit equations can be manipulated to express the data sets $\{m_i\colon\; 1 \le i \le n\}$ as linear functions of a single chosen data set m_1. The slopes and intercepts may be directly obtained from the regression or indirectly through algebraic manipulation of regression results. We note that the choice of instrument to serve as the independent variable m_1 will not affect the final RSC. Thus, m_1 should be chosen for convenience to correspond to the instrument with the highest number of direct intercomparisons against other instruments.

The RSC can easily be written as a linear function of the chosen independent variable, m_1 :

$$RSC = \; A_1 + B_1 m_1 \quad (2)$$

where $A_1 = \sum_{i=1}^{n} w_i a_{i,1}$, $B_1 = \sum_{i=1}^{n} w_i b_{i,1}$, $a_{1,1} = 0$, and $b_{1,1} = 1$.

Using the original set of regression equations the RSC can be expressed as a function of the data from any instrument (m_i). Thus, the Best Estimate Bias for the i[th] instrument can then be expressed in terms of m_i, i.e.,:

$$Best\ Estimate\ Bias_i = m_i - \; RSC$$

It is acknowledged that this approach provides a reasonable estimate of the average bias from the available intercomparison data, however, the accuracy of this estimate is limited, to a large extent, by the robustness of the regressions between the intercomparison data sets.

References

Boggs, P. T., et al. (1988), A computational examination of orthogonal distance regression, *J. of Econometrics, 38*, pp 169-201.

Fehsenfeld, F. C., et al. (2006), International Consortium for Atmospheric Research on Transport and Transformation (ICARTT): North America to Europe—Overview of the 2004 summer field study, *J. Geophys. Res., 111*, D23S01, doi:10.1029/2006JD007829.

Hoell, J. M., et al. (1985), An intercomparison of carbon monoxide measurement techniques, *J. Geophys. Res., 90*, D7, 12881-12889.

Singh, H. B., et al. (2006), Overview of the summer 2004 Intercontinental Chemical Transport Experiment-North America (INTEX-A), *J. Geophys. Res., 111*, D24S01, doi:10.1029/2006JD007905.

Zwolak, J. W., et al. (2007), Algorithm 869: ODRPACK95: A weighted orthogonal distance regression code with bound constraints, *ACMTrans.Math. Softw., 33*, 4, Article 27 (August 2007), 12 pages. DOI = 10.1145/1268776.1268782 http://doi.acm.org/10.1145/1268776.1268782.

TAbMEP Assessment: ICARTT CO Measurements

1. Introduction

Here we provide the assessment for the carbon monoxide (CO) measurements taken from multiple aircraft platforms during the summer 2004 ICARTT field campaign [*Fehsenfeld et al.*, 2006, *Singh et al*., 2006]. This assessment is based upon the five wing-tip-to-wing-tip intercomparison flights conducted during the field campaign, plus a comparison between the two NASA DC-8 instruments on all ICARTT research flights. Recommendations provided here offer TAbMEP assessed uncertainties for each of the measurements and a systematic approach to unifying the ICARTT CO data for any integrated analysis. These recommendations are directly derived from the instrument performance demonstrated during the ICARTT measurement comparison exercises and are not to be extrapolated beyond this campaign.

2. ICARTT CO Measurements

Six different CO measurement techniques were deployed on four aircraft. Table 1 summarizes these techniques and gives references for more information. Most of the CO measurements were conducted under dry conditions, i.e., the reported values are dry air mixing ratio. Two instruments measured CO at ambient conditions (marked by an "*" in Table 1). The difference, in general, between measurements made under ambient conditions and those made in a dried sample is a small but quantifiable function of the ambient humidity and is largest in the boundary layer where water is most abundant. Since the sampling humidity was not measured or reported by any of the instruments in this study, it is not possible for the panel to make a precise assessment of this difference. Based on the intercomparison between NASA DC-8 and NOAA WP-3D, the maximum difference is estimated to be less than 2.5%. For all intercomparisons considered here, the differences between measurements made under ambient and dry conditions are small and not easily distinguishable from other instrumental differences. As a general policy, the panel does not change PI reported data, however, a user of the data may wish to undertake the conversion for a particular analysis.

Table 1. CO measurements deployed on aircraft during ICARTT

Aircraft	Instrument	Reference
NASA DC-8	DACOM (Differential Absorption CO Measurement)	*Warner et al.* [2007]
NASA DC-8	WAS (Whole Air Sampler)	*Barletta et al.* [2002]
NOAA WP-3D	VUVF (Vacuum UV fluorescence)*	*Holloway et al.* [2000]
FAAM BAe-146	VUVF (Vacuum UV fluorescence)	*Gerbig et al.* [1999]
DLR Falcon	VUVF (Vacuum UV fluorescence)	*Gerbig et al.* [1999]
DLR Falcon	TDLAS (Tunable Diode Laser Absorption Spectroscopy)*	*Wienhold et al.* [1998] and *Fischer et al.* [2002]

*Measurement made at ambient humidity.

3. Summary of Results

Table 2 summarizes the assessed 2σ precisions, biases, and uncertainties. More detailed descriptions are provided to illustrate the process for assessment of bias and precision in Sections 4.1 and 4.2 respectively. The assessed 2σ precisions reported in Table 2 are equal to twice the highest adjusted precision value for that instrument listed in Table 4. Table 2 also reports an assessed bias (see Section 4.1 for details) that can be applied to maximize the consistency between the data sets. The assessed bias should be subtracted from the reported data to 'unify' the data sets. The assessed bias is derived from intercomparison periods only and may be

extrapolated to the entire mission if one assumes instrument performance remained constant throughout the mission. For one CO instrument (Falcon VUVF), the assessed bias is smaller than the uncertainty reported by the PI, so no bias adjustment need be made when combining this data set. The bias estimate for the Falcon TDLAS instrument (Table 3) is strongly influenced by a short period of the intercomparison flight when large differences were noted (see Figs. 5 and A5). If these apparent outliers were excluded, then the estimated adjustment would be significantly smaller. Consequently, we provide no assessed bias or 2σ uncertainty for this instrument as a robust statistical assessment cannot be performed. The interested researcher is encouraged to contact the PI before using the Falcon TDLAS data. The recommended 2σ uncertainty in Table 2 is the larger of either the uncertainty reported by the PI or the quadrature-sum of the assessed 2σ precision and assessed bias listed in Table 2.

Table 2. Recommended ICARTT CO measurement treatment

Aircraft/ Instrument	Reported 2σ Uncertainty	Assessed 2σ Precision	Assessed Bias	Recommended 2σ Uncertainty
NASA DC-8 DACOM	2% or 2 ppbv	2.4%	2.84 – 0.020 CO_{DACOM}	Quadrature Sum
NASA DC-8 WAS	5%	11%	-0.04 + 0.011 CO_{WAS}	Quadrature Sum
NOAA WP-3D VUVF	5%	4.0%	-3.18 + 0.023 CO_{WP3D}	Quadrature Sum
FAAM BAe-146 VUVF	None	2.8%	-7.43 + 0.004 CO_{BAe}	Quadrature Sum
DLR Falcon VUVF	5%	5.0%	0.52 – 0.015 CO_{VUVF}	Quadrature Sum
DLR Falcon TDLAS	5%	5.4%	See footnote [a]	See footnote [a]

[a]Not included since robust statistical assessment cannot be performed.

Figures 1a-1c display the precisions, biases, and recommended uncertainties for five of the six CO instruments. TDLAS on the Falcon is not included since we do not recommend a bias or 2σ uncertainty in Table 2. For four of the five instruments shown (DACOM, WAS, WP-3D VUVF and Falcon VUVF), the uncertainty is driven by the precision.

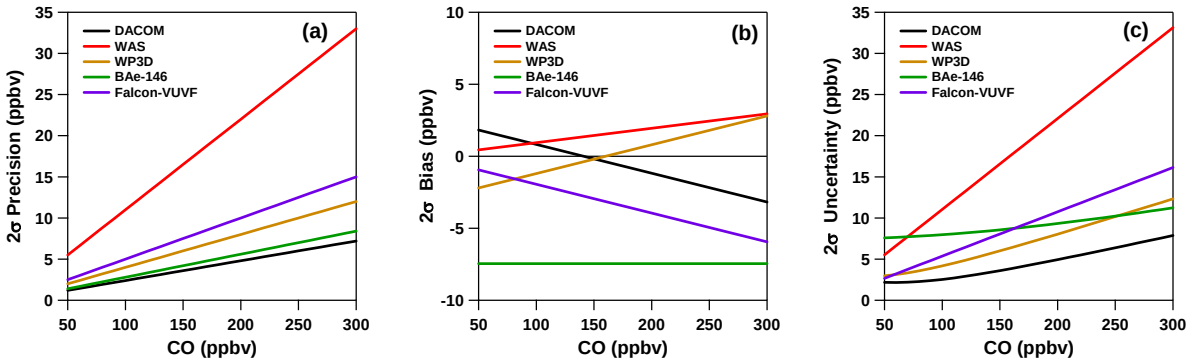

Figure 1. 2σ precision (panel a), 2σ bias (panel b), and 2σ uncertainty (panel c) for DACOM (black), WAS (red), WP-3D (gold), BAe-146 (green), and Falcon VUVF (purple) as a function of CO level. Values were calculated based upon data shown in Table 2.

4. Results and Discussion

4.1 Bias Analysis

Section 3.3 in the introduction describes the process used to determine the best estimate bias. Figure 2 shows the correlation and time series plots for each of the three WP-3D vs. DC-8 DACOM comparisons. The linear relationships listed in Table 3 were derived from the regression equations found in Figures 3 through 6. In the case of CO, there is little bias between four of the instruments (DACOM, WAS, WP-3D VUVF and Falcon VUVF), a relatively large negative bias in the BAe-146 VUVF data (see Figures 7-11), and a moderate bias in the Falcon TDLAS instrument. The Falcon bias is exaggerated by a period of large bias indicated by the vertical line of points in Figure 11. For these reasons, the BAe-146 VUVF and the Falcon TDLAS regressions are not included in the calculation of the reference standard for comparison (RSC), as defined in the introduction. The resulting RSC can be expressed as a function of the DACOM CO measurement as the following:

$$RSC_{CO} = -2.84 + 1.020 CO_{DACOM}$$

The RSC is then used to calculate the best estimate bias as described in Section 3.3 of the introduction. It should be noted that the initial choice of the reference instrument (DACOM) is arbitrary, and has no impact on the final recommendations. Table 3 summarizes the assessed measurement bias for each of the six ICARTT CO measurements. Note that additional decimal places were carried in the calculations to ensure better than 0.1 ppbv precision.

Table 3. ICARTT CO bias estimates

Aircraft/ Instrument	Linear Relationships[a]	Best Estimate Bias (a + b CO) (ppbv)
NASA DC-8 DACOM	$CO_{DACOM} = 0.00 + 1.000\ CO_{DACOM}$	$2.84 - 0.020\ CO_{DACOM}$
NASA DC-8 WAS	$CO_{WAS} = -2.91 + 1.031\ CO_{DACOM}$	$-0.04 + 0.011\ CO_{WAS}$
NOAA WP-3D VUVF	$CO_{WP3D} = -6.17 + 1.044\ CO_{DACOM}$	$-3.18 + 0.023\ CO_{WP3D}$
FAAM BAe-146 VUVF	$CO_{BAe\text{-}146} = -10.30 + 1.024\ CO_{DACOM}$ [b]	$-7.43 + 0.004\ CO_{BAe}$
DLR Falcon VUVF	$CO_{DLR\text{-}VUVF} = -2.28 + 1.006\ CO_{DACOM}$	$0.52 - 0.015\ CO_{VUVF}$
DLR Falcon TDLAS	$CO_{DLR\text{-}TDLAS} = -0.66 + 1.028\ CO_{DACOM}$ [b]	$2.18 + 0.008\ CO_{TDLAS}$

[a]Derived from Figs. A2-A5.
[b]Not included in RSC derivation, see text for details.

4.2 Precision Analysis

A detailed description of the precision assessment is given in Section 3.1 of the introduction. The IEIP precision, expected variability, observed variability, and the adjusted precision are summarized in Table 4. Based on the results presented in Table 4, the largest "adjusted precision" value is taken as a conservative precision estimate for each ICARTT CO instrument and twice that value is listed in Table 2 as the assessed 2σ precision.

Table 4. ICARTT CO precision (1σ) comparisons

Flight	Platform/ Instrument	IEIP Precision	Expected Variability	Observed Variability	Adjusted Precision
07/22	DC-8 DACOM	0.9%	1.5%	2.0%	1.2%
	WP-3D VUVF	1.2%			1.6%
07/31	DC-8 DACOM	0.8%	1.7%	1.6%	0.8%
	WP-3D VUVF	1.5%			1.5%
08/07	DC-8 DACOM	0.6%	1.5%	2.1%	0.9%
	WP-3D VUVF	1.4%			2.0%
07/28	DC-8 WAS	5.5%[a]	5.5%	4.2%	5.5%
	BAe-146 VUVF	0.5%			0.5%
08/03	BAe-146 VUVF	0.5%	1.0%	2.8%	1.4%
	Falcon VUVF	0.9%			2.5%
08/03	BAe-146 VUVF	0.5%	1.3%	2.8%	1.1%
	Falcon TDLAS	1.3%			2.7%

[a]estimated from DC-8 WAS and DC-8 DACOM comparison, see Fig. 10.

The DC-8 WAS technique provides only intermittent results with an integration time of about 1 minute. The IEIP procedures are not applicable in this case. As noted in Table 4, the DC-8 WAS precision is estimated from the standard deviation of the relative difference, i.e., [CO(DC-8 WAS) - CO(DC-8 DACOM)]/ CO(DC-8 DACOM) plotted in Figure 16, which is based on all available overlapping data from the entire ICARTT campaign period. It should also be recognized that the DC-8 WAS precision required the use of, but was not sensitive to the DC-8 DACOM IEIP analysis (see Figure 16).

To minimize the effect of bias, we make corrections for bias before computing the observed variability, as the bias may have a significant impact on the observed variability. Figures 7 – 11 show the magnitude of the bias for each intercomparison. The assessed values of the observed variability are displayed in Figure 12 – 16. The final analysis results are shown in Table 2. Over 90% of the data falls within the combined recommended uncertainties for each intercomparison, which is consistent with the TAbMEP guideline for unified data sets.

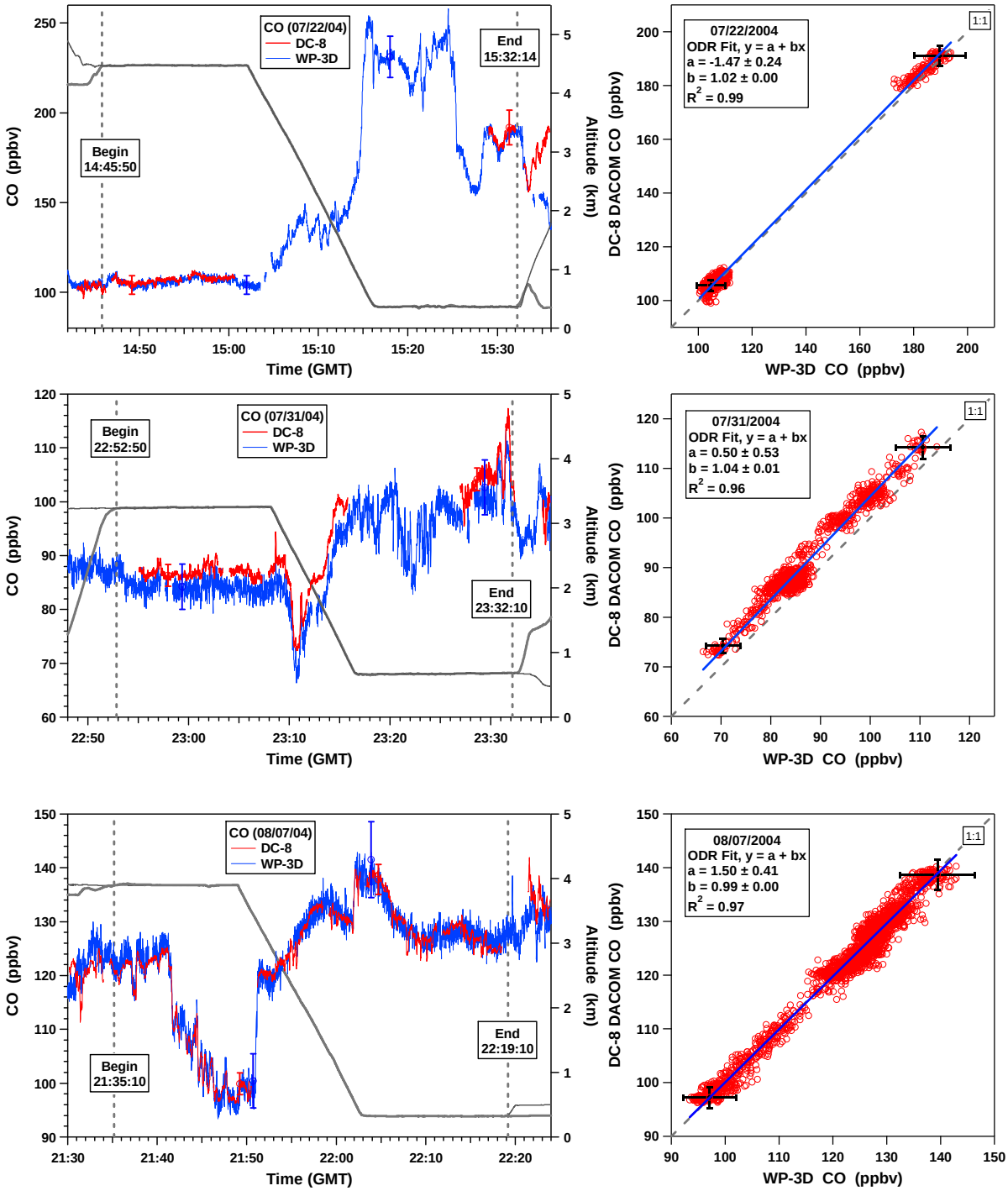

Figure 2. (left panels) Time series of CO measurements and aircraft altitudes from two aircraft on the three intercomparison flights between the NASA DC-8 (DACOM) and the NOAA WP-3D. (right panels) Correlations between the CO measurements on the two aircraft. Error bars shown depict the reported measurement uncertainties.

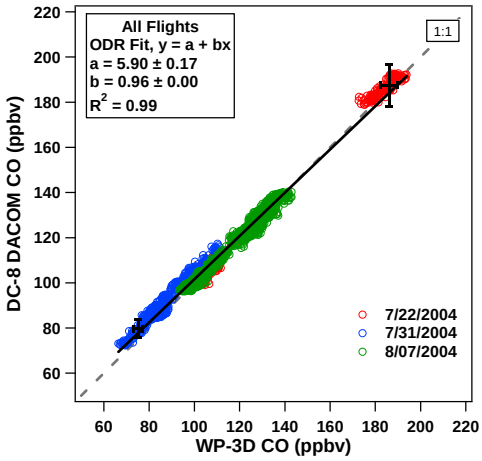

Figure 3. Combined correlation for the CO measurements on NASA DC-8 and the NOAA WP-3D for 7/22, 7/31, and 8/7 2004. Error bars shown depict the reported measurement uncertainties.

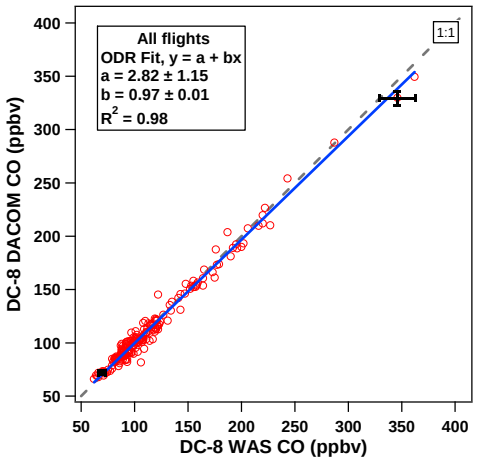

Figure 4. Correlation for the CO measurements (DACOM and WAS) on NASA DC-8 for all available data. Error bars shown depict the reported measurement uncertainties.

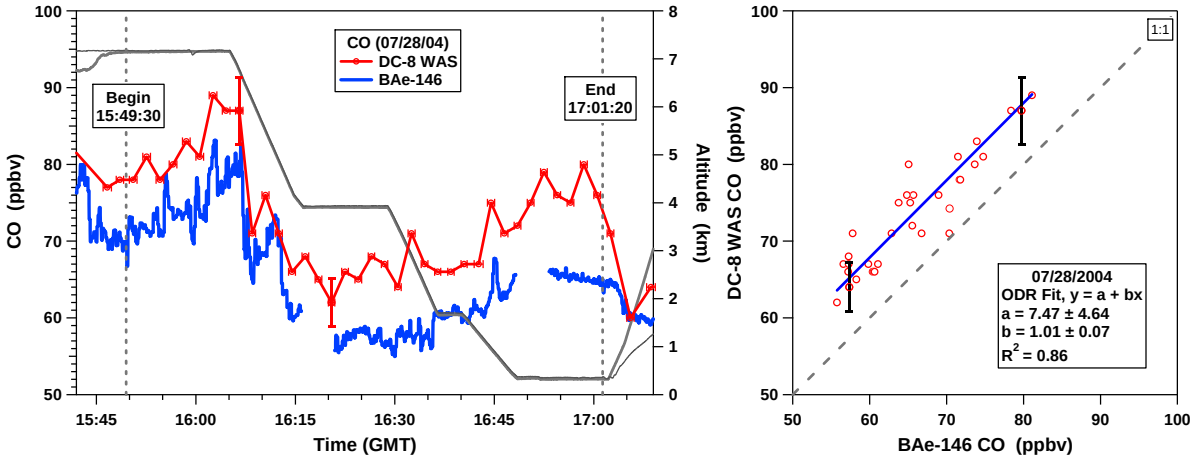

Figure 5. (left panel) Time series of CO measurements and aircraft altitudes from the intercomparison flight between the NASA DC-8 and the FAAM BAe-146. (right panel) Correlations between the CO measurements on the two aircraft. Error bars shown depict the reported measurement uncertainties.

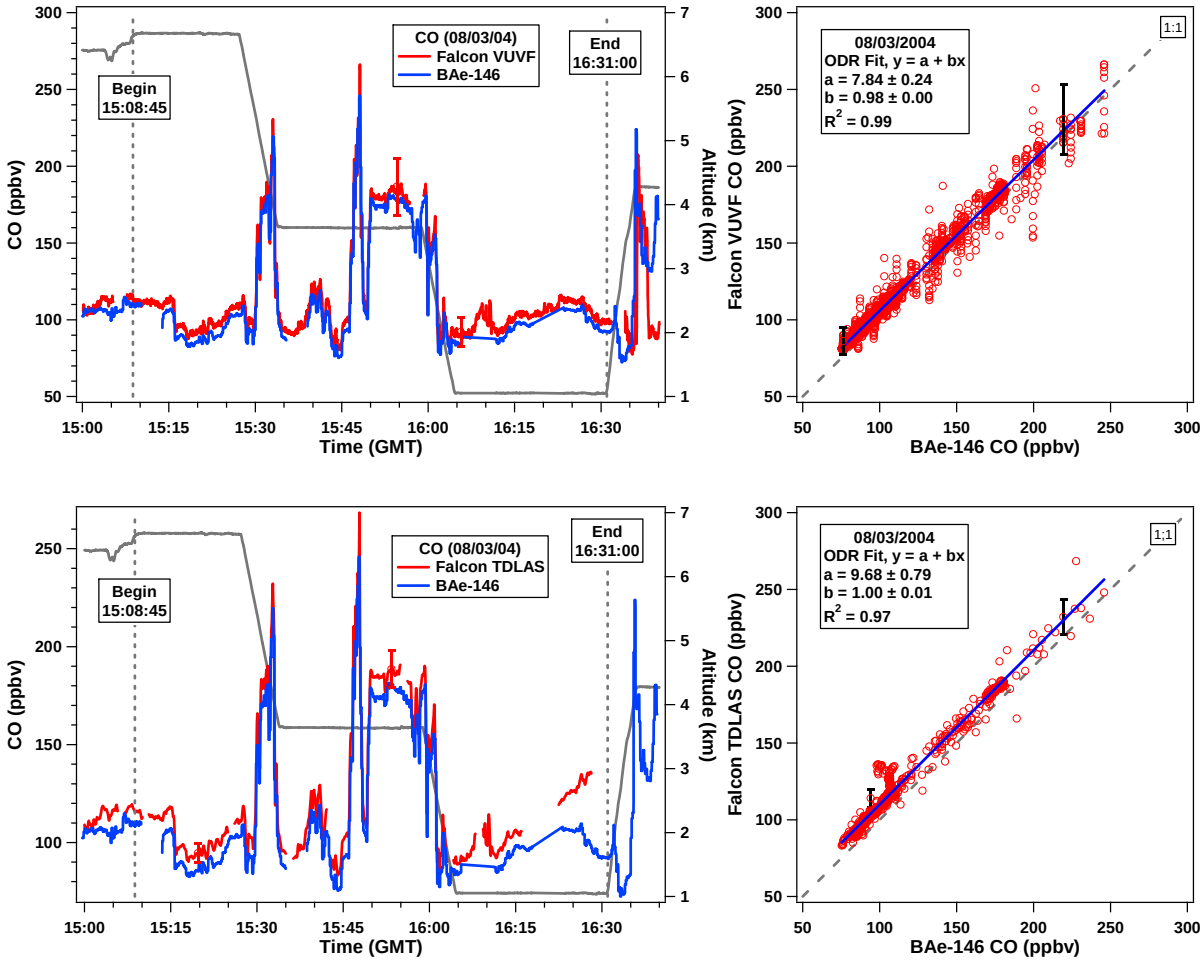

Figure 6. (left panel) Time series of CO measurements and aircraft altitudes from the intercomparison flight between the FAAM BAe-146 and the DLR Falcon. (right panel) Correlations between the CO measurements on the two aircraft. Error bars shown depict the reported measurement uncertainties.

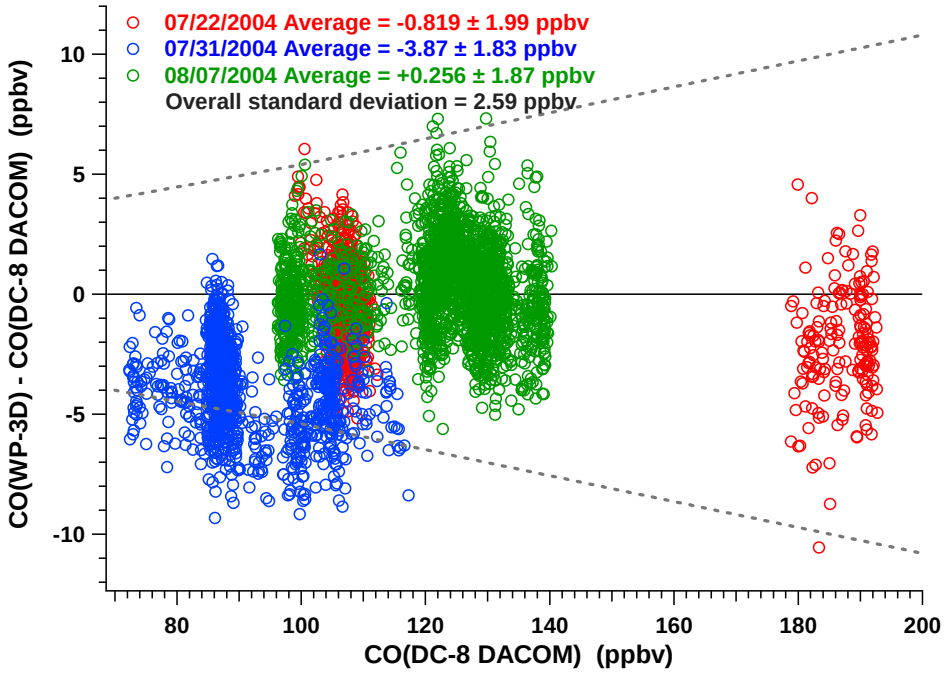

Figure 7. Difference between CO measurements from the three DC-8/WP-3D intercomparison flights as a function of the DC-8 DACOM CO. The dashed lines indicate the range of the results expected from the reported 2σ measurement uncertainties.

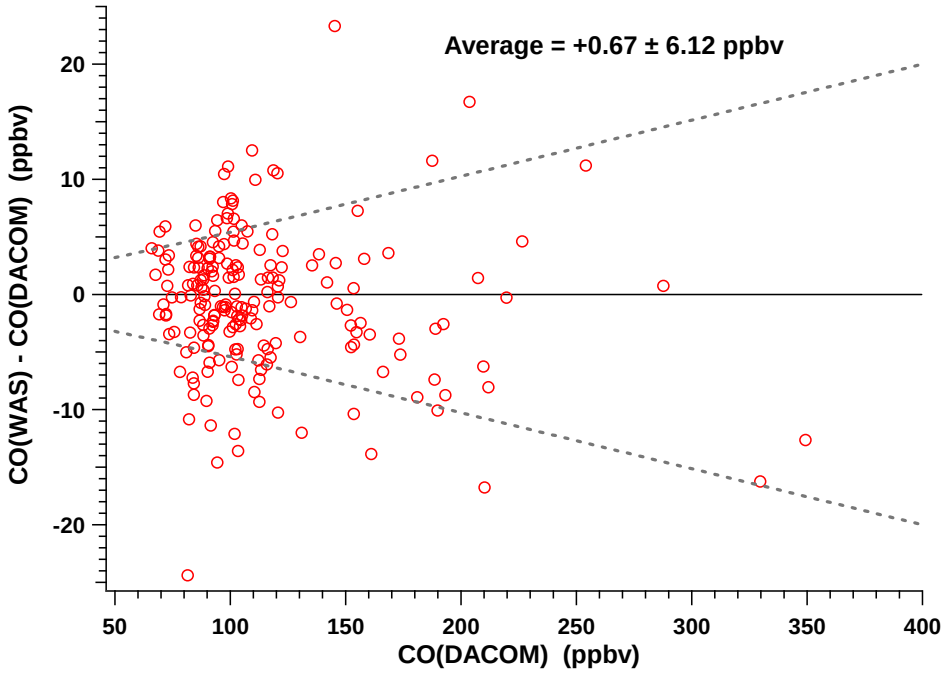

Figure 8. Difference between CO measurements from all ICARTT flights of the DC-8 as a function of the DC-8 DACOM CO. The dashed lines indicate the range of the results expected from the reported measurement uncertainties.

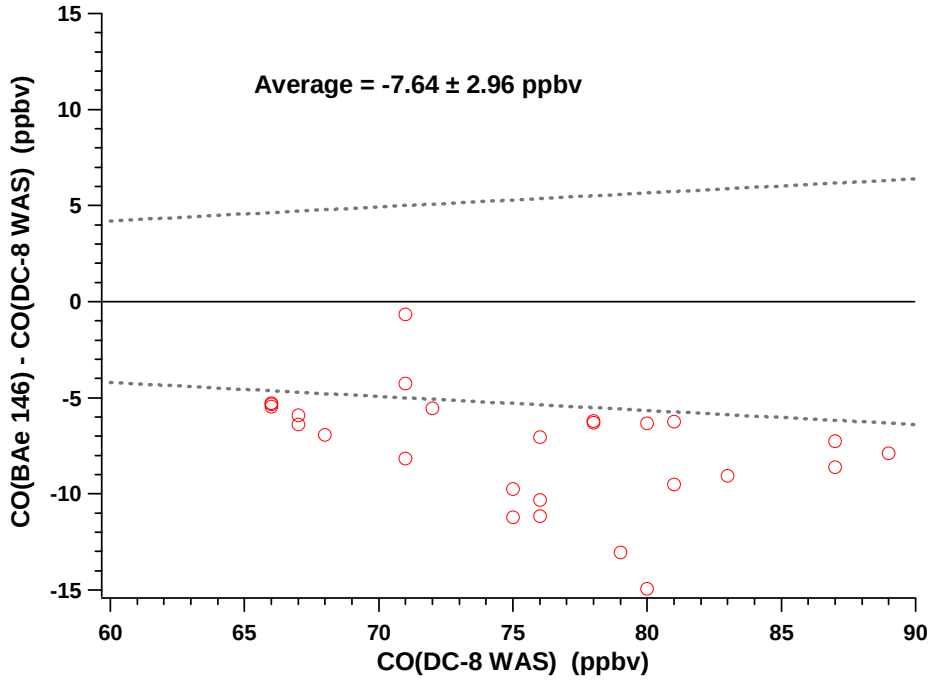

Figure 9. Difference between CO measurements from the DC-8/BAe-146 intercomparison flight (07/28) as a function of the DC-8 WAS CO. The dashed lines indicate the range of the results expected from the reported 2σ measurement uncertainties.

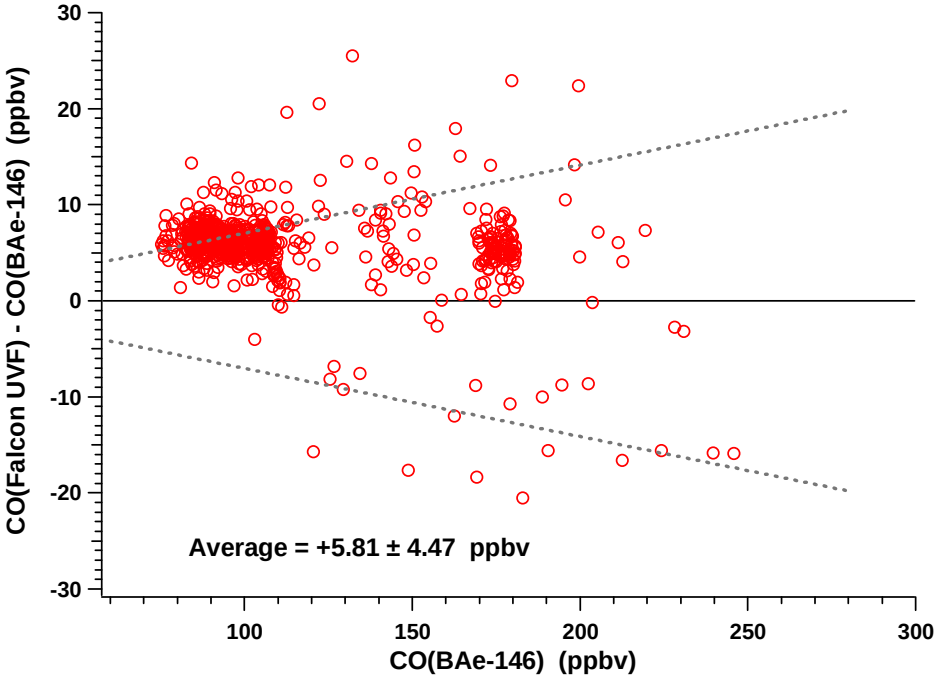

Figure 10. Difference between CO measurements from the BAe-146/DLR Falcon (VUVF) intercomparison flight (08/03) as a function of the BAe-146 VUVF CO. The dashed lines indicate the range of the results expected from the reported 2σ measurement uncertainties.

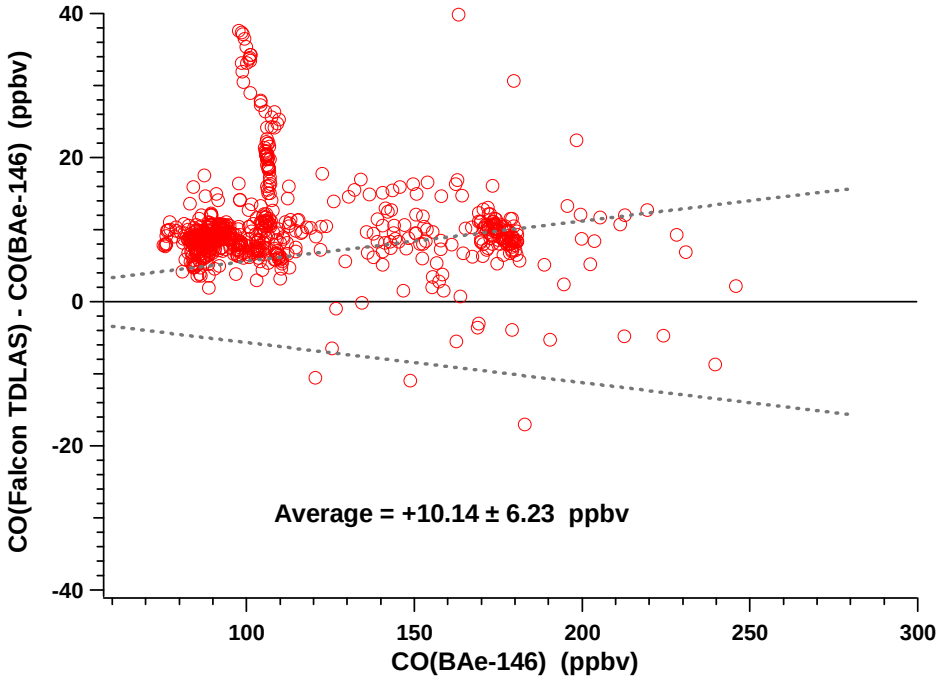

Figure 11. Difference between CO measurements reported from the BAe-146/DLR Falcon (TDLAS) intercomparison flight (08/03) as a function of the BAe-146 VUVF CO. The dashed lines indicate the range of the results expected from the reported 2σ measurement uncertainties.

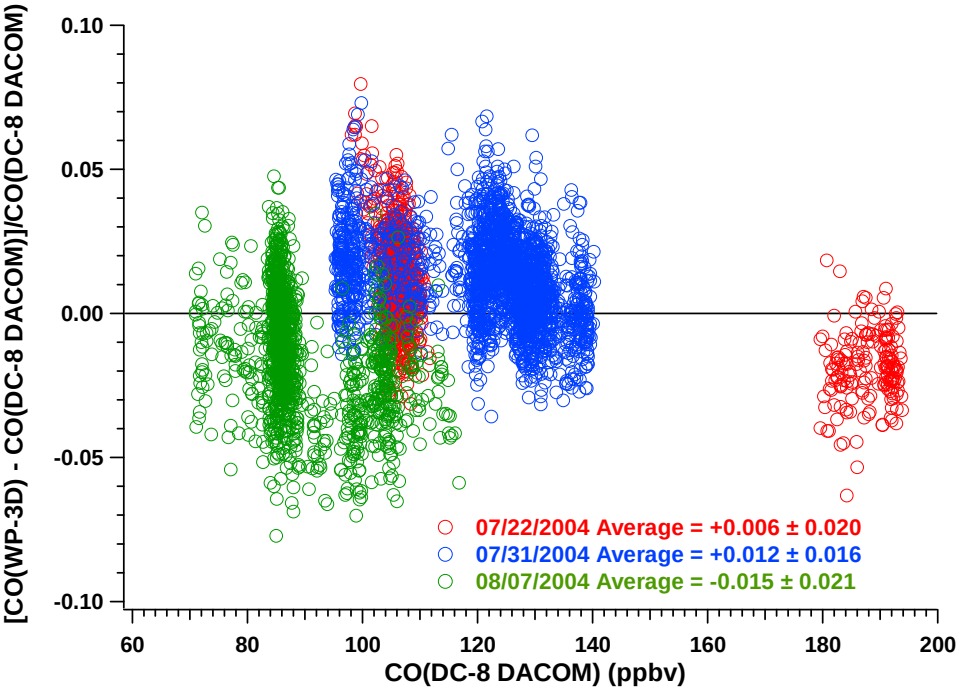

Figure 12. Relative difference between CO measurements from the three DC-8/WP-3D intercomparison flights as a function of the DC-8 DACOM CO. A correction was made to account for bias.

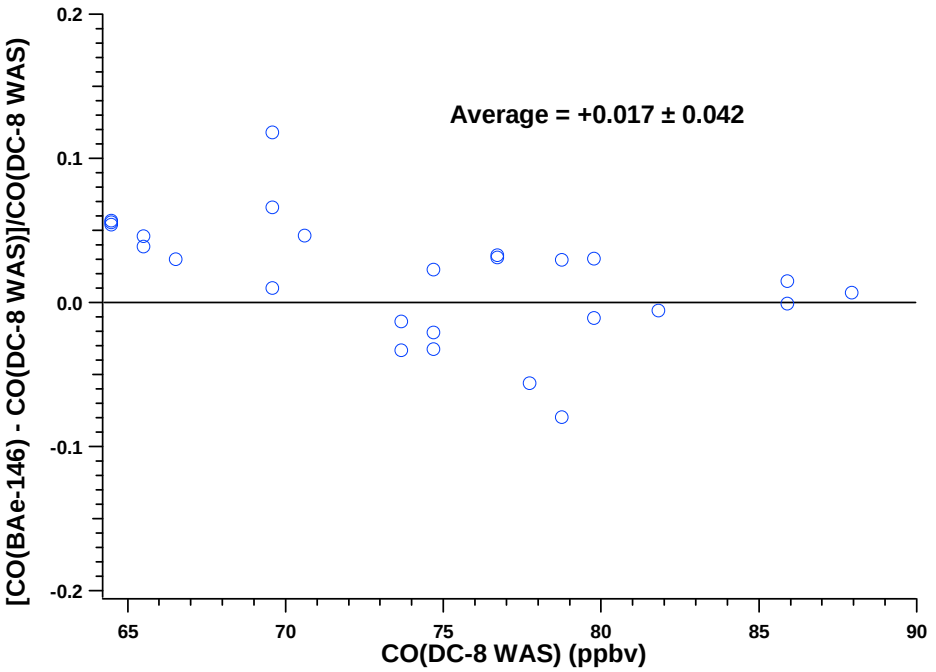

Figure 13. Relative difference between CO measurements from the DC-8/BAe-146 intercomparison flight (07/28) as a function of the DC-8 WAS CO. A correction was made to account for bias.

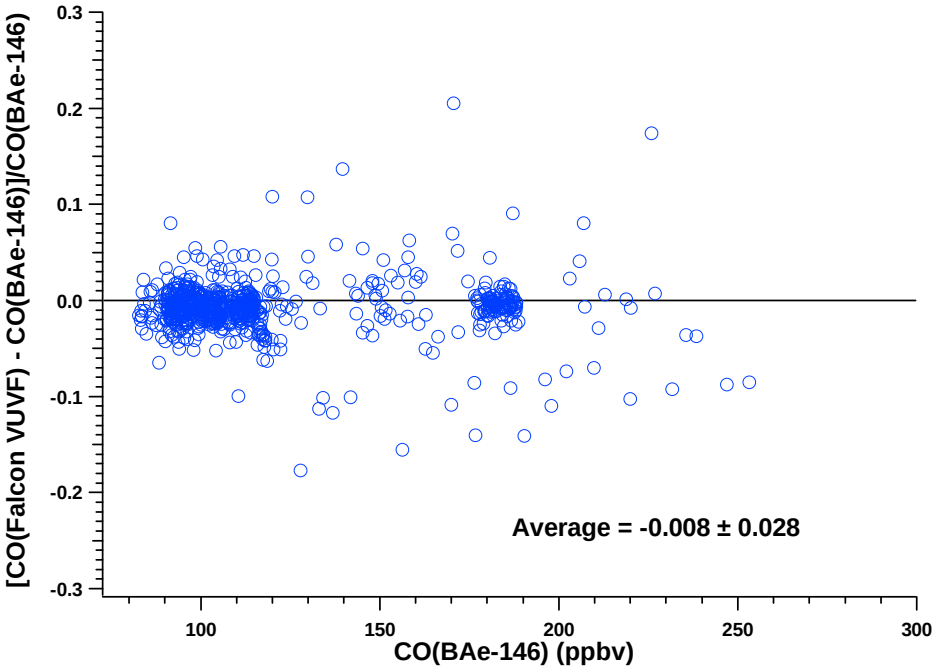

Figure 14. Relative difference between CO measurements reported from two instruments during the BAe-146/DLR Falcon (VUVF) intercomparison flight (08/03) as a function of BAe-146 VUVF CO. A correction was made to account for bias.

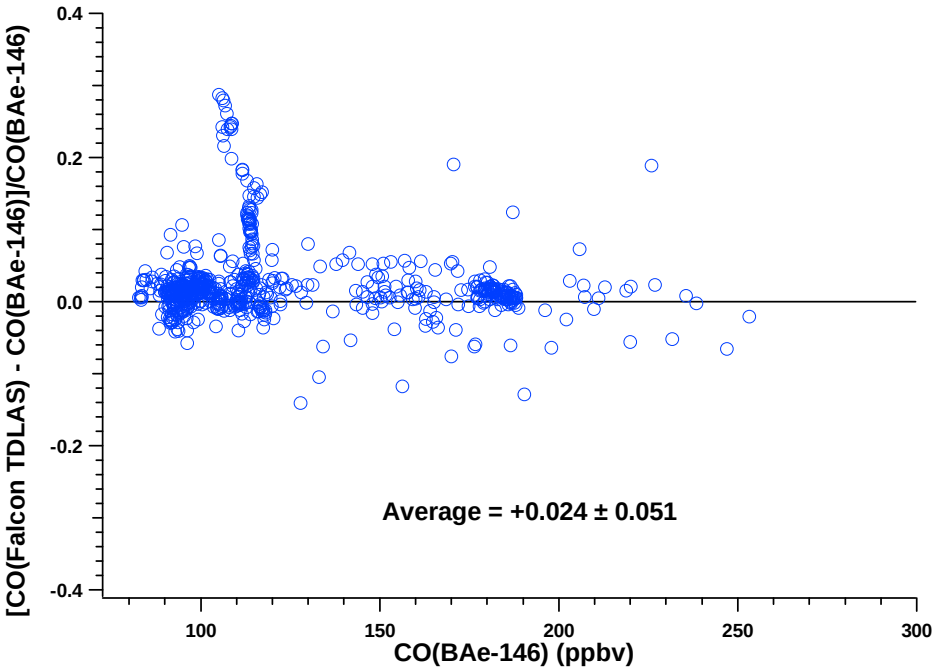

Figure 15. Relative difference between CO measurements from the BAe-146/DLR Falcon (TDLAS) intercomparison flight (08/03) as a function of the BAe-146 VUVF CO. A correction was made to account for bias.

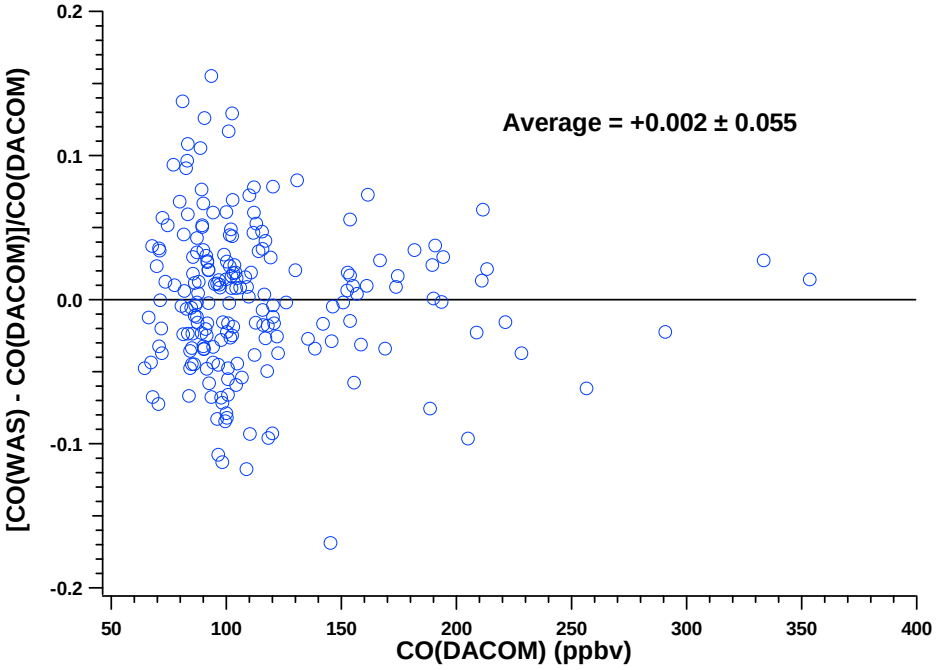

Figure 16. Relative difference between CO measurements reported from all ICARTT flights of the DC-8 as a function of the DC-8 DACOM CO. A correction was made to account for bias.

References

Barletta, B., et al. (2002), Mixing ratios of volatile organic compounds (VOCs) in the atmosphere of Karachi, Pakistan, *Atmospheric Environment, 36*, 3429-3443.

Fehsenfeld, F. C., et al. (2006), International Consortium for Atmospheric Research on Transport and Transformation (ICARTT): North America to Europe—Overview of the 2004 summer field study, *J. Geophys. Res., 111*, D23S01, doi:10.1029/2006JD007829.

Fischer, H., et al. (2002), Synoptic tracer gradients in the upper troposphere over central Canada during the Stratosphere-Troposphere Experiments by Aircraft Measurements 1998 summer campaign, *J. Geophys. Res., 107*(D8), 4064, doi:10.1029/2000JD000312.

Gerbig, C., et al. (1999), An improved fast-response VUV resonance fluorescence CO instrument, *J. Geophys. Res., 104*, 1699-1704.

Holloway, J. S., et al. (2000), Airborne intercomparison of vacuum ultraviolet fluorescence and tunable diode laser absorption measurements of tropospheric carbon monoxide, *J. Geophys. Res., 105*, 24,251–24,261.

Singh, H. B., et al. (2006), Overview of the summer 2004 Intercontinental Chemical Transport Experiment-North America (INTEX-A), *J. Geophys. Res., 111*, D24S01, doi:10.1029/2006JD007905.

Warner, J., M. M. Comer, C. D. Barnet, W. W. McMillan, W. Wolf, E. Maddy, and G. Sachse (2007), A comparison of satellite tropospheric carbon monoxide measurements from AIRS and MOPITT during INTEX-A, *J. Geophys. Res., 112*, D12S17, doi:10.1029/2006JD007925.

Wienhold, F., et al. (1998), Tristar—A tracer in situ TDLAS for atmospheric research, *Appl. Phys., B, 67*, 411 – 417.

TAbMEP Assessment: ICARTT $j(NO_2)$ Measurements

1. Introduction

Here we provide the assessment for the photolytic rate coefficient measurements of nitrogen dioxide [$j(NO_2)$]. These measurements were taken from two aircraft platforms during the summer 2004 ICARTT field campaign [*Fehsenfeld et al.*, 2006, *Singh et al*., 2006]. This assessment is based upon three wing-tip-to-wing-tip intercomparison flights conducted during the field campaign. Recommendations provided here offer TAbMEP assessed uncertainties for each of the measurements and a systematic approach to unifying the ICARTT $j(NO_2)$ data for any integrated analysis. These recommendations are directly derived from the instrument performance demonstrated during the ICARTT measurement comparison exercises and are not to be extrapolated beyond this campaign.

2. ICARTT $j(NO_2)$ Measurements

Two different $j(NO_2)$ instruments were deployed on two aircraft. Table 1 summarizes these techniques and gives references for more information.

Table 1. $j(NO_2)$ measurements deployed on aircraft during ICARTT

Aircraft	Instrument	Reference
NASA DC-8	Scanning Actinic Flux Spectroradiometer (SAFS)	*Shetter and Müller* [1999]
NOAA WP-3D	AFSR Actinic Flux Spectroradiometer (formerly: ZAPHROD)	*Stark et al.* [2007]

3. Summary of Results

Table 2 summarizes the assessed 2σ precisions, biases, and uncertainties. More detailed descriptions are provided to illustrate the process for assessment of bias and precision in Sections 4.1 and 4.2 respectively. The assessed 2σ precisions reported in Table 2 are equal to twice the highest adjusted precision value for that instrument listed in Table 4. Table 2 also reports an assessed bias (see Section 4.1 for details) that can be applied to maximize the consistency between the data sets. The assessed bias should be subtracted from the reported data to 'unify' the data sets. The assessed bias is derived from intercomparison periods only and may be extrapolated to the entire mission if one assumes instrument performance remained constant throughout the mission. The assessed 2σ uncertainty is the larger of either the uncertainty reported by the PI or the quadrature-sum of the assessed 2σ precision and assessed bias listed in Table 2.

It should be noted here that photolysis rates of $j(NO_2)$ are not directly measurable. The photolysis rate, J, is calculated through a function of the compound's absorption cross section $\sigma(\lambda)$, the quantum yield $\Phi(\lambda)$, and the actinic flux $I(\lambda)$:

$$J = \int_{\lambda_1}^{\lambda_2} \sigma(\lambda)\,\Phi(\lambda)\,I(\lambda)\,d\lambda \qquad (1)$$

The actinic flux, $I(\lambda)$, is directly observed by the spectrometers onboard both aircraft; while the cross sections and quantum yields are measured in the laboratory. Thus, the uncertainties reported in Table 2 should be viewed as a weighted actinic flux measurement uncertainty over a

given range of the solar spectrum and solar zenith angles. Users requesting more information should contact Samuel Hall at halls@ucar.edu for DC-8 or Principal Investigator Harald Stark at harald.stark@noaa.gov for WP-3D for detailed explanations.

Table 2. Recommended ICARTT $j(NO_2)$ measurement treatment

Aircraft/ Instrument	Reported Uncertainty[a]	Assessed 2σ Precision	Assessed Bias (s^{-1})	Assessed 2σ Uncertainty
NASA DC-8 SAFS	11.9%	0.96%	0.00 + 0.025 $jNO_{2\text{-DC8}}$	Quadrature Sum
NOAA WP-3D AFSR	15%	5.8%	0.00 – 0.026 $jNO_{2\text{-WP3D}}$	15% [b]

[a] User should see text or consult Samuel Hall at halls@ucar.edu for DC-8 or PI Harald Stark at harald.stark@noaa.gov for WP-3D prior to utilizing this data for explanation of uncertainty values.
[b] This recommendation based on test ranging from 0.0 to 0.02 $j(NO_2)$ (s^{-1}).

Figures 1a-1c display the precisions, biases, and recommended uncertainties for the two $j(NO_2)$ instruments. In each case the uncertainty is driven by the precision.

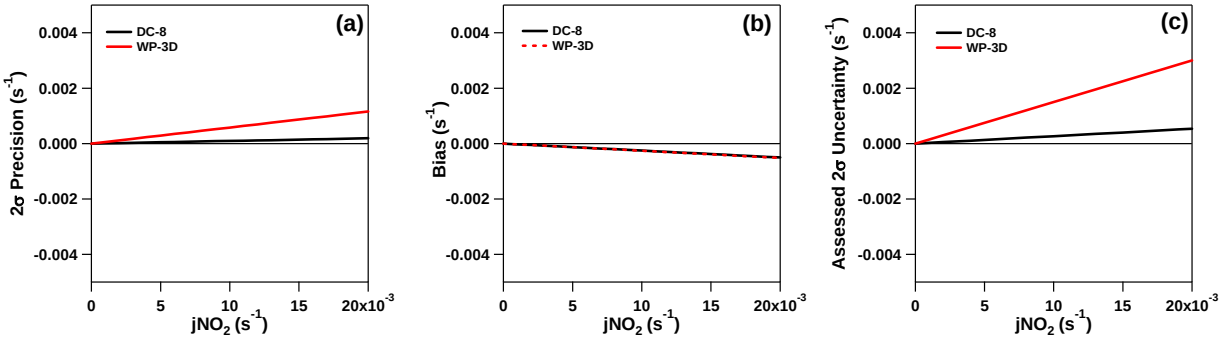

Figure 1. 2σ precision (panel a), bias (panel b), and assessed 2σ uncertainty (panel c) for DC-8 (black) and WP-3D (red) as a function of $j(NO_2)$ level. Values were calculated based upon data shown in Table 2.

4. Results and Discussion

4.1 Bias Analysis

Section 3.3 in the Introduction describes the process used to determine the best estimate bias. The linear relationships listed in Table 3 were derived from the regression equation found in Figure 3. In the case of nitrogen dioxide photolysis, the regression equation for the NOAA WP-3D, is manipulated algebraically to be expressed as a function of $j(NO_2)_{\text{-DC8}}$ shown in Table 3. The reference standard for comparison (RSC) is constructed by averaging the NOAA WP-3D and NASA DC-8. The resulting RSC can be expressed as a function of the DC-8 $j(NO_2)$ measurement as the following:

$$RSC_{jNO2} = 0.00 + 0.975\ jNO_{2\text{-DC8}}$$

The RSC is then used to calculate the best estimate bias as described in Section 3.3 of the Introduction. It should be noted that the initial choice of the reference instrument (DC-8 SAFS) is arbitrary, and has no impact on the final recommendations. Table 3 summarizes the assessed measurement bias for each of the two ICARTT $j(NO_2)$ measurements.

Table 3. ICARTT $j(NO_2)$ bias estimates

Aircraft/ Instrument	Linear Relationships [a]	Best Estimate Bias ($a + b\ jNO_2$) (s^{-1})
NASA DC-8 SAFS	$jNO_{2\text{-DC8}} = 0.00 + 1.00\ jNO_{2\text{-DC8}}$	$0.00 + 0.025\ jNO_{2\text{-DC8}}$
NOAA WP-3D AFSR	$jNO_{2\text{-WP3D}} = 0.00 + 0.95\ jNO_{2\text{-DC8}}$	$0.00 - 0.026\ jNO_{2\text{-WP3D}}$

[a]Derived from Fig. 3.

4.2 Precision Analysis

A detailed description of the precision assessment is given in Section 3.1 of the Introduction. The IEIP precision, expected variability, observed variability, and the adjusted precision are summarized in Table 4. Based on the results presented in Table 4, the largest "adjusted precision" value is taken as a conservative precision estimate for each ICARTT $j(NO_2)$ instrument and twice that value is listed in Table 2 as the assessed 2σ precision.

To minimize the effect of bias, we make corrections for bias before computing the observed variability, as the bias may have a significant impact on the observed variability. Figure 4 shows the magnitude of the bias for each intercomparison. The assessed values of the observed variability are displayed in Figure 5. The final analysis results are shown in Table 2.

Table 4. ICARTT $j(NO_2)$ precision (1σ) comparisons

Flight	Platform	IEIP Precision	Expected Variability	Observed Variability	Adjusted Precision
07/22	DC-8	0.07%	0.46%	3.00%	0.45%
	WP-3D	0.45%			2.90%
07/31	DC-8	0.45%	1.40%	1.00%	0.45%
	WP-3D	1.30%			1.30%
08/07	DC-8	0.05%	0.21%	2.00%	0.48%
	WP-3D	0.20%			1.90%

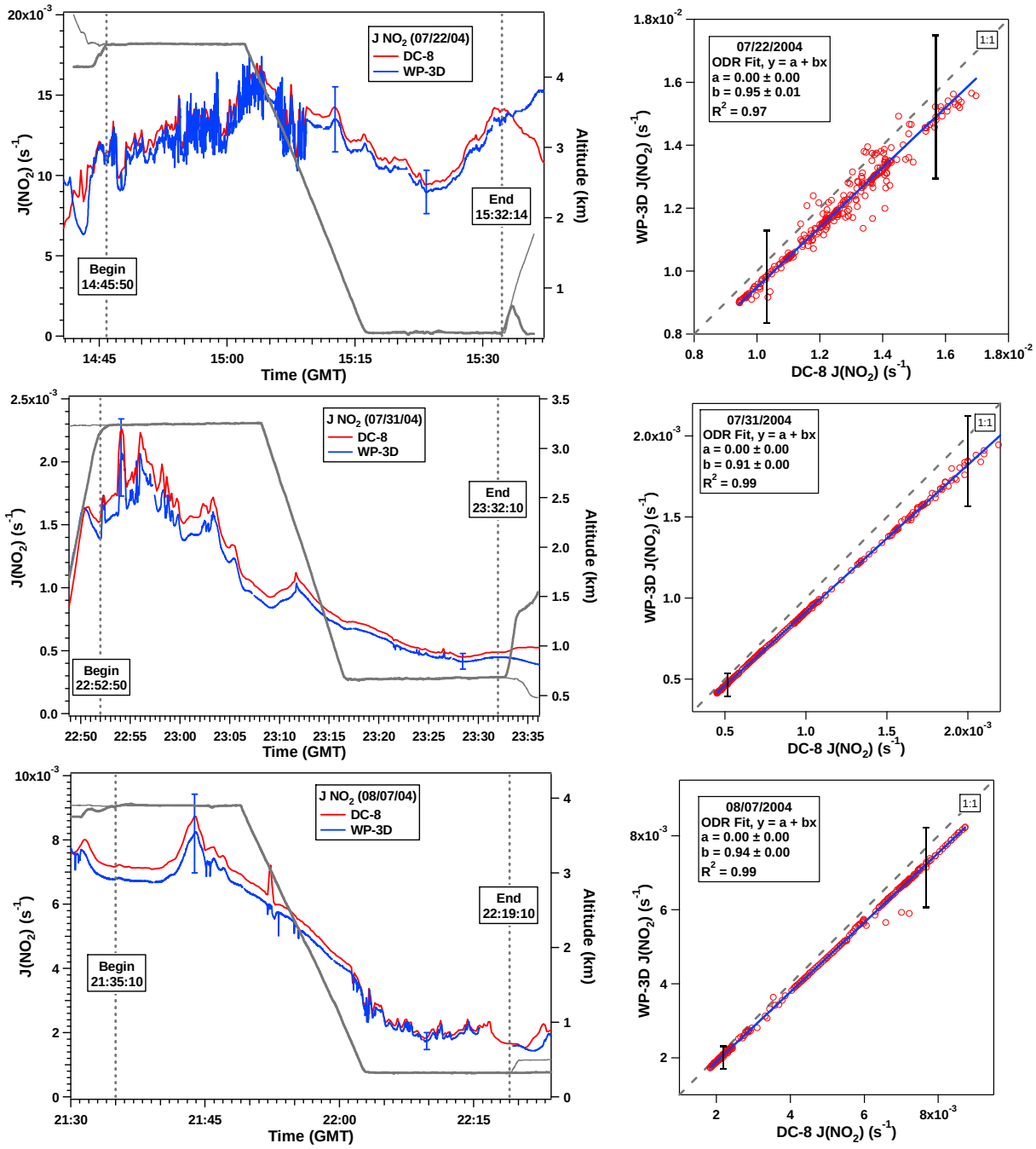

Figure 2. (left panels) Time series of j(NO_2) measurements and aircraft altitudes from two aircraft on the three intercomparison flights between the NASA DC-8 and the NOAA WP-3D. (right panels) Correlations between the j(NO_2) measurements on the two aircraft. Error bars shown depict the reported measurement uncertainties.

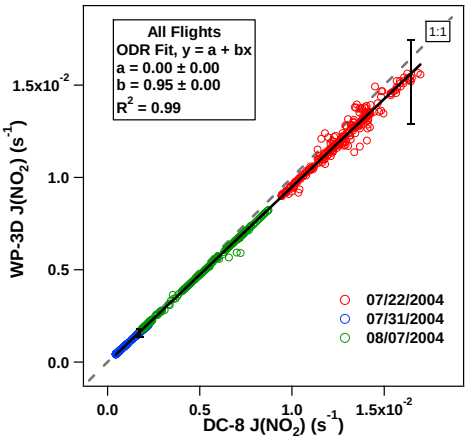

Figure 3. Correlation between the j(NO_2) measurements on the DC-8 and WP-3D for 7/22, 7/31, and 8/7 2004. Error bars shown depict the reported measurement uncertainties.

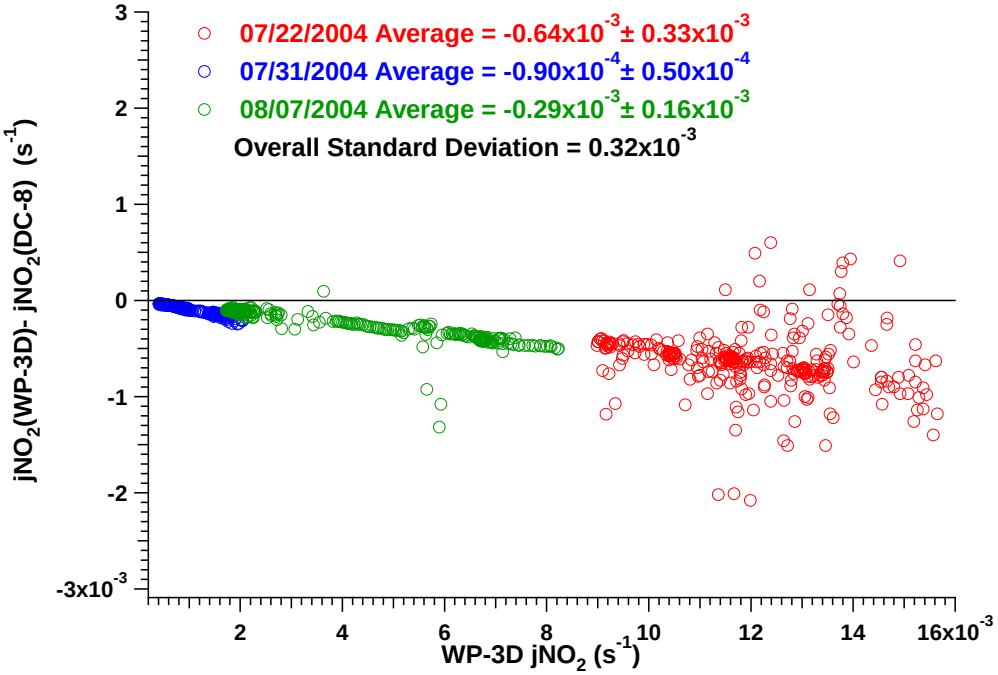

Figure 4. Difference between j(NO_2) measurements from the three DC-8/WP-3D intercomparison flights as a function of the WP-3D j(NO_2).

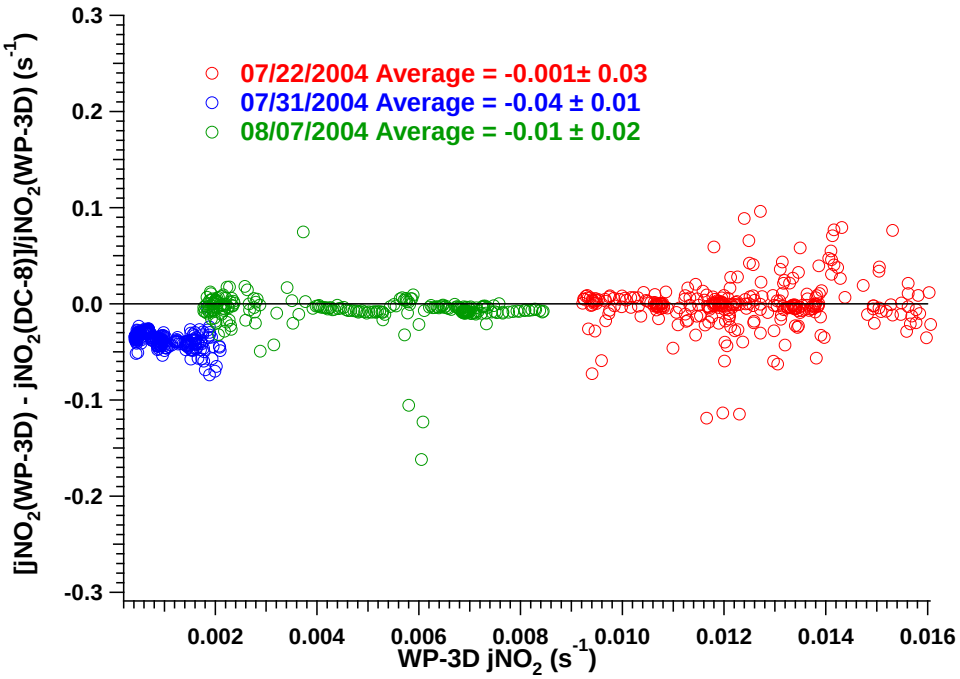

Figure 5. Relative difference between j(NO_2) measurements from the three DC-8/WP-3D intercomparison flights as a function of the WP-3D j(NO_2). A correction was made to account for bias.

References

Fehsenfeld, F. C., et al. (2006), International Consortium for Atmospheric Research on Transport and Transformation (ICARTT): North America to Europe—Overview of the 2004 summer field study, *J. Geophys. Res., 111*, D23S01, doi:10.1029/2006JD007829.

Shetter, R. E. and M. Müller (1999), Photolysis frequency measurements on the NASA DC-8 during the PEM-Tropics Mission using actinic flux spectroradiometry: Instrumentation description and results, *J. Geophys. Res., 104*, 5647-5661.

Singh, H. B., et al. (2006), Overview of the summer 2004 Intercontinental Chemical Transport Experiment-North America (INTEX-A), *J. Geophys. Res., 111*, D24S01, doi:10.1029/2006JD007905.

Stark, H., et al. (2007), Atmospheric in-Situ Measurement of Nitrate Radical (NO3) and Other Photolysis Rates Using Spectro- and Filter Radiometry, *J. Geophys. Res.,112*, D10S04, doi:10.1029/2006JD007578.

TAbMEP Assessment: ICARTT $j(O^1D)$ Measurements

1. Introduction

Here we provide the assessment for the photolytic rate coefficient measurements of ozone photolysis to $O(^1D)$, i.e. $j(O^1D)$. These measurements were taken from two aircraft platforms during the summer 2004 ICARTT field campaign [*Fehsenfeld et al.*, 2006, *Singh et al*., 2006]. This assessment is based upon three wing-tip-to-wing-tip intercomparison flights conducted during the field campaign. Recommendations provided here offer TAbMEP assessed uncertainties for each of the measurements and a systematic approach to unifying the ICARTT $j(O^1D)$ data for any integrated analysis. These recommendations are directly derived from the instrument performance demonstrated during the ICARTT measurement comparison exercises and are not to be extrapolated beyond this campaign.

2. ICARTT $j(O^1D)$ Measurements

Two different $j(O^1D)$ instruments were deployed on two aircraft. Table 1 summarizes these techniques and gives references for more information.

Table 1. $j(O^1D)$ measurements deployed on aircraft during ICARTT

Aircraft	Instrument	Reference
NASA DC-8	Scanning Actinic Flux Spectroradiometers (SAFS)	*Shetter and Müller* [1999]
NOAA WP-3D	AFSR Actinic Flux Spectroradiometer (formerly: ZAPHROD)	*Stark et al.* [2007]

3. Summary of Results

Tables 2a and 2b summarize the assessed 2σ precisions, biases, and uncertainties. More detailed descriptions are provided to illustrate the process for assessment of bias and precision in Sections 4.1 and 4.2 respectively. The assessed 2σ precisions reported in Table 2 are equal to twice the highest adjusted precision value for that instrument listed in Table 4. Table 2 also reports an assessed bias (see Section 4.1 for details) that can be applied to maximize the consistency between the data sets. The assessed bias should be subtracted from the reported data to 'unify' the data sets. The assessed bias is derived from intercomparison periods only and may be extrapolated to the entire mission if one assumes instrument performance remained constant throughout the mission. The recommended 2σ uncertainty is the larger of either the uncertainty reported by the PI or the quadrature-sum of the assessed 2σ precision and assessed bias listed in Table 2. This analysis was split into two parts, $j(O^1D)$ values > $3x10^{-5}$ (s^{-1}) and $j(O^1D)$ values < $3x10^{-5}$ (s^{-1}), in order to achieve best results.

It should be noted here that photolysis rates of $j(O^1D)$ are not directly measurable. The photolysis rate, J, is calculated through a function of the compound's absorption cross section $\sigma(\lambda)$, the quantum yield $\Phi(\lambda)$, and the actinic flux $I(\lambda)$:

$$J = \int_{\lambda_1}^{\lambda_2} \sigma(\lambda)\,\Phi(\lambda)\,I(\lambda)\,d\lambda \qquad (1)$$

The actinic flux, $I(\lambda)$, is directly observed by the spectrometers onboard both aircraft; while the cross sections and quantum yields are measured in the laboratory. Thus, the uncertainties reported in Table 2 should be viewed as a weighted actinic flux measurement uncertainty over a

given range of the solar spectrum and solar zenith angles. In the case of ozone, the cutoff in the atmospheric spectra shifts to larger wavelength as zenith solar angle increases, which makes ozone absorption weaker and harder to measure, resulting in a larger uncertainty. Users requesting more information should contact Samuel Hall at halls@ucar.edu for DC-8 or Principal Investigator Harald Stark at harald.stark@noaa.gov for WP-3D for detailed explanations.

Table 2a. Recommended ICARTT $j(O^1D)$ measurement treatment, $j(O^1D) > 3x10^{-5}$ (s^{-1})

Aircraft/ Instrument	Reported Uncertainty[a]	Assessed 2σ Precision	Assessed Bias (s^{-1})	Assessed 2σ Uncertainty
NASA DC-8 SAFS	12.3%	1.0%	$0.00 + 0.02\ j(O^1D)_{DC8}$	Quadrature Sum
NOAA WP-3D AFSR	30%	5.2%	$0.00 - 0.04\ j(O^1D)_{WP3D}$	30%[b]

[a] User should see text or consult Samuel Hall at halls@ucar.edu for DC-8 or PI Harald Stark at harald.stark@noaa.gov for WP-3D prior to utilizing this data for explanation of uncertainty values.
[b] This recommendation based on test ranging from $3x10^{-5}$ to $7x10^{-5}$ $j(O^1D)$ (s^{-1}).

Table 2b. Recommended ICARTT $j(O^1D)$ measurement treatment, $j(O^1D) < 3x10^{-5}$ (s^{-1})

Aircraft/ Instrument	Reported Uncertainty[a]	Assessed 2σ Precision	Assessed Bias (s^{-1})	Assessed 2σ Uncertainty
NASA DC-8 SAFS	12.3%	1.4%	$0.00 - 0.07\ j(O^1D)_{DC8}$	Quadrature Sum
NOAA WP-3D AFSR	30%	53%	$0.00 + 0.17\ j(O^1D)_{WP3D}$	Quadrature Sum[b]

[a] User should see text or consult Samuel Hall at halls@ucar.edu for DC-8 or PI Harald Stark at harald.stark@noaa.gov for WP-3D prior to utilizing this data for explanation of uncertainty values.
[b] This recommendation based on test ranging from $1x10^{-6}$ to $2.9x10^{-5}$ $j(O^1D)$ (s^{-1}).

Figures 1a-1c and 2a-2c display the precisions, biases, and recommended uncertainties for the two $j(O^1D)$ instruments that measured values above $3x10^{-5}$ (s^{-1}) and below $3x10^{-5}$ (s^{-1}), respectively. In both cases, the uncertainty is driven by precision.

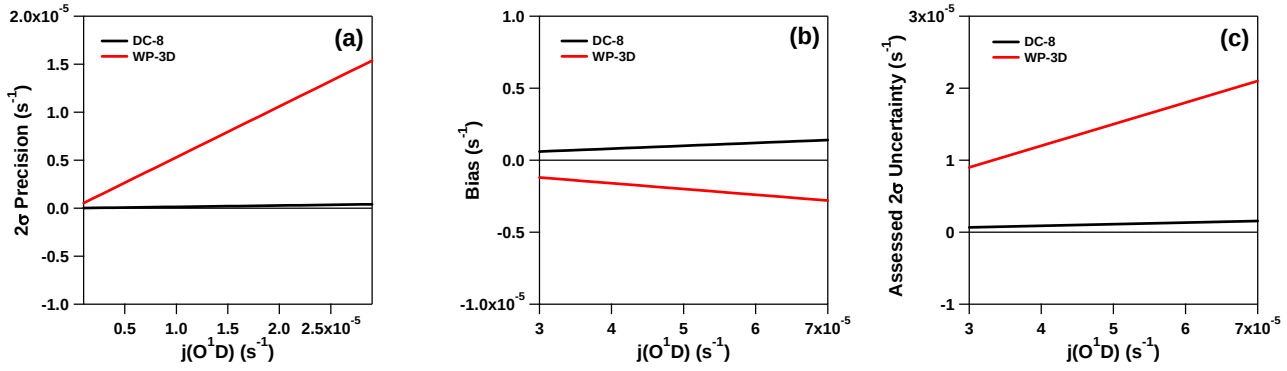

Figure 1. 2σ precision (panel a), bias (panel b), and assessed 2σ uncertainty (panel c) for DC-8 (black) and WP-3D (red) as a function of $j(O^1D)$ level. Values were calculated based upon data shown in Table 2a for $j(O^1D)$ values greater than $3x10^{-5}$ (s^{-1}).

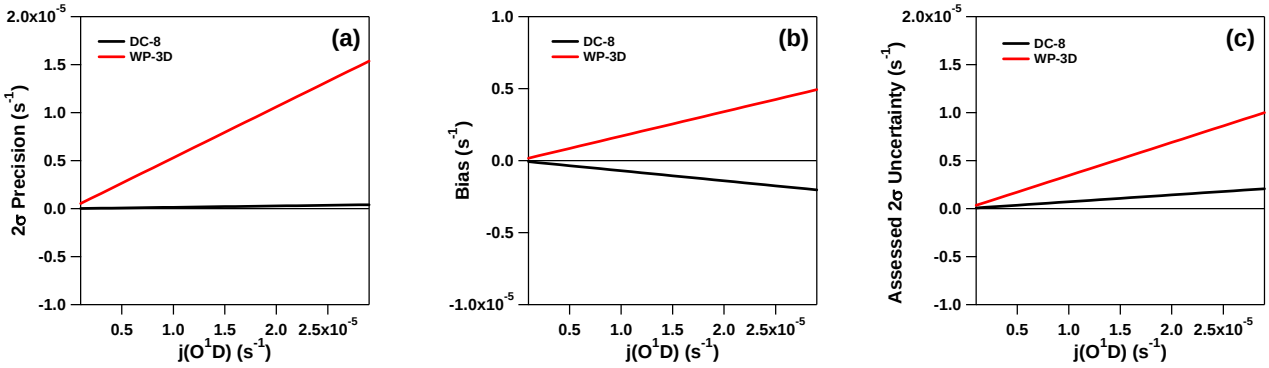

Figure 2. 2σ precision (panel a), bias (panel b), and assessed 2σ uncertainty (panel c) for DC-8 (black) and WP-3D (red) as a function of $j(O^1D)$ level. Values were calculated based upon data shown in Table 2b for $j(O^1D)$ values less than $3x10^{-5}$ (s^{-1}).

4. Results and Discussion

4.1 Bias Analysis

Section 3.3 in the introduction describes the process used to determine the best estimate bias. The linear relationships listed in Table 3a were derived from the regression equation found in Figure 3 (07/22/2004 correlation) as this was the only date with $j(O^1D)$ values greater than $3x10^{-5}$. Linear relationships listed in Table 3b were derived from the regression equation found in Figure 4 for $j(O^1D)$ values less than $3x10^{-5}$. It should be noted that the regression lines were forced to zero in all cases. The reference standard for comparison (RSC) is constructed by averaging weighted values of NOAA WP-3D and NASA DC-8. Weighted values shown in Equation 2 were used to best resolve technical difficulties that were experienced by the WP-3D AFSR instrument during the series of flights.

$$RSC = \begin{cases} \frac{2\,SAFS+AFSR}{3} & jO^1D > 3\times10^{-5} \\ \frac{3\,SAFS+AFSR}{4} & jO^1D < 3\times10^{-5} \end{cases} \quad (2)$$

The resulting RSC's can be expressed as a function of the DC-8 $j(O^1D)$ measurement as the following:

$$RSC_{jO1D} = 0.00 + 0.98\ j(O^1D)_{DC8};\ j(O^1D)\ \text{values} > 3x10^{-5}\ (s^{-1}) \quad (3)$$

$$RSC_{jO1D} = 0.00 + 1.07\ j(O^1D)_{DC8};\ j(O^1D)\ \text{values} < 3x10^{-5}\ (s^{-1}) \quad (4)$$

The RSC is then used to calculate the best estimate bias as described in Section 3.3 of the introduction. It should be noted that the initial choice of the reference instrument (DC-8 SAFS) is arbitrary, and has no impact on the final recommendations. Tables 3a and 3b summarize the assessed measurement bias for each of the two ICARTT $j(O^1D)$ measurements.

Table 3a. ICARTT $j(O^1D)$ bias estimates, $j(O^1D) > 3x10^{-5}$ (s^{-1})

Aircraft/ Instrument	Linear Relationships[a]	Best Estimate Bias ($a + b\ jO^1D$) (s^{-1})
NASA DC-8 SAFS	$0.00 + 1.00\ j(O^1D)_{DC8}$	$0.00 + 0.02\ j(O^1D)_{DC8}$
NOAA WP-3D ZAPHROD	$0.00 + 0.94\ j(O^1D)_{DC8}$	$0.00 - 0.04\ j(O^1D)_{WP3D}$

[a]Derived from Fig. 3 (7/22 correlation).

Table 3b. ICARTT $j(O^1D)$ bias estimates, $j(O^1D) < 3x10^{-5}$ (s^{-1})

Aircraft/ Instrument	Linear Relationships[a]	Best Estimate Bias ($a + b\ jO^1D$) (s^{-1})
NASA DC-8 SAFS	$0.00 + 1.00\ j(O^1D)_{DC8}$	$0.00 - 0.07\ j(O^1D)_{DC8}$
NOAA WP-3D ZAPHROD	$0.00 + 1.29\ j(O^1D)_{DC8}$	$0.00 + 0.17\ j(O^1D)_{WP3D}$

[a]Derived from Fig. 4.

4.2 Precision Analysis

A detailed description of the precision assessment is given in Section 3.1 of the introduction. The IEIP precision, expected variability, observed variability, and the adjusted precision are summarized in Table 4. Dissimilar to other TAbMEB assessment reports, the precision and variability are reported based upon the ranges of $j(O^1D)$ values instead of dates of intercomparison flights. It should be noted that flight dates and j-values do correspond with one another- $j(O^1D)$ values greater than 10^{-5} were reported on 7/22/2004, $j(O^1D)$ values below 10^{-6} were reported on 7/31/2004, and $j(O^1D)$ values between 10^{-6} and 10^{-5} were reported on 8/07/2004. Based on the results presented in Table 4, the largest "adjusted precision" value is taken as a conservative precision estimate for each ICARTT $j(O^1D)$ instrument and twice that value is listed in Tables 2a and 2b as the assessed 2σ precision.

To minimize the effect of bias, we make corrections for bias before computing the observed variability, as the bias may have a significant impact on the observed variability. Figure 6 shows the magnitude of the bias for each intercomparison. The assessed values of the observed variability are displayed in Figure 7. The final analysis results are shown in Tables 2a and 2b.

Table 4. ICARTT $j(O^1D)$ precision (1σ) comparisons

j(O1D) Range	Platform	IEIP Precision	Expected Variability	Observed Variability	Adjusted Precision
$>10^{-5}$ (7/22)	DC-8	0.3%	1.5%	2.6%	0.5%
	WP-3D	1.5%			2.6%
$<10^{-6}$ (7/31)	DC-8	0.2%	7.5%	26.5%	0.7%
	WP-3D	7.5%			26.5%
10^{-6} - 10^{-5} (8/07)	DC-8	0.3%	4.5%	7.0%	0.5%
	WP-3D	4.5%			7.0%

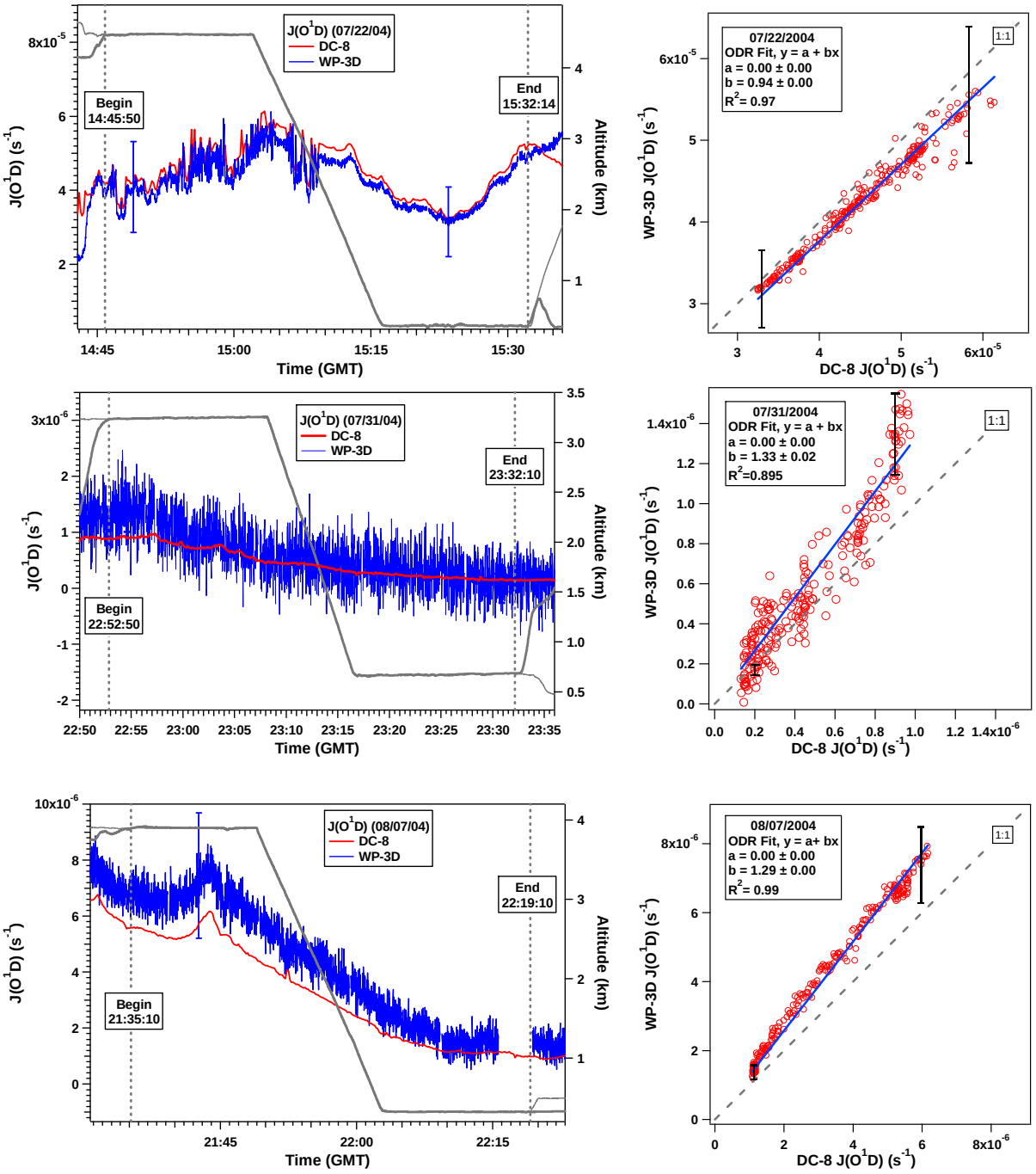

Figure 3. (left panels) Time series of $j(O^1D)$ measurements and aircraft altitudes from two aircraft on the three intercomparison flights between the NASA DC-8 and the NOAA WP-3D. (right panels) Correlations between the $j(O^1D)$ measurements on the two aircraft. Error bars shown depict the reported measurement uncertainties.

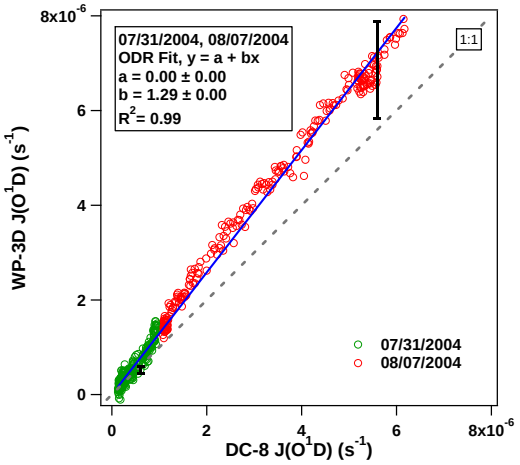

Figure 4. Correlation between the j(O^1D) measurements on the DC-8 and WP-3D for 7/31 and 8/07 2004. Error bars shown depict the reported measurement uncertainties.

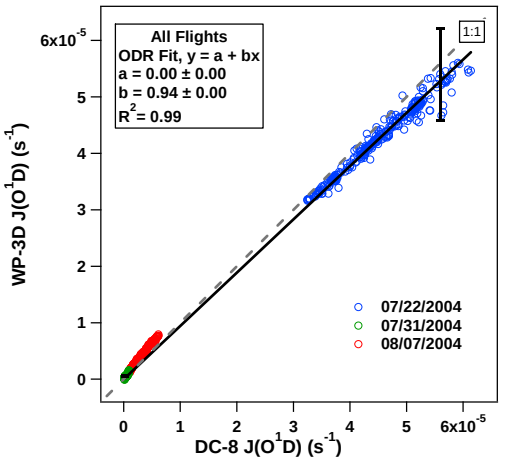

Figure 5. Correlation between the j(O^1D) measurements on the DC-8 and WP-3D for 7/22, 7/31, and 8/7 2004. Error bars shown depict the reported measurement uncertainties.

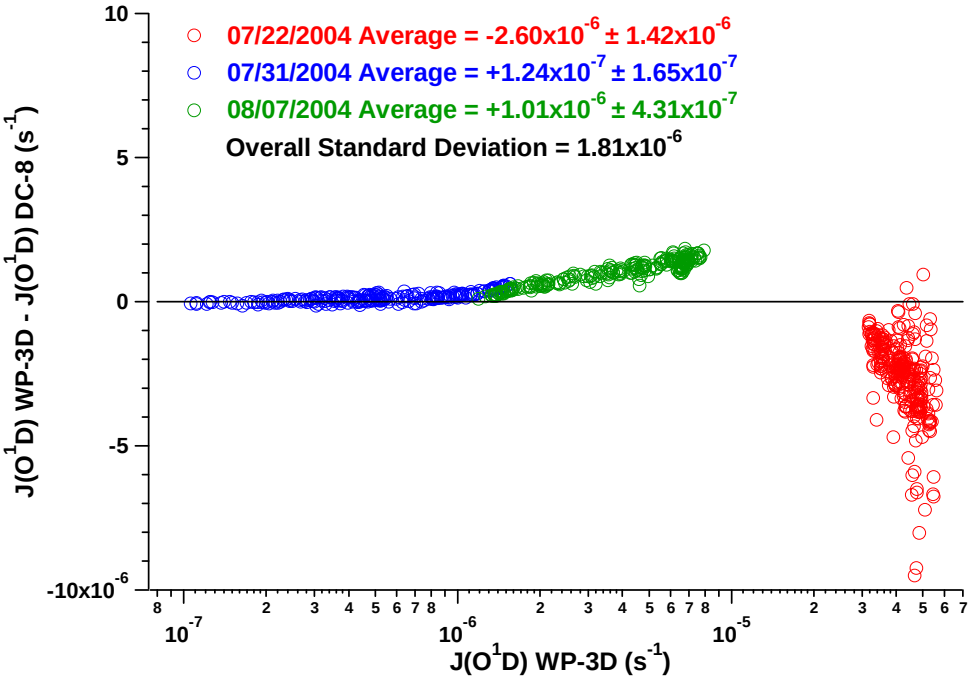

Figure 6. Difference between $j(O^1D)$ measurements from the three DC-8/WP-3D intercomparison flights as a function of the WP-3D $j(O^1D)$.

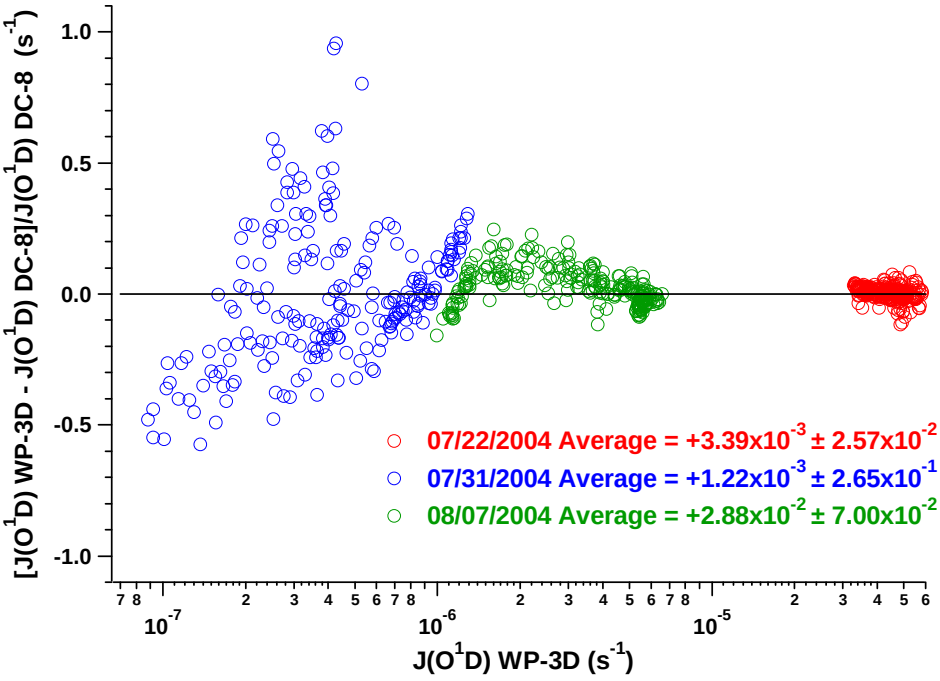

Figure 7. Relative difference between $j(O^1D)$ measurements from the three DC-8/WP-3D intercomparison flights as a function of the WP-3D $j(O^1D)$. A correction was made to account for bias.

References

Fehsenfeld, F. C., et al. (2006), International Consortium for Atmospheric Research on Transport and Transformation (ICARTT): North America to Europe—Overview of the 2004 summer field study, *J. Geophys. Res., 111*, D23S01, doi:10.1029/2006JD007829.

Shetter, R. E. and M. Müller (1999), Photolysis frequency measurements on the NASA DC-8 during the PEM-Tropics Mission using actinic flux spectroradiometry: Instrumentation description and results, *J. Geophys. Res., 104*, 5647-5661.

Singh, H. B., et al. (2006), Overview of the summer 2004 Intercontinental Chemical Transport Experiment-North America (INTEX-A), *J. Geophys. Res., 111*, D24S01, doi:10.1029/2006JD007905.

Stark, H., et al. (2007), Atmospheric in-Situ Measurement of Nitrate Radical (NO_3) and Other Photolysis Rates Using Spectro- and Filter Radiometry, *J. Geophys. Res.,112*, D10S04, doi:10.1029/2006JD007578.

TAbMEP Assessment: ICARTT O_3 Measurements

1. Introduction

Here we provide the assessment for the ozone (O_3) measurements taken from four aircraft platforms during the summer 2004 ICARTT field campaign [*Fehsenfeld et al.*, 2006, *Singh et al*., 2006]. This assessment is based upon the five wing-tip-to-wing-tip intercomparison flights conducted during the field campaign. Recommendations provided here offer TAbMEP assessed uncertainties for each of the measurements and a systematic approach to unifying the ICARTT O_3 data for any integrated analysis. These recommendations are directly derived from the instrument performance demonstrated during the ICARTT measurement comparison exercises and are not to be extrapolated beyond this campaign.

2. ICARTT O_3 Measurements

Four different O_3 instruments were deployed on the four aircraft. Table 1 summarizes these techniques and gives references for more information.

Table 1. O_3 measurements deployed on aircraft during ICARTT

Aircraft	Instrument	Reference
NASA DC-8	NO Chemiluminescence Detector (NO CLD)	*Fairlie et. al.* [2007]
NOAA WP-3D	NO CLD	*Ryerson et al.* [1998]
FAAM BAe-146	TECO 49 UV photometric (TECO UVP)	Not available
DLR Falcon	TECO UVP	Not available

3. Summary of Results

Table 2 summarizes the assessed 2σ precisions, biases, and uncertainties. More detailed descriptions are provided to illustrate the process for assessment of bias and precision in Sections 4.1 and 4.2 respectively. The assessed 2σ precisions reported in Table 2 are equal to twice the highest adjusted precision value for that instrument listed in Table 4. Table 2 also reports an assessed bias (see Section 4.1 for details) that can be applied to maximize the consistency between the data sets. The assessed bias should be subtracted from the reported data to 'unify' the data sets. The assessed bias is derived from intercomparison periods only and may be extrapolated to the entire mission if one assumes instrument performance remained constant throughout the mission. The recommended 2σ uncertainty is the larger of either the uncertainty reported by the PI or the quadrature-sum of the assessed 2σ precision and assessed bias listed in Table 2.

Table 2. Recommended ICARTT O_3 measurement treatment

Aircraft/ Instrument	Reported 2σ Uncertainty	Assessed 2σ Precision	Assessed Bias	Recommended 2σ Uncertainty[a]
NASA DC-8 NO CLD	3% or 3 ppbv	5.6%	$1.26 - 0.029\ O_{3\text{-DC8}}$	3 ppbv or Quadrature Sum[b]
NOAA WP-3D NO CLD	0.1 ppbv + 3%	4.2%	$-0.37 - 0.008\ O_{3\text{-WP3D}}$	Quadrature Sum
FAAM BAe-146 TECO UVP	None	6.4%	$-2.12 + 0.047\ O_{3\text{-BAe146}}$	Quadrature Sum
DLR Falcon TECO UVP	5%	4.0%	$-0.83 + 0.035\ O_{3\text{-Falcon}}$	2 ppbv[c] or 5%

[a] Recommendations based on test ranging from 10 to 100 ppbv.
[b] Recommended 2σ uncertainty is 3ppbv for $O_{3\text{-DC8}} < 56$ ppbv.
[c] Derived from absolute precision IEIP analysis.

Figures 1a-1c display the precisions, biases, and recommended uncertainties for the four O_3 instruments. Except for low O_3 values measured by the TECO UVP aboard the Falcon (and to a lesser extent the NO CLD aboard the DC-8), the uncertainty is driven by the precision.

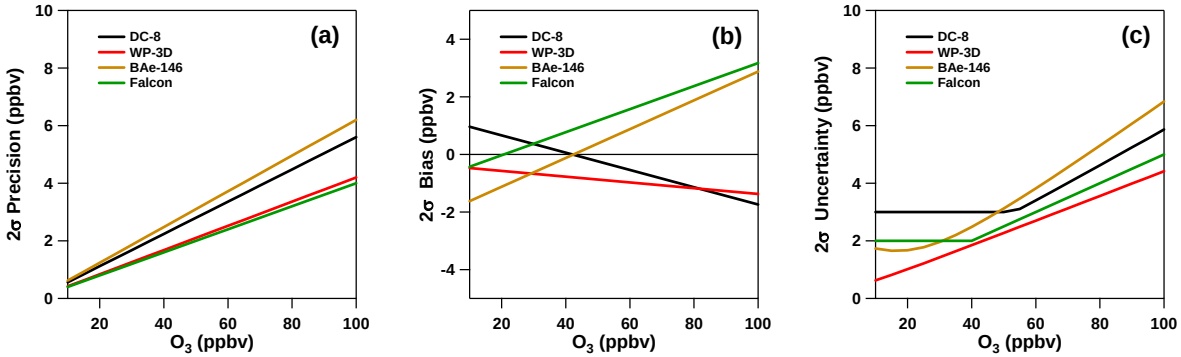

Figure 1. 2σ precision (panel a), 2σ bias (panel b), and 2σ uncertainty (panel c) for DC-8 (black), WP-3D (red), BAe-146 (gold), and Falcon (green) as a function of O_3 level. Values were calculated based upon data shown in Table 2.

4. Results and Discussion

4.1 Bias Analysis

Section 3.3 in the introduction describes the process used to determine the best estimate bias. Figure 2 shows the correlation and time series plots for each of the three WP-3D vs. DC-8 comparisons. The linear relationships listed in Table 3 were derived from the regression equations found in Figures 3 through 5. In the case of ozone, the regression equations for the NOAA WP-3D, FAAM BAe-146, and DLR Falcon are manipulated algebraically to be expressed as a function of $O_{3\text{-}DC8}$ shown in Table 3. The reference standard for comparison (RSC), as defined in the introduction, is constructed by averaging the NOAA WP-3D and NASA DC-8 and DLR Falcon measurements, as they are best maintained and calibrated instruments. The BAe-146 is not included in constructing RSC since the instrument calibration record is incomplete. The resulting RSC can be expressed as a function of the DC-8 O_3 measurement as the following:

$$RSC_{O3} = -1.26 + 1.029\ O_{3\text{-}DC8}$$

The RSC is then used to calculate the best estimate bias as described in Section 3.3 of the introduction. It should be noted that the initial choice of the reference instrument (DC-8 NO CLD) is arbitrary, and has no impact on the final recommendations. Table 3 summarizes the assessed measurement bias for each of the four ICARTT O_3 measurements. Note that additional decimal places were carried in the calculations to ensure better than 0.1 ppbv precision.

Table 3. ICARTT O_3 bias estimates

Aircraft/ Instrument	Linear Relationships[a]	Best Estimate Bias ($a + b\ O_3$) (ppbv)
NASA DC-8 NO CLD	$O_{3\text{-DC8}} = 0.00 + 1.00\ O_{3\text{-DC8}}$	$1.26 - 0.029\ O_{3\text{-DC8}}$
NOAA WP-3D NO CLD	$O_{3\text{-WP3D}} = -1.61 + 1.020\ O_{3\text{-DC8}}$	$-0.37 - 0.008\ O_{3\text{-WP3D}}$
FAAM BAe-146 TECO UVP	$O_{3\text{-BAe146}} = -3.54 + 1.079\ O_{3\text{-DC8}}$[b]	$-2.12 + 0.047\ O_{3\text{-BAe146}}$
DLR Falcon TECO UVP	$O_{3\text{-Falcon}} = -2.16 + 1.066\ O_{3\text{-DC8}}$	$-0.83 + 0.035\ O_{3\text{-Falcon}}$

[a]Derived from Figs. A2-A4.
[b]Not included in RSC derivation, text for details.

4.2 Precision Analysis

A detailed description of the precision assessment is given in Section 3.1 of the introduction. The IEIP precision, expected variability, observed variability, and the adjusted precision are summarized in Table 4. Based on the results presented in Table 4, the largest "adjusted precision" value is taken as a conservative precision estimate for each ICARTT O_3 instrument and twice that value is listed in Table 2 as the assessed 2σ precision.

To minimize the effect of bias, we make corrections for bias before computing the observed variability, as the bias may have a significant impact on the observed variability. Figures 6 – 8 show the magnitude of the bias for each intercomparison. The assessed values of the observed variability are displayed in Figures 9 – 11. The final analysis results are shown in Table 2. Over 90% of the data falls within the combined recommended uncertainties for each intercomparison, which is consistent with the TAbMEP guideline for unified data sets.

Table 4. ICARTT O_3 precision (1σ) comparisons

Flight	Platform	IEIP Precision	Expected Variability	Observed Variability	Adjusted Precision
07/22	DC-8	1.2%	1.8%	2.7%	1.8%
	WP-3D	1.4%			2.1%
07/31	DC-8	1.3%	1.3%	2.9%	2.3%
	WP-3D	1.0%			1.8%
08/07	DC-8	1.2%	1.6%	2.3%	1.8%
	WP-3D	1.0%			1.5%
07/28	DC-8	1.2%	1.8%	4.2%	2.8%
	BAe-146	1.4%			3.2%
08/03	BAe-146	0.9%	2.2%	2.1%	0.9%
	Falcon	2.0%			2.0%

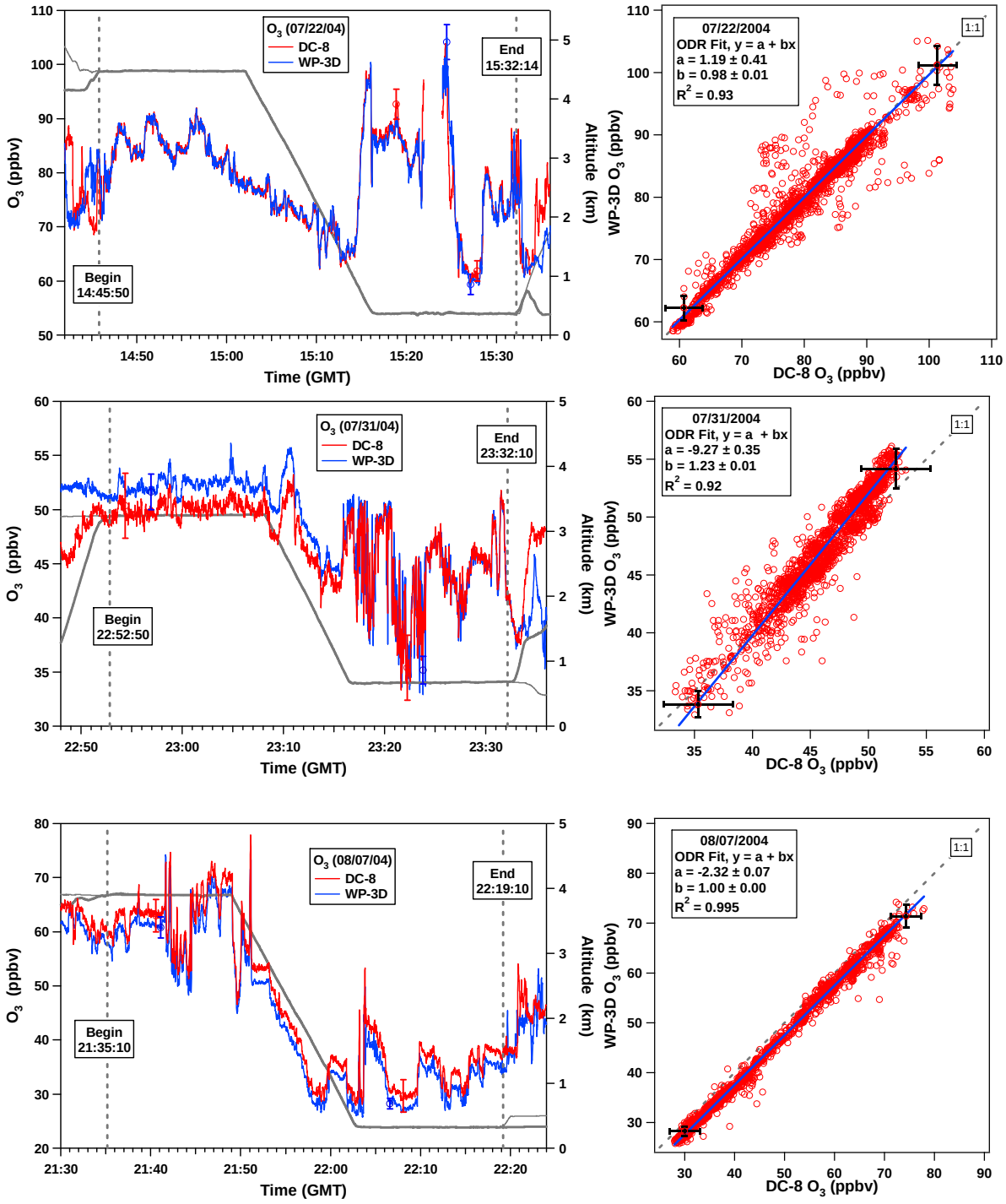

Figure 2. (left panels) Time series of O_3 measurements and aircraft altitudes from two aircraft on the three intercomparison flights between the NASA DC-8 and the NOAA WP-3D. (right panels) Correlations between the O_3 measurements on the two aircraft. Error bars shown depict the reported measurement uncertainties.

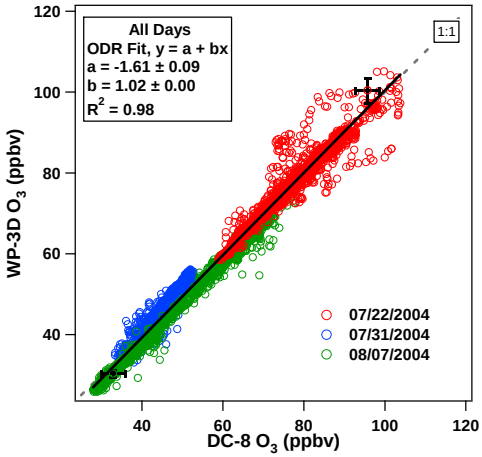

Figure 3. Correlation between the O_3 measurements on the DC-8 and WP-3D for 7/22, 7/31, and 8/7 2004. Error bars shown depict the reported measurement uncertainties.

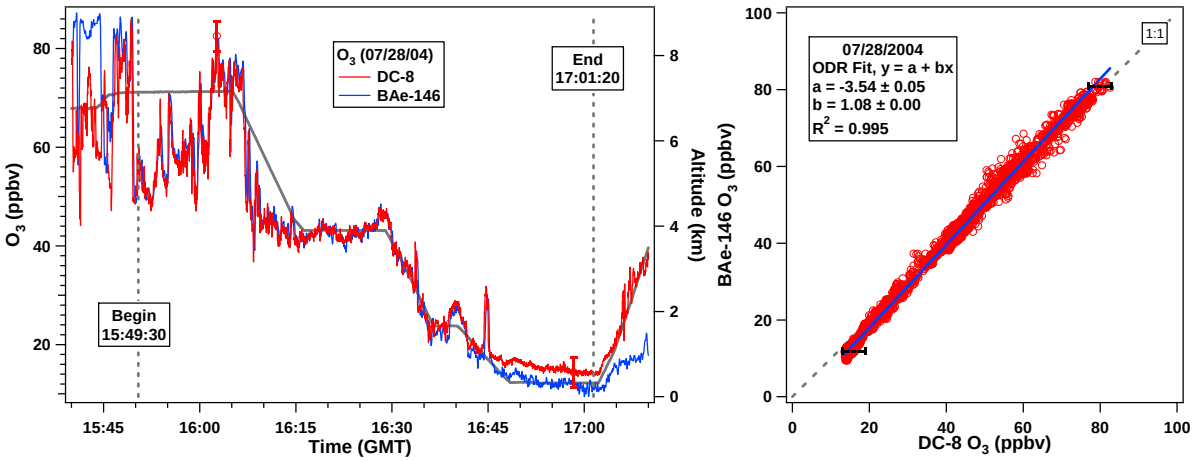

Figure 4. (left panel) Time series of O_3 measurements and aircraft altitudes from the intercomparison flight between the NASA DC-8 and the FAAM BAe-146. (right panel) Correlations between the O_3 measurements on the two aircraft. Error bars shown depict the reported measurement uncertainties.

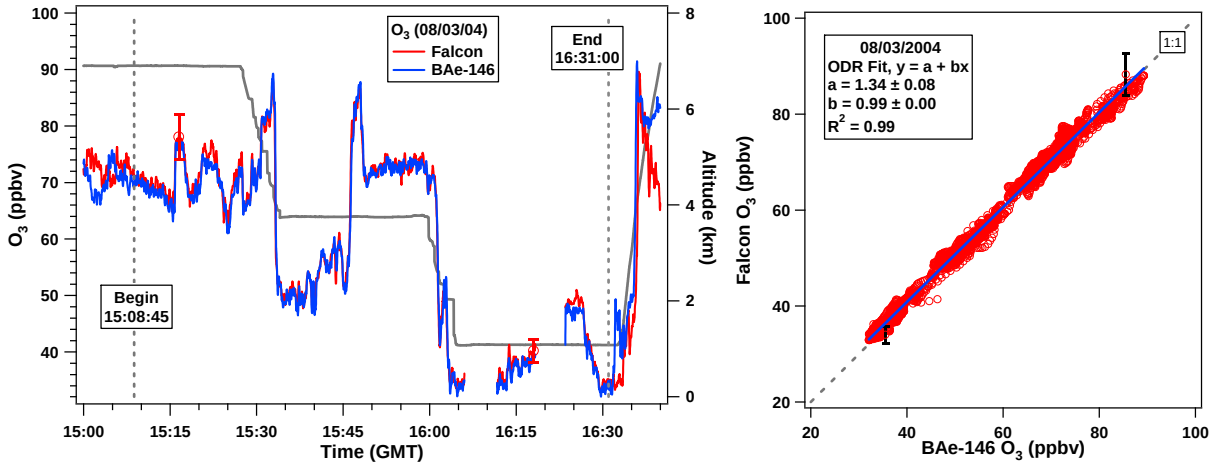

Figure 5. (left panel) Time series of O_3 measurements and aircraft altitudes from the intercomparison flight between the FAAM BAe-146 and the DLR Falcon. (right panel) Correlations between the O_3 measurements on the two aircraft. Error bars shown depict the reported measurement uncertainties.

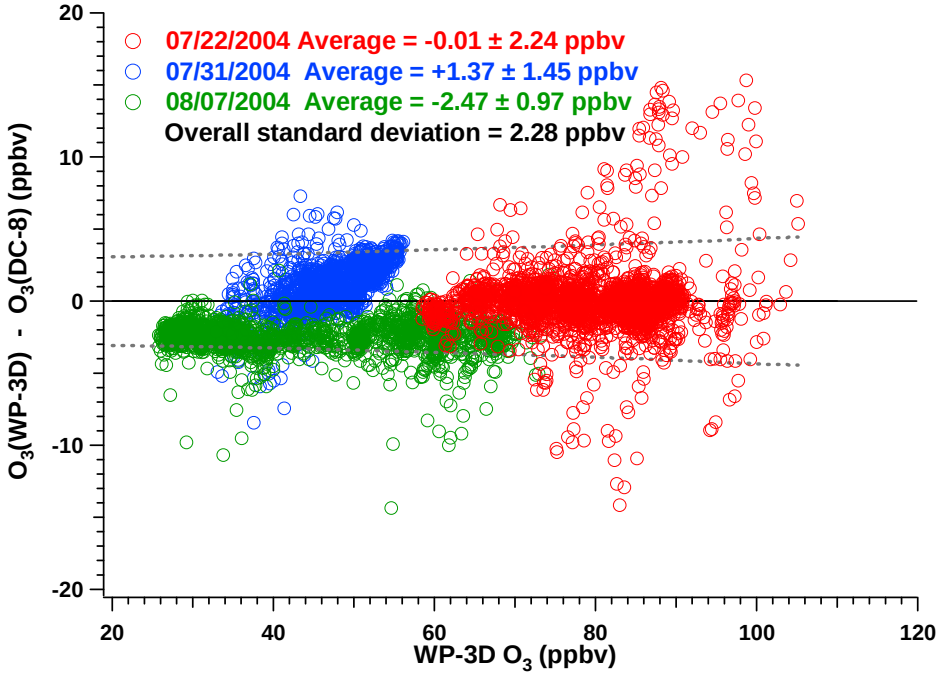

Figure 6. Difference between O_3 measurements from the three DC-8/WP-3D intercomparison flights as a function of the WP-3D O_3. The dashed lines indicate the range of the results expected from the reported 2σ measurement uncertainties.

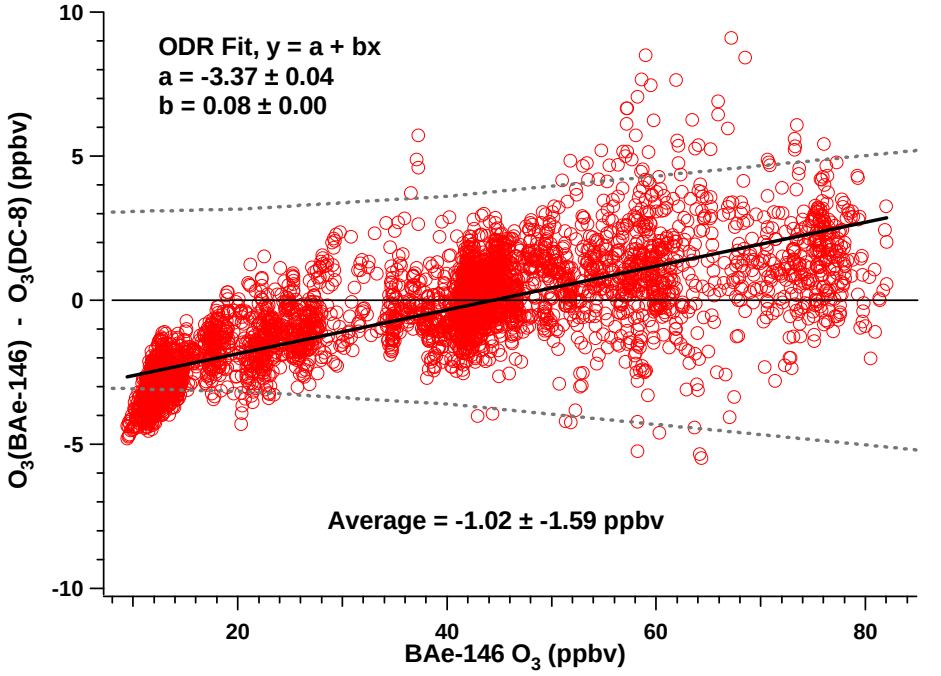

Figure 7. Difference between O_3 measurements from the DC-8/BAe-146 intercomparison flight (07/28) as a function of the BAe-146 O_3. The dashed lines indicate the range of the results expected from the reported 2σ measurement uncertainties. For the purposes of this graph, BAe-146 uncertainty was assumed to be 5% based on similar instruments.

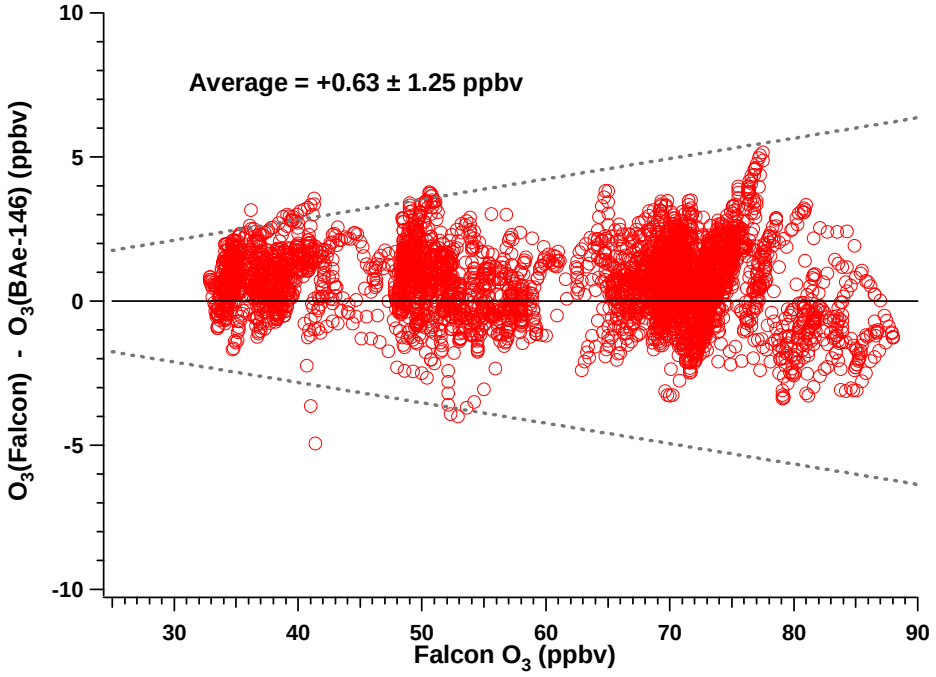

Figure 8. Difference between O_3 measurements from the BAe-146/Falcon intercomparison flight (08/03) as a function of the Falcon O_3. The dashed lines indicate the range of the results expected from the reported 2σ measurement uncertainties. For the purposes of this graph, BAe-146 uncertainty was assumed to be 5% based on similar instruments.

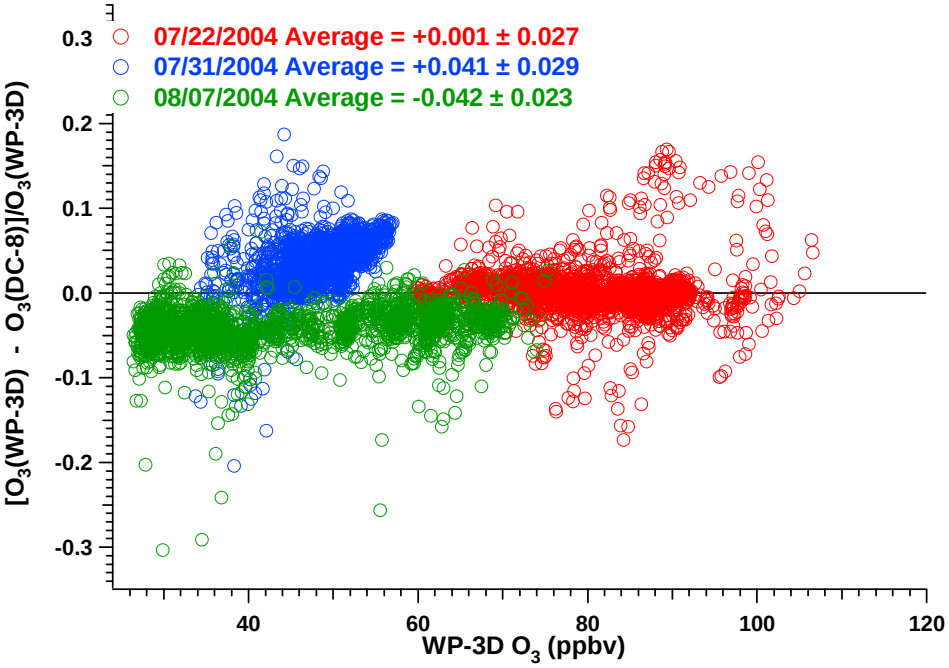

Figure 9. Relative difference between O_3 measurements from the three DC-8/WP-3D intercomparison flights as a function of the WP-3D O_3. A correction was made to account for bias.

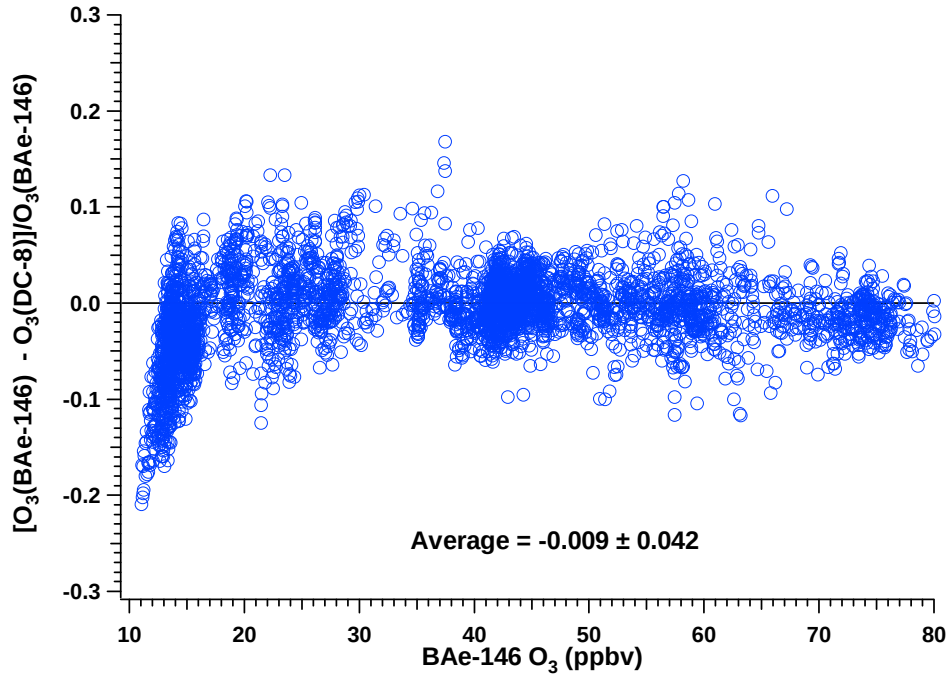

Figure 10. Relative difference between O_3 measurements from the DC-8/BAe-146 intercomparison flight (07/28) as a function of the BAe-146 O_3. A correction was made to account for bias.

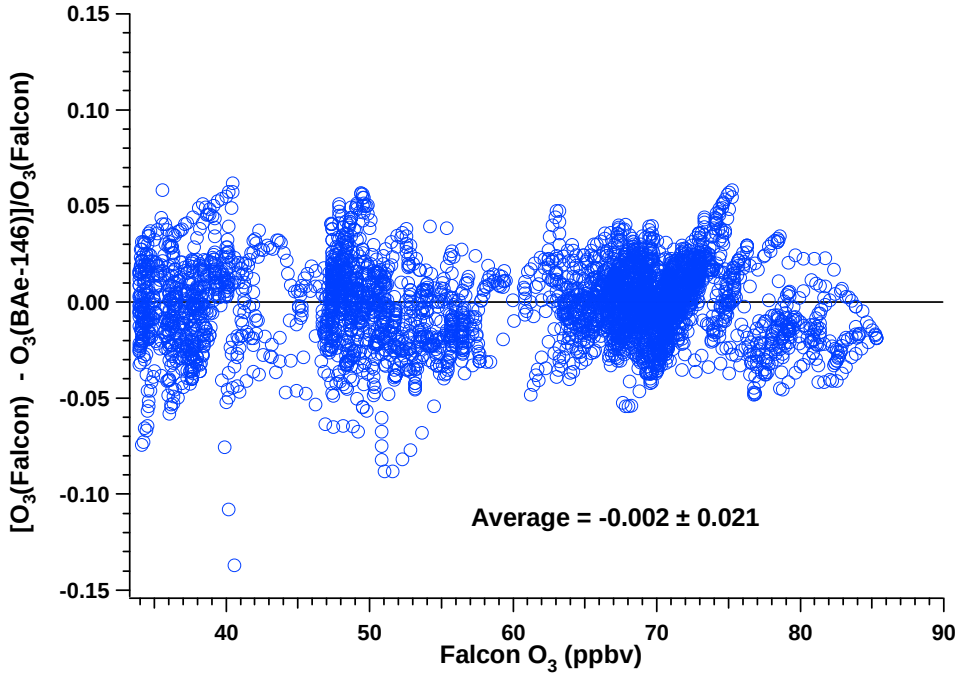

Figure 11. Relative difference between O_3 measurements from the BAe-146/Falcon intercomparison flights as a function of the Falcon O_3. A correction was made to account for bias.

References

Fairlie, T. D., M. A. Avery, R. B. Pierce, J. Al-Saadi, J. Dibb, and G. Sachse (2007), Impact of multiscale dynamical processes and mixing on the chemical composition of the upper troposphere and lower stratosphere during the Intercontinental Chemical Transport Experiment–North America, J. Geophys. Res., 112, D16S90, doi:10.1029/2006JD007923.

Fehsenfeld, F. C., et al. (2006), International Consortium for Atmospheric Research on Transport and Transformation (ICARTT): North America to Europe—Overview of the 2004 summer field study, *J. Geophys. Res., 111*, D23S01, doi:10.1029/2006JD007829.

Ryerson, T. B., et al. (1998), Emissions lifetimes and ozone formation in power plant plumes, *J. Geophys. Res., 103*, D17, pp. 22,569-22,583.

Singh, H. B., et al. (2006), Overview of the summer 2004 Intercontinental Chemical Transport Experiment-North America (INTEX-A), *J. Geophys. Res., 111*, D24S01, doi:10.1029/2006JD007905.

TAbMEP Assessment: ICARTT Temperature Measurements

1. Introduction

Here we provide the assessment for the temperature measurements taken from three aircraft platforms during the summer 2004 ICARTT field campaign [*Fehsenfeld et al.*, 2006, *Singh et al*., 2006]. This assessment is based upon the four wing-tip-to-wing-tip intercomparison flights conducted during the field campaign. Recommendations provided here offer TAbMEP assessed uncertainties for each of the measurements and a systematic approach to unifying the ICARTT temperature data for any integrated analysis. These recommendations are directly derived from the instrument performance demonstrated during the ICARTT measurement comparison exercises and are not to be extrapolated beyond this campaign.

2. ICARTT Temperature Measurements

Three different temperature instruments were deployed on three aircraft. Table 1 summarizes these techniques and gives references for more information.

Table 1. Temperature measurements deployed on aircraft during ICARTT

Aircraft	Instrument	Reference
NASA DC-8	Rosemount Temperature Sensor (deiced) (RTS)	*Stickney et al.* [1990]
NOAA WP-3D	Rosemount Temperature Sensor (non-deiced) (RTS)	Not available
FAAM BAe-146	Rosemount Temperature Sensors (RTS)[a]	Not available

[a]Two sensors, one deiced and one non-deiced. The lower of the two temperatures was used as per PI instruction.

3. Summary of Results

Table 2 summarizes the assessed 2σ precisions, biases, and uncertainties. More detailed descriptions are provided to illustrate the process for assessment of bias and precision in Sections 4.1 and 4.2 respectively. The assessed 2σ precisions reported in Table 2 are equal to twice the highest adjusted precision value for that instrument listed in Table 4. Table 2 also reports an assessed bias (see Section 4.1 for details) that can be applied to maximize the consistency between the data sets. The assessed bias should be subtracted from the reported data to 'unify' the data sets. The assessed bias is derived from intercomparison periods only and may be extrapolated to the entire mission if one assumes instrument performance remained constant throughout the mission. The recommended 2σ uncertainty is the larger of either the uncertainty reported by the PI or the quadrature-sum of the assessed 2σ precision and assessed bias listed in Table 2.

Table 2. Recommended ICARTT Temperature measurement treatment

Aircraft/ Instrument	Reported 2σ Uncertainty (K)	Assessed 2σ Precision	Assessed Bias (K)	Recommended 2σ Uncertainty
NASA DC-8 RTS	0.5	0.26	$2.17 - 0.0093\ Temp_{DC8}$	0.5 or Quadrature Sum[a]
NOAA WP-3D RTS	0.4	0.26	$-0.35+0.0014\ Temp_{WP3D}$	0.4
FAAM BAe-146 RTS	0.4	0.22	$-1.78+0.0078\ Temp_{BAe146}$	0.4 or Quadrature Sum[b]

[a]0.5 is recommended for temperatures up to 280 K, thereafter the quadrature sum is recommended.
[b]0.4 is the recommended for temperatures up to 272 K, thereafter the quadrature sum is recommended.

Figures 1a through 1c display the precisions, biases, and recommended uncertainties for the three temperature instruments. For all aircraft measurements, the temperature uncertainty is typically driven by precision below approximately 270 K and by bias above approximately 270 K.

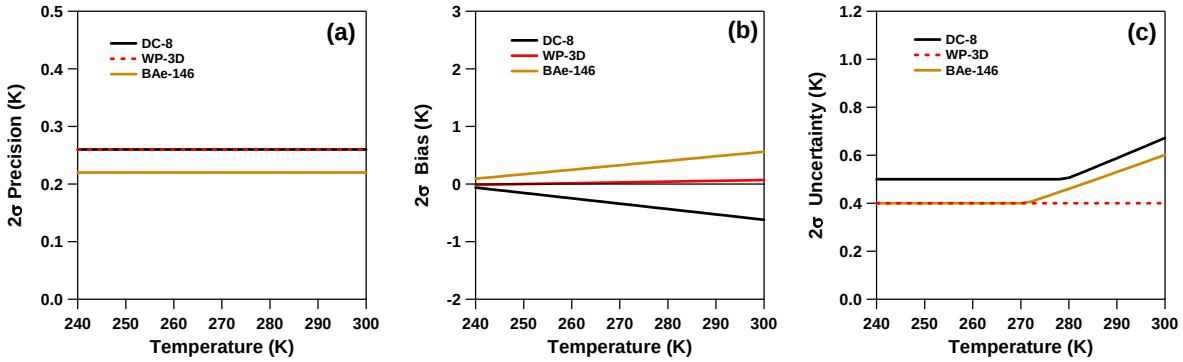

Figure 1. 2σ precision (panel a), 2σ bias (panel b), and 2σ uncertainty (panel c) for DC-8 (black), WP-3D (red), and BAe-146 (gold) as a function of temperature. Values were calculated based upon data shown in Table 2.

4. Results and Discussion

4.1 Bias Analysis

Section 3.3 in the introduction describes the process used to determine the best estimate bias. The linear relationships listed in Table 3 were derived from the regression equations found in Figures 2 through 5. The reference standard for comparison (RSC), as defined in the introduction, is constructed by averaging the NOAA WP-3D, NASA DC-8 and BAe-146 measurements. The resulting RSC can be expressed as a function of the DC-8 temperature measurement as the following:

$$RSC_{Temp} = -2.167 + 1.0093\ Temp_{DC8}$$

The RSC is then used to calculate the best estimate bias as described in Section 3.3 of the introduction. It should be noted that the initial choice of the reference instrument (DC-8) is arbitrary, and has no impact on the final recommendations. Table 3 summarizes the assessed measurement bias for each of the three ICARTT temperature measurements. Note that additional decimal places were carried in the calculations to ensure better than 0.1 K precision.

Table 3. ICARTT Temperature bias estimates

Aircraft/ Instrument	Linear Relationships[a]	Best Estimate Bias (a + b Temp) (K)
NASA DC-8 RTS	$Temp_{DC8} = 0.0 + 1.00\ Temp_{DC8}$	$2.17 - 0.0093\ Temp_{DC8}$
NOAA WP-3D RTS	$Temp_{WP3D} = -2.52 + 1.011\ Temp_{DC8}$	$-0.35 + 0.0014\ Temp_{WP3D}$
FAAM BAe-146 RTS	$Temp_{BAe146} = -3.98 + 1.017\ Temp_{DC8}$	$-1.78 + 0.0078\ Temp_{BAe146}$

[a]Derived from Figs. 3-5.

4.2 Precision Analysis

A detailed description of the precision assessment is given in Section 3.1 of the introduction. The IEIP precision, expected variability, observed variability, and the adjusted precision are summarized in Table 4. Based on the results presented in Table 4, the largest "adjusted precision" value is taken as a conservative precision estimate for each ICARTT temperature instrument and twice that value is listed in Table 2 as the assessed 2σ precision.

To minimize the effect of bias, we make corrections for bias before computing the observed variability, as the bias may have a significant impact on the observed variability. Figures 6 and 7 show the magnitude of the bias for each intercomparison. The assessed values of the observed variability are displayed in Figure 8 and 9. The final analysis results are shown in Table 2. Over 90% of the data falls within the combined recommended uncertainties for each intercomparison, which is consistent with the TAbMEP guideline for unified data sets.

Table 4. ICARTT Temperature precision (1σ) comparisons

Flight	Platform	IEIP Precision (K)	Expected Variability (K)	Observed Variability (K)	Adjusted Precision (K)
07/22	DC-8	0.13	0.16	0.13	0.13
	WP-3D	0.09			0.09
07/31	DC-8	0.09	0.13	0.18	0.13
	WP-3D	0.09			0.13
08/07	DC-8	0.12	0.15	0.12	0.12
	WP-3D	0.09			0.09
07/28	DC-8	0.12	0.14	0.11	0.12
	BAe-146	0.07			0.07

Note: Error bars are included wherever possible in the following Figures 2-5, although some may not be visible.

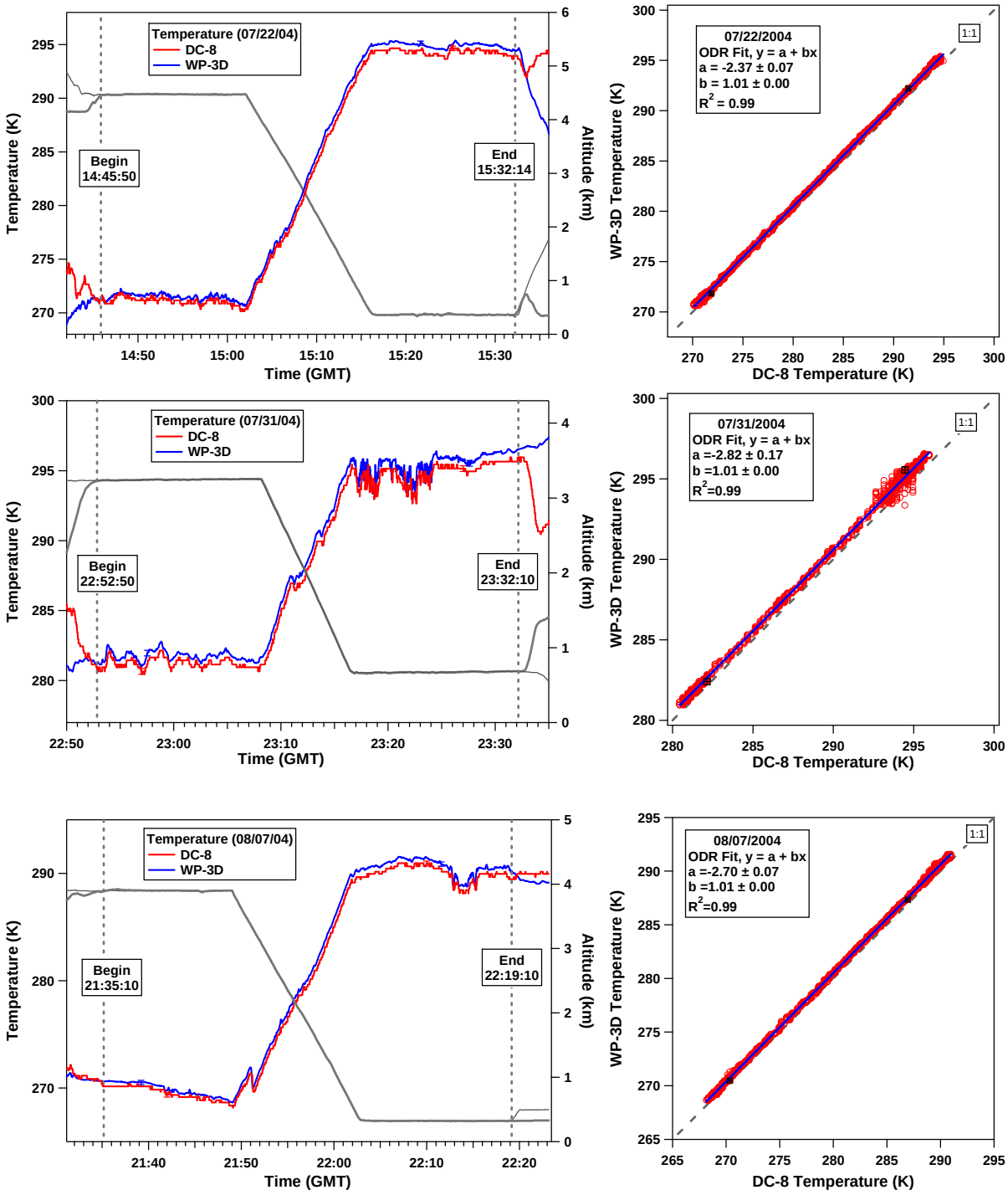

Figure 2. (left panels) Time series of temperature measurements and aircraft altitudes from two aircraft on the three intercomparison flights between the NASA DC-8 and the NOAA WP-3D. (right panels) Correlations between the temperature measurements on the two aircraft. Error bars shown depict the reported measurement uncertainties.

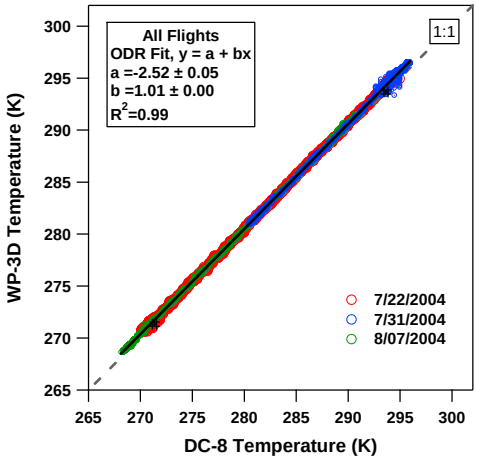

Figure 3. Correlation between the temperature measurements on the DC-8 and WP-3D for 7/22, 7/31, and 8/7 2004. Error bars shown depict the reported measurement uncertainties.

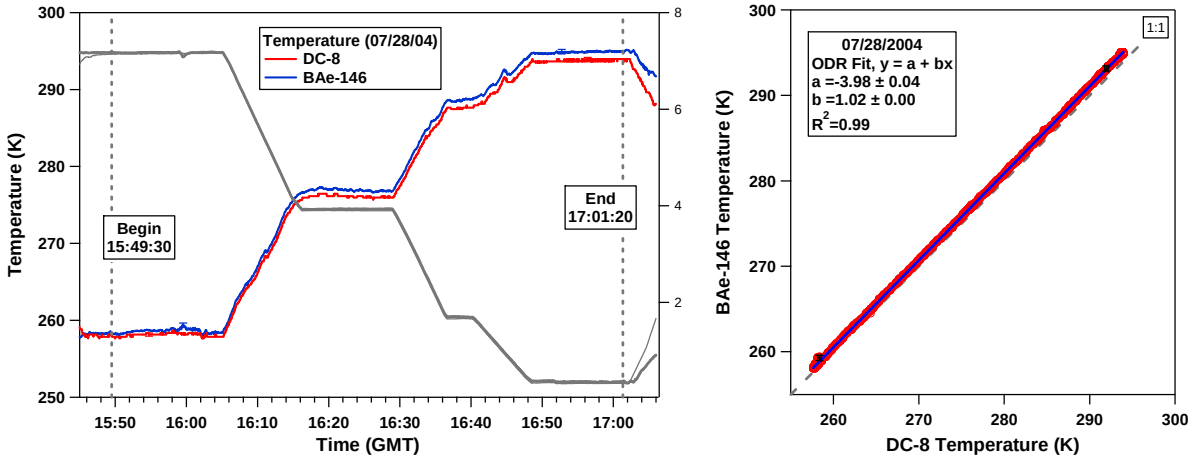

Figure 4. (left panel) Time series of temperature measurements and aircraft altitudes from the intercomparison flight between the NASA DC-8 and the FAAM BAe-146. (right panel) Correlations between the temperature measurements on the two aircraft. Error bars shown depict the reported measurement uncertainties.

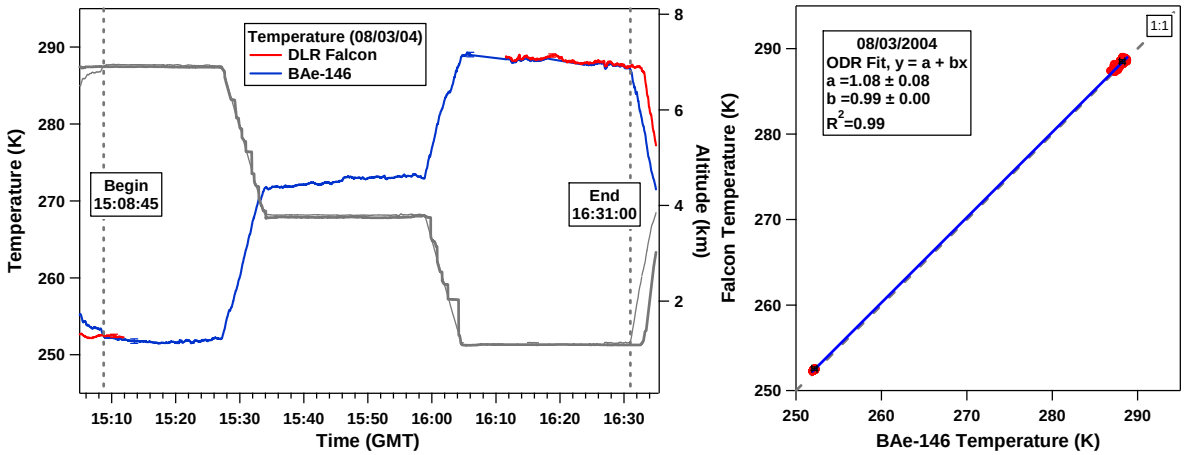

Figure 5. (left panel) Time series of temperature measurements and aircraft altitudes from the intercomparison flight between the FAAM BAe-146 and the DLR Falcon. (right panel) Correlations between the temperature measurements on the two aircraft. Error bars shown depict the reported measurement uncertainties.

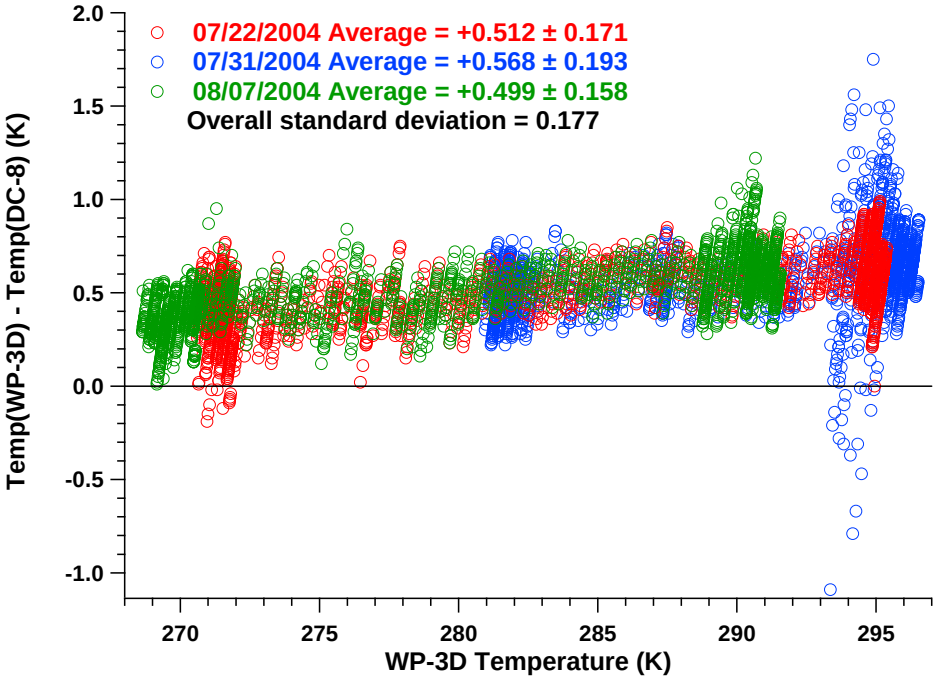

Figure 6. Difference between temperature measurements from the three DC-8/WP-3D intercomparison flights as a function of the WP-3D temperature.

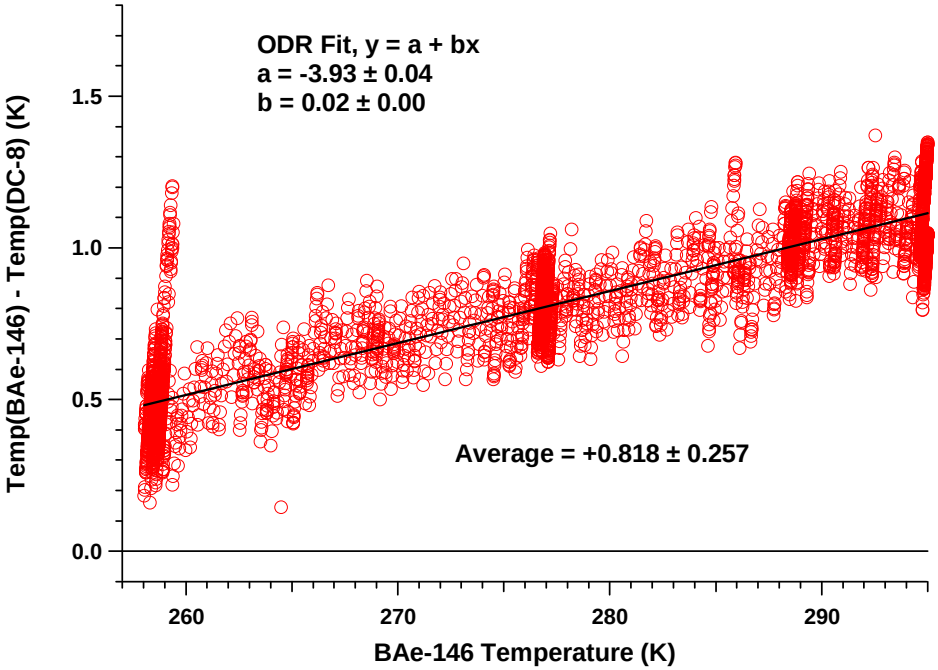

Figure 7. Difference between temperature measurements from the DC-8/BAe-146 intercomparison flight (07/28) as a function of the BAe-146 temperature.

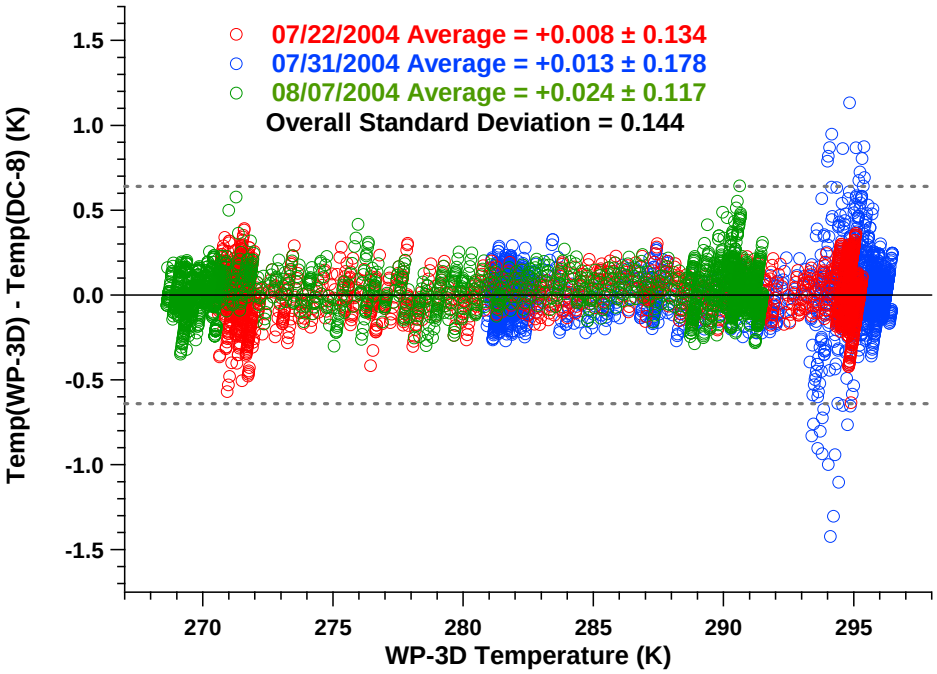

Figure 8. Difference between unified measurements of temperature from the three DC-8/WP-3D intercomparison flights as a function of the WP-3D temperature. Corrections were made to all data sets to account for bias. The dashed lines indicate the range of the results expected from the reported 2σ measurement uncertainties.

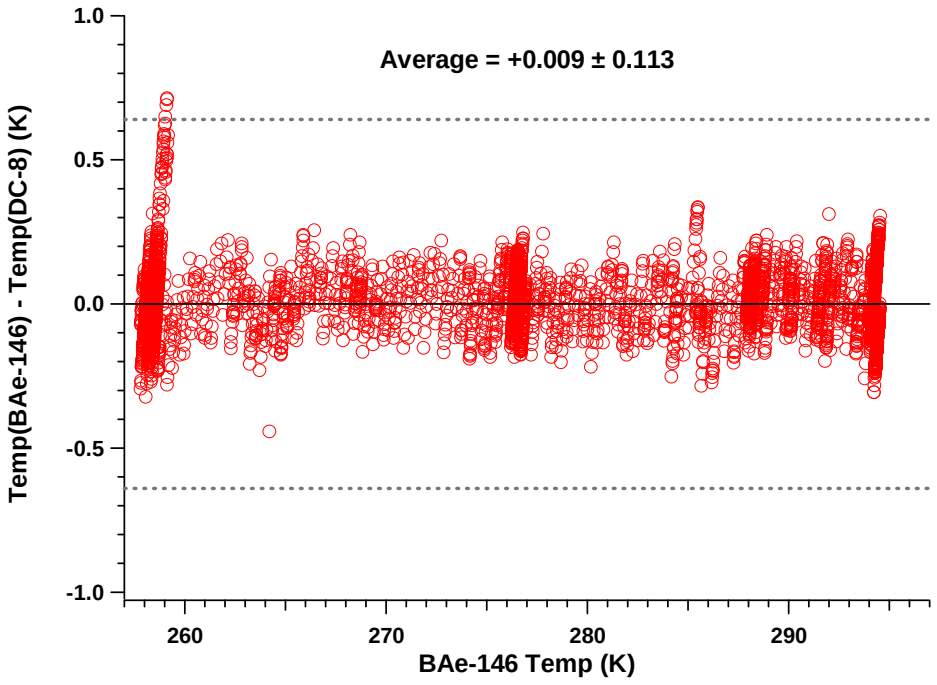

Figure 9. Difference between unified measurements of temperature from the DC-8/BAe-146 intercomparison flight (07/28) as a function of the BAe-146 temperature. Corrections were made to all data sets to account for bias. The dashed lines indicate the range of the results expected from the reported 2σ measurement uncertainties.

References

Fehsenfeld, F. C., et al. (2006), International Consortium for Atmospheric Research on Transport and Transformation (ICARTT): North America to Europe—Overview of the 2004 summer field study, *J. Geophys. Res., 111*, D23S01, doi:10.1029/2006JD007829.

Singh, H. B., et al. (2006), Overview of the summer 2004 Intercontinental Chemical Transport Experiment-North America (INTEX-A), *J. Geophys. Res., 111*, D24S01, doi:10.1029/2006JD007905.

Stickney, Truman M., et al. (1990), *Rosemount Total Temperature Sensors. Tech Rep*. 5755, Rev B, Rosemount, Inc.

TAbMEP Assessment: ICARTT H_2O Measurements

1. Introduction

Here we provide the assessment for the water (H_2O) measurements taken from three aircraft platforms during the summer 2004 ICARTT field campaign [*Fehsenfeld et al.*, 2006, *Singh et al*., 2006]. The inter-platform assessment is based upon four wing-tip-to-wing-tip intercomparison flights conducted during the field campaign. The two instruments on the DC-8 are compared using all available data from the mission. There is no H_2O data reported by the DLR Falcon due to an instrument breakdown. Recommendations provided here offer TAbMEP assessed biases for each of the measurements which can be used to unify the ICARTT H_2O data to achieve better consistency for integrated analysis. These recommendations are directly derived from the instrument performance demonstrated during the ICARTT measurement comparison exercises and are not to be extrapolated beyond this campaign.

2. ICARTT H_2O Measurements

Four different H_2O instruments were deployed on the three aircraft. Table 1 summarizes these techniques and gives references for more information.

Table 1. H_2O measurements deployed on aircraft during ICARTT

Aircraft	Instrument	Reference
NASA DC-8	Diode Laser Hygrometer (DLH)	*Diskin et al.* [2002]
NASA DC-8	Cryo-hygrometer (Cryo)	*Buck and Clark* [1991]
NOAA WP-3D	Cryo-hygrometer (Cryo)	Not available
FAAM BAe-146	Hygrometer (Hygro)	Not available

3. Summary of Results

Table 2 summarizes the assessed biases. More detailed descriptions are provided to illustrate the process for assessment of bias and precision in Sections 4.1 and 4.2 respectively. The assessed 2σ precisions normally reported in Table 2 for other species are equal to twice the highest adjusted precision value for that instrument listed in Table 5. It was not possible to derive adjusted precisions (see Section 4.2 for details) therefore no assessed 2σ precisions are reported

Table 2. Recommended ICARTT H_2O measurement treatment

Aircraft/ Instrument	Reported 2σ Uncertainty	Assessed 2σ Precision	Assessed Bias (g/kg)	Recommended 2σ Uncertainty
NASA DC-8 DLH	5%	n/a	K0=0.00732, K1=0.0259, K2=-0.0106, K3=0.000345[a]	n/a
NASA DC-8 Cryo	5%	n/a	K0=-0.00825, K1=-0.0716, K2=0.0294, K3=-0.00271, K4=0.0000777[b]	n/a
NOAA WP-3D Cryo	None	n/a	$-0.02645 - 0.01145\ H_2O_{WP3D} + 0.01134\ H_2O_{WP3D}^2$	n/a
FAAM BAe-146 Hygro	None	n/a	$0.150 - 0.0374\ H_2O_{BAe146} + 0.00163\ H_2O_{BAe146}^2$	n/a

[a] Correction in the form $K0 + K1*DLH + K2*DLH^2 + K3*DLH^3$

[b] Correction in the form $K0 + K1*Cryo + K2*Cryo^2 + K3*Cryo^3 + K4*Cryo^4$

in Table 2. Table 2 reports an assessed bias (see Section 4.1 for details) that can be applied to maximize the consistency between the data sets. The assessed bias should be subtracted from the reported data to 'unify' the data sets. For the inter-platform comparisons the assessed bias is derived from intercomparison periods only and may be extrapolated to the entire mission if one assumes instrument performance remained constant throughout the mission. No recommended 2σ uncertainty is reported since there is no assessed 2σ precision.

Figure 1 provides a quick glance of the magnitude of the bias for four H_2O instruments. The curves reflect the range of measurements for each instrument during the intercomparison period. This figure shows that the absolute bias is higher at high concentrations, however, when compared to concentration levels, the relative bias is highest at the lowest values (e.g. about 80% at 0.01 g kg^{-1} vs. about 5% at 20 g kg^{-1}). The bias correction is our best estimate of the central tendency but may not accurately reflect the bias on a point to point basis (see later discussion in Section 4.1).

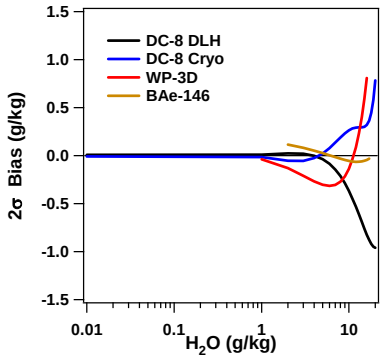

Figure 1. 2σ bias for DC-8 DLH (black), DC-8 cryo (blue), WP-3D (red), and BAe-146 (gold), as a function of H_2O level. Values were calculated based upon data shown in Table 2. The range of the curves with respect to H_2O level reflects the range of measurements of each instrument during the intercomparison period.

4. Results and Discussion

4.1 Bias Analysis

Section 3.3 in the introduction describes the process used to determine the best estimated bias. Figures 2-6 show the correlation and time series plots for each intercomparison included in this assessment. For H_2O measurements, the DC-8 DLH versus DC-8 Cryo intercomparison is taken as the standard for all H_2O analysis since both instruments are well maintained and calibrated, and the comparison was encompassed the largest range of water mixing ratio values. The standard method for determining bias as described in the introduction is not applicable for H_2O. Because the performance of the two instruments involved have very different dependence on ambient conditions, the Reference Standard for Comparison (RSC) is not taken as an average of the two. Rather it emphasizes the better performing instrument while de-emphasizes the other for a given range of conditions. The ICARTT field campaign was the first time DLH reported data for very high concentrations (> 10 g/kg) , and was thought to have some accuracy issues in that range. Therefore, the cryo-hygrometer is weighted more heavily at high concentrations. The cryo-hygrometer technique is subject to difficulties at low dew point (e.g., water/ice ambiguity, see discussion in section 4.1), thus DLH is weighted more heavily in this case. The two

instruments are weighted equally in the intermediate range, where both are known to perform well. The two instruments are weighted equally in the intermediate range, where both are known to perform well. The resulting RSC is defined as follows:

$$RSC_{H2O} = \begin{cases} \dfrac{DLH + 2\,Cryo_{DC8}}{3} & Cryo_{DC8} > 10\ g/kg \\ \dfrac{2\,DLH + Cryo_{DC8}}{3} & \text{Dew point} < -15^{\circ}C \\ \dfrac{DLH + Cryo_{DC8}}{2} & \text{All other points} \end{cases}$$

Unlike the other species, the RSC for H_2O can be considered as the better measure of the average H_2O concentration sampled by NASA DC-8 aircraft, not necessarily on a point-to-point basis. This reflects that the RSC is derived by combining measurements of differing temporal response characteristics. Using the RSC, the best representation of the bias can be determined through regression analysis as shown in Figures 8-11. This is believed to be an effective way to determine the mean bias between the measurements.

To quantify the bias for each of the four ICARTT H_2O measurements, the difference between the individual measurements and the RSC is plotted against the measurement mixing ratio in Figures 8-11. For the all instruments, polynomials are used as they can better represent the best estimate biases (black lines), over the largest concentration range. The equations for these lines are the bias and are reported in Table 3 as the best estimate bias. It is noted here that Figures 8 – 11 show large variability for all four instruments. For example, the BAe-146 bias scatter is so large that one cannot help wondering the meaning of the bias correction, other than it may better reflect the central tendency. In the case of WP-3D in Figure 10, the fit could be quite different if the data from 07/22/2004 (red) is not included. However, there is no reason for excluding it. The panel strongly recommends that the bias estimates be treated as the correction for central tendency, but may not effectively remove the potential bias on a point to point basis.

Table 3. ICARTT H_2O bias estimates

Aircraft/ Instrument	Linear Relationships	Best Estimate Bias (g/kg)
NASA DC-8 DLH	n/a	K0=0.00732, K1=0.0259, K2=-0.0106, K3=0.000345[a]
NASA DC-8 Cryo	n/a	K0=-0.00825, K1=-0.0716, K2=0.0294, K3=-0.00271, K4=0.0000777[b]
NOAA WP-3D Cryo	n/a	$-0.02645 - 0.01145\ H_2O_{WP3D} + 0.01134\ H_2O_{WP3D}^2$
FAAM BAe-146 Hygro	n/a	$0.150 - 0.0374\ H_2O_{BAe} + 0.00163\ H_2O_{BAe}^2$

[a] $K0+K1*DLH+K2*DLH^2+K3*DLH^3$

[b] $K0+K1*Cryo+K2*Cryo^2+K3*Cryo^3+K4*Cryo^4$

To better illustrate the bias variability and the complexity of the comparison, Figure 12 (a - d) shows four cases of ICARTT comparisons between DC-8 DLH and cryo ranging from boundary layer to upper free troposphere. Figure 12 (a - d) depicts DLH (red) and cryo (blue) mixing

ratios (g/kg) during level flight leg segments in the lower panel and the residual (DLH – cryo, green) in the upper panel, both as functions of time. In general, at low H_2O concentrations, the residual is fairly stable, though slightly positive (upper panel, Figure 12d), ranging between 0.04 and 0.08 g/kg. At higher H_2O the residual is larger and varies considerably more (upper panel, Figure 12a), ranging between -1.6 and -0.8 g/kg. This systematic shift in the H_2O data is captured by the best estimate bias shown in Table 3.

In addition to this systematic shift, there are other systematic differences at times not easily characterized by the estimated bias which limit the effectiveness of the bias correction based on all data. Complications can occur when there are abrupt changes in H_2O levels. This is illustrated in Figure 12b with H_2O levels that are highly variable. The residual (upper panel) has a fairly stable baseline near zero, but there are frequent and significant deviations from the baseline. One explanation for the deviations is a cryo time response lag relative to DLH. Several examples can be seen at ~19:30, 19:38, and between 19:35 and 19:36. In addition, at these times (as well as at 19:23) cryo overshoots the DLH data, resulting in the previously mentioned spikes in the residual as well as the spike at 19:23. Finally, at about 19:32 DLH and cryo are nearly anti-correlated. The time lag response issue is also present, though less dramatically, in Figure 12d between 19:31 and 19:32. Another complicating factor to the bias correction is cryo having a slower response to changes in H_2O relative to DLH. Though difficult to discern in these plots, it is noticeable when regions are expanded horizontally (e.g. Figure 12b between 19:39:30 and 19:40:00 and between 19:41:00 and 19:41:30). This detail is present when more subtle changes in H_2O occur as well. In Figure 12a the spikes in the residual at ~14:49, 14:52, 14:53, and between 14:59 and 15:00 are the result of additional structure in the DLH data that is not present in the cryo data. Finally, even when the residual is relatively constant (Figure 12c) and near zero for much of the level flight leg, there are still unexplained deviations, e.g., -0.5 g/kg at about 17:14:00. These complicating factors combine to limit our ability to effectively remove bias from the data on a point by point basis.

Another way to characterize the effectiveness of the bias correction is to test if the bias corrected relative residual, as shown in Figure 13, falls within PI reported uncertainties. In this case, both DC-8 DLH and DC-8 cryo data were corrected using the best estimate bias listed in Table 3. The overall average is <0.1% and standard deviation is 12.8%. As shown in Figure 13, however, the difference between the bias-corrected DC-8 DLH and cryo data remains to be a finite positive or negative value at various RSC values and appears to be a function of the RSC. This trend can be characterized by dividing mixing ratio levels into three regimes, i.e., less than 0.2 g/kg, between 0.2 and 1 g/kg, and above 1 g/kg, yielding different values for the standard deviation (see Table 4). Since there is substantial variability in the standard deviation after bias correction, it is likely that the bias cannot be systematically removed and no value for observed variability can be given in Table 5.

Table 4. DC-8 DLH vs. Cryo

RSC	< 0.2	0.2 ≤ RSC < 1	≥ 1
Observed Variability	-4.0 ± 16.8%	10.8 ± 10.5%	-2.8 ± 8.15%

This uncertainty is also affected by ambiguity between supercooled water and ice in the cryo measurements. This ambiguity exists for dew points between 0°C and -40°C when the cryo instrument cannot distinguish between liquid water and ice on its detection mirror. To illustrate

this ambiguity, Figure 14 shows DC-8 DLH and DC-8 cryo percent residual as a function of dew point and RSC mixing ratio (g/kg). For dew points between 0°C and -40°C the spread in the data changes (greater spread at colder dew points) as a result of the ambiguity. The upper bound of the uncertainty, shown as a black line, ranges from 0 to 40% depending on dew point. Without a systematic way to incorporate this into the bias equation, it contributes to the larger than expected uncertainty.

4.2 Precision Analysis

A detailed description of the precision assessment is given in Section 3.1 of the introduction. The IEIP precision and expected variability are summarized in Table 5. Observed variability and adjusted precision are also normally presented in Table 5, however in this case the bias between the measurements cannot be effectively removed by our procedures and the magnitude of the remaining bias may be comparable to the precision. Therefore, the observed variability analysis is unlikely to provide a reasonable assessment of the long-term precision as it was intended to. Without an observed variability, adjusted precision cannot be calculated.

IEIP procedures were applied to both the DC-8 DLH and cryo data from the entire INTEX-NA period. The DC-8 cryo data presented challenges in deriving a precision estimate due to the slow response time of the instrument. In order to derive an estimate, longer time intervals were needed (possible for entire INTEX-NA time period, but not for individual intercomparison periods). Because the DLH had a better precision than cryo and the cryo data was not ideal for this analysis, DLH was chosen as the basis for comparison with other instruments and only DLH IEIP precisions are listed for the individual intercomparison periods in Table 5.

Table 5. ICARTT H_2O precision (1σ) comparisons

Flight	Platform	IEIP Precision	Expected Variability	Observed Variability	Adjusted Precision
07/22	DC-8 DLH	1.5%	2.3%		
	WP-3D	1.8%			
07/31	DC-8 DLH	1.5%	2.1%		
	WP-3D	1.5%			
08/07	DC-8 DLH	2.4%	3.1%		
	WP-3D	2.0%			
07/28	DC-8 DLH	2.5%	7.4%		
	BAe-146	7.0%			
All flights	DC-8 DLH	1.0%	2.1%		
	DC-8 Cryo	1.8%			

4.3 Conversion Equations

The following equations were used to convert dew/frost point (T_d in K) to mixing ratio (g/kg).

$$e_w = 10^{[23.5518-(2937.4/T_d)]} \times T_d{}^{(-4.9283)} \qquad (4.3.1)$$

$$e_i = 10^{[11.4816-(2705.21/T_d)]} \times T_d^{(-0.32286)} \quad (4.3.2)$$

e_w = partial pressure of water vapor over water (mb)

e_i = partial pressure of water vapor over ice (mb)

$$q\ (g/kg) = \frac{622 \times e_{w,i}}{P_s - (0.378 \times e_{w,i})} \quad (4.3.3)$$

q = mixing ratio (g/kg)
P_S = static pressure (mb)

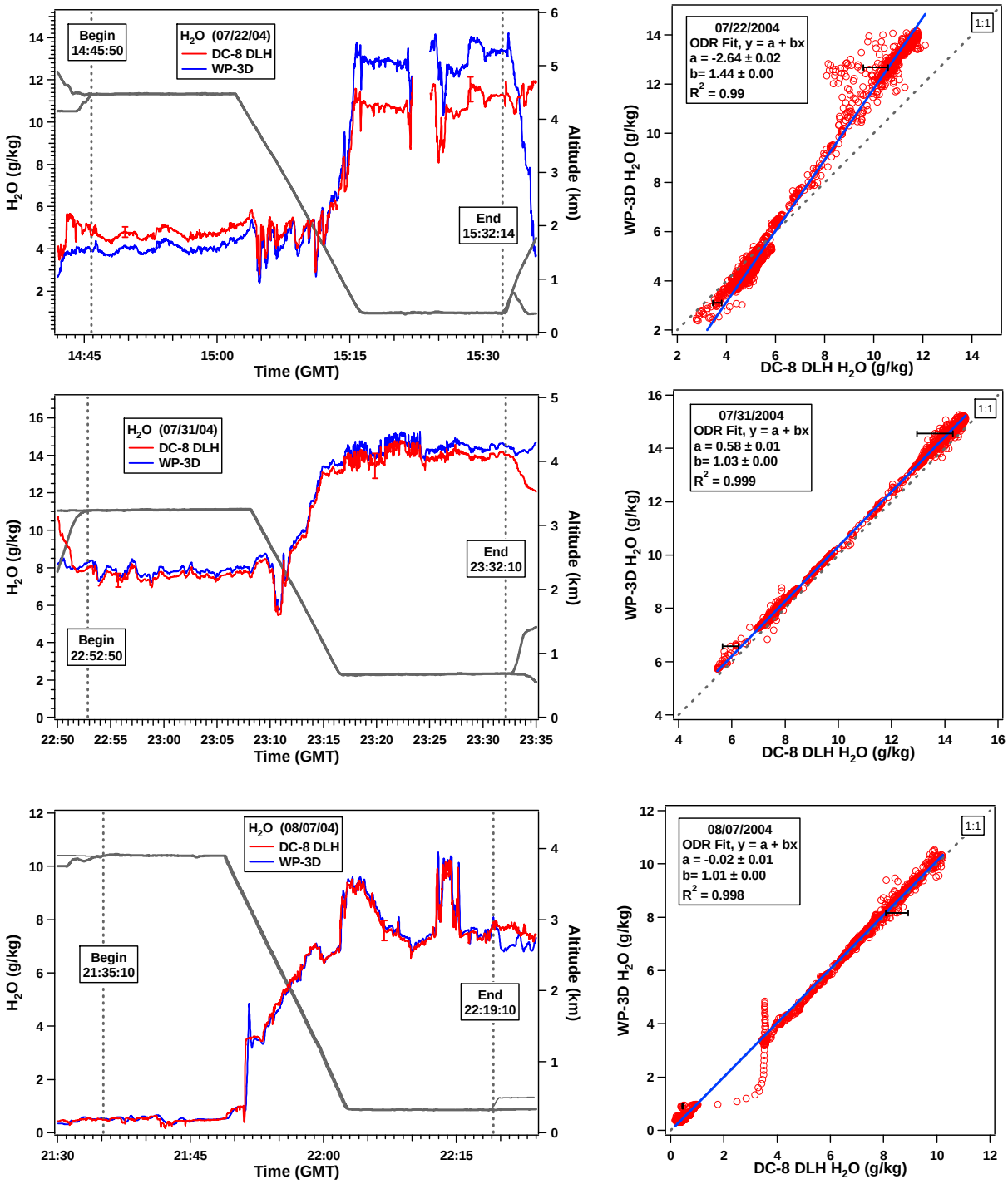

Figure 2. (left panels) Time series of DC-8 DLH and WP-3D cryo H_2O measurements and aircraft altitudes on the three intercomparison flights. (right panels) Correlations between the H_2O measurements on the two aircraft. Error bars shown depict the reported measurement uncertainties.

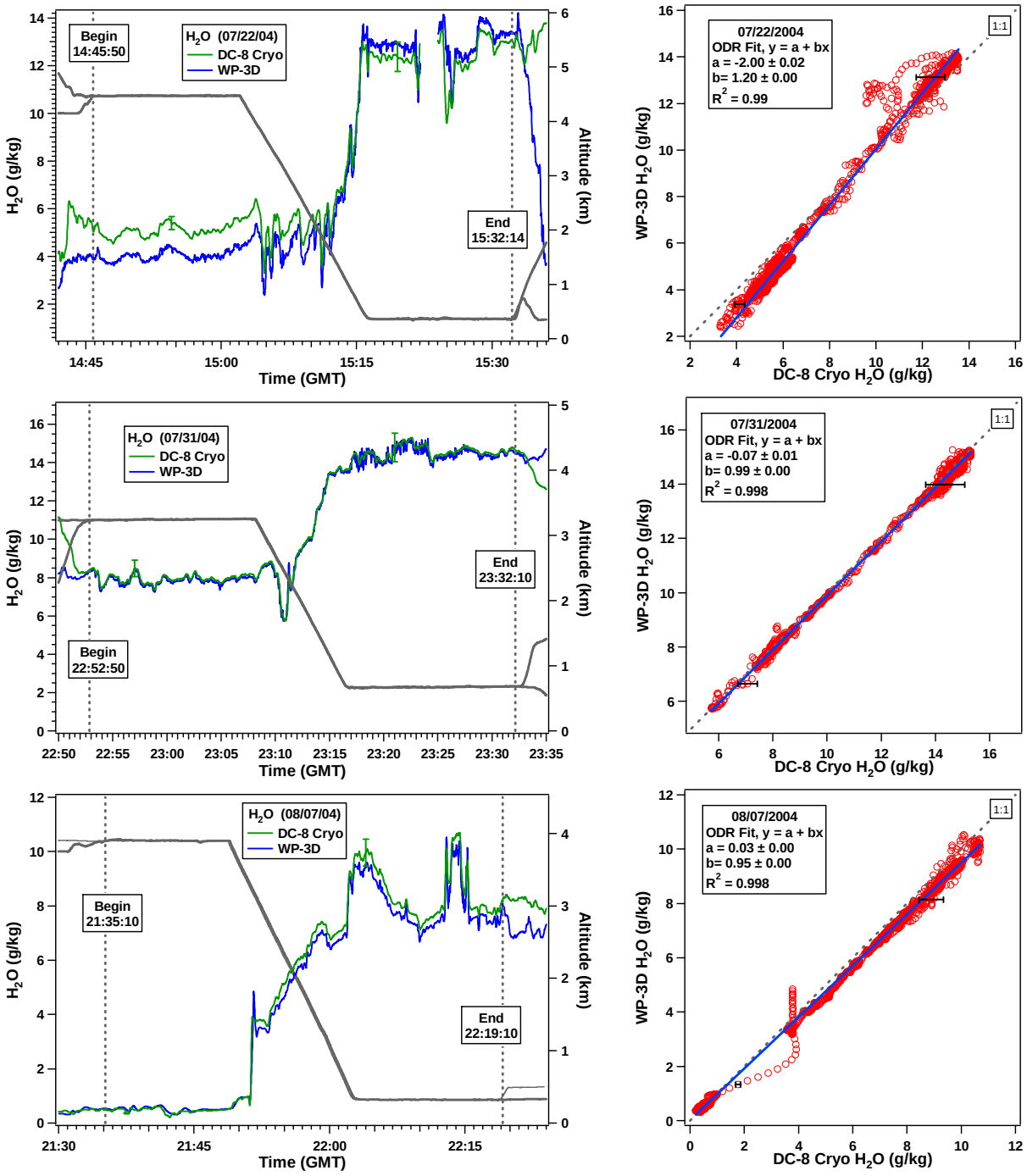

Figure 3. (left panels) Time series of DC-8 cryo and WP-3D cryo H_2O measurements and aircraft altitudes on the three intercomparison flights. (right panels) Correlations between the H_2O measurements on the two aircraft. Error bars shown depict the reported measurement uncertainties.

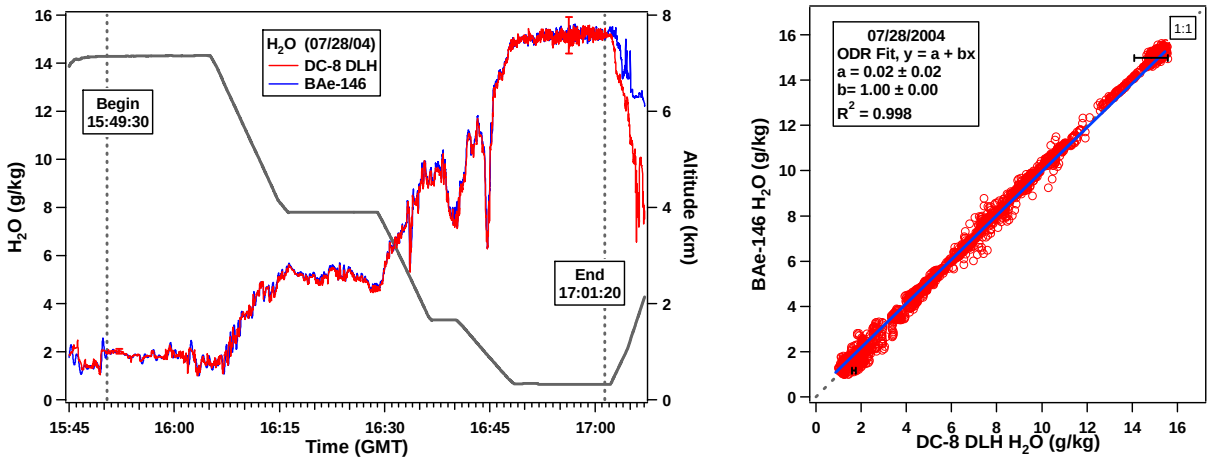

Figure 4. (left panel) Time series of H_2O measurements and aircraft altitudes from the intercomparison flight between the NASA DC-8 DLH and the FAAM BAe-146 hygro. (right panel) Correlations between the H_2O measurements on the two aircraft. Error bars shown depict the reported measurement uncertainties.

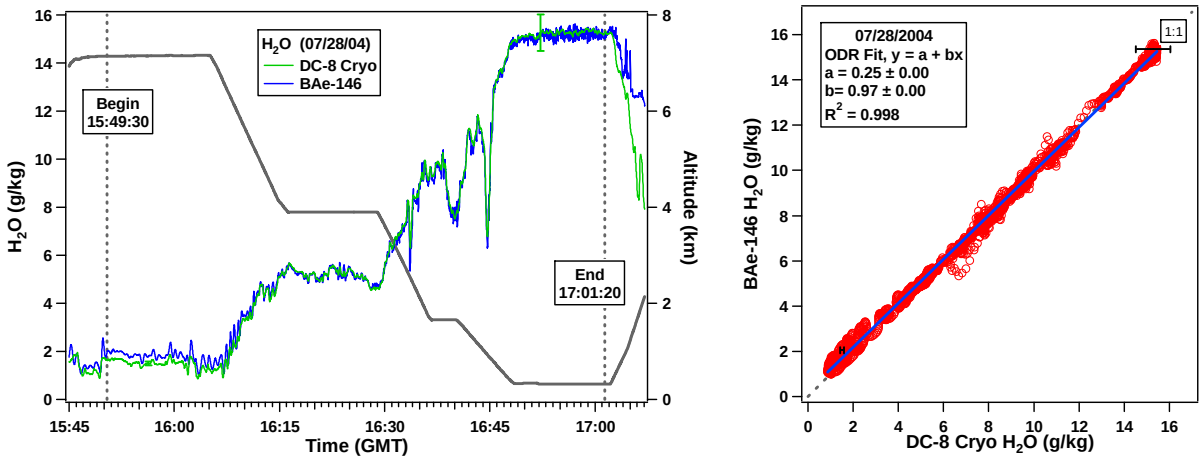

Figure 5. (left panel) Time series of H_2O measurements and aircraft altitudes from the intercomparison flight between the NASA DC-8 cryo and the FAAM BAe-146 hygro. (right panel) Correlations between the H_2O measurements on the two aircraft. Error bars shown depict the reported measurement uncertainties.

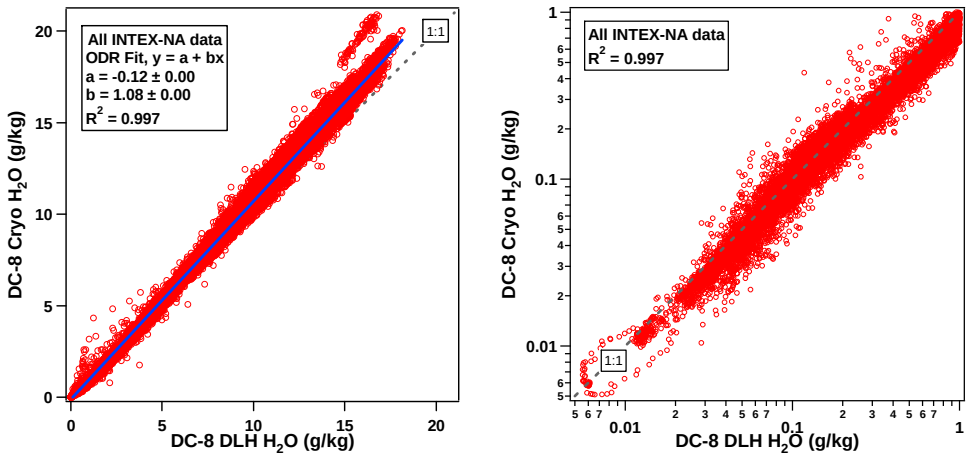

Figure 6. Correlation of DC-8 DLH and Cryo H_2O measurements for all INTEX-NA flights.

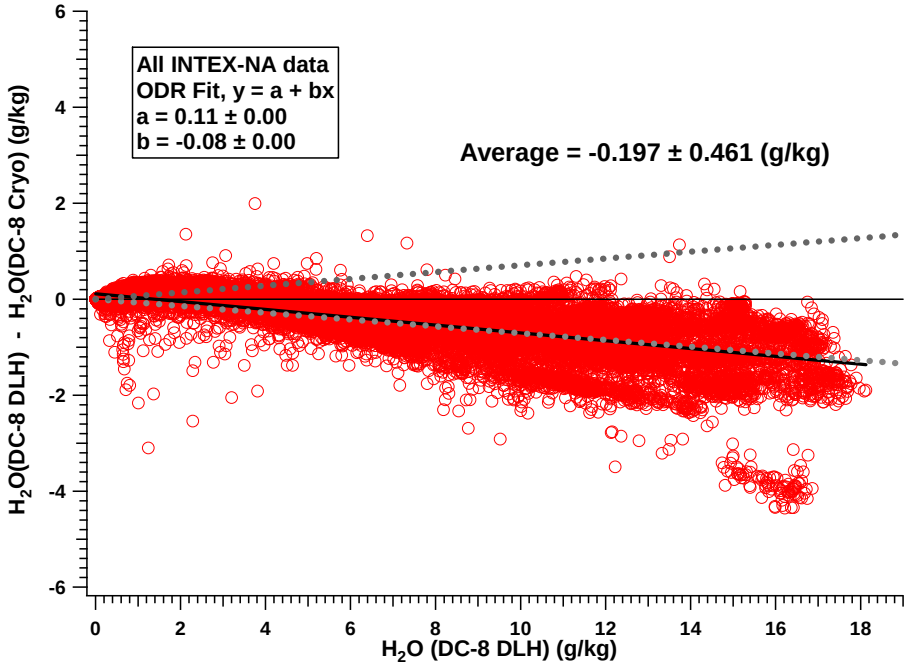

Figure 7. Difference between H_2O measurements from DC-8 DLH and DC-8 cryo for all intercomparison flights as a function of DC-8 DLH H_2O. The dashed lines indicate the range of the results expected from the reported 2σ measurement uncertainties.

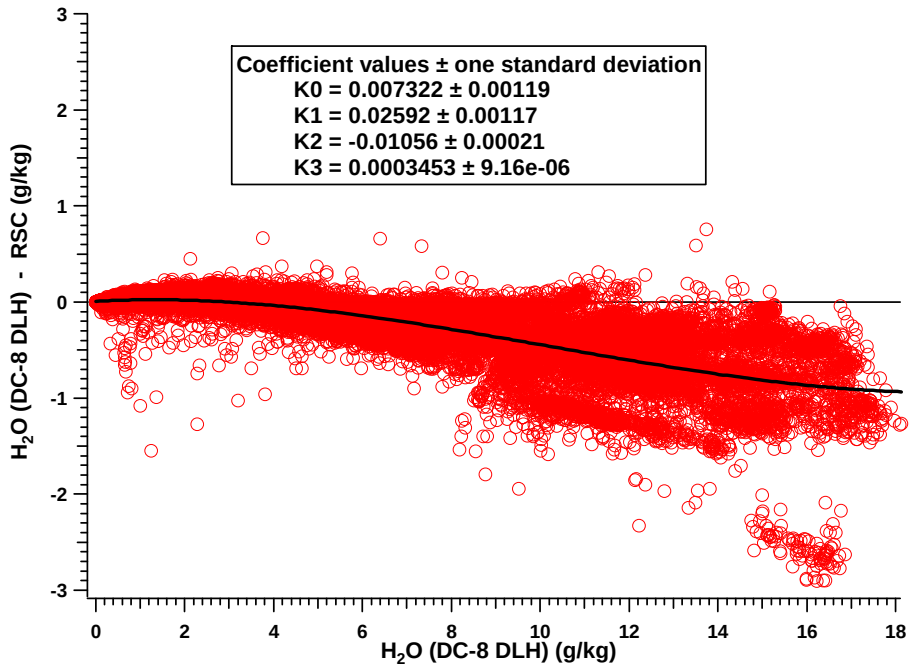

Figure 8. Difference between H_2O measurements from DC-8 DLH and RSC for all INTEX-NA flights as a function of DLH.

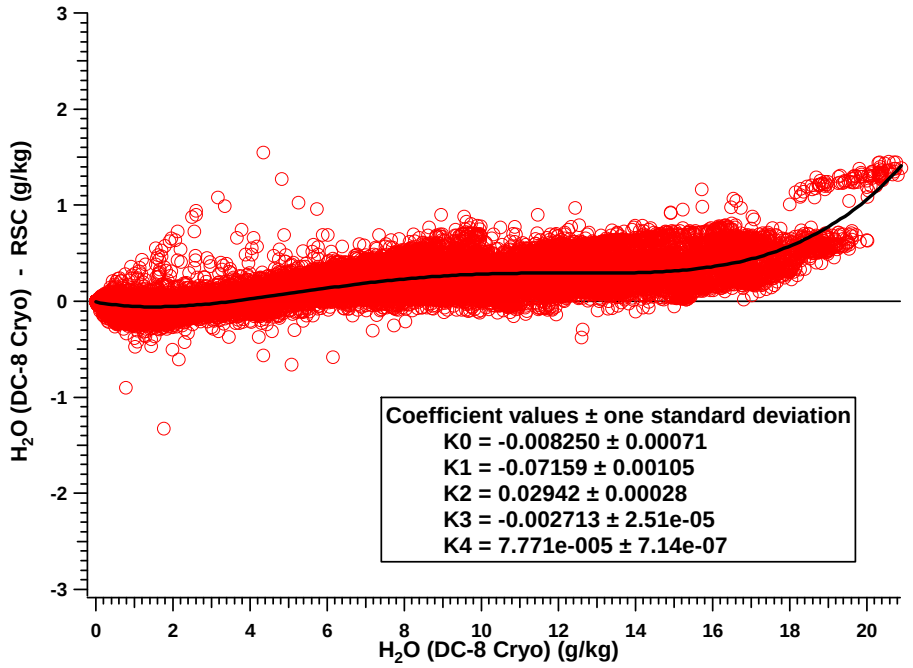

Figure 9. Difference between H_2O measurements from DC-8 cryo and RSC for all INTEX-NA flights as a function of DC-8 cryo.

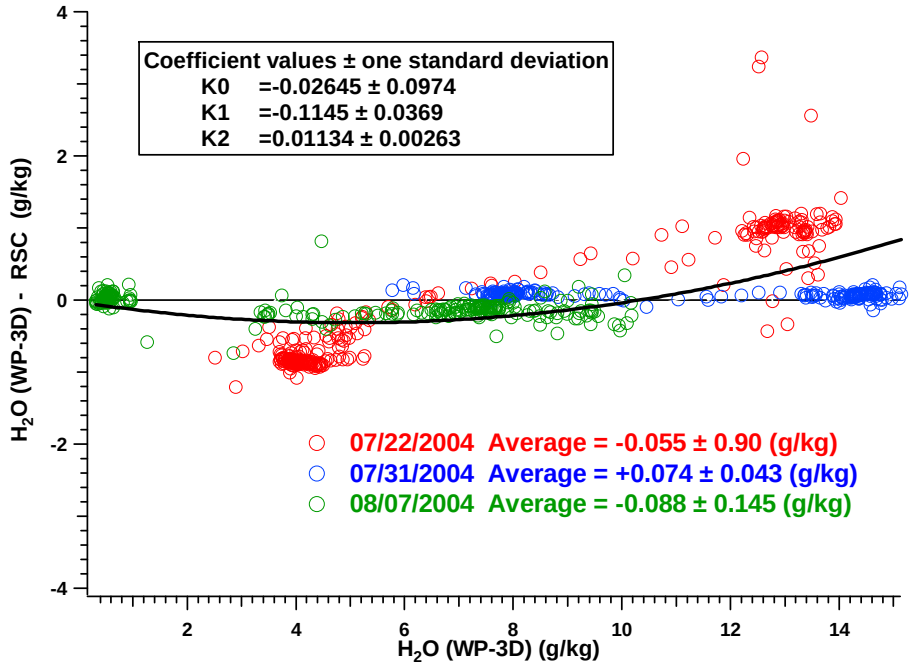

Figure 10. Difference between H_2O measurements from three DC-8/WP-3D intercomparison flights as a function of WP-3D H_2O. No uncertainty bounds are included because WP-3D did not report uncertainty.

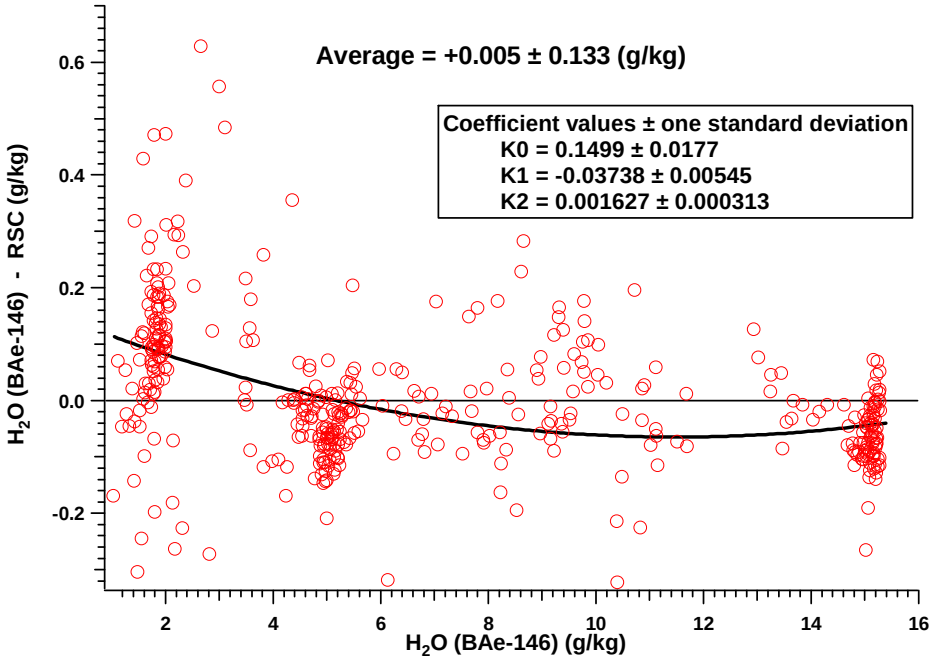

Figure 11. Difference between H_2O measurements from the DC-8/BAe-146 intercomparison flight (07/28) as a function of the BAe-146 H_2O. No uncertainty bounds are included because BAe-146 did not report uncertainty.

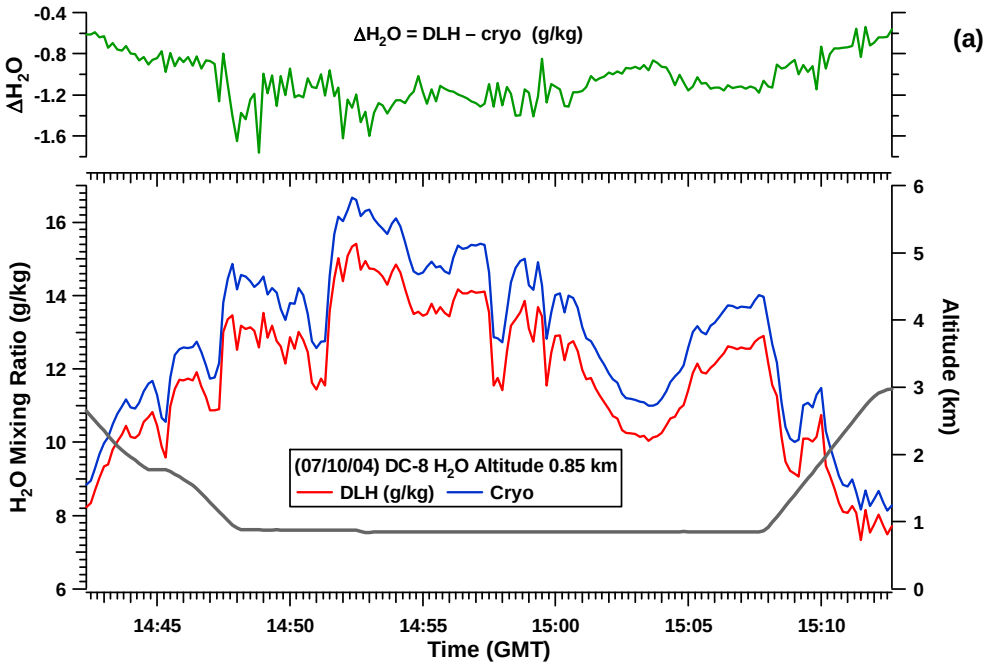
(a)
ΔH2O = DLH – cryo (g/kg)
ΔH2O
-0.4
-0.8
-1.2
-1.6
H2O Mixing Ratio (g/kg)
16
14
12
10
8
6
Altitude (km)
6
5
4
3
2
1
0
(07/10/04) DC-8 H2O Altitude 0.85 km
DLH (g/kg)
Cryo
14:45
14:50
14:55
15:00
15:05
15:10
Time (GMT)

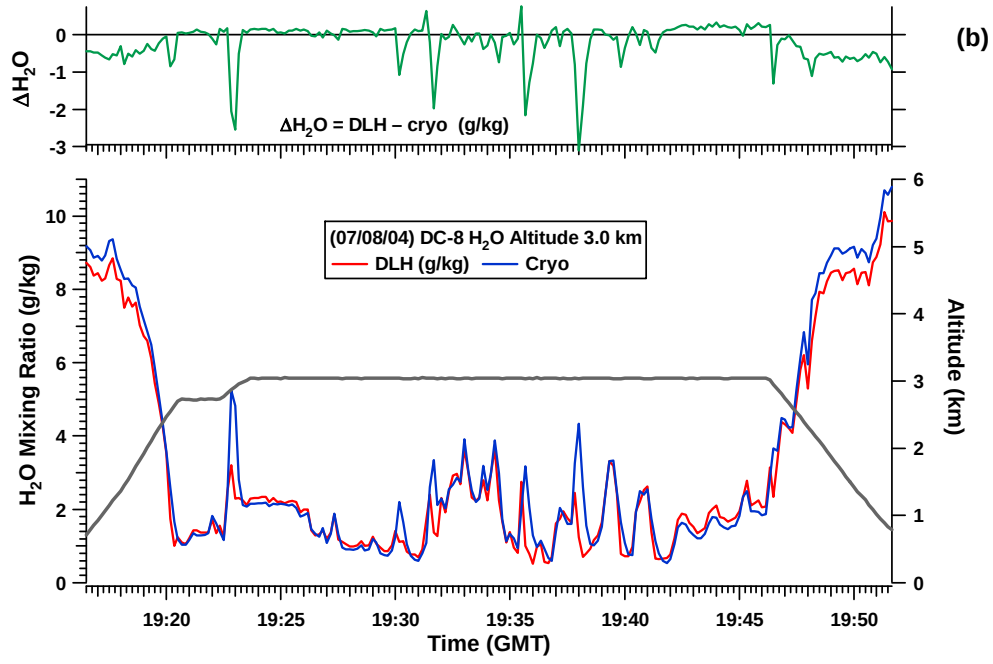
(b)
ΔH2O
0
-1
-2
-3
ΔH2O = DLH – cryo (g/kg)
H2O Mixing Ratio (g/kg)
10
8
6
4
2
0
Altitude (km)
6
5
4
3
2
1
0
(07/08/04) DC-8 H2O Altitude 3.0 km
DLH (g/kg)
Cryo
19:20
19:25
19:30
19:35
19:40
19:45
19:50
Time (GMT)

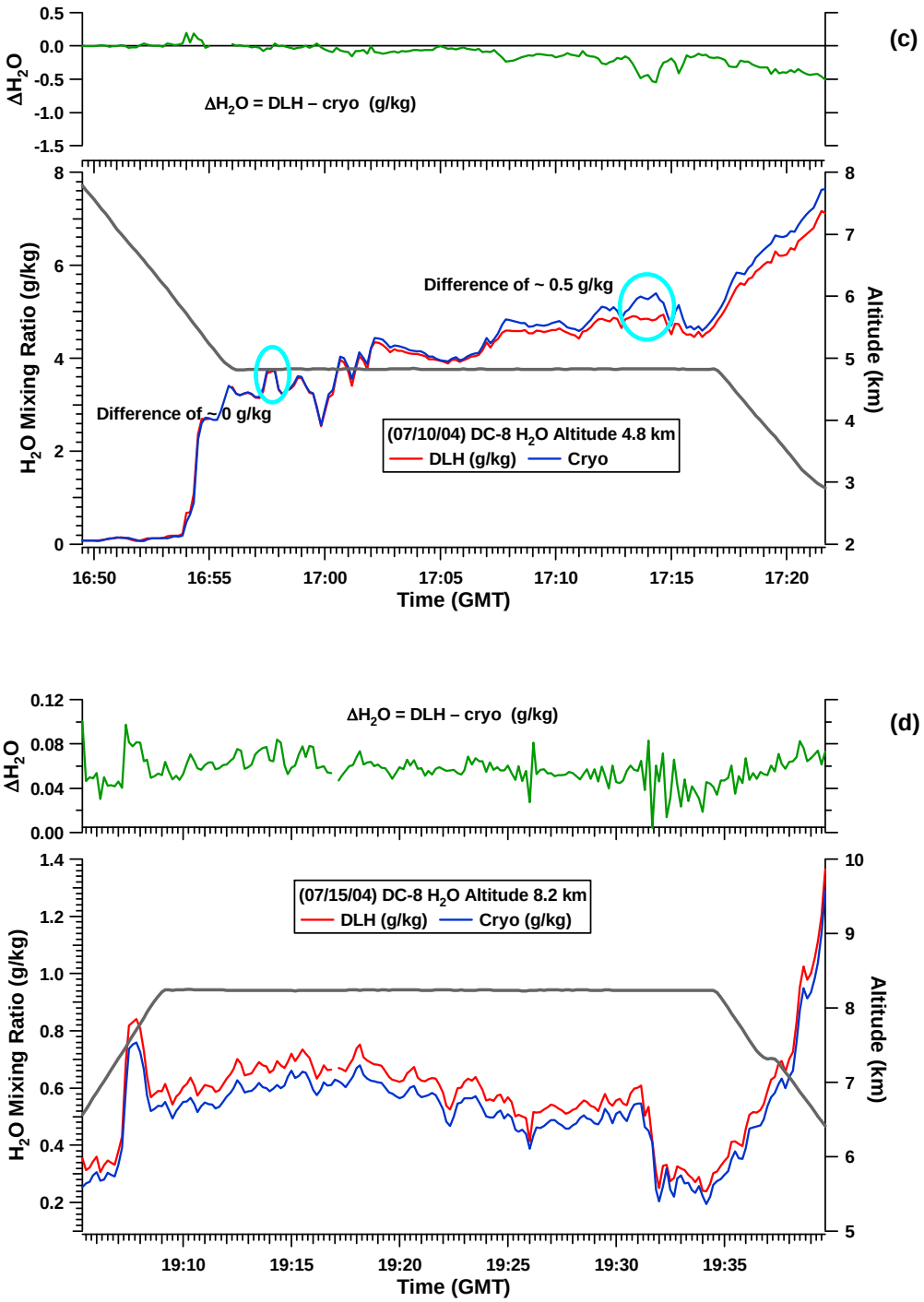

Figure 12. DC-8 DLH, cryo, and dew point during four level leg segments during flights on July 08 (b), July 10 (a and c), and July 15, 2004 (d).

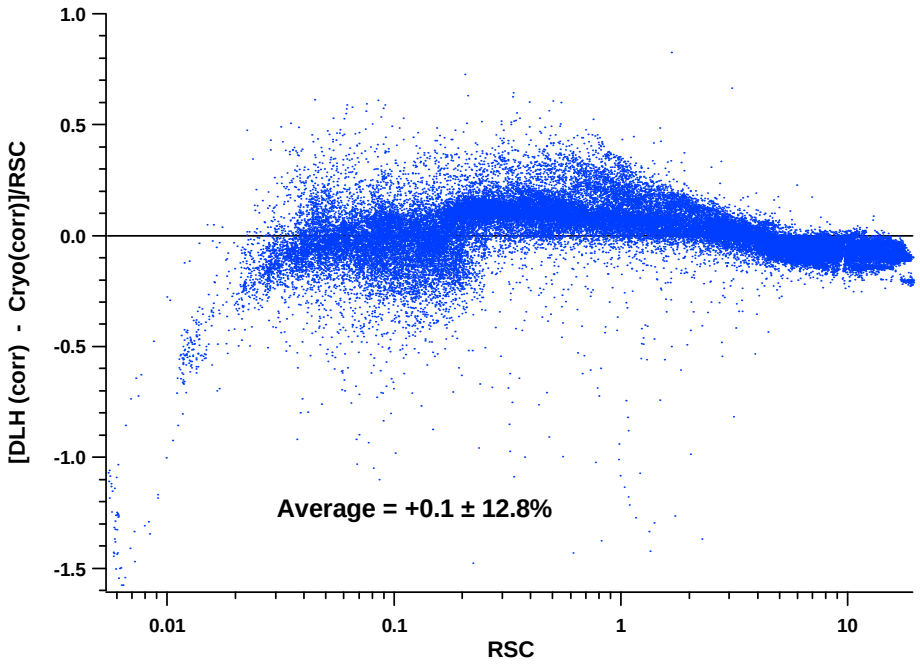

Figure 13. Relative difference between bias corrected H_2O measurements from DC-8 DLH and DC-8 Cryo for all INTEX-NA flights as a function of RSC.

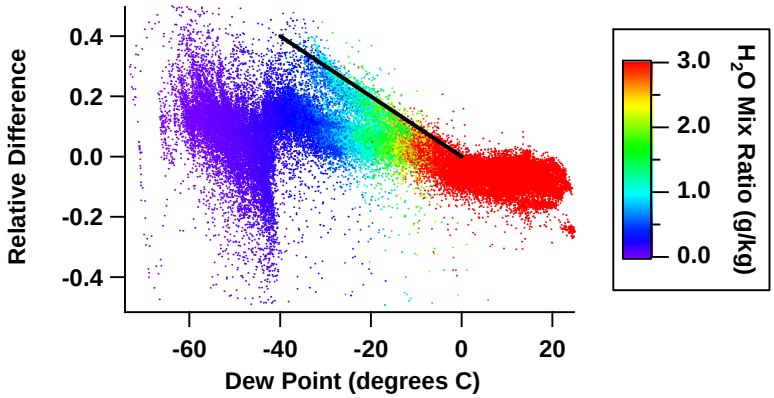

Figure 14. Relative difference between DC-8 DLH and cryo as a function of dew point.

References

Buck, A. L. and R. Clark, "Development of a Cryogenic Dew/Frost Point Hygrometer," Proc. American Meteorological Society, Jan 1991.

Diskin, G. S., et al. (2002), Open-Path Airborne Tunable Diode Laser Hygrometer, *Diode Lasers and Applications in Atmospheric Sensing*, SPIE Proceedings 4817, A. Fried, editor, 196-204.

Fehsenfeld, F. C., et al. (2006), International Consortium for Atmospheric Research on Transport and Transformation (ICARTT): North America to Europe—Overview of the 2004 summer field study, *J. Geophys. Res., 111*, D23S01, doi:10.1029/2006JD007829.

Singh, H. B., et al. (2006), Overview of the summer 2004 Intercontinental Chemical Transport Experiment-North America (INTEX-A), *J. Geophys. Res., 111*, D24S01, doi:10.1029/2006JD007905.

TAbMEP Assessment: ICARTT Wind Direction Measurements

1. Introduction

Here we provide the assessment for the wind direction measurements taken from two aircraft platforms during the summer 2004 ICARTT field campaign [*Fehsenfeld et al.*, 2006, *Singh et al*., 2006]. This assessment is based upon the two wing-tip-to-wing-tip intercomparison flights conducted during the field campaign. Recommendations provided here offer TAbMEP assessed uncertainties for each of the measurements and a systematic approach to unifying the ICARTT wind direction data for any integrated analysis. These recommendations are directly derived from the instrument performance demonstrated during the ICARTT measurement comparison exercises and are not to be extrapolated beyond this campaign.

2. ICARTT Wind Direction Measurements

Due to the data reporting problems for BAe-146, the ICARTT wind direction intercomparison was limited to between the DC-8 and WP-3D. Table 1 summarizes the measurement techniques and gives references for more information. A brief description of the DC-8 measurement is also given in the Wind Direction Appendix.

Table 1. Wind Direction measurements deployed on aircraft during ICARTT

Aircraft	Instrument	Reference
NASA DC-8	Delco Carousel IV-3 Inertial Navigation System (INS)	*Delco Electronics* [1977]
NOAA WP-3D	Not Available	Not Available

3. Summary of Results

Table 2 summarizes the assessed 2σ precisions, biases, and uncertainties. More detailed descriptions are provided to illustrate the process for assessment of bias and precision in Sections 4.1 and 4.2 respectively. The assessed 2σ precisions reported in Table 2 are equal to twice the highest adjusted precision value for that instrument listed in Table 4. Table 2 also reports an assessed bias (see Section 4.1 for details) that can be applied to maximize the consistency between the data sets. The assessed bias should be subtracted from the reported data to 'unify' the data sets. The assessed bias is derived from intercomparison periods only and may be extrapolated to the entire mission if one assumes instrument performance remained constant throughout the mission. The recommended 2σ uncertainty is the larger of either the uncertainty reported by the PI or the quadrature-sum of the assessed 2σ precision and assessed bias listed in Table 2. It is noted here that the actual wind direction measurement uncertainty varies with the relative direction of the aircraft heading and wind direction. The error tends to maximize when the wind direction and aircraft heading are parallel and tends to minimize when the wind direction and aircraft heading are orthogonal (see Wind Direction Appendix for further details).

Table 2. Recommended ICARTT Wind Direction measurement treatment

Aircraft/ Instrument	Reported 2σ Uncertainty	Assessed 2σ Precision	Assessed Bias (deg)	Recommended 2σ Uncertainty
NASA DC-8 INS	N/A	5.2%	$3.21 - 0.015\text{WindDir}_{DC8}$	Quadrature Sum
NOAA WP-3D Not Available	N/A	8.6%	$-3.12 + 0.015\text{WindDir}_{WP3D}$	Quadrature Sum

Figures 1a through 1c display the precisions, biases, and recommended uncertainties for the two

wind direction instruments. For all aircraft measurements, the wind direction uncertainty is driven by the precision.

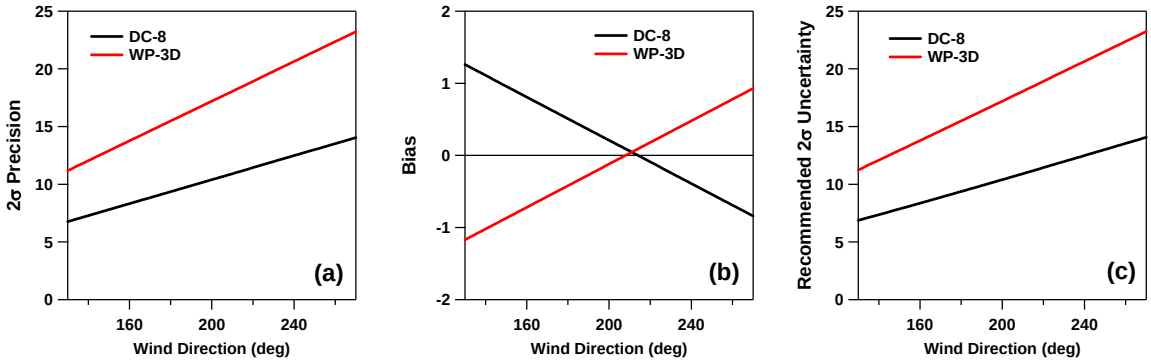

Figure 1. 2σ precision (panel a), bias (panel b), and 2σ uncertainty (panel c) for DC-8 (black) and WP-3D (red) as a function of wind direction. Values were calculated based upon data shown in Table 2.

4. Results and Discussion

4.1 Bias Analysis

Section 3.3 in the introduction describes the process used to determine the best estimate bias. The linear relationships listed in Table 3 were derived from the regression equations found in Figure 3. Note that data from the 8/07/2004 intercomparison flight is not included in this report because the PI identified measurement problems on the DC-8. The reference standard for comparison (RSC), as defined in the introduction, is constructed by averaging the NOAA WP-3D and NASA DC-8. The resulting RSC can be expressed as a function of the DC-8 wind direction measurement as the following:

$$RSC_{WindDir} = -3.21 + 1.015WindDir_{DC8}$$

The RSC is then used to calculate the best estimate bias as described in Section 3.3 of the introduction. It should be noted that the initial choice of the reference instrument (DC-8) is arbitrary, and has no impact on the final recommendations. Table 3 summarizes the assessed measurement bias for each of the two ICARTT wind direction measurements.

Table 3. ICARTT Wind Direction bias estimates

Aircraft/ Instrument	Linear Relationships[a]	Best Estimate Bias (a + b WindDir) (deg)
NASA DC-8 INS	$WindDir_{DC8} = 0.0 + 1.00\ WindDir_{DC8}$	$3.21 - 0.015WindDir_{DC8}$
NOAA WP-3D Not Available	$WindDir_{WP3D} = -6.42 + 1.03WindDir_{DC8}$	$-3.12 + 0.015WindDir_{WP3D}$

[a]Derived from Fig 3.

4.2 Precision Analysis

A detailed description of the precision assessment is given in section 3.1 of the introduction. The IEIP precision, expected variability, observed variability, and the adjusted precision are summarized in Table 4. Based on the results presented in Table 4, the largest "adjusted

precision" value is taken as a conservative precision estimate for each ICARTT wind direction instrument and twice that value is listed in Table 2 as the assessed 2σ precision.

To minimize the effect of bias, we make corrections for bias before computing the observed variability, as the bias may have a significant impact on the observed variability. Figure 4 shows the magnitude of the bias for each intercomparison. The assessed values of the observed variability are displayed in Figure 5. The final analysis results are shown in Table 2. Over 90% of the data falls within the combined recommended uncertainties for each intercomparison, which is consistent with the TAbMEP guideline for unified data sets.

Table 4. ICARTT Wind Direction precision (1σ) comparisons

Flight	Platform	IEIP Precision	Expected Variability	Observed Variability	Adjusted Precision
07/22	DC-8	0.22%	0.43%	5.0%	2.6%
	WP-3D	0.37%			4.3%
07/31	DC-8	0.23%	0.26%	0.70%	0.61%
	WP-3D	0.13%			0.34%

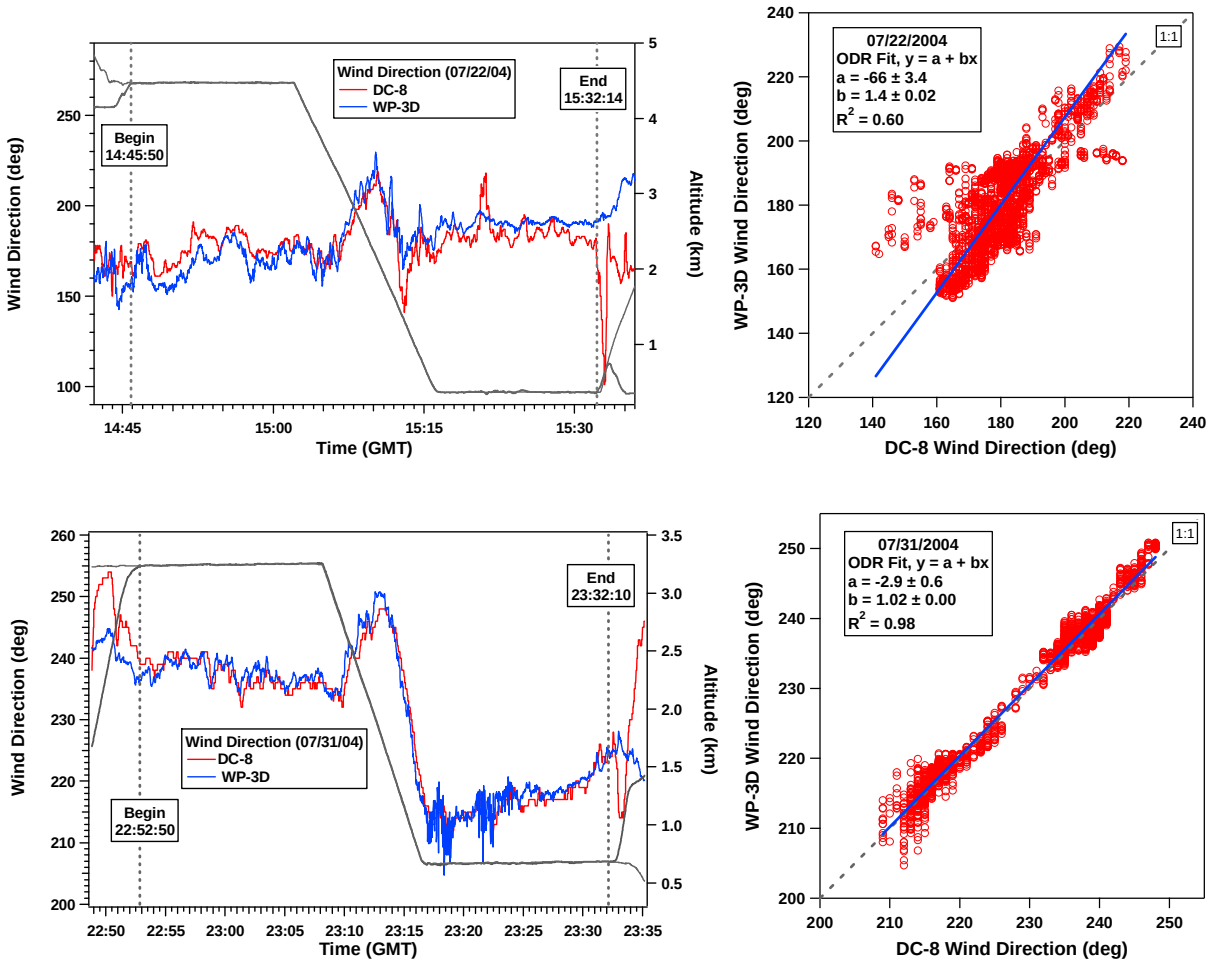

Figure 2. (left panels) Time series of wind direction, wind speed, and heading measurements and aircraft altitudes from two aircraft on the two intercomparison flights between the NASA DC-8 and the NOAA WP-3D. (right panels) Correlations between the wind direction measurements on the two aircraft.

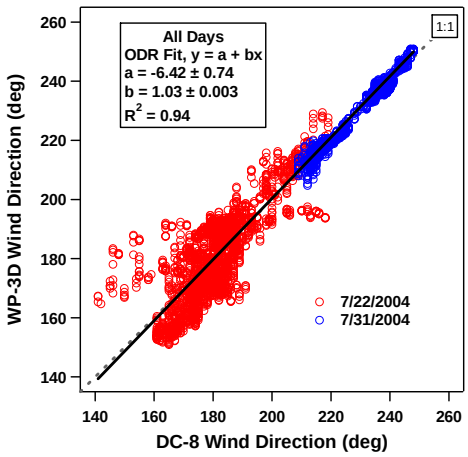

Figure 3. Correlation between the wind direction measurements on the DC-8 and WP-3D for 7/22, and 7/31/2004.

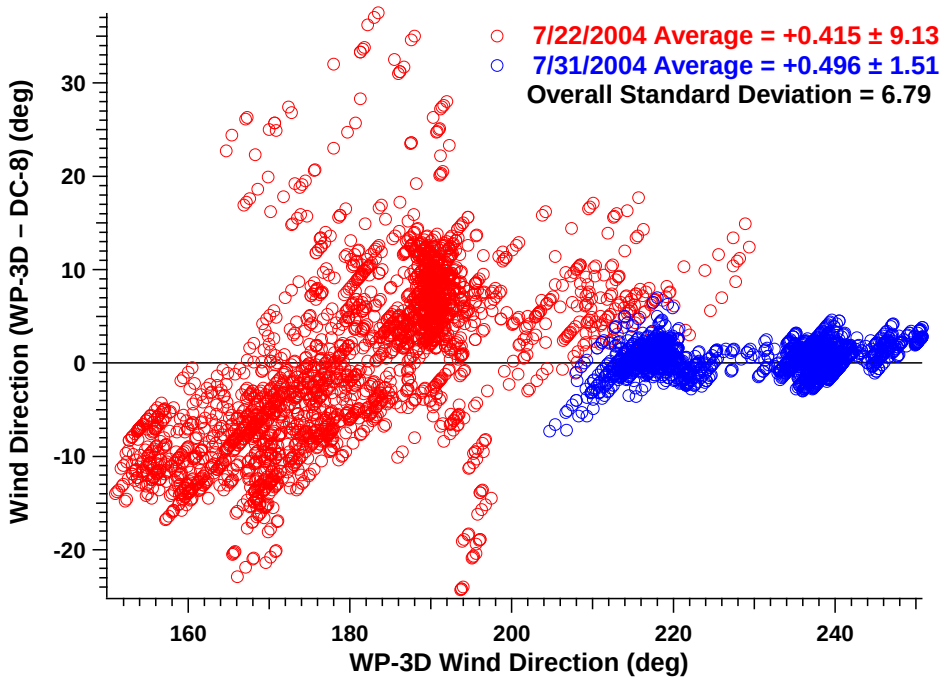

Figure 4. Difference between wind direction measurements from the two DC-8/WP-3D intercomparison flights as a function of the WP-3D wind direction.

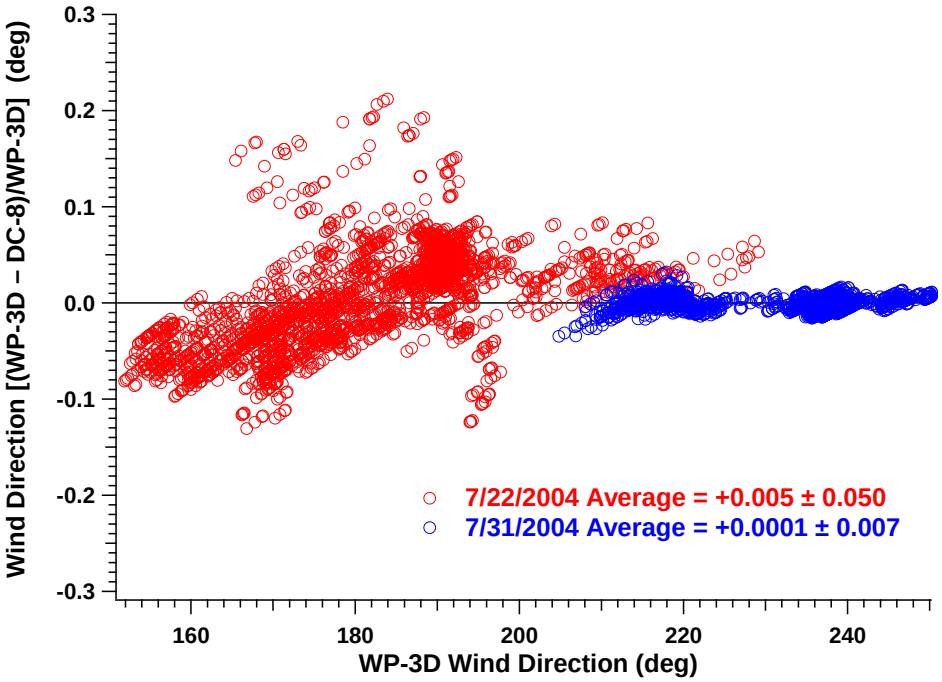

Figure 5. Relative difference between unified measurements of wind direction from the two DC-8/WP-3D intercomparison flights as a function of the WP-3D wind direction. Corrections were made to all data sets to account for bias.

References

Fehsenfeld, F. C., et al. (2006), International Consortium for Atmospheric Research on Transport and Transformation (ICARTT): North America to Europe—Overview of the 2004 summer field study, *J. Geophys. Res., 111*, D23S01, doi:10.1029/2006JD007829.

Singh, H. B., et al. (2006), Overview of the summer 2004 Intercontinental Chemical Transport Experiment-North America (INTEX-A), *J. Geophys. Res., 111*, D24S01, doi:10.1029/2006JD007905.

Wind Direction Appendix

DC-8 Aircraft Measurements of Wind Speed and Wind Direction

The DC-8 aircraft wind speed and wind direction are calculated parameters derived via the aircraft inertial navigation system and air data computer. As shown in the figure on the right, these quantities are obtained using vector subtraction between the vector defined by aircraft heading and true airspeed (i.e., air vector) and ground track and ground speed (i.e., ground vector). The difficulty in obtaining accurate wind speed and wind direction is partially due to the air vector and ground vectors being much larger in magnitude than that of the wind vector. The specified wind speed measurement precision of 3 ms-1 is based on the overall assessment. The uncertainties associated with the calculated wind speed and wind direction also depend on the uncertainties in the air vector and ground vector. Uncertainties associated with wind direction are usually larger for lower wind speed conditions. In general, the wind direction readings are considered to be valid if the wind speed is above 3 ms-1. For the same wind speed, the wind direction and wind speed uncertainties are largest when the wind vector is parallel to the air vector and smallest when the wind vector is perpendicular to the air vector. The wind speed and wind direction uncertainties are also influenced by the flight path, where straight and level flight legs produce the best results.

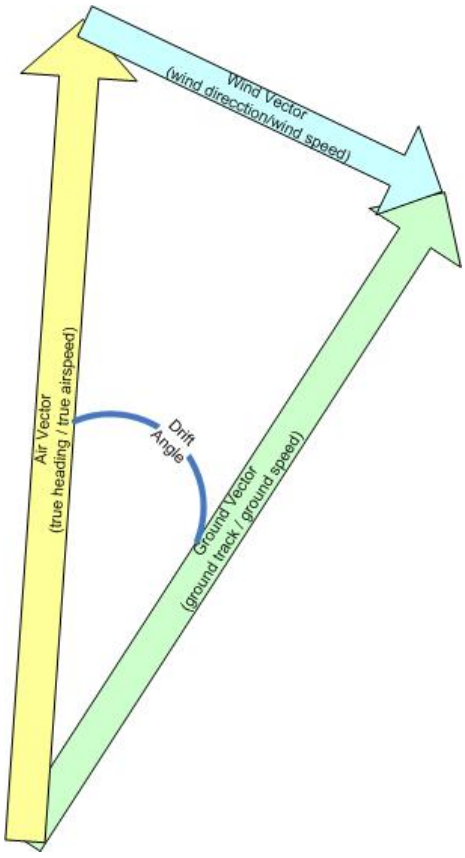

TAbMEP Assessment: ICARTT Wind Speed Measurements

1. Introduction

Here we provide the assessment for the wind speed measurements taken from two aircraft platforms during the summer 2004 ICARTT field campaign [*Fehsenfeld et al.*, 2006, *Singh et al*., 2006]. This assessment is based upon the three wing-tip-to-wing-tip intercomparison flights conducted during the field campaign. Recommendations provided here offer TAbMEP assessed uncertainties for each of the measurements and a systematic approach to unifying the ICARTT wind speed data for any integrated analysis. These recommendations are directly derived from the instrument performance demonstrated during the ICARTT measurement comparison exercises and are not to be extrapolated beyond this campaign.

2. ICARTT Wind speed Measurements

Due to the data reporting problems for BAe-146, the ICARTT wind speed intercomparison was limited to between the DC-8 and WP-3D. Table 1 summarizes the measurement techniques and gives references for more information. A brief description of the DC-8 measurement is also given in the Wind Speed Appendix.

Table 1. Wind Speed measurements deployed on aircraft during ICARTT

Aircraft	Instrument	Reference
NASA DC-8	Delco Carousel IV-3 Inertial Navigation System (INS)	*Delco Electronics* [1977]
NOAA WP-3D	Not Available	Not Available

3. Summary of Results

Table 2 summarizes the assessed 2σ precisions, biases, and uncertainties. More detailed descriptions are provided to illustrate the process for assessment of bias and precision in Sections 4.1 and 4.2 respectively. The assessed 2σ precisions reported in Table 2 are equal to twice the highest adjusted precision value for that instrument listed in Table 4. Table 2 also reports an assessed bias (see Section 4.1 for details) that can be applied to maximize the consistency between the data sets. The assessed bias should be subtracted from the reported data to 'unify' the data sets. The assessed bias is derived from intercomparison periods only and may be extrapolated to the entire mission if one assumes instrument performance remained constant throughout the mission. The recommended 2σ uncertainty is the larger of either the uncertainty reported by the PI or the quadrature-sum of the assessed 2σ precision and assessed bias listed in Table 2. It is noted here that the actual wind speed measurement uncertainty varies with the relative direction of the aircraft heading and wind direction. The error tends to maximize when the wind direction and aircraft heading are parallel and tends to minimize when the wind direction and aircraft heading are orthogonal (see Wind Speed Appendix for further details).

Table 2. Recommended ICARTT Wind Speed measurement treatment

Aircraft/ Instrument	Reported Uncertainty[a] (m/s)	Assessed 2σ Precision (m/s)	Assessed Bias (m/s)	Recommended 2σ Uncertainty[b]
NASA DC-8 INS	3.1	2.9	$-0.045 + 0.01\text{WindSpeed}_{DC8}$	3.1
NOAA WP-3D Not Available	3.1	0.9	$0.046 - 0.01\text{WindSpeed}_{WP3D}$	3.1

[a]See text for details or contact PIs for more information. (J. Barrick on DC-8, john.d.barrick@nasa.gov)
[b]These recommendations based on tests ranging from 0.1 to 30 (m s^{-1}).

Figures 1a through 1c display the precisions, biases, and recommended uncertainties for the two wind speed instruments. For all aircraft measurements, the PI reported uncertainty is adequate for wind speed from 0.1 to 30 m s^{-1}.

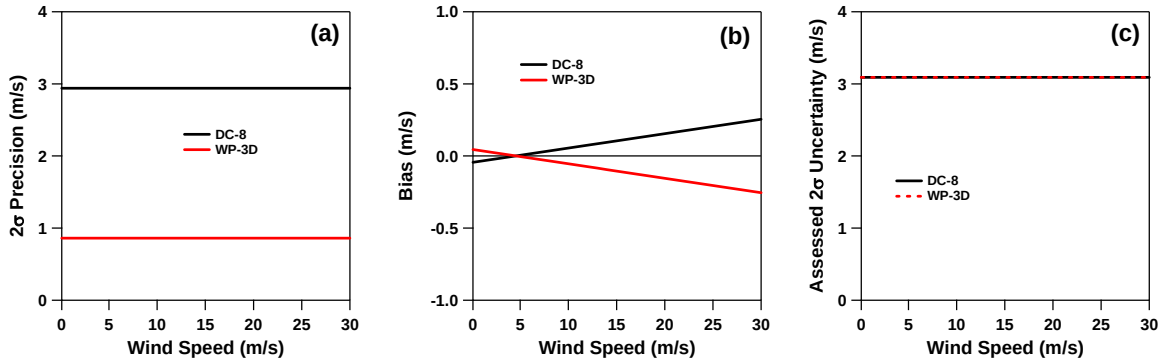

Figure 1. 2σ precision (panel a), bias (panel b), and 2σ uncertainty (panel c) for DC-8 (black) and WP-3D (red) as a function of wind speed. Values were calculated based upon data shown in Table 2.

4. Results and Discussion

4.1 Bias Analysis

Section 3.3 in the introduction describes the process used to determine the best estimate bias. The linear relationships listed in Table 3 were derived from the regression equations found in Figure 3. The reference standard for comparison (RSC), as defined in the introduction, is constructed by averaging the NOAA WP-3D and NASA DC-8. The resulting RSC can be expressed as a function of the DC-8 wind speed measurement as the following:

$$\text{RSC}_{\text{WindSpeed}} = 0.045 + 0.99\ \text{WindSpeed}_{DC8}$$

The RSC is then used to calculate the best estimate bias as described in section 3.3 of the introduction. It should be noted that the initial choice of the reference instrument (DC-8) is arbitrary, and has no impact on the final recommendations. Table 3 summarizes the assessed measurement bias for each of the two ICARTT wind speed measurements.

Table 3. ICARTT Wind Speed bias estimates

Aircraft/ Instrument	Linear Relationships[a]	Best Estimate Bias (a + b WindSpeed) (m/s)
NASA DC-8 INS	$WindSpeed_{DC8} = 0.00 + 1.00 WindSpeed_{DC8}$	$-0.045 + 0.01 WindSpeed_{DC8}$
NOAA WP-3D Not Available	$WindSpeed_{WP3D} = 0.09 + 0.98 WindSpeed_{DC8}$	$0.046 - 0.01 WindSpeed_{WP3D}$

[a]Derived from Fig. 3.

4.2 Precision Analysis

A detailed description of the precision assessment is given in section 3.1 of the introduction. The IEIP precision, expected variability, observed variability, and the adjusted precision are summarized in Table 4. Based on the results presented in Table 4, the largest "adjusted precision" value is taken as a conservative precision estimate for each ICARTT wind speed instrument and twice that value is listed in Table 2 as the assessed 2σ precision.

To minimize the effect of bias, we make corrections for bias before computing the observed variability, as the bias may have a significant impact on the observed variability. Figure 4 shows the magnitude of the bias for each intercomparison. The assessed values of the observed variability are displayed in Figure 5. The final analysis results are shown in Table 2. Over 90% of the data falls within the combined recommended uncertainties for each intercomparison, which is consistent with the TAbMEP guideline for unified data sets.

Table 4. ICARTT Wind Speed precision (1σ) comparisons

Flight	Platform	IEIP Precision (m/s)	Expected Variability (m/s)	Observed Variability (m/s)	Adjusted Precision (m/s)
07/22	DC-8	0.30	0.31	0.61	0.59
	WP-3D	0.08			0.16
07/31	DC-8	0.26	0.28	0.57	0.52
	WP-3D	0.11			0.22
08/07	DC-8	0.27	0.28	1.52	1.46
	WP-3D	0.08			0.43

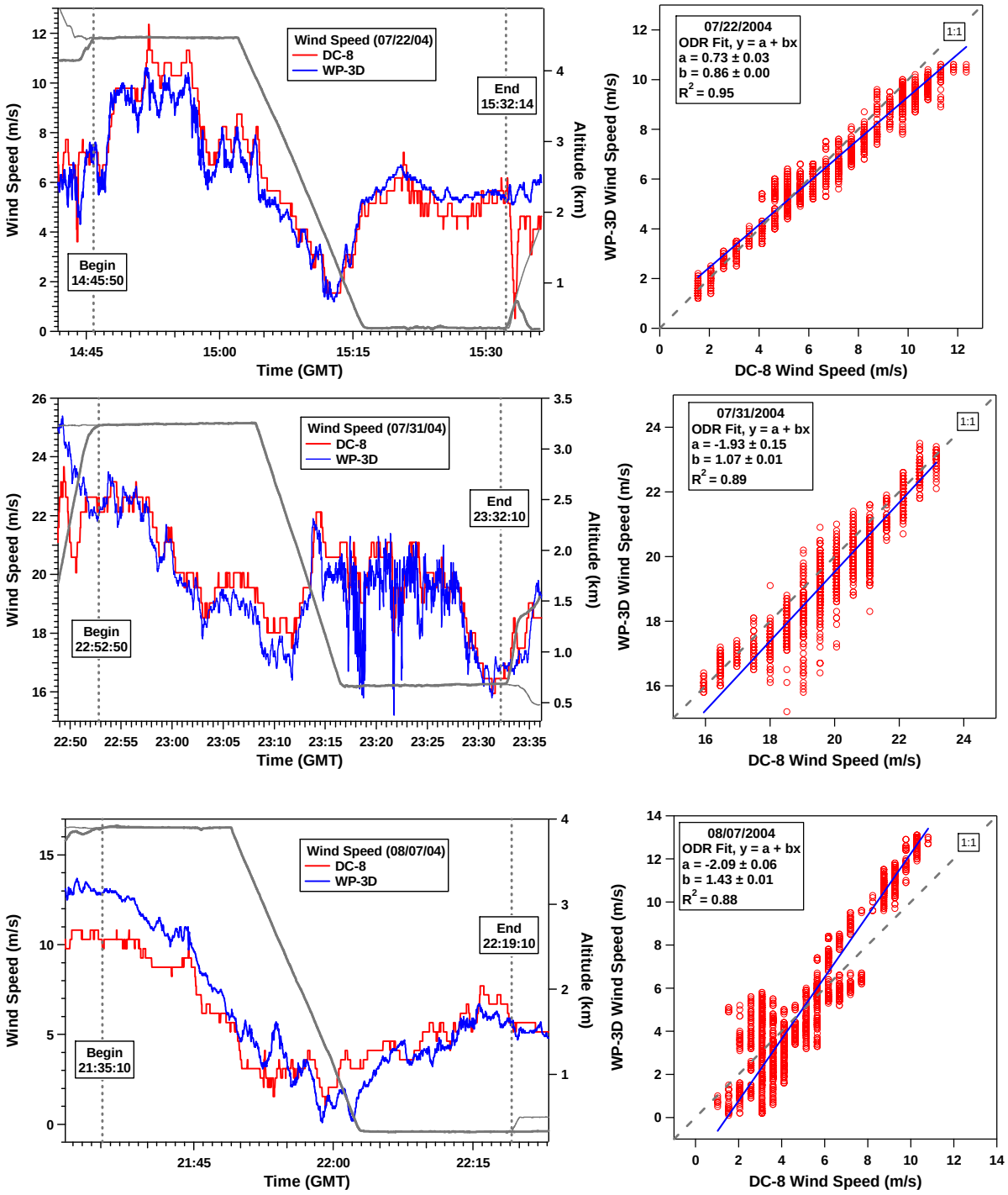

Figure 2. (left panels) Time series of wind speed measurements and aircraft altitudes from two aircraft on the three intercomparison flights between the NASA DC-8 and the NOAA WP-3D. (right panels) Correlations between the wind speed measurements on the two aircraft.

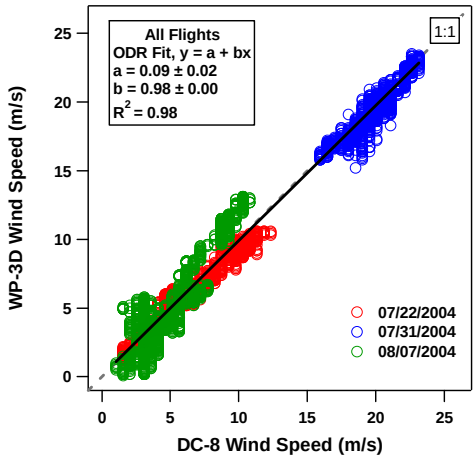

Figure 3. Correlation between the wind speed measurements on the DC-8 and WP-3D for 7/22, 7/31, and 8/7 2004.

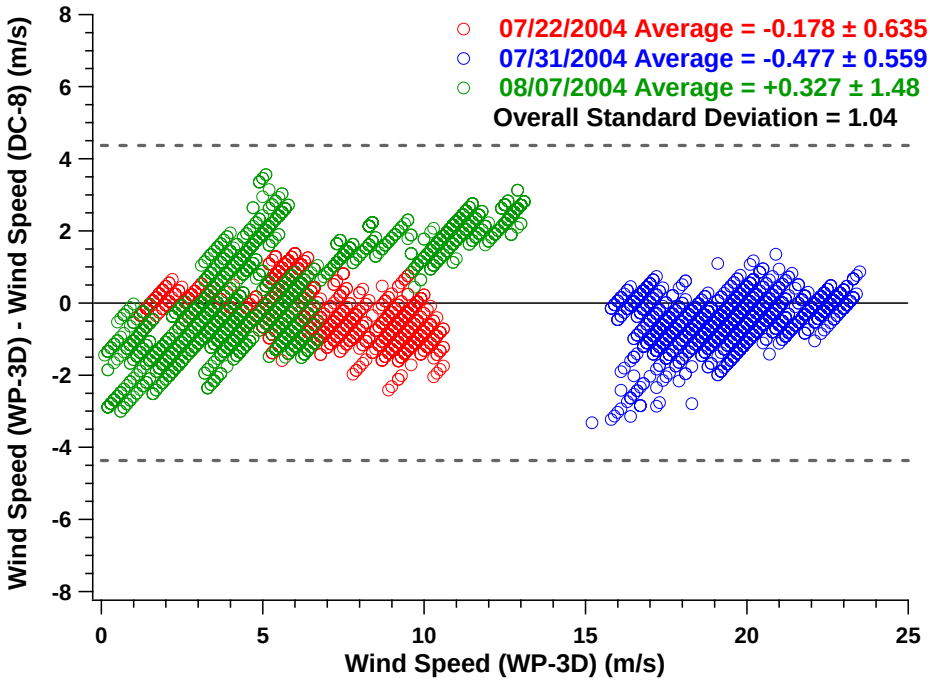

Figure 4. Difference between wind speed measurements from the three DC-8/WP-3D intercomparison flights as a function of the WP-3D wind speed. The dashed lines indicate the range of results expected from the reported measurement uncertainties.

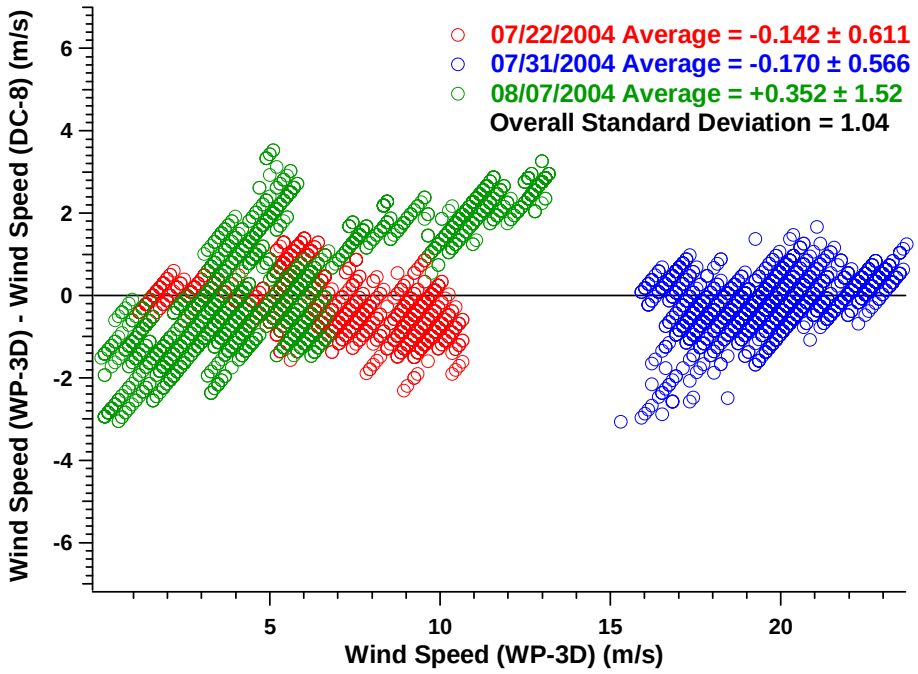

Figure 5. Difference between unified measurements of wind speed from the three DC-8/WP-3D intercomparison flights as a function of the WP-3D wind speed. Corrections were made to all data sets to account for bias.

References

Fehsenfeld, F. C., et al. (2006), International Consortium for Atmospheric Research on Transport and Transformation (ICARTT): North America to Europe—Overview of the 2004 summer field study, *J. Geophys. Res., 111*, D23S01, doi:10.1029/2006JD007829.

Singh, H. B., et al. (2006), Overview of the summer 2004 Intercontinental Chemical Transport Experiment-North America (INTEX-A), *J. Geophys. Res., 111*, D24S01, doi:10.1029/2006JD007905.

Wind Speed Appendix

DC-8 Aircraft Measurements of Wind Speed and Wind Direction

The DC-8 aircraft wind speed and wind direction are calculated parameters derived via the aircraft inertial navigation system and air data computer. As shown in the figure on the right, these quantities are obtained using vector subtraction between the vector defined by aircraft heading and true airspeed (i.e., air vector) and ground track and ground speed (i.e., ground vector). The difficulty in obtaining accurate wind speed and wind direction is partially due to the air vector and ground vectors being much larger in magnitude than that of the wind vector. The specified wind speed measurement precision of 3 ms-1 is based on the overall assessment. The uncertainties associated with the calculated wind speed and wind direction also depend on the uncertainties in the air vector and ground vector. Uncertainties associated with wind direction are usually larger for lower wind speed conditions. In general, the wind direction readings are considered to be valid if the wind speed is above 3 ms-1. For the same wind speed, the wind direction and wind speed uncertainties are largest when the wind vector is parallel to the air vector and smallest when the wind vector is perpendicular to the air vector. The wind speed and wind direction uncertainties are also influenced by the flight path, where straight and level flight legs produce the best results.

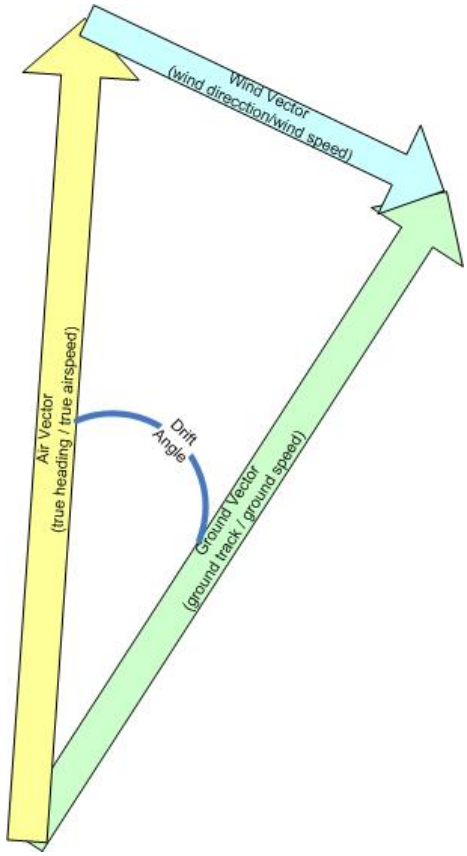

TAbMEP Report: ICARTT NO Measurements

1. Introduction

Here we present the results from the nitrogen oxide (NO) measurement comparisons conducted on four aircraft platforms during the summer 2004 ICARTT field campaign [*Fehsenfeld et al.*, 2006, *Singh et al*., 2006]. This report is based upon the five wing-tip-to-wing-tip intercomparison flights conducted during the field campaign. Low NO conditions encountered during the comparisons prevent us from carrying out a meaningful assessment, thus recommendations are not given in terms of the measurement uncertainties. This report serves as a record for ICARTT NO measurement comparisons.

2. ICARTT NO Measurements

Four different NO instruments were deployed on the four aircraft. It is noted here that the designated DC-8 instrument experienced serious malfunctions and had to be replaced during the campaign with a commercial grade instrument. Table 1 summarizes these techniques and gives references for more information.

Table 1. NO measurements deployed on aircraft during ICARTT

Aircraft	Instrument	Reference
NASA DC-8	NO Chemiluminescence Detector (NO CLD)	Contact PI: brune@meteo.psu.edu
NOAA WP-3D	NO Chemiluminescence Detector (NO CLD)	*Ryerson et al.* [1998]
FAAM BAe-146	NO Chemiluminescence Detector (NO CLD)	Contact PI: m.j.evans.ac.uk
DLR Falcon	NO Chemiluminescence Detector (NO CLD)	Contact PI: hans.schlager@dlr.de

3. Summary of Results

Figure 1 shows the time series plots for comparisons between NASA DC-8 and NOAA WP-3D NO measurements. Between these two measurements, the DC-8 measurement PI reports significantly higher uncertainties. As all three comparisons were conducted at relatively low NO conditions, over 90% of the reported DC-8 values were under LODs (limit of detection), denoted by the grey symbols. The LOD value is defined as the 2 times the 1σ uncertainty reported by the PI. This severely limits our ability to make a meaningful assessment because the ICARTT intercomparison between DC-8 and WP-3D does not provide sufficient data to conduct any robust statistical analysis. It should be clarified here that WP-3D reported values are generally above their LOD and the observed NO trends were found to be correlated with other chemical tracers, e.g., CO. Table 2 provides a summary of the PI reported uncertainties for each of the instruments involved in the intercomparisons. Please note the point by point uncertainty given by PI is a strong function of NO value itself.

Table 2. ICARTT NO PI reported uncertainty for intercomparison period

Aircraft/Instrument	Reported 1σ Uncertainty
NASA DC-8 NO CLD	Point by point, average: 37% for NO values above LOD
NOAA WP-3D NO CLD	5 pptv + 2.5%
FAAM BAe-146 NO CLD	Point by point, average: 41% for NO values above LOD
DLR Falcon NO CLD	2.5%

[a]The average encompasses only the comparison periods for DC-8/WP-3D and DC-8/BAe-146
[b]The average encompasses only the comparison periods for DC-8/BAe-146 and BAe-146/Falcon

Taking the data at face value, the DC-8 NO measurement is, on average, about 32% higher than those of WP-3D for DC-8 NO levels above 10 pptv. The average reported 1σ uncertainty for DC-8 above LOD intercomparison points is 41%; while the WP-3D 1σ uncertainty is reported as 34% on average for the intercomparison points. For comparison between the NASA DC-8 and FAAM BAe-146, Figure 2 displays a very similar situation to what is displayed in Figure 1. Most of the comparison data points fall under 2σ LODs. Again, the LOD values for DC-8 and BAe-146 are defined as 2 times the 1σ uncertainties reported by the corresponding PIs. For DC-8 NO higher than 10 pptv, the average difference between the DC-8 and BAe-146 measurements is 52%, DC-8 being higher. The average reported 1σ uncertainty for DC-8 above LOD intercomparison points is 33%; while the average for BAe-146 1σ uncertainty above LOD is 40%. Figure 3 shows that low NO conditions were again encountered during the FAAM BAe-146 and DLR Falcon comparison. Less than 3% of BAe-146 data are above 2σ LODs. On average, the Falcon NO measurement is about 14% lower than those of the BAe-146 for BAe-146 NO levels above 10 pptv. The average reported 1σ uncertainty for BAe-146 above LOD intercomparison points is 42%; while the PI reported Falcon uncertainty is 2.5% (1σ).

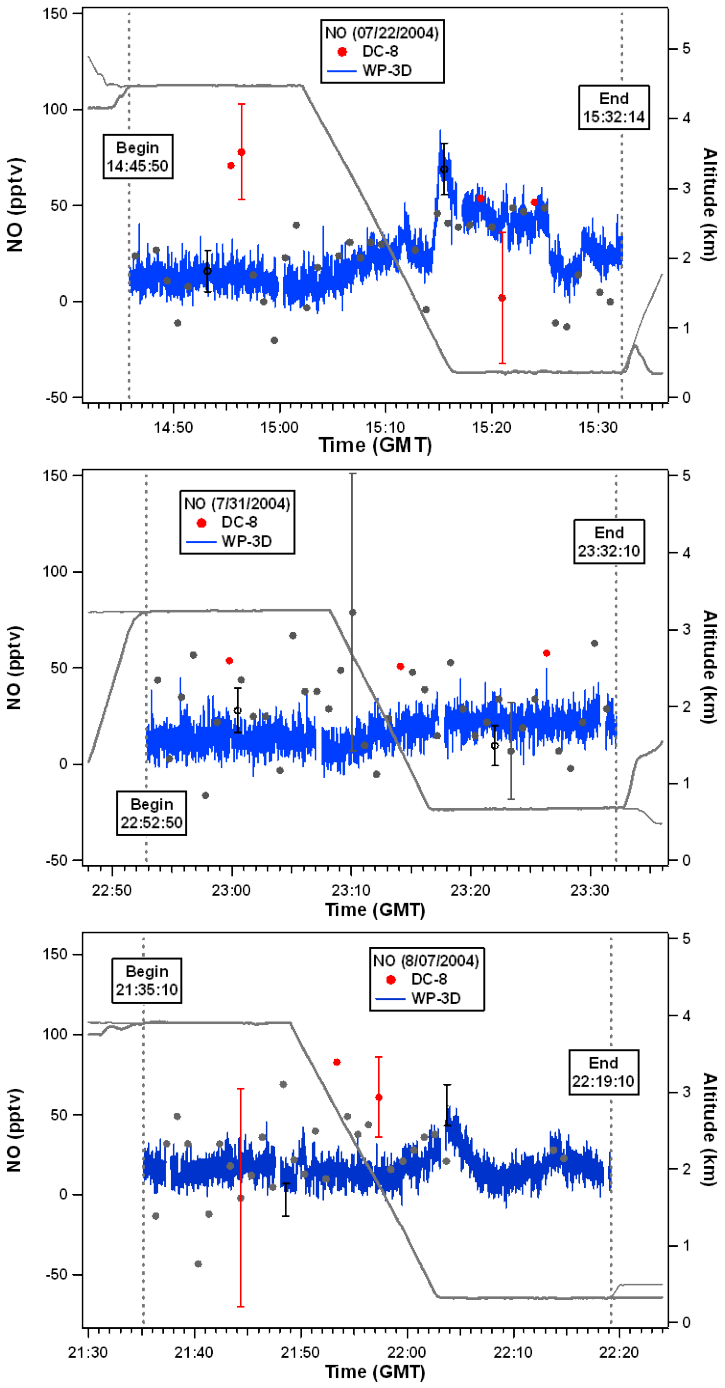

Figure 1. Time series of NO measurements and aircraft altitudes from the three intercomparison flights between the NASA DC-8 and the NOAA WP-3D. Error bars represent the PI reported uncertainty. Gray symbols represent DC-8 measurements that are under limit of detection (LOD). The LOD level is defined as 2 times the 1σ uncertainty reported by PI.

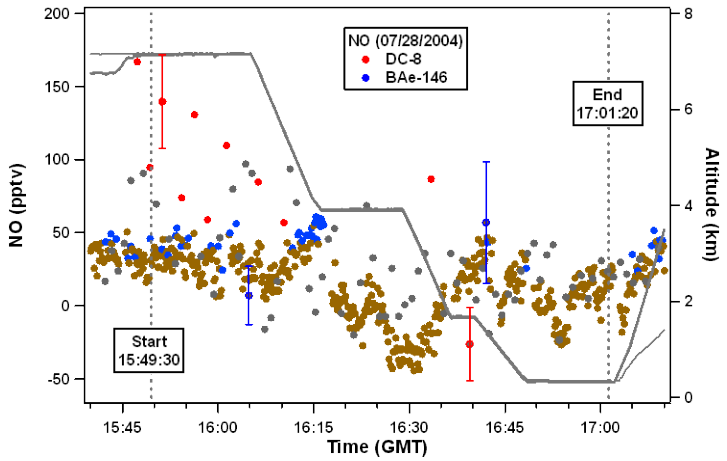

Figure 2. Time series of NO measurements and aircraft altitudes from the intercomparison flight between the NASA DC-8 and the FAAM BAe-146. Error bars represent the PI reported uncertainty. Gray and brown symbols, respectively, represent DC-8 and BAe-146 measurements that are under limit of detection (LOD). The LOD level is defined as 2 times the 1σ uncertainty reported by PI.

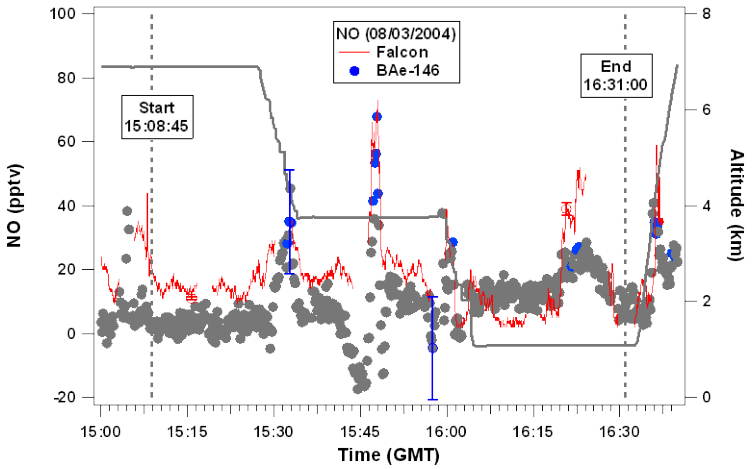

Figure 3. Time series of NO measurements and aircraft altitudes from the intercomparison flight between the FAAM BAe-146 and the DLR Falcon. Error bars represent the PI reported uncertainty. Gray symbols represent BAe-146 measurements that are under limit of detection (LOD). The LOD level is defined as 2 times the 1σ uncertainty reported by PI.

References

Fehsenfeld, F. C., et al. (2006), International Consortium for Atmospheric Research on Transport and Transformation (ICARTT): North America to Europe—Overview of the 2004 summer field study, *J. Geophys. Res., 111*, D23S01, doi:10.1029/2006JD007829.

Ryerson, T.B., et al. (1998), Emissions lifetimes and ozone formation in power plant plumes, *J. Geophys. Res., 103,* D17, 22569-22583

Singh, H. B., et al. (2006), Overview of the summer 2004 Intercontinental Chemical Transport Experiment-North America (INTEX-A), *J. Geophys. Res., 111*, D24S01, doi:10.1029/2006JD007905.

TAbMEP Assessment: ICARTT CH_4 Measurements

1. Introduction

Here we provide the assessment for the methane (CH_4) measurements during the summer 2004 ICARTT field campaign [*Fehsenfeld et al.*, 2006, *Singh et al*., 2006]. This assessment is based upon the three wing-tip-to-wing-tip intercomparison flights conducted during the field campaign. Recommendations provided here offer TAbMEP assessed biases for each of the measurements and a systematic approach to unifying the ICARTT CH_4 data for any integrated analysis. These recommendations are directly derived from the instrument performance demonstrated during the ICARTT measurement comparison exercises and are not to be extrapolated beyond this campaign.

2. ICARTT CH_4 Measurements

During the ICARTT campaign, there were two CH_4 measurements deployed on NASA DC-8 and NOAA WP-3D aircraft. Table 1 summarizes these techniques and gives references for more information.

Table 1. CH_4 measurements deployed on aircraft during ICARTT

Aircraft	Instrument	Reference
NASA DC-8	Whole Air Sampler (WAS)	*Simpson et al.* [2002, 2006]
NOAA WP-3D	Whole Air Sampler (WAS)	Contact PI: eatlas@rsmas.miami.edu

3. Summary of Results

Table 2 summarizes the assessed biases as well as PI reported uncertainties for each of the two CH_4 measurements involved in the intercomparisons. More detailed descriptions are provided to illustrate the process for the bias assessment in Section 4.1. The TAbMEP-prescribed IEIP procedures cannot be applied to the ICARTT CH_4 measurement for precision assessments. This is because the reported data have large time gaps and a small data population (see Section 3.1 of the introduction). The assessed bias reported in Table 2 (see Section 4.1 for details) can be applied to maximize the consistency between the data sets, by subtracting the bias value from the reported data to 'unify' the data sets. If one assumes instrument performance remained constant throughout the mission, the assessed bias may be extrapolated to the entire mission although it is derived from intercomparison periods only.

Table 2. Recommended ICARTT CH_4 measurement treatment

Aircraft/ Instrument	Reported 2σ Uncertainty	Assessed Bias (ppbv)
NASA DC-8 WAS	Precision: 0.2% Accuracy: 1%	$-38.86 + 0.0249\ CH_{4\ \text{DC-8}}$
NOAA WP-3D WAS	Precision: 0.4% Accuracy: 1%	$40.90 - 0.0262\ CH_{4\ \text{WP-3D}}$

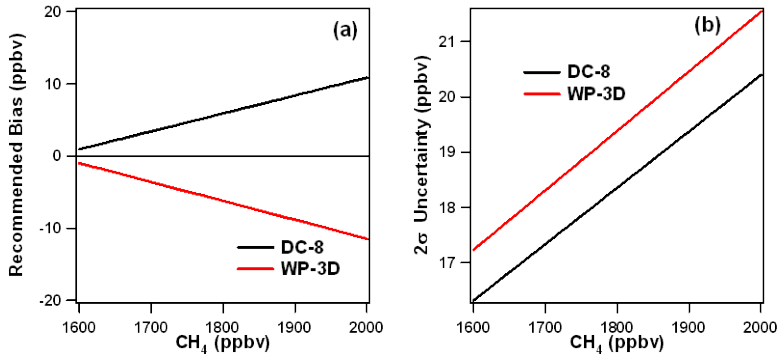

Figure 1. Recommended bias (panel a) and PI reported 2σ uncertainty (panel b) for DC-8 (black) and WP-3D (red) as a function of CH_4 level. Values were calculated based upon data shown in Table 2.

4. Results and Discussion

4.1 Bias Analysis

Section 3.3 in the introduction describes the process used to determine the best estimate bias. Figure 2 shows the time series plots for each of the three WP-3D vs. DC-8 comparisons. As shown in the Figure, the data sets have similar trends for 07/22 and 07/31. There are some differences in trend for 08/07, but the absolute difference is less than 25 ppbv for points in which the DC-8 and WP-3D sampling intervals overlapped. Figure 4 displays the residuals (i.e., the difference between DC-8 and WP-3D) which are less than 25 ppbv, which is about 1.3%, well within the combined uncertainties. Unlike the DC-8 data, the WP-3D CH_4 is not reported under dry conditions. The WP-3D PI also noted potential condensation problems in the canister and sampling lines. It was determined that there was insufficient information to appropriately account for the moisture level for the wet to dry conversion. This is one of the factors contributing to the differences between WP-3D and DC-8 measurements. For 2 out of 3 flights, there are only 3 or 4 overlapping points with a small range of variation (3 - 5 ppbv). It is not statistically significant to show the linear regression for these flights. Therefore, linear regression is performed over the data combined from all three flights. The linear relationships listed in Table 3 were derived from the regression equation found in Figure 3. The reference standard for comparison (RSC), as defined in the introduction, is constructed by averaging the NOAA WP-3D and NASA DC-8 measurements with equal weights. The resulting RSC can be expressed as a function of the DC-8 CH_4 measurement by the following:

$$RSC_{CH4} = 38.861 + 0.975\ CH_{4\text{-}DC8}$$

The RSC is then used to calculate the best estimate bias as described in Section 3.3 of the introduction. It should be noted that the initial choice of the reference instrument (DC-8 WAS) is arbitrary, and has no impact on the final recommendations. Table 3 summarizes the assessed measurement bias for each of the two ICARTT CH_4 measurements. Note that additional decimal places were carried in the calculations to ensure better precision. It is also noted that the intercept in the equations listed in Table 3 should not be viewed as an offset. These linear equations are used to best describe the linear relation between the WP-3D and DC-8 measurements.

The WAS technique for measuring VOCs presents some challenges in analyzing the data. The DC-8 data have an integration time of approximately 60-70 seconds, while the WP-3D data have an integration time between 6-11 seconds. For these measurements to be considered

simultaneous and correlated, the start and stop times of the WP-3D data must fall within the start and stop times of the DC-8 data. In order to maximize the data coverage for statistical analysis, one exception is made to this rule. If the shorter (WP-3D) integration time falls outside the longer integration time by no more than two seconds, the data points are also considered to be simultaneous. Only the PI reported data are used in this assessment, and no interpolation is included. It is noted here the integration time difference may potentially be another factor leading to the difference between the DC-8 and WP-3D measurements.

Table 3. ICARTT CH_4 bias estimates

Aircraft/ Instrument	**Linear Relationships**	**Best Estimate Bias ($a + b\ CH_4$) (ppbv)**
NASA DC-8 WAS	$CH_{4\ DC\text{-}8} = 0.00 + 1.000\ CH_{4\ DC\text{-}8}$	$-38.86 + 0.0249\ CH_{4\ DC\text{-}8}$
NASA WP-3D WAS	$CH_{4\ WP\text{-}3D} = 77.72 + 0.950\ CH_{4\ DC\text{-}8}$	$40.90 - 0.0262\ CH_{4\ WP\text{-}3D}$

4.2 Precision Analysis

A detailed description of the precision assessment is given in Section 3.1 of the introduction. The IEIP precision, expected variability, and adjusted precision could not be calculated for CH_4 because of the small number of points and large time gaps between measurements.

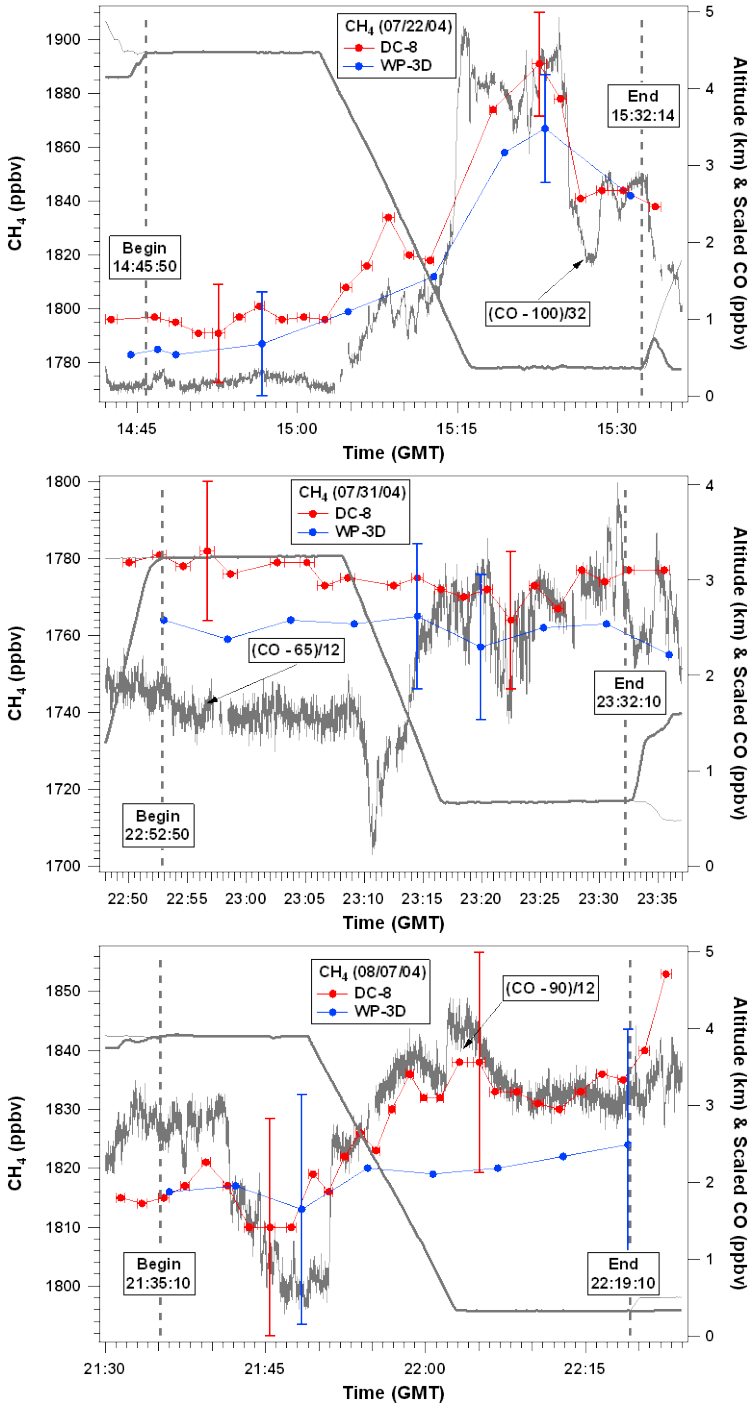

Figure 2. Time series of CH_4 measurements and aircraft altitudes from two aircraft on the three intercomparison flights between the NASA DC-8 and the NOAA WP-3D. Y-axis error bars represent the PI reported uncertainty and x-axis error bars represent the instrument integration time. X-axis error bars were not included for the WP-3D due to the small integration times.

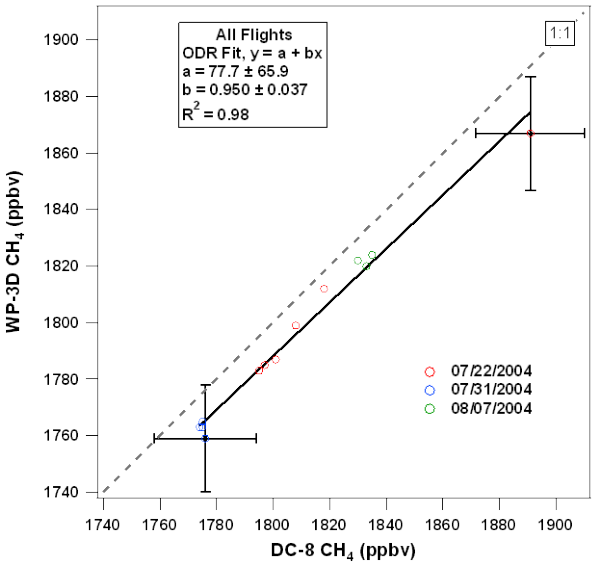

Figure 3. Combined correlation for the CH_4 measurements on NASA DC-8 and the NOAA WP-3D for 7/22, 7/31, and 8/07 2004. Error bars represent the PI reported uncertainty.

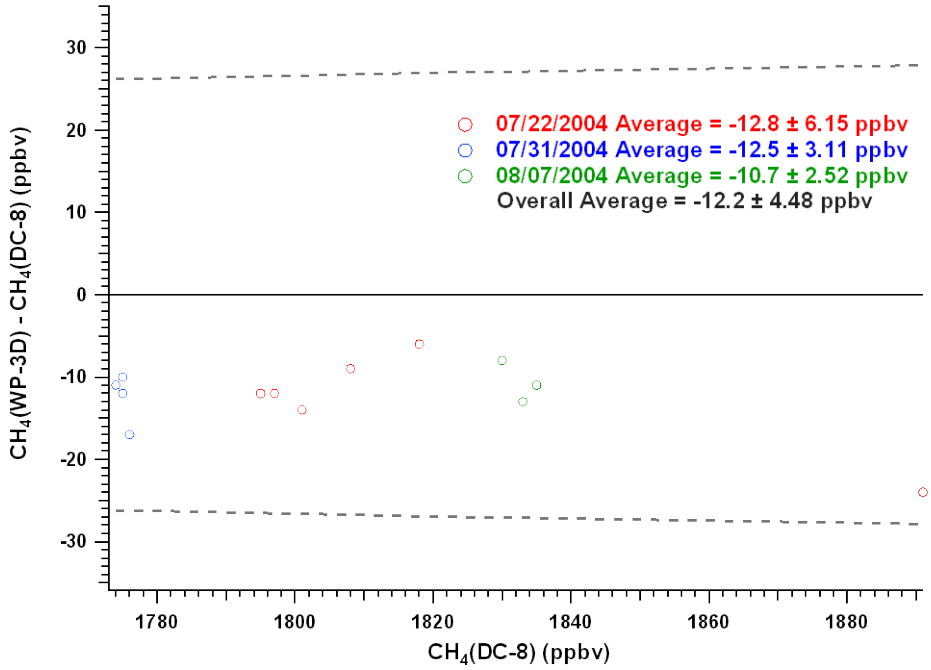

Figure 4. Difference between CH_4 measurements from the three DC-8/WP-3D intercomparison flights as a function of the DC-8 CH_4. The dashed lines indicate the range of the results expected from the reported measurement uncertainties.

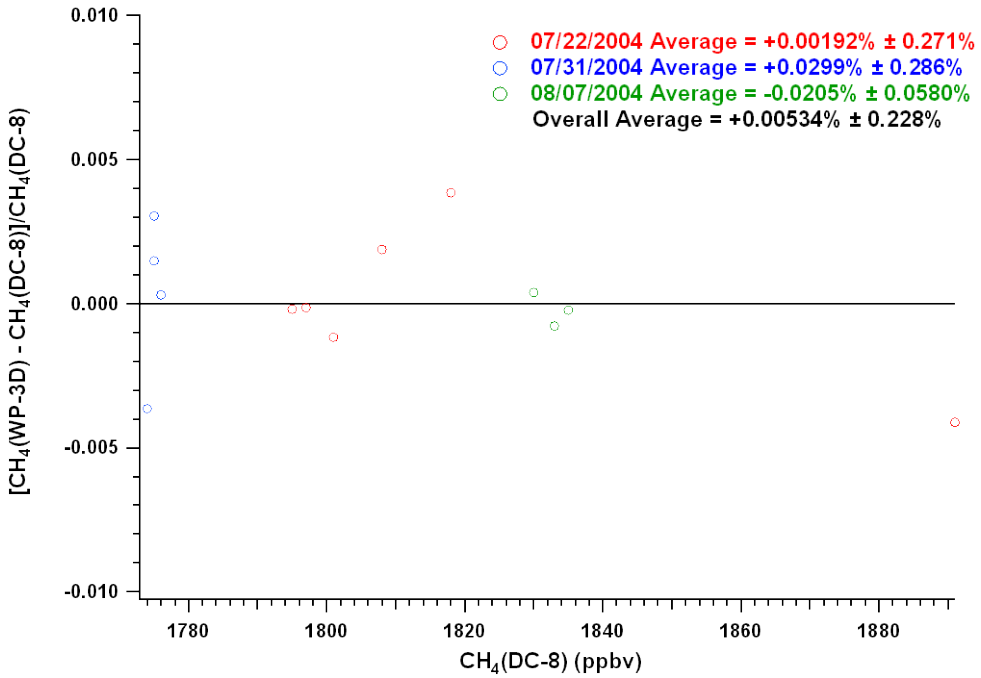

Figure 5. Relative difference between CH_4 measurements from the three DC-8/WP-3D intercomparison flights as a function of DC-8 CH_4. A correction was made to account for bias.

References

Fehsenfeld, F. C., et al. (2006), International Consortium for Atmospheric Research on Transport and Transformation (ICARTT): North America to Europe—Overview of the 2004 summer field study, *J. Geophys. Res., 111*, D23S01, doi:10.1029/2006JD007829.

Simpson, I. J., D. R. Blake, F. S. Rowland, and T.-Y. Chen (2002), Implications of the Recent Fluctuations in the Growth Rate of Tropospheric Methane, *Geophysical Research Letters, 29* 10.1029/2001GL014521.

Simpson, I. J., F. S. Rowland, S. Meinardi, and D. R. Blake (2006), Influence of Biomass Burning During Recent Fluctuations in the Slow Growth of Tropospheric Methane, *Geophysical Research Letters,* 33, L22808, 10.1029/2006GL027330.

Singh, H. B., et al. (2006), Overview of the summer 2004 Intercontinental Chemical Transport Experiment-North America (INTEX-A), *J. Geophys. Res., 111*, D24S01, doi:10.1029/2006JD007905.

TAbMEP Assessment: ICARTT Propane Measurements

1. Introduction

Here we provide the assessment for the propane (C_3H_8) measurements during the summer 2004 ICARTT field campaign [*Fehsenfeld et al.*, 2006, *Singh et al*., 2006]. The inter-platform assessment is based upon the four wing-tip-to-wing-tip intercomparison flights conducted during the field campaign. The two techniques for the WP-3D are compared using all available data from the mission. Recommendations provided here offer TAbMEP assessed biases for each of the measurements and a systematic approach to unifying the ICARTT propane data for any integrated analysis. These recommendations are directly derived from the instrument performance demonstrated during the ICARTT measurement comparison exercises and are not to be extrapolated beyond this campaign.

2. ICARTT Propane Measurements

Three whole air sampler instruments were deployed on three aircraft. Table 1 summarizes these techniques and gives references for more information.

Table 1. Propane measurements deployed on aircraft during ICARTT

Aircraft	Instrument	Reference
NASA DC-8	Whole Air Sampler (WAS)	*Colman et al.* [2001]
NOAA WP-3D	Whole Air Sampler (WAS) Flame Ionization Detection (FID)	Contact PI: eatlas@rsmas.miami.edu
	Whole Air Sampler (WAS) Mass Spectrometer Detection (MSD)	Contact PI: eatlas@rsmas.miami.edu
FAAM BAe-146	Whole Air Sampler (WAS)	*Hopkins et al.* [2003]

3. Summary of Results

Table 2 summarizes the assessed biases as well as PI reported uncertainties for each of the four propane measurements involved in the intercomparisons. More detailed descriptions are provided to illustrate the process for the bias assessment in Section 4.1. The TAbMEP-prescribed IEIP procedures cannot be applied to the ICARTT propane measurements for precision assessment. This is because the reported data have large time gaps and a small data population (see Section 3.1 of the introduction). The assessed bias reported in Table 2 (see Section 4.1 for details) can be applied to maximize the consistency between the data sets, by subtracting the value from the reported data to 'unify' the data sets. If one assumes instrument performance remained constant throughout the mission, the assessed bias may be extrapolated to the entire mission although it is derived from intercomparison periods only.

Table 2. Recommended ICARTT Propane measurement treatment

Aircraft/Instrument	Reported 2σ Uncertainty	Assessed Bias (pptv)
NASA DC-8 WAS	10%	$-7.465 - 0.0222\ C_3H_{8\ DC\text{-}8}$
NOAA WP-3D WAS FID	10%	$12.65 - 0.0621\ C_3H_{8\ FID}$
NOAA WP-3D WAS MSD	10%	$12.33 - 0.0601\ C_3H_{8\ MSD}$
FAAM BAe-146 WAS	Point by Point, average: 32%[a]	$-7.830 + 0.138\ C_3H_{8\ BAe\text{-}146}$

[a] The average encompasses only the comparison period for DC-8/BAe-146.

Figures 1 a and b display the PI reported uncertainties and recommended biases for the four propane instruments.

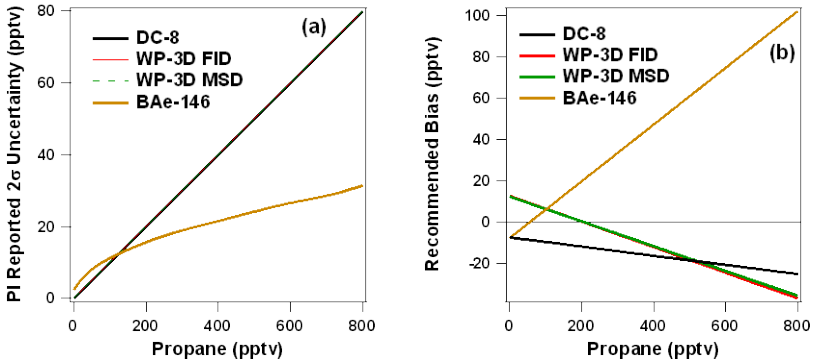

Figure 1. PI reported 2σ uncertainty (panel a) and recommended bias (panel b) for DC-8 (black), WP-3D FID (red), WP-3D MSD (green), and BAe-146 (gold) as a function of propane level. Values were calculated based upon data shown in Table 2. The BAe-146 PI reported uncertainty was calculated using a function derived from the 60 second merge file.

4. Results and Discussion

4.1 Bias Analysis

Section 3.3 in the introduction describes the process used to determine the best estimate bias. Figures 2 and 4 show the time series plots for the DC-8/WP-3D and DC-8/BAe-146 comparisons. The DC-8 is consistently lower than both WP-3D and BAe-146 by 13 pptv and 4 pptv on average respectively. The two techniques used on the WP-3D were compared for all flights using the WAS merge file, shown in Figure 5. On average the FID data were less than 0.5 pptv larger than the MSD data. Figures 6 – 9 show the magnitude of the bias for each intercomparison and Figures 10 – 13 show the corresponding relative residuals.

For 2 of the 3 DC-8/WP-3D flights, there are only 3 or 4 overlapping points with a small range of variation (less than 100 pptv). It is not statistically significant to show the linear regression for these flights. Therefore, linear regression is performed over the data combined from all three DC-8/WP-3D flights. The linear relationships listed in Table 3 were derived from the regression equations found in Figures 3 and 4. The regression equations are expressed as a function of C_3H_8 DC-8 shown in Table 3. The reference standard for comparison (RSC), as defined in the introduction, is constructed by a weighted average of the DC-8, both WP-3D techniques, and the BAe-146. The PI consensus was to give the DC-8 a weight of 2, the FID technique 1.5, the MSD technique 0.5, and the BAe-146 one. (i.e. [2DC-8 + 1.5FID + 0.5MSD + BAe-146]/5) The resulting RSC can be expressed as a function of the DC-8 C_3H_8 measurements as the following:

$$RSC_{C3H8} = 7.465 + 1.022\ C_3H_{8\text{-}DC8}$$

The RSC is then used to calculate the best estimate bias as described in Section 3.3 of the introduction. It should be noted that the initial choice of the reference instrument (DC-8 WAS) is arbitrary, and has no impact on the final recommendations. Table 3 summarizes the assessed measurement bias for each of the four ICARTT propane measurements. Note that additional

decimal places were carried in the calculations to ensure better precision. It is also noted that the intercept in the equations listed in Table 3 should not be viewed as an offset. These linear equations are used to best describe the linear relation between the measurements.

The WAS technique for measuring VOCs presents some challenges in analyzing the data. The DC-8 data have an integration time of approximately 60-70 seconds, while the WP-3D data have an integration time between 6-11 seconds. For these measurements to be considered simultaneous and correlated, the start and stop times of the WP-3D data must fall within the start and stop times of the DC-8 data. In order to maximize the data coverage for statistical analysis, one exception is made to this rule. If the shorter (WP-3D) integration time falls outside the longer integration time by no more than two seconds, the data points are also considered to be simultaneous. BAe-146 integration times range from approximately 30-60 seconds. Since the DC-8 and BAe-146 have similar integration times, the measurements are considered correlated if the midpoint of DC-8 or BAe-146 fall within the start and stop time of the other measurement. Only the PI reported data are used in this assessment, and no interpolation is included. It is noted here the integration time difference may potentially be another factor leading to the difference between measurements.

Table 3. ICARTT Propane bias estimates

Aircraft/ Instrument	**Linear Relationships**	**Best Estimate Bias ($a + b\ C_3H_8$) (pptv)**
NASA DC-8 WAS	$C_3H_{8\ DC\text{-}8} = 0.00 + 1.000\ C_3H_{8\ DC\text{-}8}$	$-7.465 - 0.0222\ C_3H_{8\ DC\text{-}8}$
NOAA WP-3D WAS FID	$C_3H_{8\ WP\text{-}3D} = 18.9 + 0.962\ C_3H_{8\ DC\text{-}8}$	$12.65 - 0.0621\ C_3H_{8\ FID}$
NOAA WP-3D WAS MSD	$C_3H_{8\ WP\text{-}3D} = 18.7 + 0.964\ C_3H_{8\ DC\text{-}8}$	$12.33 - 0.0601\ C_3H_{8\ MSD}$
FAAM BAe-146 WAS	$C_3H_{8\ BAe\text{-}146} = -0.423 + 1.19\ C_3H_{8\ DC\text{-}8}$	$- 7.830 + 0.138\ C_3H_{8\ BAe\text{-}146}$

As a part of ICARTT intercomparison standard exchange exercises, University of California, Irvine (UCI) prepared the common VOC samples that were sent to University of Miami (Miami), University of New Hampshire (UNH), and University of York (York) for their lab analyses. Some of these same institutions had instruments on the following planes during ICARTT: UCI on the DC-8, Miami on the WP-3D, and York on the BAe-146. The comparison incorporated 9 species, which included propane. We believe that the inclusion of this comparison result will help the readers better understand the airborne intercomparison analysis. The difference in this lab comparison between the DC-8 and WP-3D instruments was 3 pptv, WP-3D being higher, with a DC-8 instrument reading of 1427 pptv. From the same lab comparison, the difference between the DC-8 and BAe-146 was 12 pptv, DC-8 being higher. Comparing the ICARTT flights to this lab comparison shows slightly different relationships for both the DC-8/WP-3D and the DC-8/BAe-146 intercomparisons. The average lab comparison level of 1424 pptv is much higher than levels experience during the intercomparison flights which range from approximately 0 to 800 pptv. Also, the intercomparison flights do not provide a large number of data points for comparison. These are possible contributions to the difference between the lab comparison and the intercomparison flights.

4.2 Precision Analysis

A detailed description of the precision assessment is given in Section 3.1 of the introduction. The IEIP precision, expected variability, and adjusted precision could not be calculated for propane because of the small number of points and large time gaps between measurements.

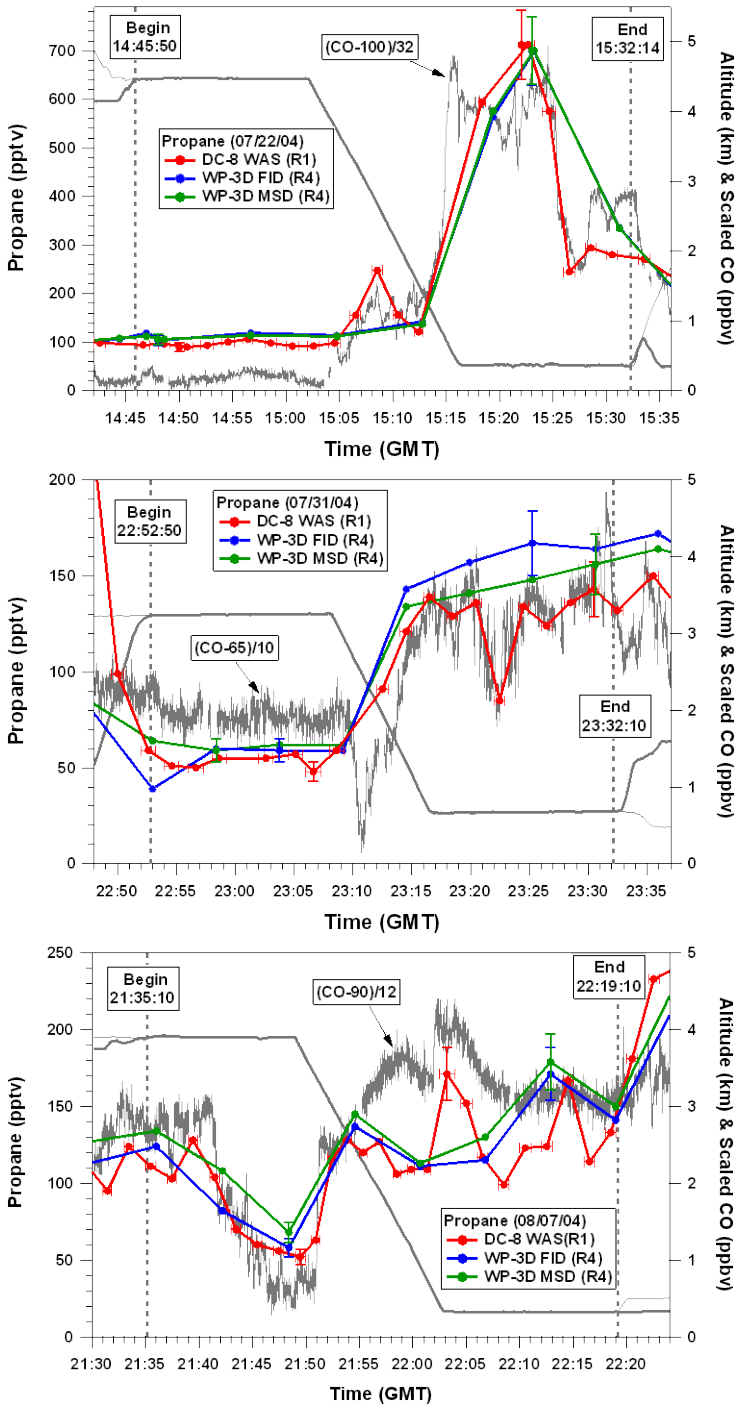

Figure 2. Time series of propane measurements and aircraft altitudes from two aircraft on the three intercomparison flights between the NASA DC-8 and the NOAA WP-3D. Error bars represent the PI reported uncertainty. In parenthesis next to the plane is the data version number.

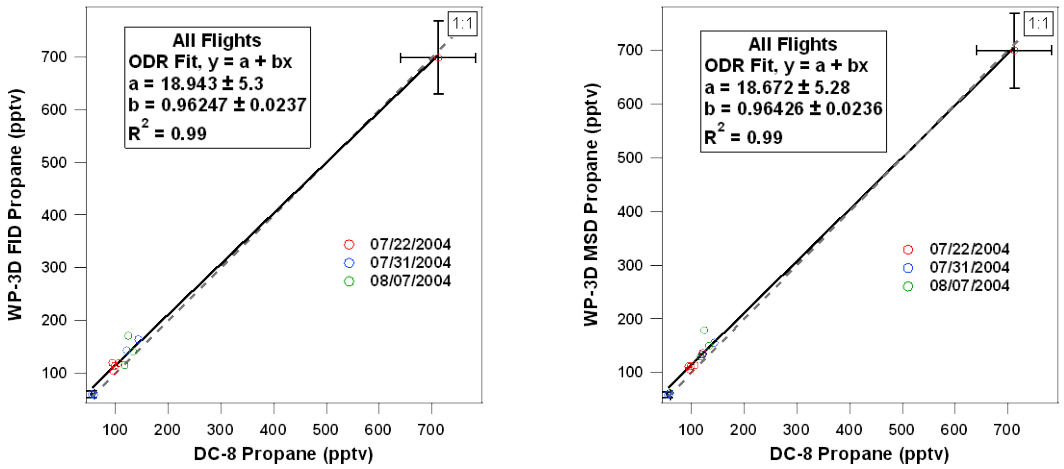

Figure 3. Combined correlation for the propane measurements on NASA DC-8 and the NOAA WP-3D for 7/22, 7/31, and 8/07 2004. (left panel) WP-3D FID and (right panel) WP-3D MSD. Error bars represent the PI reported uncertainty.

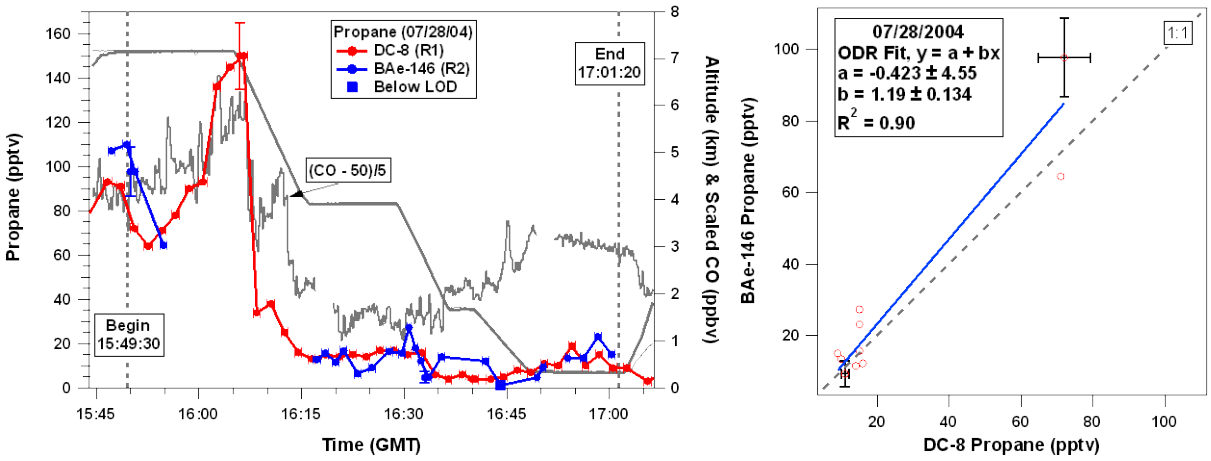

Figure 4. (left panel) Time series of propane measurements and aircraft altitudes from the intercomparison flight between the NASA DC-8 and the FAAM BAe-146. In parenthesis next to the plane is the data version number. (right panel) Correlation between the propane measurements on the two aircraft. Error bars represent the PI reported uncertainty.

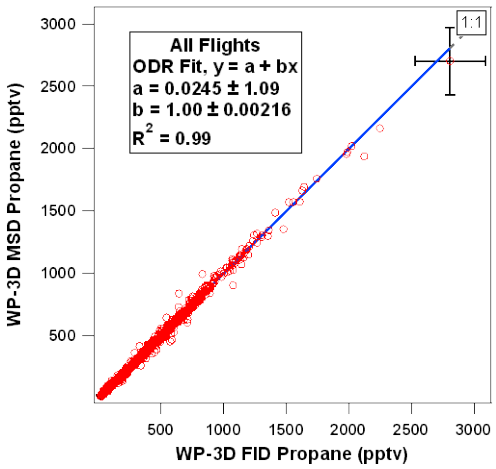

Figure 5. Correlation of WP-3D FID and MSD propane measurements for all ICARTT flights. Data taken from the WAS merge file.

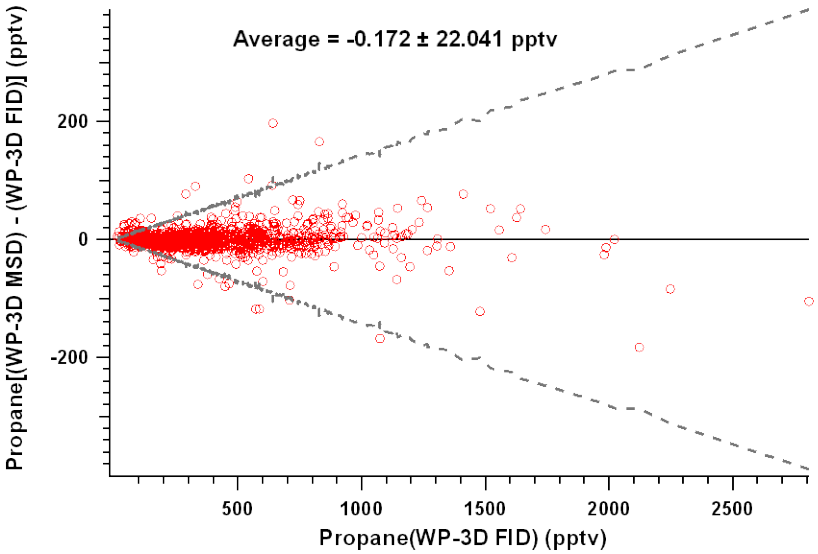

Figure 6. Difference between propane measurements from WP-3D FID and WP-3D MSD for all flights as a function of WP-3D FID propane. The dashed lines indicate the range of results expected from the reported 2σ measurement uncertainties.

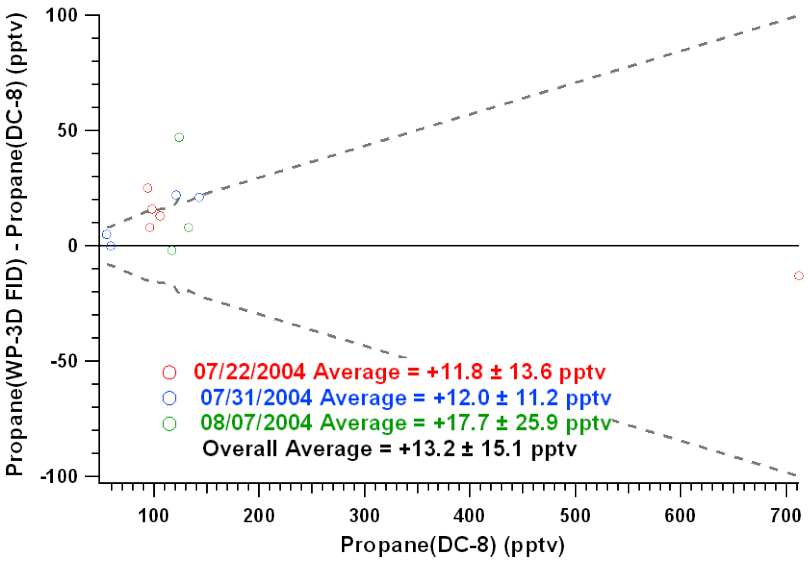

Figure 7. Difference between propane measurements from the three DC-8/WP-3D FID intercomparison flights as a function of DC-8 propane. The dashed lines indicate the range of results expected from the reported 2σ measurement uncertainties.

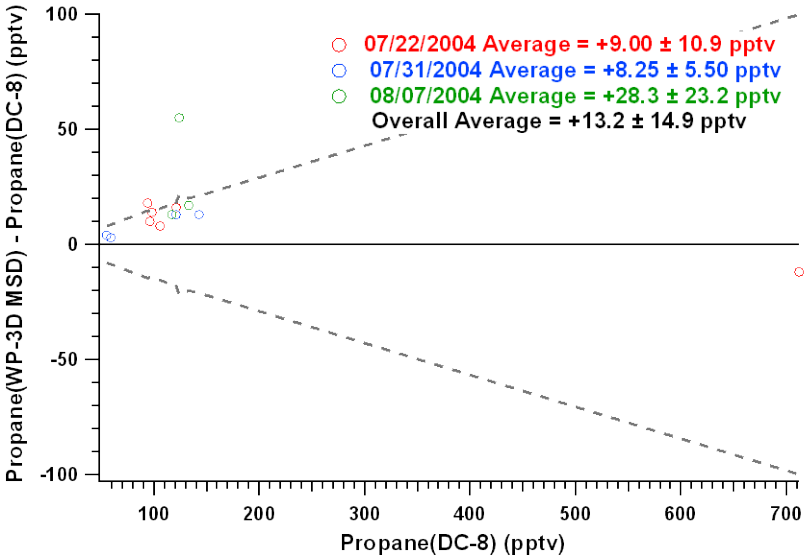

Figure 8. Difference between propane measurements from the three DC-8/WP-3D MSD intercomparison flights as a function of DC-8 propane. The dashed lines indicate the range of results expected from the reported 2σ measurement uncertainties.

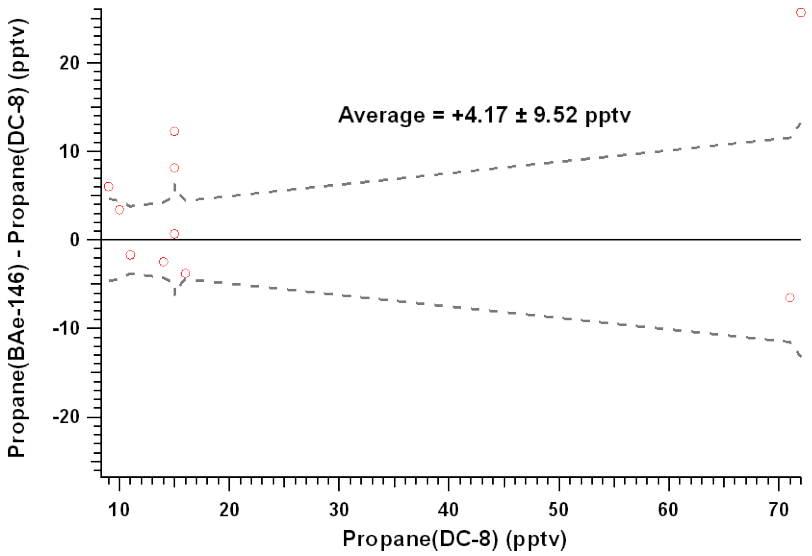

Figure 9. Difference between propane measurements from the DC-8/BAe-146 intercomparison flight as a function of DC-8 propane. The dashed lines indicate the range of results expected from the reported 2σ measurement uncertainties.

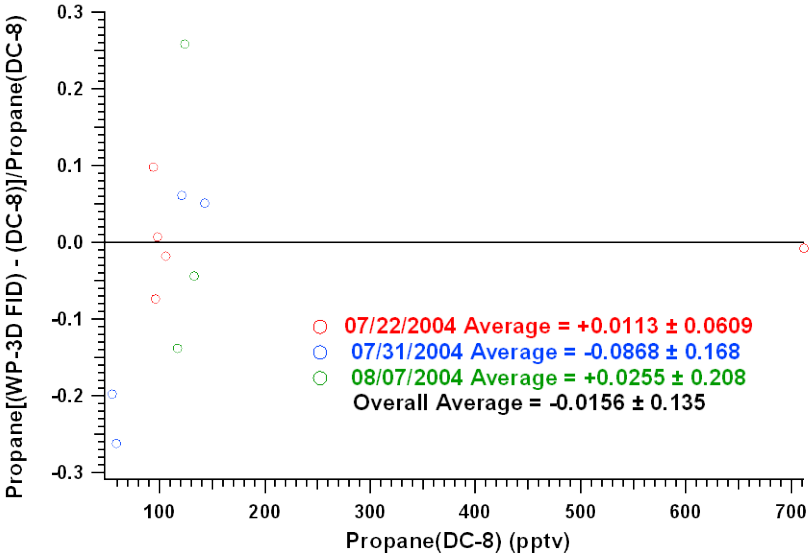

Figure 10. Relative difference between propane measurements from the three DC-8/WP-3D FID intercomparison flights as a function of DC-8 propane. A correction was made to account for bias.

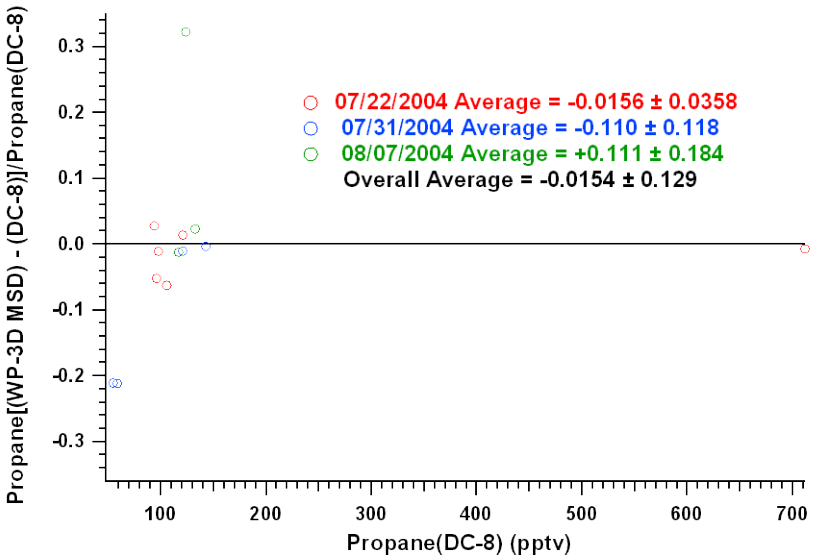

Figure 11. Relative difference between propane measurements from the three DC-8/WP-3D MSD intercomparison flights as a function of DC-8 propane. A correction was made to account for bias.

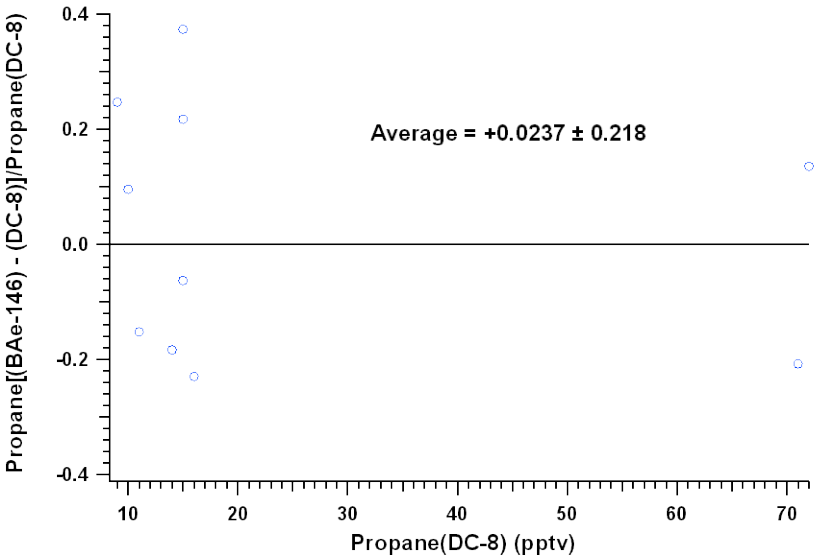

Figure 12. Relative difference between propane measurements from the DC-8/BAe-146 intercomparison flight as a function of DC-8 propane. A correction was made to account for bias.

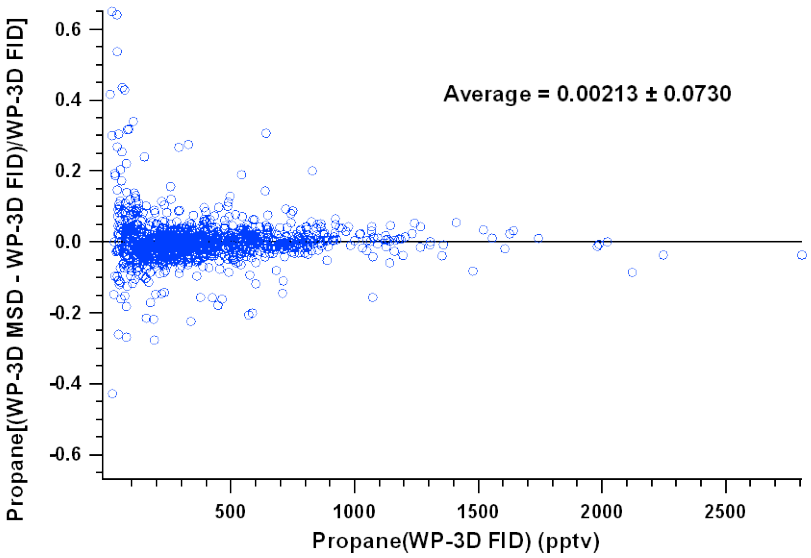

Figure 13. Relative difference between propane measurements from WP-3D FID and WP-3D MSD for all flights as a function of WP-3D FID propane.

References

Colman, J.J., et al. (2001), Description of the analysis of a wide range of volatile organic compounds in whole air samples collected during PEM-Tropics A and B, *Anal. Chem* ., 73, 3723-3731.

Fehsenfeld, F. C., et al. (2006), International Consortium for Atmospheric Research on Transport and Transformation (ICARTT): North America to Europe—Overview of the 2004 summer field study, *J. Geophys. Res., 111*, D23S01, doi:10.1029/2006JD007829.

Hopkins, J. R., K. A. Read, and A. C. Lewis. (2003), A Column Method For Long-term Monitoring Of Non-Methane Hydrocarbons (NMHCs) and Oxygenated Volatile Organic Compounds, *Journal of Environmental Monitoring*, 5 (1), 8-13.

Singh, H. B., et al. (2006), Overview of the summer 2004 Intercontinental Chemical Transport Experiment-North America (INTEX-A), *J. Geophys. Res., 111*, D24S01, doi:10.1029/2006JD007905.

TAbMEP Assessment: ICARTT C_2H_6 Measurements

1. Introduction

Here we provide the assessment for the ethane (C_2H_6) measurements during the summer 2004 ICARTT field campaign [*Fehsenfeld et al.*, 2006, *Singh et al*., 2006]. This assessment is based upon the four wing-tip-to-wing-tip intercomparison flights conducted during the field campaign. Recommendations provided here offer TAbMEP assessed biases for each of the measurements and a systematic approach to unifying the ICARTT C_2H_6 data for any integrated analysis. These recommendations are directly derived from the instrument performance demonstrated during the ICARTT measurement comparison exercises and are not to be extrapolated beyond this campaign.

2. ICARTT C_2H_6 Measurements

Three whole air sampler instruments were deployed on three aircraft. Table 1 summarizes these techniques and gives references for more information.

Table 1. C_2H_6 measurements deployed on aircraft during ICARTT

Aircraft	Instrument	Reference
NASA DC-8	Whole Air Sampler (WAS)	*Colman et al.* [2001]
NOAA WP-3D	Whole Air Sampler (WAS)	Contact PI: eatlas@rsmas.miami.edu
FAAM BAe-146	Whole Air Sampler (WAS)	*Hopkins et al.* [2003]

3. Summary of Results

Table 2 summarizes the assessed biases as well as PI reported uncertainties for each of the three C_2H_6 measurements involved in the intercomparisons. More detailed descriptions are provided to illustrate the process for the bias assessment in Section 4.1. The TAbMEP-prescribed IEIP procedures cannot be applied to the ICARTT C_2H_6 measurements for precision assessment. This is because the reported data have large time gaps and a small data population (see Section 3.1 of the introduction). The assessed bias reported in Table 2 (see Section 4.1 for details) can be applied to maximize the consistency between the data sets, by subtracting the value from the reported data to 'unify' the data sets. If one assumes instrument performance remained constant throughout the mission, the assessed bias may be extrapolated to the entire mission although it is derived from intercomparison periods only.

Table 2. Recommended ICARTT C_2H_6 measurement treatment

Aircraft/Instrument	Reported 2σ Uncertainty	Assessed Bias (pptv)
NASA DC-8 WAS	10%	$-14.92 - 0.0521\ C_2H_{6\ \text{DC-8}}$
NOAA WP-3D WAS	5%	$47.75 - 0.0725\ C_2H_{6\ \text{WP-3D}}$
FAAM BAe-146 WAS	Point by Point, average: 5.4%[a]	$-49.15 + 0.190\ C_2H_{6\ \text{BAe-146}}$

[a] The average encompasses only the comparison period for DC-8/BAe-146.

Figures 1 a and b display the PI reported uncertainties and recommended biases for the three ethane instruments.

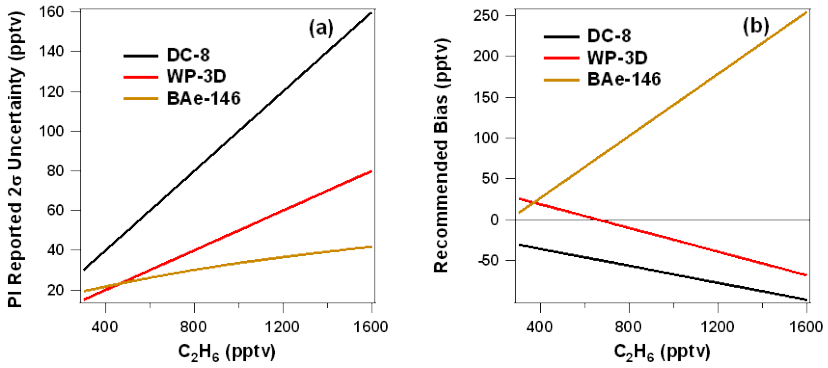

Figure 1. PI reported 2σ uncertainty (panel a) and recommended bias (panel b) for DC-8 (black), WP-3D (red), and BAe-146 (gold) as a function of C_2H_6 level. Values were calculated based upon data shown in Table 2. The BAe-146 PI reported uncertainty was calculated using a function derived from the 60 second merge file.

4. Results and Discussion

4.1 Bias Analysis

Section 3.3 in the introduction describes the process used to determine the best estimate bias. Figures 2 and 4 show the time series plots for the DC-8/WP-3D and DC-8/BAe-146 comparisons. The DC-8 is consistently lower than both WP-3D and BAe-146 by 45 pptv and 67 pptv on average respectively. Figures 5 and 6 show the magnitude of the bias for each intercomparison and Figures 7 and 8 show the corresponding relative residuals.

For 2 of the 3 DC-8/WP-3D flights, there are only 3 or 4 overlapping points with a small range of variation (about 20-40 pptv). It is not statistically significant to show the linear regression for these flights. Therefore, linear regression is performed over the data combined from all three DC-8/WP-3D flights shown in Figure 3. The linear relationships listed in Table 3 were derived from the regression equations found in Figures 3 and 4. The reference standard for comparison (RSC), as defined in the introduction, is constructed by averaging the NOAA WP-3D and NASA DC-8 measurements with equal weights of two each and the FAAM BAe-146 with a weight of one. (i.e. [2DC-8 + 2WP-3D + BAe-146]/5) The resulting RSC can be expressed as a function of the DC-8 C_2H_6 measurements as the following:

$$RSC_{C2H6} = 14.921 + 1.052\ C_2H_{6\text{-}DC8}$$

The RSC is then used to calculate the best estimate bias as described in Section 3.3 of the introduction. It should be noted that the initial choice of the reference instrument (DC-8 WAS) is arbitrary, and has no impact on the final recommendations. Table 3 summarizes the assessed measurement bias for each of the three ICARTT C_2H_6 measurements. Note that additional decimal places were carried in the calculations to ensure better precision. It is also noted that the intercept in the equations listed in Table 3 should not be viewed as an offset. These linear equations are used to best describe the linear relation between the measurements.

The WAS technique for measuring VOCs presents some challenges in analyzing the data. The DC-8 data have an integration time of approximately 60-70 seconds, while the WP-3D data have an integration time between 6-11 seconds. For these measurements to be considered simultaneous and correlated, the start and stop times of the WP-3D data must fall within the start

and stop times of the DC-8 data. In order to maximize the data coverage for statistical analysis, one exception is made to this rule. If the shorter (WP-3D) integration time falls outside the longer integration time by no more than two seconds, the data points are also considered to be simultaneous. BAe-146 integration times range from approximately 30-60 seconds. Since the DC-8 and BAe-146 have similar integration times, the measurements are considered correlated if the midpoint of DC-8 or BAe-146 fall within the start and stop time of the other measurement. Only the PI reported data are used in this assessment, and no interpolation is included. It is noted here the integration time difference may potentially be another factor leading to the difference between measurements.

Table 3. ICARTT C_2H_6 bias estimates

Aircraft/ Instrument	Linear Relationships	Best Estimate Bias ($a + b\ C_2H_6$) (pptv)
NASA DC-8 WAS	$C_2H_{6\ DC\text{-}8} = 0.00 + 1.000\ C_2H_{6\ DC\text{-}8}$	$-14.92 - 0.0521\ C_2H_{6\ DC\text{-}8}$
NOAA WP-3D WAS	$C_2H_{6\ WP\text{-}3D} = 58.43 + 0.981\ C_2H_{6\ DC\text{-}8}$	$47.75 - 0.0725\ C_2H_{6\ WP\text{-}3D}$
FAAM BAe-146 WAS	$C_2H_{6\ BAe\text{-}146} = -42.26 + 1.3\ C_2H_{6\ DC\text{-}8}$	$-49.15 + 0.190\ C_2H_{6\ BAe\text{-}146}$

As a part of ICARTT intercomparison standard exchange exercises, University of California, Irvine (UCI) prepared the common VOC samples that were sent to University of Miami (Miami), University of New Hampshire (UNH), and University of York (York) for their lab analyses. Some of these same institutions had instruments on the following planes during ICARTT: UCI on the DC-8, Miami on the WP-3D, and York on the BAe-146. The comparison incorporated 9 species, which included ethane. We believe that the inclusion of this comparison result will help the readers better understand the airborne intercomparison analysis. The difference in this lab comparison between the DC-8 and WP-3D instruments was 35 pptv, WP-3D being higher, at a DC-8 instrument reading of 1183 pptv. From the same lab comparison, the difference between the DC-8 and BAe-146 was 67 pptv, BAe-146 being higher. Comparing the ICARTT flights to this lab comparison shows fairly similar results. The difference for the DC-8/WP-3D flights is 10 pptv higher, whereas the difference for the DC-8/BAe-146 flights is the same as the lab comparison. Since instrument performance can vary depending on calibration and environmental factors, and the time intervals were not the same for all instruments, this difference between intercomparisons does not seem unnaturally large.

4.2 Precision Analysis

A detailed description of the precision assessment is given in Section 3.1 of the introduction. The IEIP precision, expected variability, and adjusted precision could not be calculated for C_2H_6 because of the small number of points and large time gaps between measurements.

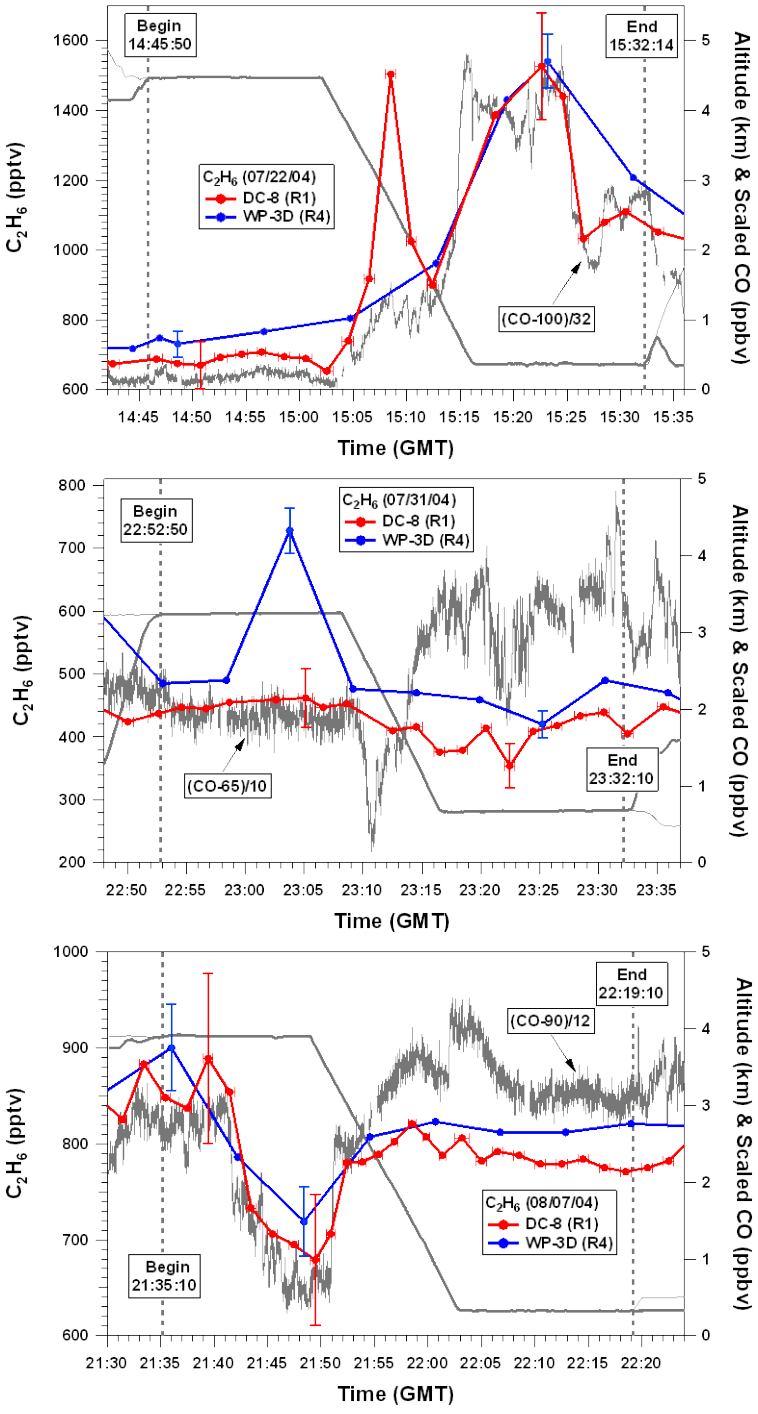

Figure 2. Time series of C_2H_6 measurements and aircraft altitudes from two aircraft on the three intercomparison flights between the NASA DC-8 and the NOAA WP-3D. Error bars represent the PI reported uncertainty. In parenthesis next to the plane is the data version number.

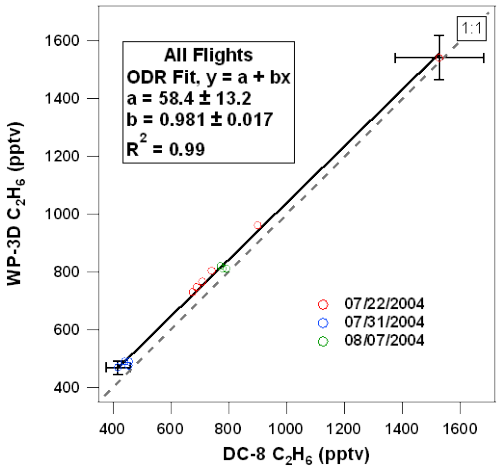

Figure 3. Combined correlation for the C_2H_6 measurements on NASA DC-8 and the NOAA WP-3D for 7/22, 7/31, and 8/07 2004. Error bars represent the PI reported uncertainty.

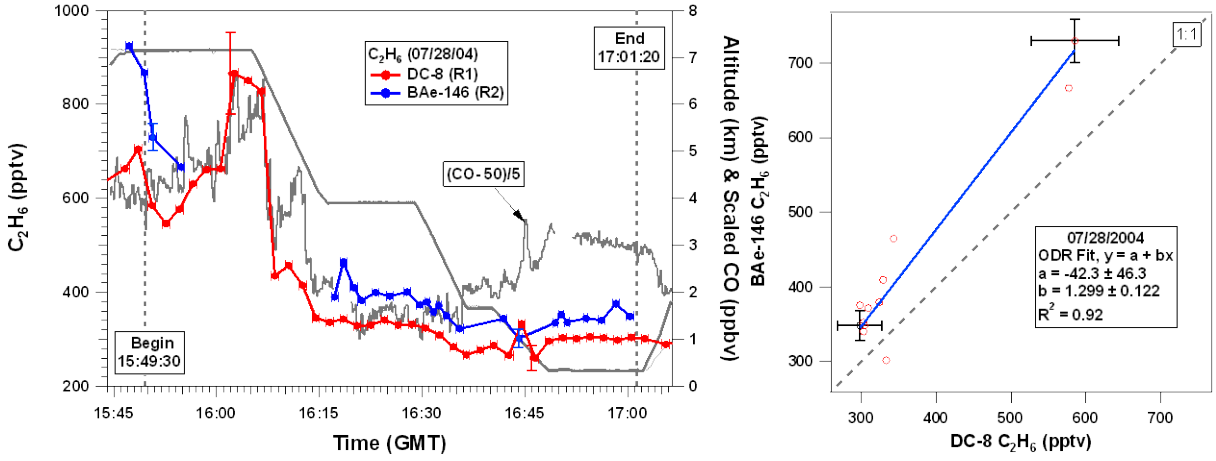

Figure 4. (left panel) Time series of C_2H_6 measurements and aircraft altitudes from the intercomparison flight between the NASA DC-8 and the FAAM BAe-146. In parenthesis next to the plane is the data version number. (right panel) Correlation between the C_2H_6 measurements on the two aircraft. Error bars represent the PI reported uncertainty.

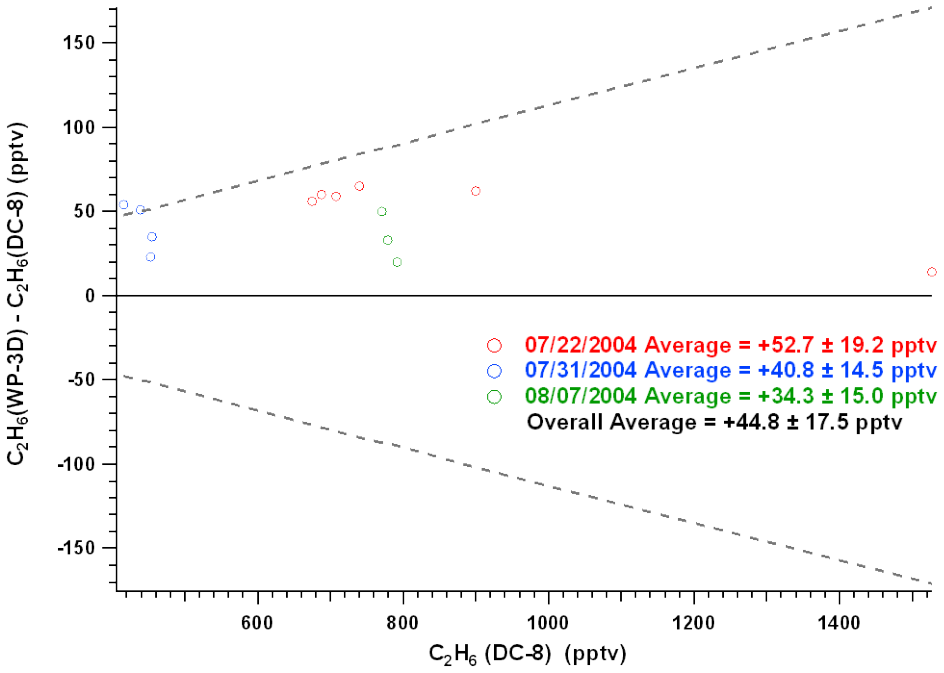

Figure 5. Difference between C_2H_6 measurements from the three DC-8/WP-3D intercomparison flights as a function of the DC-8 C_2H_6. The dashed lines indicate the range of the results expected from the reported measurement uncertainties.

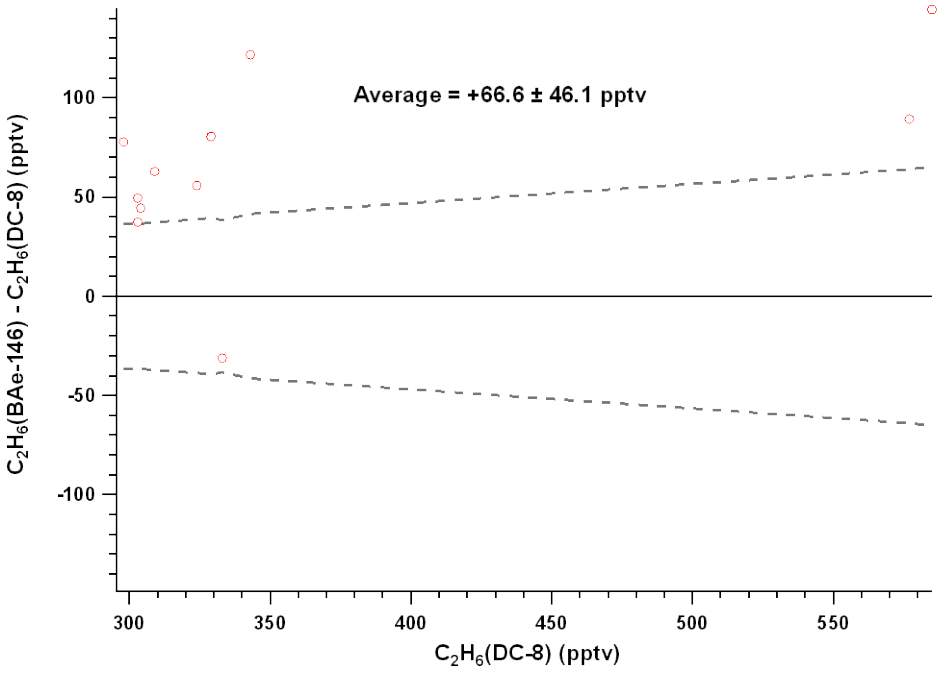

Figure 6. Difference between C_2H_6 measurements from the DC-8/BAe-146 intercomparison flight as a function of the DC-8 C_2H_6. The dashed lines indicate the range of the results expected from the reported measurement uncertainties.

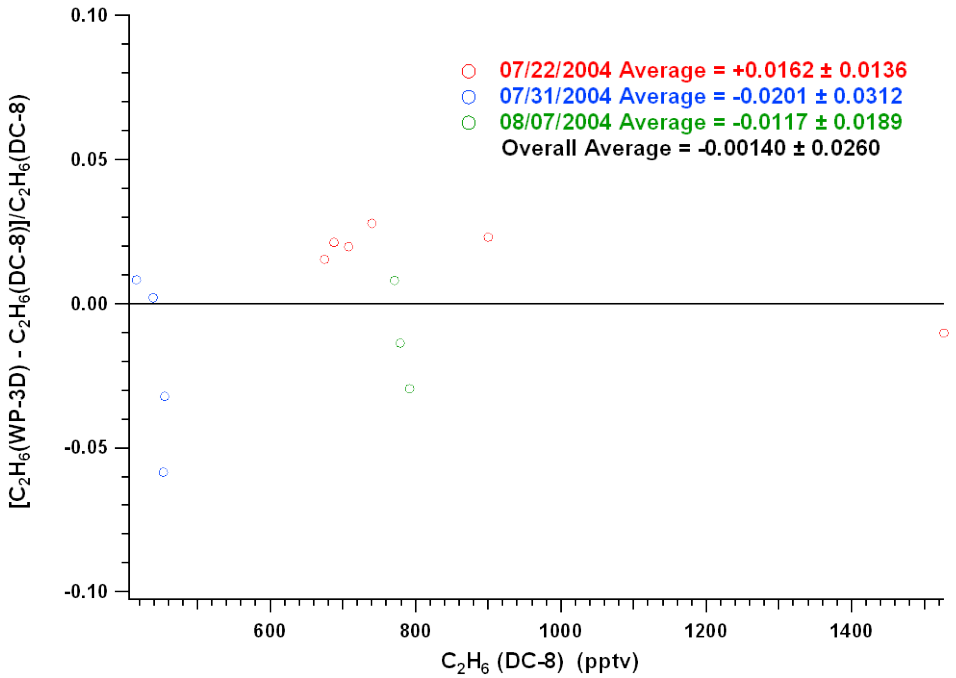

Figure 7. Relative difference between C_2H_6 measurements from the three DC-8/WP-3D intercomparison flights as a function of DC-8 C_2H_6. A correction was made to account for bias.

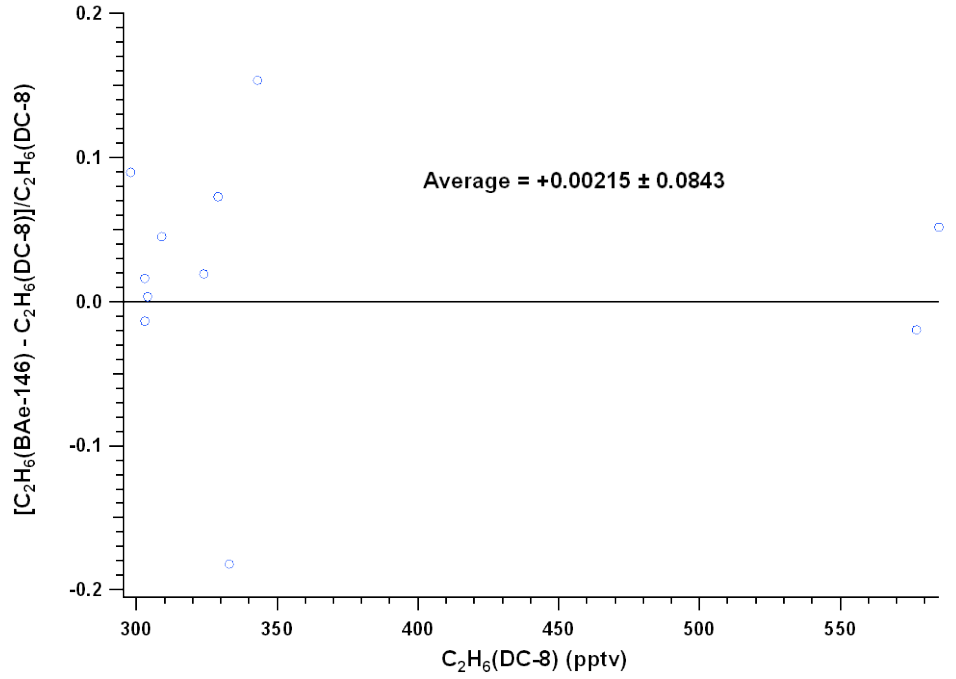

Figure 8. Relative difference between C_2H_6 measurements from the DC-8/BAe-146 intercomparison flight as a function of DC-8 C_2H_6. A correction was made to account for bias.

References

Colman, J.J., et al. (2001), Description of the analysis of a wide range of volatile organic compounds in whole air samples collected during PEM-Tropics A and B, *Anal. Chem* ., 73, 3723-3731.

Fehsenfeld, F. C., et al. (2006), International Consortium for Atmospheric Research on Transport and Transformation (ICARTT): North America to Europe—Overview of the 2004 summer field study, *J. Geophys. Res., 111*, D23S01, doi:10.1029/2006JD007829.

Hopkins, J. R., K. A. Read, and A. C. Lewis. (2003), A Column Method For Long-term Monitoring Of Non-Methane Hydrocarbons (NMHCs) and Oxygenated Volatile Organic Compounds, *Journal of Environmental Monitoring*, 5 (1), 8-13.

Singh, H. B., et al. (2006), Overview of the summer 2004 Intercontinental Chemical Transport Experiment-North America (INTEX-A), *J. Geophys. Res., 111*, D24S01, doi:10.1029/2006JD007905.

TAbMEP Assessment: ICARTT *n*-Butane Measurements

1. Introduction

Here we provide the assessment for the *n*-butane (C_4H_{10}) measurements during the summer 2004 ICARTT field campaign [*Fehsenfeld et al.*, 2006, *Singh et al*., 2006]. This assessment is based upon the four wing-tip-to-wing-tip intercomparison flights conducted during the field campaign. Recommendations provided here offer TAbMEP assessed biases for each of the measurements and a systematic approach to unifying the ICARTT *n*-butane data for any integrated analysis. These recommendations are directly derived from the instrument performance demonstrated during the ICARTT measurement comparison exercises and are not to be extrapolated beyond this campaign.

2. ICARTT *n*-Butane Measurements

Three whole air sampler instruments were deployed on three aircraft. Table 1 summarizes these techniques and gives references for more information.

Table 1. *n*-Butane measurements deployed on aircraft during ICARTT

Aircraft	Instrument	Reference
NASA DC-8	Whole Air Sampler (WAS)	*Colman et al.* [2001]
NOAA WP-3D	Whole Air Sampler (WAS)	Contact PI: eatlas@rsmas.miami.edu
FAAM BAe-146	Whole Air Sampler (WAS)	*Hopkins et al.* [2003]

3. Summary of Results

Table 2 summarizes the assessed biases as well as PI reported uncertainties for each of the three *n*-butane measurements involved in the intercomparisons. More detailed descriptions are provided to illustrate the process for the bias assessment in Section 4.1. The TAbMEP-prescribed IEIP procedures cannot be applied to the ICARTT *n*-butane measurements for precision assessment. This is because the reported data have large time gaps and a small data population (see Section 3.1 of the introduction). The assessed bias reported in Table 2 (see Section 4.1 for details) can be applied to maximize the consistency between the data sets, by subtracting the value from the reported data to 'unify' the data sets. If one assumes instrument performance remained constant throughout the mission, the assessed bias may be extrapolated to the entire mission although it is derived from intercomparison periods only. No assessed bias is included for the FAAM BAe-146 because there were only two overlapping points both platforms reported non-LOD (limit of detection) values. Although good agreement is shown for these points, there are two other overlapping points where DC-8 reported LOD but BAe-146 gave values around 6 pptv. Given these mixed results, no definitive assessment can be made with reasonable level of confidence.

The DC-8 and WP-3D uncertainties reported by PIs are a percentage. This may not be adequate at very low end concentration levels. Ideally, the measurement uncertainty may be better represented in the form of x pptv or y%. Based on the intercomparison data, the TAbMEP analysis cannot provide such assessment. Data users should contact the respective PIs about the proper uncertainties when dealing with the low end of measurements, e.g., < ~20 pptv.

Table 2. Recommended ICARTT *n*-butane measurement treatment

Aircraft/Instrument	Reported 2σ Uncertainty	Assessed Bias (pptv)
NASA DC-8 WAS	10%	$-2.631 + 0.0705\ C_4H_{10\ DC\text{-}8}$
NOAA WP-3D WAS	10%	$3.063 - 0.0821\ C_4H_{10\ WP\text{-}3D}$
FAAM BAe-146 WAS	Point by Point, average: 48%[a]	N/A

[a] The average encompasses only the comparison period for DC-8/BAe-146.

Figures 1 a and b display the PI reported uncertainties and recommended biases for the three *n*-butane instruments.

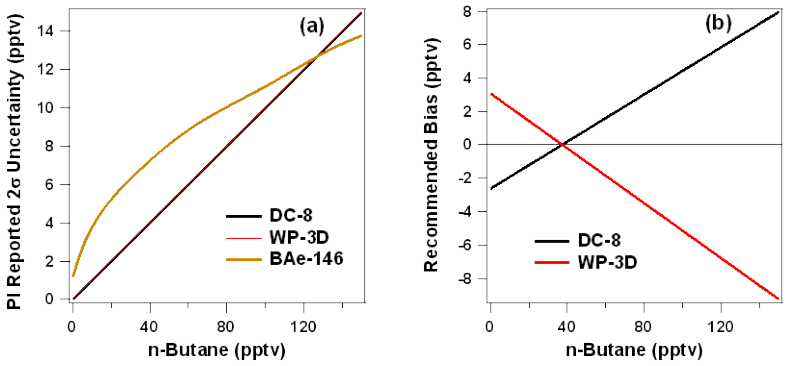

Figure 1. PI reported 2σ uncertainty (panel a) and recommended bias (panel b) for DC-8 (black), WP-3D (red), and BAe-146 (gold) as a function of *n*-butane level. Values were calculated based upon data shown in Table 2. The BAe-146 PI reported uncertainty was calculated using a function derived from the 60 second merge file.

4. Results and Discussion

4.1 Bias Analysis

Section 3.3 in the introduction describes the process used to determine the best estimate bias. Figures 2 and 4 show the time series plots for the DC-8/WP-3D and DC-8/BAe-146 comparisons. The DC-8 is generally lower than the WP-3D by 1 pptv on average, with a majority of the variance about 4 pptv. Figure 4 shows four overlapping points. For two of them at the beginning of the intercomparison period, both BAe-146 and DC-8 reported values and have agreement within 0.5 pptv; while the difference for the other two overlapping points can be as large as 6 pptv where DC-8 consistently reported LOD values. Figure 5 shows the magnitude of the bias for the intercomparison and Figure 6 shows the corresponding relative residuals. Both plots suggest that the PI reported uncertainties may not be adequate for the lowest part of data set, e.g. < ~20 pptv.

For 2 of the 3 DC-8/WP-3D flights, there are only 3 or 4 overlapping points with a small range of variation (about 10 - 60 pptv). It is not statistically significant to show the linear regression for these flights. Therefore, linear regression is performed over the data combined from all three DC-8/WP-3D flights. The linear relationships listed in Table 3 were derived from the regression equation found in Figure 3. The reference standard for comparison (RSC), as defined in the introduction, is constructed by averaging the NOAA WP-3D and NASA DC-8 measurements with equal weights. The FAAM BAe-146 is not included in the calculation of the reference standard for comparison. As discussed earlier, there were only four comparison points and LOD

values were involved with two of the four points. Both factors restricted our ability to perform a robust assessment between BAe-146 and DC-8 measurements. The resulting RSC can be expressed as a function of the DC-8 C_4H_{10} measurements as the following:

$$RSC_{C4H10} = 2.631 + 0.929\ C_4H_{10\text{-}DC8}$$

The RSC is then used to calculate the best estimate bias as described in Section 3.3 of the introduction. It should be noted that the initial choice of the reference instrument (DC-8 WAS) is arbitrary, and has no impact on the final recommendations. Table 3 summarizes the assessed measurement bias for two of the ICARTT *n*-butane measurements. Note that additional decimal places were carried in the calculations to ensure better precision. It is also noted that the intercept in the equations listed in Table 3 should not be viewed as an offset. These linear equations are used to best describe the linear relation between the measurements.

The WAS technique for measuring VOCs presents some challenges in analyzing the data. The DC-8 data have an integration time of approximately 60-70 seconds, while the WP-3D data have an integration time between 6-11 seconds. For these measurements to be considered simultaneous and correlated, the start and stop times of the WP-3D data must fall within the start and stop times of the DC-8 data. In order to maximize the data coverage for statistical analysis, one exception is made to this rule. If the shorter (WP-3D) integration time falls outside the longer integration time by no more than two seconds, the data points are also considered to be simultaneous. BAe-146 integration times range from approximately 30-60 seconds. Since the DC-8 and BAe-146 have similar integration times, the measurements are considered correlated if the midpoint of DC-8 or BAe-146 fall within the start and stop time of the other measurement. In the case of the *n*-butane DC-8/BAe-146 comparison, several points were below the LOD and are not used for comparison analysis. Only the PI reported data are used in this assessment, and no interpolation is included. It is noted here the integration time difference may potentially be another factor leading to the difference between measurements.

Table 3. ICARTT *n*-Butane bias estimates

Aircraft/ Instrument	Linear Relationships	Best Estimate Bias ($a + b\ C_4H_{10}$) (pptv)
NASA DC-8 WAS	$C_4H_{10\ DC\text{-}8} = 0.00 + 1.000\ C_4H_{10\ DC\text{-}8}$	$-2.631 + 0.0705\ C_4H_{10\ DC\text{-}8}$
NOAA WP-3D WAS	$C_4H_{10\ WP\text{-}3D} = 5.26 + 0.859\ C_4H_{10\ DC\text{-}8}$	$3.063 - 0.0821\ C_4H_{10\ WP\text{-}3D}$
FAAM BAe-146 WAS	N/A	N/A

As a part of ICARTT intercomparison standard exchange exercises, University of California, Irvine (UCI) prepared the common VOC samples that were sent to University of Miami (Miami), University of New Hampshire (UNH), and University of York (York) for their lab analyses. Some of these same institutions had instruments on the following planes during ICARTT: UCI on the DC-8, Miami on the WP-3D, and York on the BAe-146. The comparison incorporated 9 species, which included *n*-butane. We believe that the inclusion of this comparison result will help the readers better understand the airborne intercomparison analysis. The difference in this lab comparison between the DC-8 and WP-3D instruments was 6 pptv, WP-3D being higher, at a

DC-8 instrument reading of 434 pptv. From the same lab comparison, the difference between the DC-8 and BAe-146 was 7 pptv, BAe-146 being higher. Comparing the ICARTT flights to this lab comparison shows fairly similar results even though the flights only provide a few comparison points.

4.2 Precision Analysis

A detailed description of the precision assessment is given in Section 3.1 of the introduction. The IEIP precision, expected variability, and adjusted precision could not be calculated for *n*-butane because of the small number of points and large time gaps between measurements.

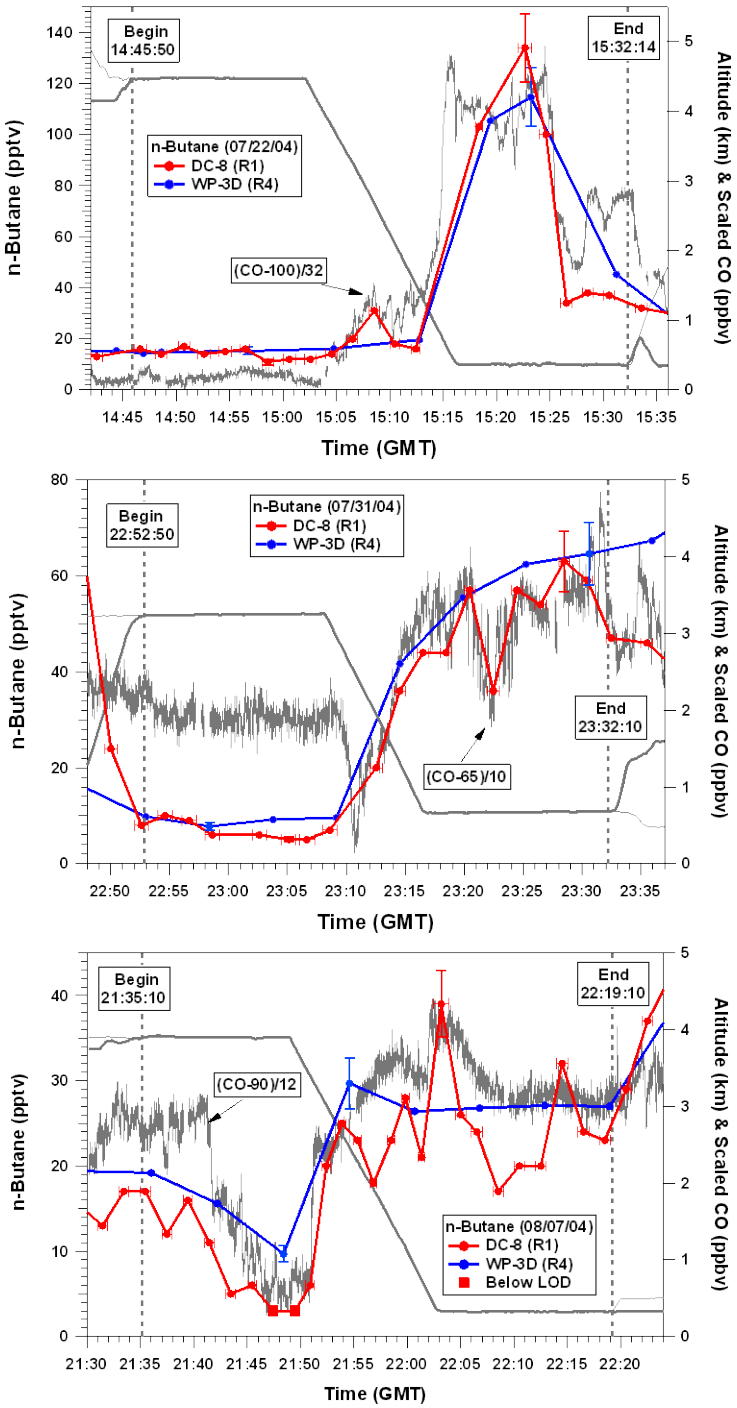

Figure 2. Time series of *n*-butane measurements and aircraft altitudes from two aircraft on the three intercomparison flights between the NASA DC-8 and the NOAA WP-3D. Error bars represent the PI reported uncertainty. In parenthesis next to the plane is the data version number.

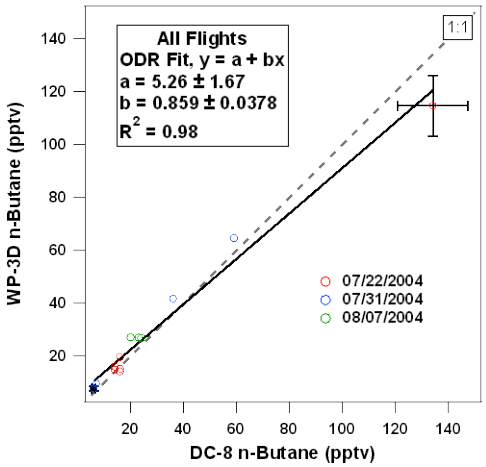

Figure 3. Combined correlation for the *n*-butane measurements on NASA DC-8 and the NOAA WP-3D for 7/22, 7/31, and 8/07 2004. Error bars represent the PI reported uncertainty.

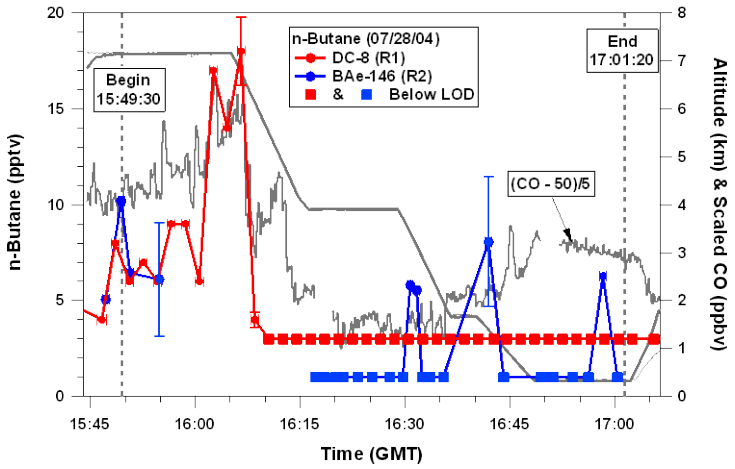

Figure 4. Time series of *n*-butane measurements and aircraft altitudes from the intercomparison flight between the NASA DC-8 and the FAAM BAe-146. Error bars represent the PI reported uncertainty. In parenthesis next to the plane is the data version number.

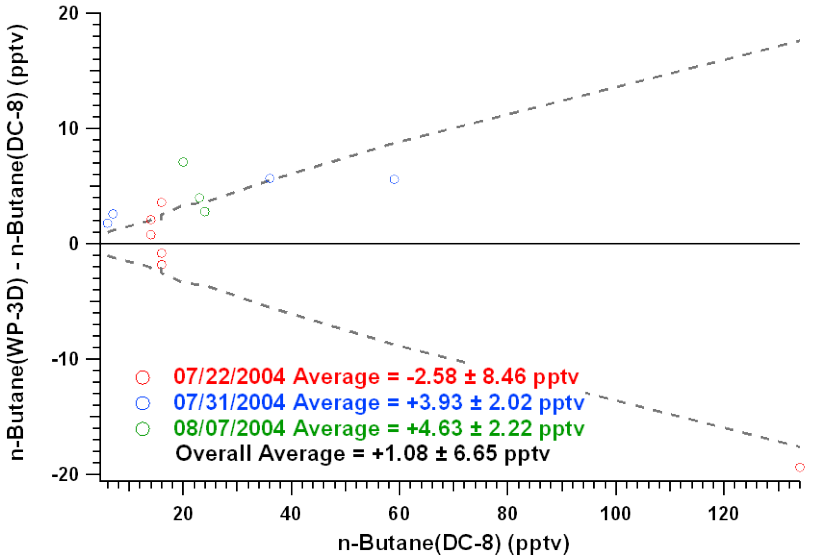

Figure 5. Difference between *n*-butane measurements from the three DC-8/WP-3D intercomparison flights as a function of DC-8 *n*-butane. The dashed lines indicate the range of results expected from the reported 2σ measurement uncertainties.

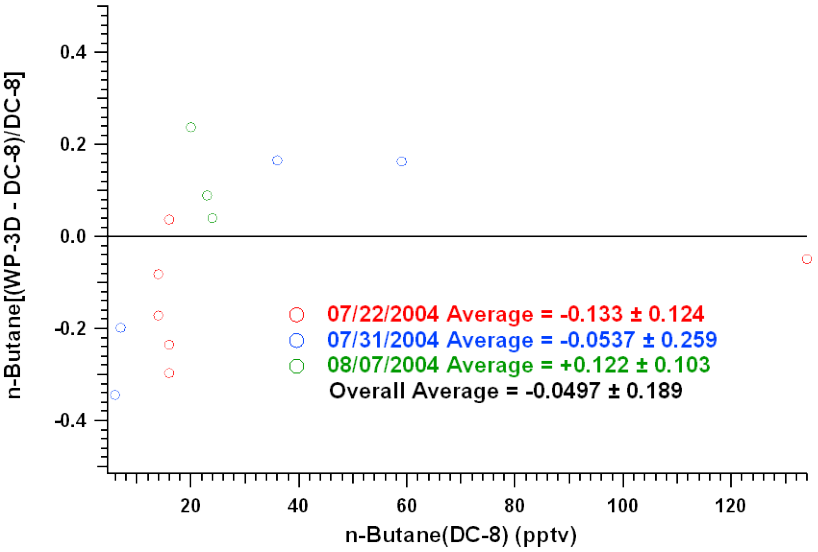

Figure 6. Relative difference between *n*-butane measurements from the three DC-8/WP-3D intercomparison flights as a function of DC-8 *n*-butane. A correction was made to account for bias.

References

Colman, J.J., et al. (2001), Description of the analysis of a wide range of volatile organic compounds in whole air samples collected during PEM-Tropics A and B, *Anal. Chem* ., 73, 3723-3731.

Fehsenfeld, F. C., et al. (2006), International Consortium for Atmospheric Research on Transport and Transformation (ICARTT): North America to Europe—Overview of the 2004 summer field study, *J. Geophys. Res., 111*, D23S01, doi:10.1029/2006JD007829.

Hopkins, J. R., K. A. Read, and A. C. Lewis. (2003), A Column Method For Long-term Monitoring Of Non-Methane Hydrocarbons (NMHCs) and Oxygenated Volatile Organic Compounds, *Journal of Environmental Monitoring*, 5 (1), 8-13.

Singh, H. B., et al. (2006), Overview of the summer 2004 Intercontinental Chemical Transport Experiment-North America (INTEX-A), *J. Geophys. Res., 111*, D24S01, doi:10.1029/2006JD007905.

TAbMEP Assessment: ICARTT NO_2 Measurements

1. Introduction

Here we provide the assessment for the nitrogen dioxide (NO_2) measurements taken from two aircraft platforms during the summer 2004 ICARTT field campaign [*Fehsenfeld et al.*, 2006, *Singh et al*., 2006]. This assessment is based upon the three wing-tip-to-wing-tip DC-8/WP-3D intercomparison flights conducted during the field campaign. Detailed analyses were not conducted on the BAe-146 data due to instrument problems during installation. Recommendations provided here offer TAbMEP assessed uncertainties for each of the measurements and a systematic approach to unifying the ICARTT NO_2 data for any integrated analysis. These recommendations are directly derived from the instrument performance demonstrated during the ICARTT measurement comparison exercises and are not to be extrapolated beyond this campaign.

2. ICARTT NO_2 Measurements

Two different NO_2 instruments were deployed on the two aircraft. Table 1 summarizes these techniques and gives references for more information.

Table 1. NO_2 measurements deployed on aircraft during ICARTT

Aircraft	Instrument	Reference
NASA DC-8	Thermal Dissociation-Laser Induced Fluorescence (TD-LIF)	*Thornton et al.* [2000]
NOAA WP-3D	UV Photolysis followed by NO chemiluminescense (P-CL)	*Ryerson et al.* [2000]

3. Summary of Results

Table 2 summarizes the assessed 2σ precisions, biases, and uncertainties for the DC-8 and WP-3D instruments for 20 second data. These assessments listed in Table 2 are only recommended for the NO_2 concentrations observed during the intercomparisons (0 – 800 pptv). For the DC-8 and WP-3D analyses, detailed descriptions are provided to illustrate the process for assessment of bias and precision in Sections 4.1 and 4.2 respectively. The assessed 2σ precisions reported in Table 2 are equal to twice the highest adjusted precision value for that instrument listed in Table 4, which should be treated as the upper limit value. It is clearly shown in Section 4.2 that the measurement precision is a strong function of the ambient NO_2 levels and improves significantly at higher levels. The precision estimate given in Table 2 is largely driven by the data population concentrated at low NO_2 values. Table 2 also reports an assessed bias (see Section 4.1 for details) that can be applied to maximize the consistency between the data sets. The assessed bias should be subtracted from the reported data to 'unify' the data sets. The assessed 2σ uncertainty is taken as the PI reported uncertainty because the PI uncertainty sufficiently covers all difference between the two instruments (see section 4.2). The data sets are consistent and suitable for integrated analysis. The assessed bias is well within the accuracy values reported for DC-8 and WP-3D measurements.

Table 2. Recommended ICARTT NO_2 measurement treatment

Aircraft/ Instrument	Reported 2σ Uncertainty	Assessed 2σ Precision	Assessed Bias (pptv)	Assessed 2σ Uncertainty
NASA DC-8 TD-LIF	Accuracy: 5% Point by point, average: 62%[a]	50%	-0.52 – 0.0311 $NO_{2\text{-}DC8}$	PI uncertainty
NOAA WP-3D P-CL	Accuracy: 8% Precision: ± 40 pptv	32%	0.49 + 0.0292 $NO_{2\text{-}WP3D}$	PI uncertainty

[a] The average encompasses only the comparison periods for the DC-8/WP-3D.

Figures 1a through 1c display the precisions, biases, and recommended uncertainties for the two NO_2 instruments. The assessed measurement biases are well within the accuracy values provided by the DC-8 and WP-3D PIs.

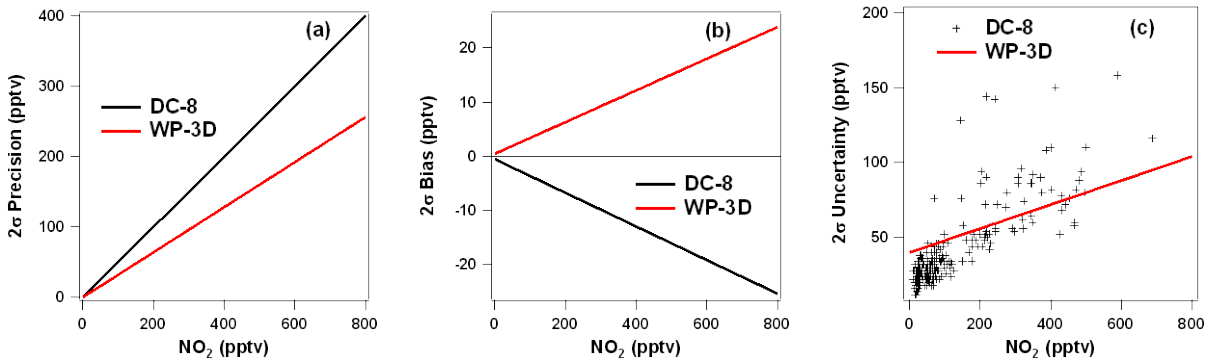

Figure 1. 2σ precision (panel a), 2σ bias (panel b), and 2σ uncertainty (panel c) for DC-8 (black) and WP-3D (red) as a function of NO_2. Values were calculated based upon data shown in Table 2. The DC-8 uncertainty is the PI reported point by point uncertainty during the DC-8/WP-3D comparison periods.

4. Results and Discussion

4.1 Bias Analysis

Section 3.3 in the Introduction describes the process used to determine the best estimate bias. Figure 2 shows the time series plots and correlations for each of the WP-3D vs. DC-8 comparisons. The time series plots are based on 1 second data for both the DC-8 and WP-3D, and the correlations are based on 20 second data. The PI reported 20 second DC-8 data was used and the PI reported WP-3D 1 second data was averaged into the DC-8 time intervals. The linear relationships listed in Table 3 were derived from the regression equation shown in Figure 3. The data used in Figure 3 was 20 second data. The 20 second average was chosen to minimize noise and better represent the overall trend, given that there is a substantial portion of data at very low values, i.e., <60 pptv. The reference standard for comparison (RSC), as defined in the Introduction, is constructed by averaging the NOAA WP-3D and NASA DC-8. The resulting RSC can be expressed as a function of the DC-8 NO_2 measurement as the following:

$$RSC_{NO2} = 0.52 + 1.031\ NO_{2\text{-}DC8}$$

The RSC is then used to calculate the best estimate bias as described in Section 3.3 of the Introduction. It should be noted that the initial choice of the reference instrument (DC-8) is

arbitrary, and has no impact on the final recommendations. Table 3 summarizes the assessed measurement bias for the WP-3D and DC-8 ICARTT NO_2 measurements. Note that additional decimal places were carried in the calculations to ensure better precision.

Table 3. ICARTT NO_2 bias estimates

Aircraft/ Instrument	Linear Relationships[a]	Best Estimate Bias (a + b NO_2) (pptv)
NASA DC-8 TD-LIF	$NO_{2\text{-DC8}} = 0.00 + 1.000\ NO_{2\text{-DC8}}$	$-0.52 - 0.031\ NO_{2\text{-DC8}}$
NOAA WP-3D P-CL	$NO_{2\text{-WP3D}} = 1.05 + 1.062\ NO_{2\text{-DC8}}$	$0.49 + 0.029\ NO_{2\text{-WP3D}}$

[a]Derived from Fig. 3.

4.2 Precision Analysis

A detailed description of the precision assessment is given in Section 3.1 of the Introduction. The IEIP precision, expected variability, observed variability, and the adjusted precision are summarized in Table 4. Based on the results presented in Table 4, the largest "adjusted precision" value is taken as a conservative precision estimate for each ICARTT NO_2 instrument and twice that value is listed in Table 2 as the assessed 2σ precision. It should be noted that IEIP is dependent on concentration and this can account for the large difference between the IEIP for the DC-8 instrument between 07/22 and 08/07. The average DC-8 concentration on 07/22 is 399 pptv, whereas the average concentration on 08/07 is 109 pptv. The aforementioned averages are for the entire flight (not just comparison periods) because IEIP is calculated for the entire flight.

To minimize the effect of bias, we make corrections for bias before computing the observed variability, as the bias may have a significant impact on the observed variability. Figure 4 shows the magnitude of the bias for each intercomparison. As shown in the figure, the residuals are well within the 2σ PI reported uncertainties. The assessed values of the observed variability are displayed in Figure 5. As can be seen in this figure, the variability is dependent on concentration. On 07/22 and 08/07 the variability is much higher because the sampling during the comparison period was at lower concentration levels, whereas 07/31 was at higher concentration levels and has a much lower variability.

The final analysis results are shown in Table 2. Well over 90% of the data falls within the combined PI reported uncertainties for each intercomparison, which is consistent with the TAbMEP guideline for unified data sets. Therefore, no change to the PI uncertainty is recommended.

Table 4. ICARTT NO_2 precision (1σ) comparisons

Flight	Platform	IEIP Precision	Expected Variability	Observed Variability	Adjusted Precision
07/22	DC-8	15%	19%	26%	21%
	WP-3D	12%			16%
07/31	DC-8	15%	19%	9%	25%
	WP-3D	12%			12%
08/07	DC-8	23%	27%	24%	23%
	WP-3D	15%			15%

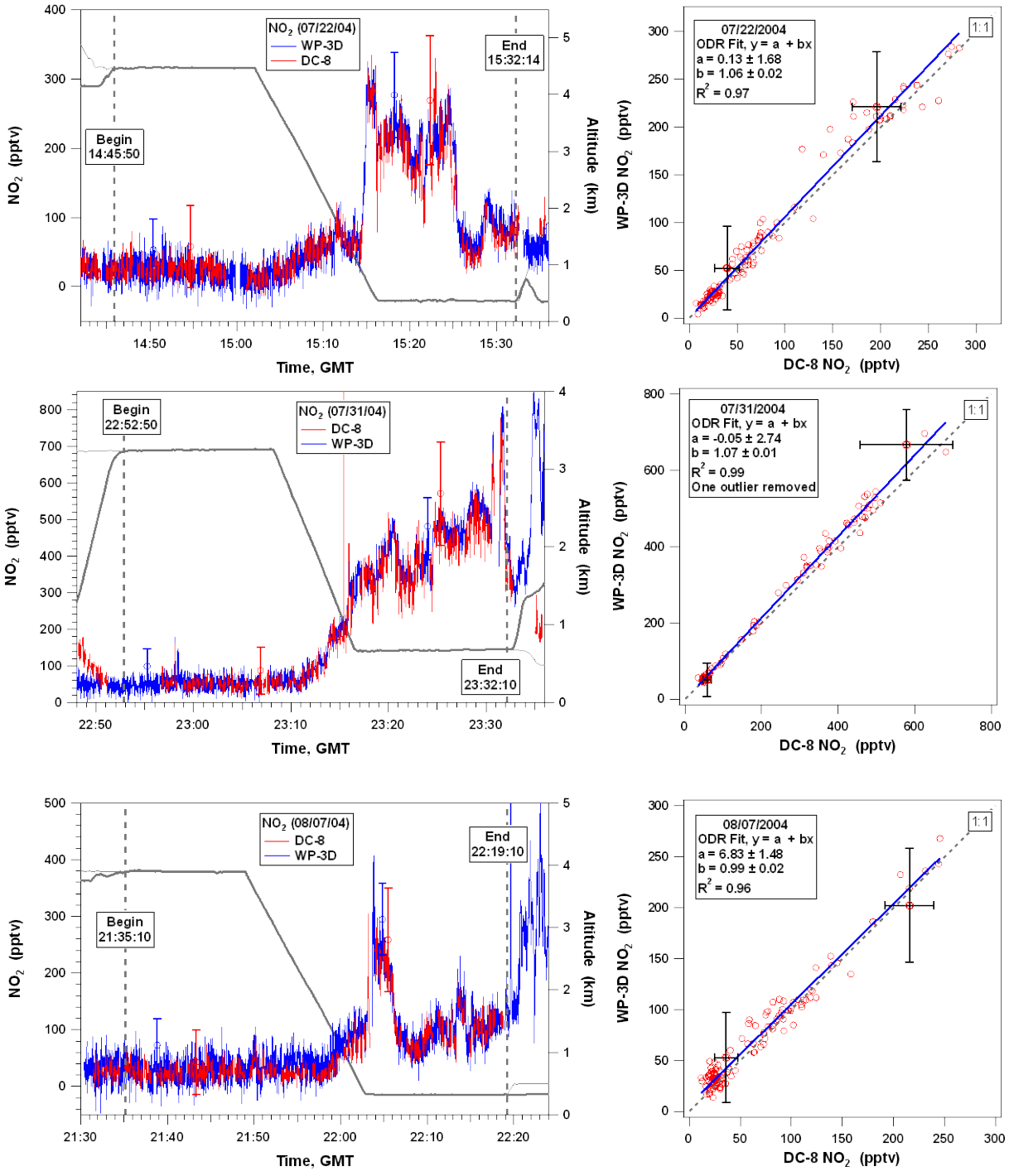

Figure 2. (left panels) Time series of NO_2 measurements and aircraft altitudes from two aircraft on the three intercomparison flights between the NASA DC-8 and the NOAA WP-3D. Note that the DC-8 and WP-3D data is 1 second in the time series plot. (right panels) Correlations between 20 second averages of the NO_2 measurements on the two aircraft. PI reported DC-8 20 second data is used in the regression figures and WP-3D 1 second data was averaged into the DC-8 time intervals.

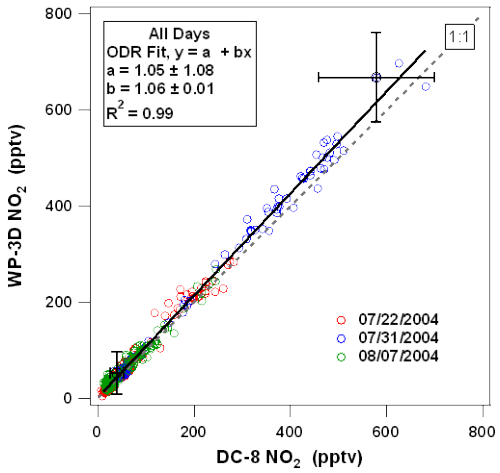

Figure 3. Correlation between 20 second averages of the NO_2 measurements on the DC-8 and WP-3D for 7/22, 7/31, and 8/7 2004.

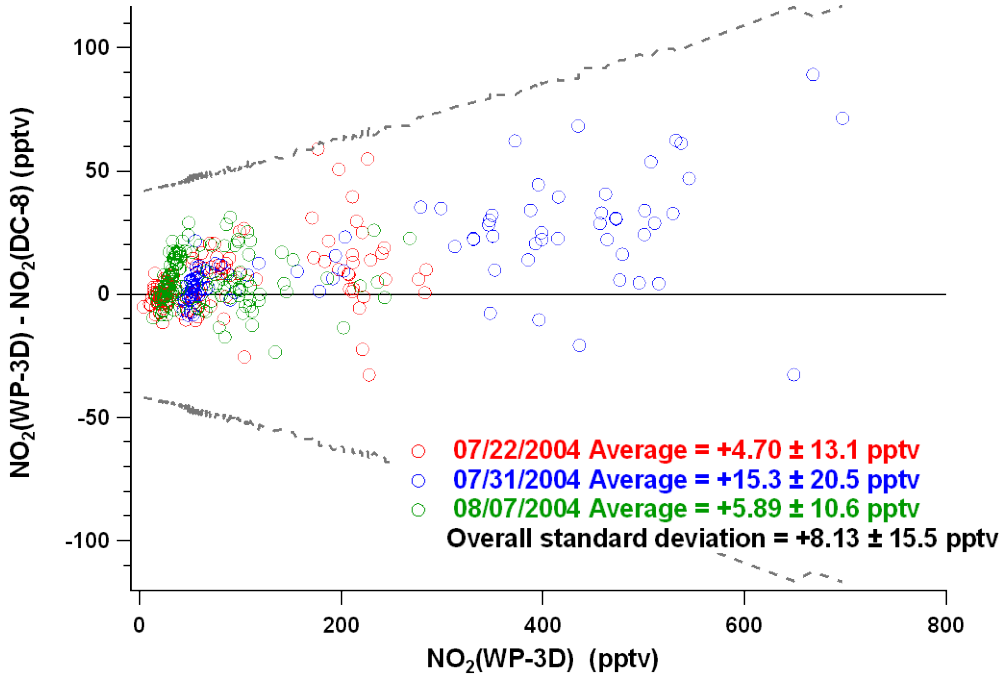

Figure 4. Difference between NO_2 measurements from the three DC-8/WP-3D intercomparison flights as a function of the WP-3D NO_2. The dashed lines indicate the range of the results expected from the reported 2σ measurement uncertainties.

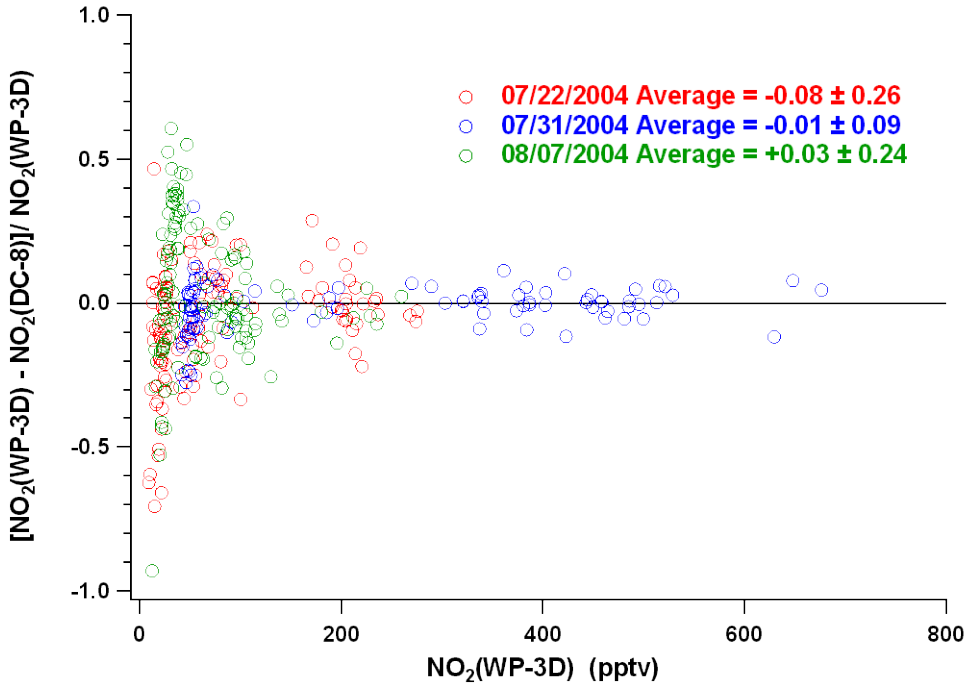

Figure 5. Relative difference between NO_2 measurements from the three DC-8/WP-3D intercomparison flights as a function of the WP-3D NO_2. A correction was made to account for bias. One outlier at about -2 is not shown for 07/22.

References

Fehsenfeld, F. C., et al. (2006), International Consortium for Atmospheric Research on Transport and Transformation (ICARTT): North America to Europe—Overview of the 2004 summer field study, *J. Geophys. Res., 111*, D23S01, doi:10.1029/2006JD007829.

Ryerson, T.B., E. J. Williams, and F. C. Fehsenfeld. (2000), An efficient photolysis system for fast-response NO_2 measurements, *J. Geophys. Res.,* 105(D21), 26,447–26,461, doi:10.1029/2000JD900389.

Singh, H. B., et al. (2006), Overview of the summer 2004 Intercontinental Chemical Transport Experiment-North America (INTEX-A), *J. Geophys. Res., 111*, D24S01, doi:10.1029/2006JD007905.

Thornton, J. A., P. J. Wooldridge, and R. C. Cohen (2000), Atmospheric NO_2: In Situ Laser-Induced Fluorescence Detection at Parts per Trillion Mixing Ratios, *Analytical Chemistry, 72*, 528.

TAbMEP Assessment: ICARTT HNO_3 Measurements

1. Introduction

Here we provide the assessment for the nitric acid (HNO_3) measurements during the summer 2004 ICARTT field campaign [*Fehsenfeld et al.*, 2006, *Singh et al*., 2006]. The inter-platform assessment is based upon the three wing-tip-to-wing-tip intercomparison flights conducted during the field campaign. The two DC-8 instruments are compared using all available data from the mission (flights 6 – 20). Recommendations provided here offer TAbMEP assessed uncertainties for each of the measurements and a systematic approach to unifying the ICARTT HNO_3 data for any integrated analysis. These recommendations are directly derived from the instrument performance demonstrated during the ICARTT measurement comparison exercises and are not to be extrapolated beyond this campaign.

2. ICARTT HNO_3 Measurements

Three different HNO_3 instruments were deployed on two aircraft. Table 1 summarizes these techniques and gives references for more information. The two CIMS systems report data integrated for less than 1 second and the MC system has an integration time of ~100 seconds.

Table 1. HNO_3 measurements deployed on aircraft during ICARTT

Aircraft	Instrument	Reference
NASA DC-8	Mist chamber (MC)	*Scheuer et al.* [2010]
NASA DC-8	Chemical ionization mass spectrometer (CIMS)	*Crounse et al.* [2006]
NOAA WP-3D	Chemical ionization mass spectrometer (CIMS)	*Neuman et al.* [2002, 2006]

3. Summary of Results

Table 2 summarizes the assessed 2σ precisions, biases, and uncertainties, along with PI reported uncertainties. More detailed descriptions are provided to illustrate the process for assessment of bias and precision in Sections 4.1 and 4.2 respectively. The assessed 2σ precisions reported in Table 2 are equal to twice the highest adjusted precision value for that instrument listed in Table 5. Table 2 also reports an assessed bias (see Section 4.1 for details) that can be applied to maximize the consistency between the data sets. The assessed bias should be subtracted from the reported data to 'unify' the data sets when conducting an integrated analysis. The assessed bias is derived from intercomparison periods only and may be extrapolated to the entire mission if one assumes instrument performance remained constant throughout the mission. The recommended 2σ uncertainty in Table 2 is the larger of either the uncertainty reported by the PI or the quadrature-sum of the assessed 2σ precision and assessed bias listed in Table 2.

This intercomparison has led to the identification of a problem with the DC-8 CIMS stratospheric data. *The DC-8 CIMS PI has indicated that he will resubmit his data files by removing the stratospheric data and reprocessing the data based on the ICARTT water assessment report. We opt to keep the comparison of stratospheric data in the current version of the assessment to be consistent with the current data archive status. This report will be updated when the revised data is posted in the archive.* It is noted that the DC-8 CIMS PI uncertainty is reported point by point at 90% confidence level. This is slightly different from the others, which are reported as 2σ uncertainty (95% CI).

Table 2. Recommended ICARTT HNO_3 measurement treatment

Aircraft/ Instrument	Reported 2σ Uncertainty	Assessed 2σ Precision	Assessed Bias (pptv)	Recommended 2σ Uncertainty
NASA DC-8 MC	60-70% for < 25 pptv 40% for 25-100 pptv 30% for >100 pptv	44%	-6.9 – 0.12 $HNO_{3DC\text{-}8MC}$	Quadrature Sum[b]
NASA DC-8 CIMS	Point by point, average: 40%[a]	43%	2.4 – 0.099 $HNO_{3DC\text{-}8CIMS}$	0 – 255 pptv: Point by point > 255 pptv: Quadrature Sum
NOAA WP-3D CIMS	Precision: 40 pptv Accuracy: 100 pptv + 30%	43%	-1.8 + 0.13 $HNO_{3WP\text{-}3D}$	0 – 672 pptv: precision: 40 pptv, accuracy: 100 pptv + 30% > 672 pptv: Quadrature Sum

[a] The average encompasses all DC-8 CIMS data not including points below the LOD because these points greatly skewed the average.
[b] There is a small range (11-24 pptv) where the PI uncertainty is larger than the quadrature sum.

Figures 1a – c display the assessed precisions, biases, and recommended uncertainties for the three HNO_3 instruments. For the three instruments (DC-8 MC, DC-8 CIMS, and WP-3D) the uncertainty is driven by the precision.

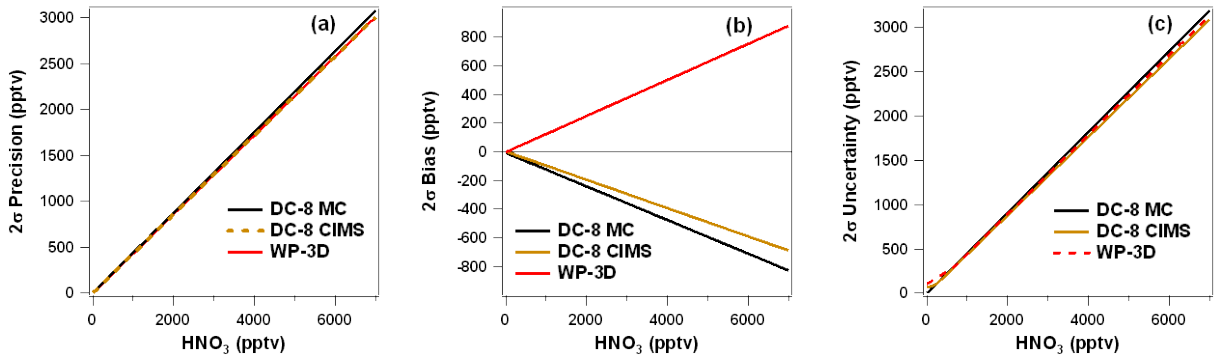

Figure 1. Assessed 2σ precision (panel a), assessed 2σ bias (panel b), and recommended 2σ uncertainty (panel c) for DC-8 MC (black), DC-8 CIMS (gold), and WP-3D (red) as a function of HNO_3 level. Values were calculated based upon data shown in Table 2.

4. Results and Discussion

4.1 Bias Analysis

Section 3.3 in the introduction describes the process used to determine the best estimate bias. Figure 2 shows the time series plots for each of the three WP-3D vs. DC-8 HNO_3 comparisons. There was no DC-8 CIMS data during the comparison period for 08/07/2004. Regression

analysis was conducted between the HNO_3 measurements. Figure 3a displays the correlation between DC-8 MC and CIMS data. The DC-8 CIMS data were averaged into the overlapping DC-8 MC measurement time intervals. The WP-3D CIMS measurement is compared with both the DC-8 MC and CIMS systems in Figure 4a and 4b. Similarly, the WP-3D CIMS data were also averaged into the overlapping DC-8 MC measurement time intervals.

Table 3. ICARTT HNO_3 bias estimates

Aircraft/ Instrument	Linear Relationships (pptv)	Best Estimate Bias (a + b HNO_3) (pptv)
NASA DC-8 MC	$HNO_{3DC\text{-}8MC} = 0.00 + 1.00\ HNO_{3DC\text{-}8MC}$	$-6.9 - 0.12\ HNO_{3DC\text{-}8MC}$
NASA DC-8 CIMS	$HNO_{3DC\text{-}8CIMS} = 8.47 + 1.02\ HNO_{3DC\text{-}8MC}$	$2.4 - 0.099\ HNO_{3DC\text{-}8CIMS}$
NOAA WP-3D CIMS	$HNO_{3WP\text{-}3D} = 5.87 + 1.28\ HNO_{3DC\text{-}8MC}$	$-1.8 + 0.13\ HNO_{3WP\text{-}3D}$
NOAA WP-3D CIMS[a]	$HNO_{3WP\text{-}3D} = 12.1 + 1.39\ HNO_{3DC\text{-}8CIMS}$	N/A
NASA DC-8 CIMS*	$HNO_{3DC\text{-}8CIMS*} = 4.84 + 1.09\ HNO_{3DC\text{-}8MC}$	N/A
NOAA WP-3D CIMS*	$HNO_{3WP\text{-}3D*} = 20.7 + 1.42\ HNO_{3DC\text{-}8MC}$	N/A

[a] This equation was used in the derivation of * equations.
* Derived from regression equations.

The summary of the regression analyses is given in Table 3 along with the best estimate bias which is defined as the difference between the individual measurement and the reference standard for comparison (RSC). Detailed description of RSC and the best estimated bias can be found in the introduction section. For ICARTT HNO_3 measurements, the RSC is constructed using all the available comparison information. Because there were two instruments on the DC-8, the RSC is found by averaging five regressions, three of which are direct from the correlation graphs and two of which come from combining regression equations in order to use all comparisons. The three comparisons from the correlation graphs are: DC-8 MC vs DC-8 MC, DC-8 MC vs DC-8 CIMS, and DC-8 MC vs WP-3D. The WP-3D* is the linear equation derived from the WP-3D vs DC-8 CIMS and DC-8 MC vs DC-8 CIMS equations. Similarly, the DC-8 CIMS* is from the DC-8 CIMS vs WP-3D and WP-3D vs DC-8 MC. The DC-8 MC vs DC-8 MC and DC-8 MC vs DC-8 CIMS direct regression equations were given equal weights of one. The DC-8 MC vs WP-3D direct regression equations and the two derived linear equations were given weights of 0.5 (i.e. [MC + DC8 CIMS + 0.5 WP-3D + 0.5 WP-3D* + 0.5 CIMS*]/3.5). The resulting RSC can be expressed as a function of the DC-8 MC HNO_3 measurement as the following:

$$RSC = 6.914 + 1.117\ HNO_{3DC\text{-}8MC}$$

The RSC is then used to calculate the best estimate bias as described in Section 3.3 of the introduction. It should be noted that the initial choice of the reference instrument (DC-8 MC) is arbitrary, and has no impact on the final recommendations. Table 3 summarizes the assessed measurement bias for each of the three ICARTT HNO_3 measurements. Note that additional decimal places were carried in the calculations to ensure better precision. It is also noted that the

intercept in the equations listed in Table 3 should not be viewed as an offset. These linear equations are used to best describe the linear relation between the WP-3D and DC-8 measurements.

The possibility that the DC-8 MC and CIMS comparison was dependent on water was explored by looking at the difference between the two measurements versus water. This dependence is evident in Figure A1. This was further investigated through the analysis of the individual flights. An example of this can be seen in Figure A2 for flight 8 on 07/15/2004. From this Figure, it can be summarized that at low water levels the DC-8 CIMS measurement is larger than the DC-8 MC and at high water levels the DC-8 MC is larger. It is noted that the water vapor at which the difference between CIMS and MC switches sign is variable from flight to flight. Figure 5a – 5c shows how the linear relationship between the two measurements changes based on water level. At diode laser hygrometer (DLH) H_2O below 1000 ppmv the slope (2.02) is significantly larger than the overall comparison (1.02). It is also noted that this group of data has the lowest R^2 value. At higher water levels the linear relationship is much more similar to the overall comparison as shown in Figure 5b and 5c. It can also be seen that the color code suggests that at lower water vapor CIMS tend to be higher than MC while MC tend to be higher at the opposition conditions. The regression line should be considered as a net average for the data group. A summary of the comparison between DC-8 MC and CIMS is given in Table 4 as a function of water vapor mixing ratio. Also given are the best estimate biases. Table 4 highlights the difference between DC-8 MC and CIMS, which is variable and at least partially dependent on water vapor. This is especially relevant considering the fact that low water vapor points remain in the DC-8 CIMS HNO_3 data archive. At the same time, the data user should recognize that the equations provided in Table 4 may improve the data consistency to a certain extent. The limitation can clearly be seen in Figure 9b.

Table 4. ICARTT HNO_3 DC-8 CIMS bias at various water levels

Aircraft/ Instrument	Range of DLH Water	Linear Relationships	Best Estimate Bias (a + b HNO_3) (pptv)
NASA DC-8 CIMS	$[H_2O] < 1000$ ppmv	$HNO_{3DC\text{-}8CIMS} = -115 + 2.02\ HNO_{3DC\text{-}8MC}$	$-71 + 0.45\ HNO_{3DC\text{-}8CIMS}$
	$1000 \leq [H_2O] \leq 15000$ ppmv	$HNO_{3DC\text{-}8CIMS} = -48.1 + 1.06\ HNO_{3DC\text{-}8MC}$	$-58 - 0.058\ HNO_{3DC\text{-}8CIMS}$
	$[H_2O] > 15000$ ppmv	$HNO_{3DC\text{-}8CIMS} = -154 + 1.05\ HNO_{3DC\text{-}8MC}$	$-171 - 0.063\ HNO_{3DC\text{-}8CIMS}$

The potential effect of fine nitrate interference on the MC measurement is also explored here through examining the dependence of the difference between MC and CIMS values on the fine nitrate measurement by PILs, which is shown in Figure A3. For more information on the PILS measurement contact Rodney Weber at rweber@eas.gatech.edu. There is a definite trend shown and the regression line suggests that the difference between the instruments may be explained by the fine nitrate. At the same time, it should also be noted that there are a significant number of cases that the difference is well beyond the observed fine nitrate level, especially for the part where the fine nitrate is less than 100 pptv. The PILs measurement showed only ~7% of data with values larger than 100 pptv for the entire INTEX-A campaign. Figure A4 shows that the linear relationship at the lowest nitrate levels (under LOD) is similar to the overall linear relationship between DC-8 MC and CIMS shown in Figure 3a. Therefore, it is reasonable to

conjecture that the fine nitrate interference should not have a major influence on the difference between the DC-8 MC and DC-8 CIMS systems. This reflects the general low nitrate concentration observed in the DC-8 sampling region.

4.2 Precision Analysis

A detailed description of the precision assessment is given in Section 3.1 of the introduction. The IEIP precision, expected variability, observed variability, and adjusted precision are summarized in Table 5. Based on the results in Table 5, the largest "adjusted precision" value was taken as a conservative precision estimate for each ICARTT HNO_3 instrument and twice that value is listed in Table 2 as the assessed 2σ precision.

Table 5. ICARTT HNO_3 precision (1σ) comparison

Flight	Platform	IEIP Precision	Expected Variability	Observed Variability	Adjusted Precision
07/22	DC-8 MC	15%	16.8%	23.6%	22%
	WP-3D	7.5%			11%
07/31	DC-8 MC	15%	21.2%	15.8%	15%
	WP-3D	15%			15%
08/07	DC-8 MC	15%	19.2%	22.4%	18%
	WP-3D	12%			14.4%

Flight	Platform	IEIP Precision	Expected Variability	Observed Variability	Adjusted Precision
07/22	DC-8 CIMS	7.5%	10.6%	28.9%	21.5%
	WP-3D	7.5%			21.5%
07/31	DC-8 CIMS	7.5%	16.8%	17.3%	8.5%
	WP-3D	15%			17%
08/07	DC-8 CIMS	12%	17.0%	N/A[a]	N/A
	WP-3D	12%			N/A

[a] DC-8 CIMS did not have any measurements during the comparison period.

To minimize the effect of bias in precision assessment, we make corrections for bias before computing the observed variability, as the bias may have a significant impact on the observed variability. Figures 6 – 8 show the magnitude of the bias for each intercomparison. The assessed values of the observed variability are displayed in Figures 10 – 11. The observed variability estimated from the DC-8 MC and DC-8 CIMS comparison, shown in Figure 9a is not used to derive adjusted precision. This is because the observed variability is influenced by the bias related water vapor, which should not be considered as precision issues. Figure 9b shows a smaller spread as the data for water < 1000 ppmv which was corrected using the equation provided in Table 4. This correction has reduced the observed variability by more than 20%, which indicates the observed variability is an inadequate measure of precision. The final analysis results are shown in Table 2, which is based on the intercomparison periods between DC-8 and WP-3D. As all intercomparisons were conducted below 5 km and the water vapor effect on the observed variability is not significant, analysis of the data demonstrates that Table 2 provides a reasonable estimate of the precisions.

As shown in Figure 7 and 8, over 90% of the data falls within the combined recommended uncertainties for both of the DC-8 vs. WP-3D comparisons, which is consistent with the TAbMEP guideline for unified data sets. The DC-8 MC vs. DC-8 CIMS comparison does not meet this guideline most likely due to the aforementioned larger variability at low water levels, even with additional bias correction as shown in Figure 9a and 9b.

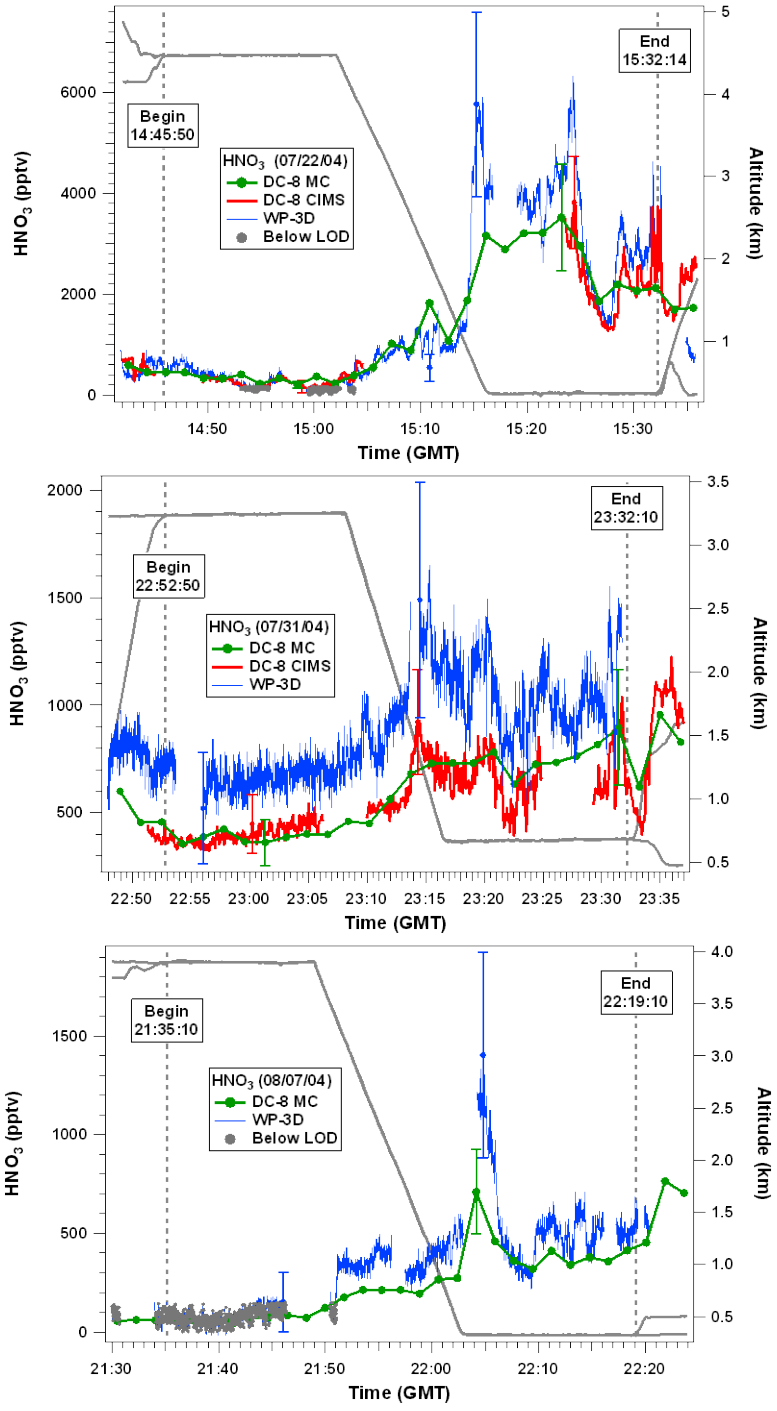

Figure 2. Time series of HNO_3 measurements and aircraft altitudes from two aircraft on the three intercomparison flights between the NASA DC-8 and the NOAA WP-3D. Error bars represent the PI reported uncertainty.

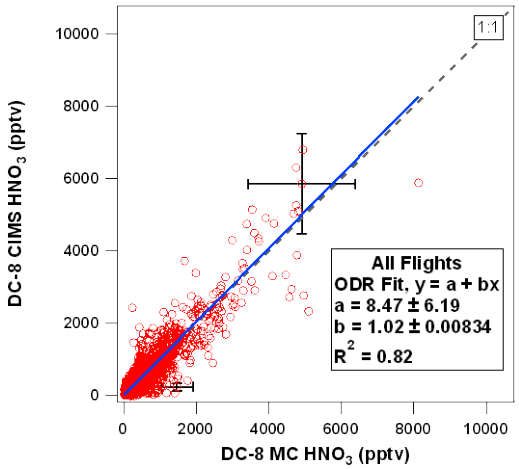

Figure 3. Correlation of DC-8 MC and CIMS HNO_3 measurements for all ICARTT flights. Data was taken from the UNHMC merge file.

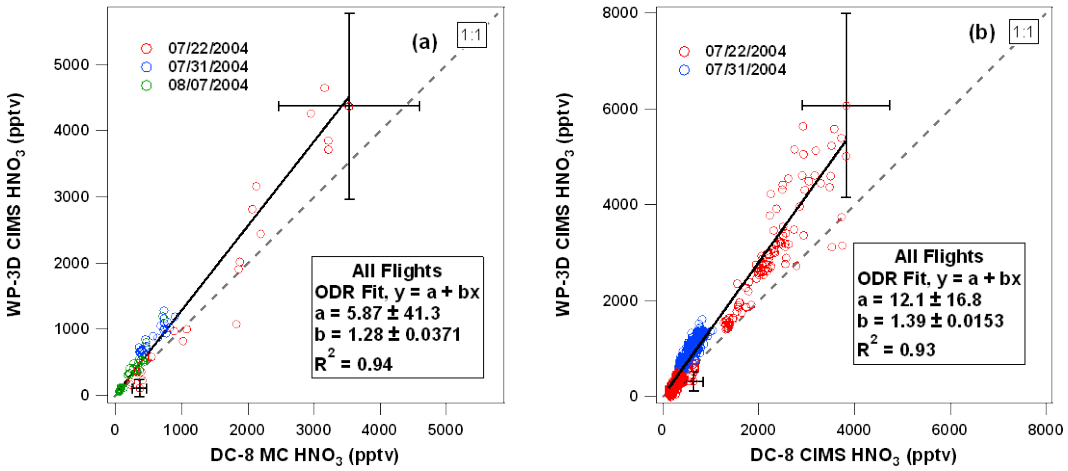

Figure 4. Combined correlation for the HNO_3 measurements on the NASA DC-8 and the NOAA WP-3D for 7/22, 7/31, and 8/07 2004. (left panel) DC-8 MC and (right panel) DC-8 CIMS. Error bars represent the PI reported uncertainty.

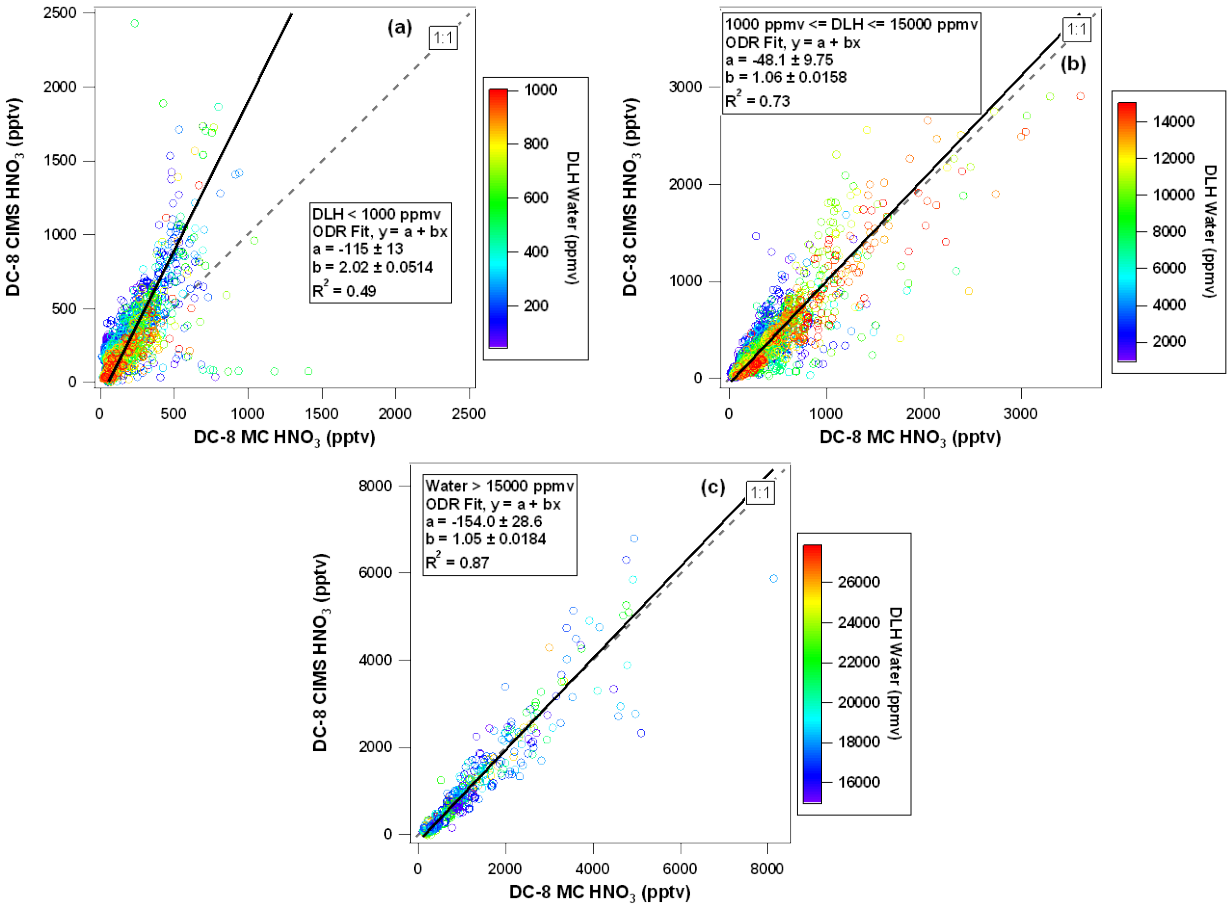

Figure 5. Correlation of DC-8 MC and CIMS HNO_3 measurements at different ranges of DLH H_2O: (top left panel) water < 1000 ppmv, (top right panel) water between 1000 and 15000 ppmv, and (bottom panel) water > 15000 ppmv. The correlations are colored by DLH H_2O level.

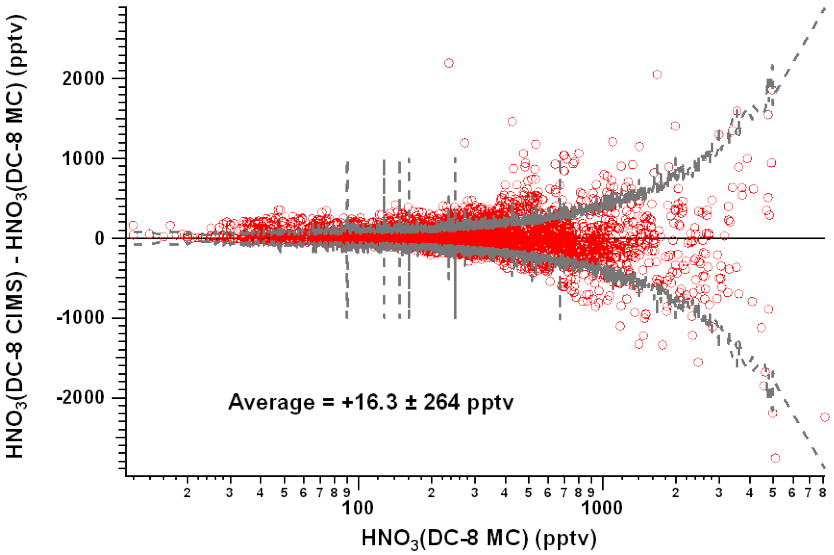

Figure 6. Difference between HNO_3 measurements from DC-8 MC and CIMS for all flights as a function of DC-8 MC HNO_3. The dashed lines indicate the range of results expected from the reported 2σ measurement uncertainties.

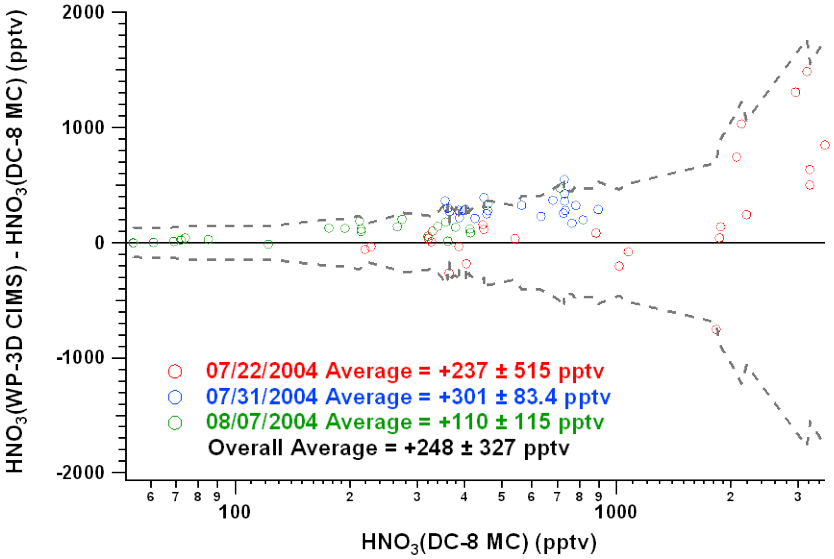

Figure 7. Difference between HNO_3 measurements from the three DC-8 MC and WP-3D intercomparison flights as a function of DC-8 MC HNO_3. The dashed lines indicate the range of results expected from the reported 2σ measurement uncertainties.

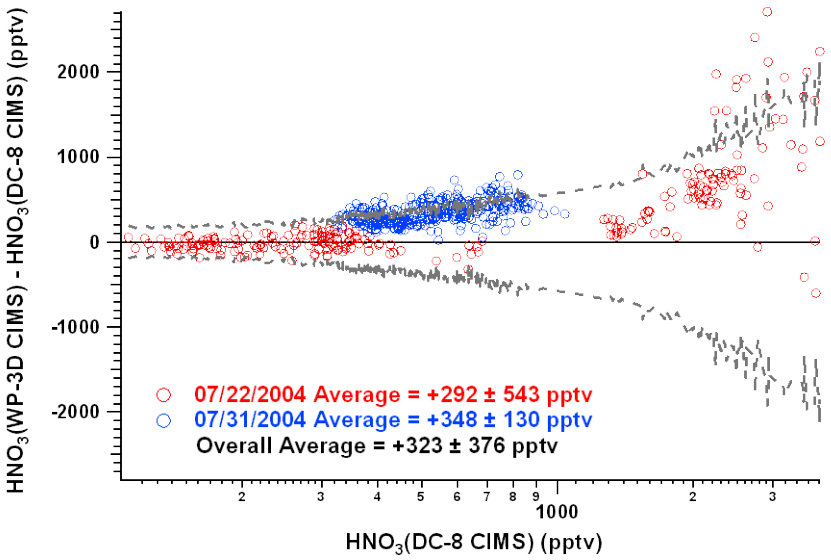

Figure 8. Difference between the HNO_3 measurements from the two DC-8 CIMS and WP-3D intercomparison flights as a function of DC-8 CIMS HNO_3. The dashed lines indicate the range of results expected from the reported 2σ measurement uncertainties.

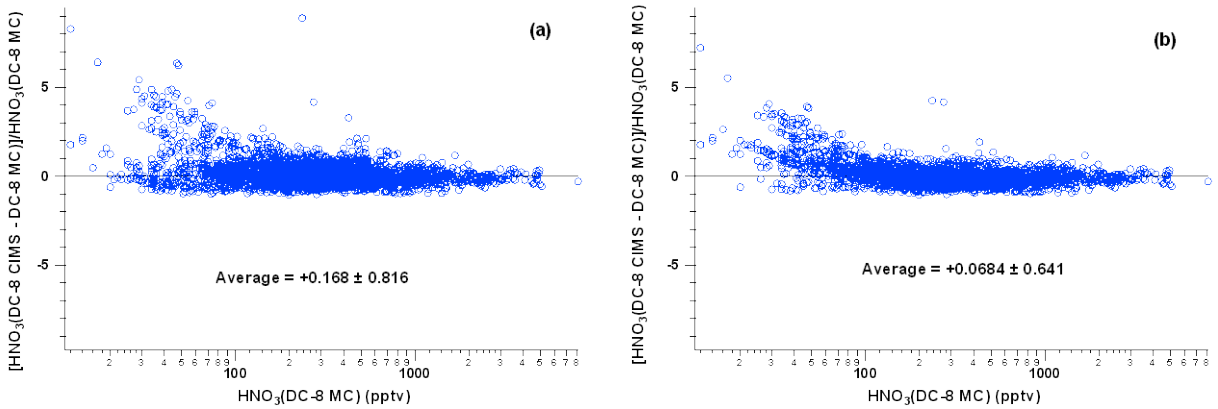

Figure 9. Relative difference between HNO_3 measurements from DC-8 MC and CIMS for all flights as a function of DC-8 MC HNO_3. (left panel) A correction was made to account for bias. (right panel) Two corrections were used, one for water < 1000 ppmv, and the general correction to account for bias.

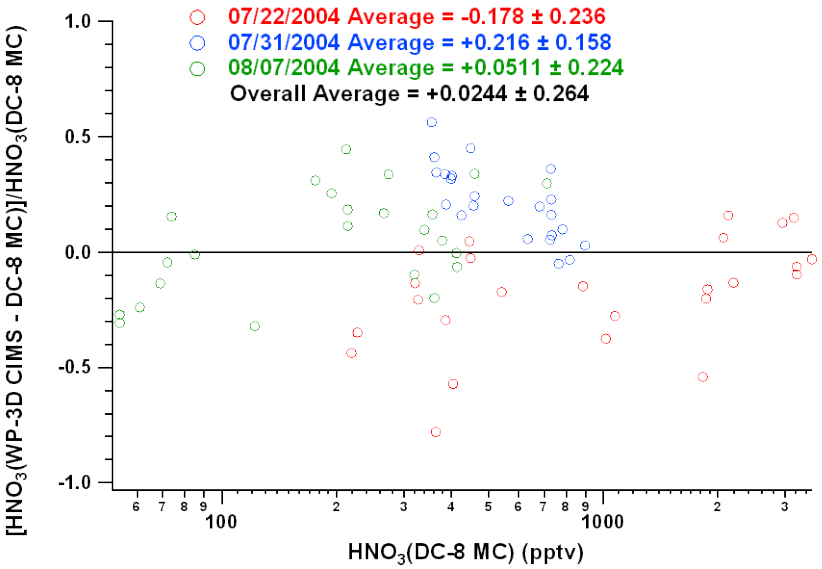

Figure 10. Relative difference between HNO_3 measurements for the three DC-8 MC and WP-3D intercomparison flights as a function of DC-8 MC HNO_3. A correction was made to account for bias.

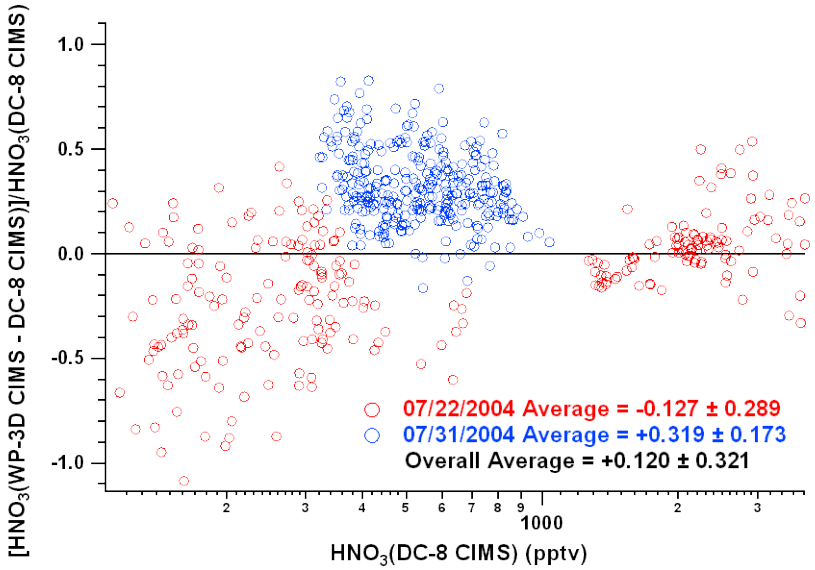

Figure 11. Relative difference between HNO_3 measurements for the two DC-8 CIMS and WP-3D intercomparison flights as a function of DC-8 CIMS HNO_3. A correction was made to account for bias.

Appendix

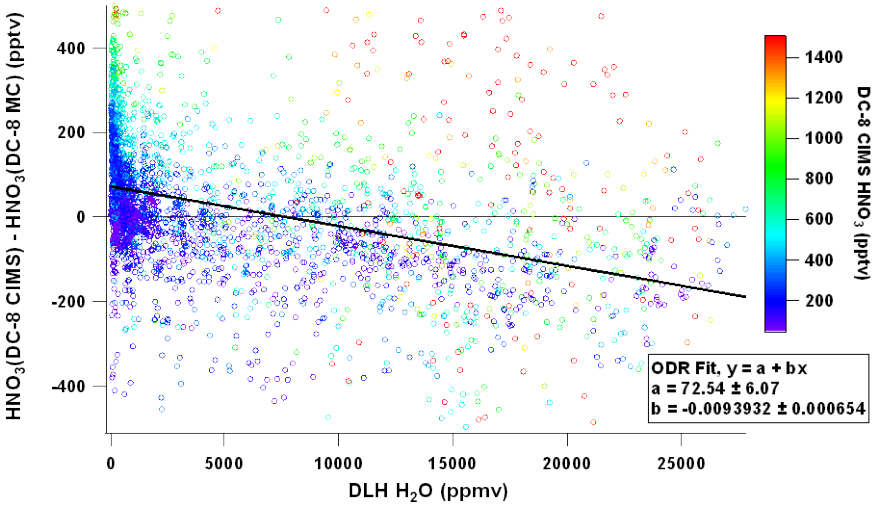

Figure A1. Difference between HNO_3 measurements from DC-8 MC and CIMS for all flights as a function of DLH H_2O and colored by DC-8 CIMS HNO_3. Some data points are not shown because the plot is zoomed in to accentuate the relationship between the residual and DLH at low HNO_3 levels.

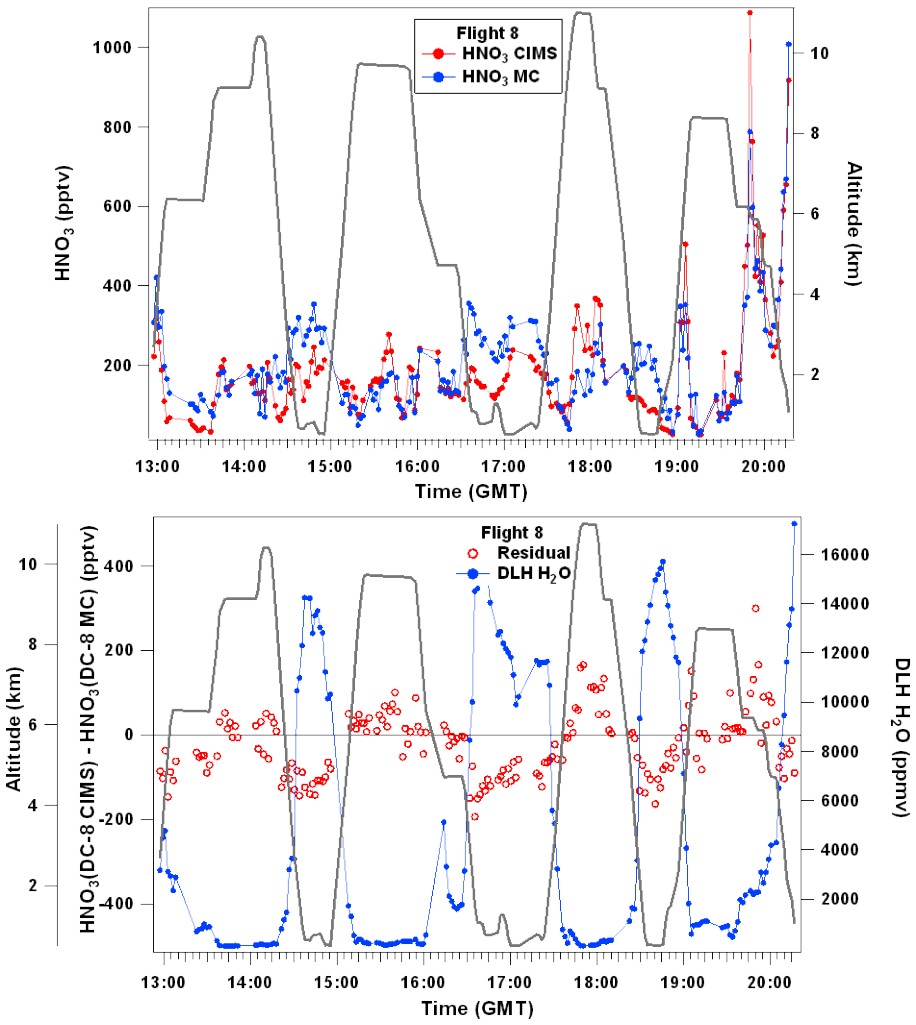

Figure A2. (top panel) Time series plot of HNO_3 measurements and aircraft altitudes from the DC-8 aircraft on flight 8 (07/15/04). (bottom panel) Time series plot of difference between DC-8 MC and CIMS, altitude, and DLH H_2O for flight 8 (07/15/04).

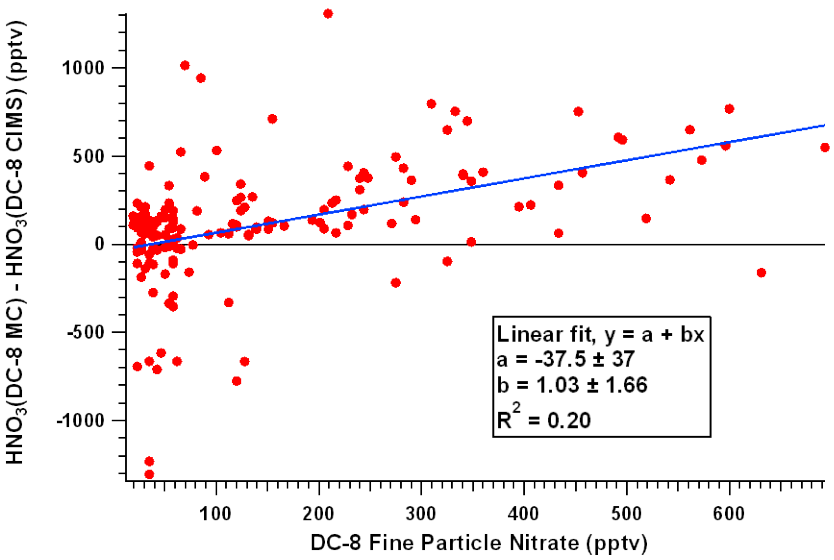

Figure A3. Difference between DC-8 HNO_3 measurements (MC – CIMS) as a function of fine nitrate.

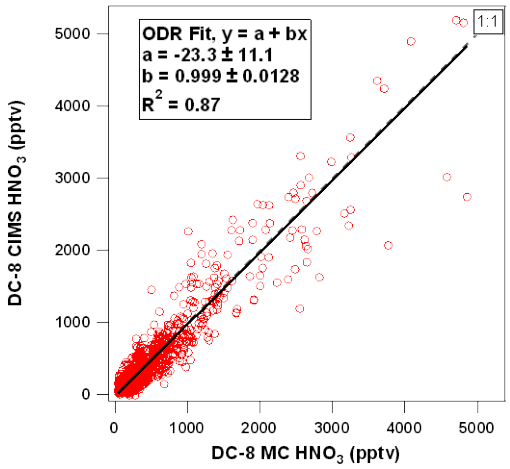

Figure A4. Correlation of DC-8 MC and CIMS HNO_3 measurements for all available fine nitrate below LOD, i.e., minimum fine nitrate interference.

References

Crounse, J. D., K. A. McKinney, A. J. Kwan, and P. O. Wennberg (2006), Measurement of gas-phase hydroperoxides by chemical ionization mass spectrometry (CIMS), *Anal. Chem.,* 78 (19); 6726-6732.

Fehsenfeld, F. C., et al. (2006), International Consortium for Atmospheric Research on Transport and Transformation (ICARTT): North America to Europe—Overview of the 2004 summer field study, *J. Geophys. Res., 111*, D23S01, doi:10.1029/2006JD007829.

Neuman, J. A., et al. (2002), Fast-response airborne in situ measurements of HNO_3 during the Texas 2000 Air Quality Study, *J. Geophys. Res.,* 107(D20), 4436, doi:10.1029/2001JD001437.

Neuman, J. A., et al. (2006), Reactive nitrogen transport and photochemistry in urban pluems over the North Atlantic Ocean, *J. Geophys. Res.,* 111, D23S54, doi:10.10129/2005JD007010.

Scheuer, E., et al. (2010), Evidence of nitric acid in warm cirrus anvil clouds during the NASA TC4 campaign, *J. Geophys. Res.,* D00J03, doi:10.1029/2009JD012716.

Singh, H. B., et al. (2006), Overview of the summer 2004 Intercontinental Chemical Transport Experiment-North America (INTEX-A), *J. Geophys. Res., 111*, D24S01, doi:10.1029/2006JD007905.

TAbMEP Assessment: ICARTT Ethyne Measurements

1. Introduction

Here we provide the assessment for the ethyne (C_2H_2) measurements taken from three aircraft platforms during the summer 2004 ICARTT field campaign [*Fehsenfeld et al.*, 2006, *Singh et al.*, 2006]. This assessment is based upon the four wing-tip-to-wing-tip intercomparison flights conducted during the field campaign. Recommendations provided here offer TAbMEP assessed biases for each of the measurements and a systematic approach to unifying the ICARTT ethyne data for any integrated analysis. These recommendations are directly derived from the instrument performance demonstrated during the ICARTT measurement comparison exercises and are not to be extrapolated beyond this campaign.

2. ICARTT Ethyne Measurements

Three whole air sampler instruments were deployed on three aircraft. Table 1 summarizes these techniques and gives references for more information.

Table 1. Ethyne measurements deployed on aircraft during ICARTT

Aircraft	Instrument	Reference
NASA DC-8	Whole Air Sampler (WAS)	*Colman et al.* [2001]
NOAA WP-3D	Whole Air Sampler (WAS)	Contact PI: eatlas@rsmas.miami.edu
FAAM BAe-146	Whole Air Sampler (WAS)	*Hopkins et al.* [2003]

3. Summary of Results

Table 2 summarizes the assessed biases as well as the PI reported uncertainties for each of the three ethyne measurements involved in the intercomparisons. More detailed descriptions are provided to illustrate the process of the bias assessment in Section 4.1. The TAbMEP-prescribed IEIP procedures cannot be applied to the ICARTT ethyne measurements for precision assessment. This is because the reported data have large time gaps and a small data population (see Section 3.1 of the introduction). The assessed bias reported in Table 2 (see Section 4.1 for details) can be applied to maximize the consistency between the data sets, by subtracting the value from the reported data to 'unify' the data sets. If one assumes instrument performance remained constant throughout the mission, the assessed bias may be extrapolated to the entire mission although it is derived from intercomparison periods only.

Figure 1 illustrates the PI reported uncertainty and the assessed bias from Table 2. It can be seen in the figure that the DC-8 uncertainty is larger than the DC-8 bias for most conditions, whereas for the WP-3D and BAe-146 the bias is larger than the uncertainty for a significant portion of the range shown in Figure 1. Furthermore, it should be noted that there are two comparison points with actual readings from DC-8 while BAe-146 reported points below the LOD (limit of detection). This is not accounted for by the assessed bias given in Table 2 and may suggest large bias under certain circumstances.

Table 2. Recommended ICARTT Ethyne measurement treatment

Aircraft/Instrument	Reported 2σ Uncertainty	Assessed Bias
NASA DC-8 WAS	10%	$-10.1 + 0.0905\ C_2H_{2\ DC\text{-}8}$
NOAA WP-3D WAS	10%	$-28.8 + 0.255\ C_2H_{2\ WP\text{-}3D}$
FAAM BAe-146 WAS	Point by Point, average: 15%[a]	$-6.4 - 0.117\ C_2H_{2\ BAe\text{-}146}$

[a] The average encompasses the entire flight, 24% for the comparison period for the DC-8/BAe-146.

The DC-8 and WP-3D uncertainties reported by PIs are a percentage. This may not be adequate at very low end concentration levels. Ideally, the measurement uncertainty may be better represented in the form of x pptv or y%. Based on the intercomparison data, the TAbMEP analysis cannot provide such assessment. Data users should contact the respective PIs about the proper uncertainties when dealing with the low end of measurements, e.g., < 10 pptv.

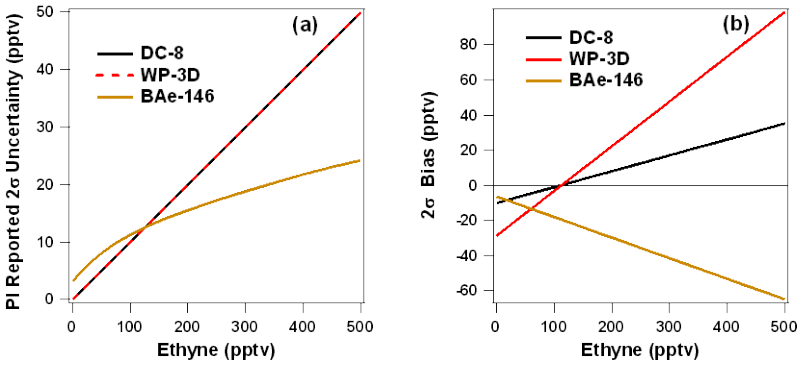

Figure 1. PI reported 2σ uncertainty (panel a) and recommended bias (panel b) for DC-8 (black), WP-3D (red), and BAe-146 (gold) as a function of ethyne level. Values were calculated based upon data shown in Table 2. The BAe-146 PI reported uncertainty was calculated using a function derived from the 60 second merge file.

4. Results and Discussion

4.1 Bias Analysis

Section 3.3 in the introduction describes the process used to determine the best estimate bias. Figures 2 and 4 show the time series plots for the DC-8/WP-3D and DC-8/BAe-146 comparisons. The DC-8 is on average higher than the WP-3D by 5 pptv. Figure 4 clearly shows examples of time periods where the BAe-146 WAS recorded a point below LOD and the DC-8 WAS had a value. The DC-8 is consistently lower on average than BAe-146 by 7 pptv. Figures 5 and 6 show the magnitude of the bias for each intercomparison and Figures 7 and 8 show the corresponding relative residuals.

For two of the three DC-8/WP-3D flights, there are only 3 or 4 overlapping points. It is not statistically significant to show the linear regression individually for these flights. Therefore, linear regression is performed over the data combined from all three DC-8/WP-3D flights shown in Figure 3. The linear relationships listed in Table 3 were derived from the regression equations found in Figures 3 and 4. Note the regression line shown in Figure 4 does not include the points that the BAe-146 reported as under the LOD. For plotting purposes, zero was assigned to the BAe-146 values as the LOD was undefined. The reference standard for comparison (RSC), as defined in the introduction, is constructed by averaging the NASA DC-8 and NOAA WP-3D measurements with equal weights of one. The FAAM BAe-146 was not included in the RSC calculation because the range of comparison is small and the points below the LOD were not assigned any value. The resulting RSC can be expressed as a function of the DC-8 C_2H_2 measurements as the following:

$$RSC_{C2H2} = 10.13 + 0.909\ C_2H_{2\text{-}DC8}$$

The RSC is then used to calculate the best estimate bias as described in Section 3.3 of the introduction. It should be noted that the initial choice of the reference instrument (DC-8 WAS) is arbitrary, and has no impact on the final recommendations. Table 3 summarizes the assessed measurement bias for each of the three ICARTT ethyne measurements. Note that additional decimal places were carried in the calculations to ensure better precision. It is also noted that the intercept in the equations listed in Table 3 should not be viewed as an offset. These linear equations are used to best describe the linear relation between the measurements.

The WAS technique for measuring VOCs presents some challenges in analyzing the data. The DC-8 data have an integration time of approximately 60-70 seconds, while the WP-3D data have an integration time between 6-11 seconds. For these measurements to be considered simultaneous and able to used in the regression analysis, the start and stop times of the WP-3D data must fall within the start and stop times of the DC-8 data. In order to maximize the data coverage for statistical analysis, one exception is made to this rule. If the shorter (WP-3D) integration time falls outside the longer integration time by no more than two seconds, the data points are also considered to be simultaneous. BAe-146 integration times range from approximately 30-60 seconds. Since the DC-8 and BAe-146 have similar integration times, the measurements are considered eligible for regression analysis if the midpoint of DC-8 or BAe-146 fall within the start and stop time of the other measurement. Only the PI reported data is used in this assessment, no interpolation is included. It is noted here the integration time difference may potentially be another factor leading to the difference between measurements.

Table 3. ICARTT Ethyne bias estimates

Aircraft/ Instrument	**Linear Relationships**	**Best Estimate Bias ($a + b\ C_2H_2$) (pptv)**
NASA DC-8 WAS	$C_2H_{2\ DC\text{-}8} = 0.00 + 1.000\ C_2H_{2\ DC\text{-}8}$	$-10.13 + 0.0905\ C_2H_{2\ DC\text{-}8}$
NASA WP-3D WAS	$C_2H_{2\ WP\text{-}3D} = 20.5 + 0.819\ C_2H_{2\ DC\text{-}8}$	$-28.77 + 0.255\ C_2H_{2\ WP\text{-}3D}$
FAAM BAe-146 WAS	$C_2H_{2\ BAe\text{-}146} = -4.08 + 1.50\ C_2H_{2\ DC\text{-}8}$	$-6.415 - 0.117\ C_2H_{2\ BAe\text{-}146}$

As a part of ICARTT intercomparison standard exchange exercises, University of California, Irvine (UCI) prepared the common VOC samples that were sent to University of Miami (Miami), University of New Hampshire (UNH), and University of York (York) for their lab analyses. Some of these same institutions had instruments on the following planes during ICARTT: UCI on the DC-8, Miami on the WP-3D, and York on the BAe-146. The comparison incorporated 9 species, which included ethyne. We believe that the inclusion of this comparison result will help the readers better understand the airborne intercomparison analysis. The difference in this lab comparison between the DC-8 and WP-3D instruments was 3 pptv, WP-3D being higher, at a DC-8 instrument reading of 532 pptv. From the same lab comparison, the difference between the DC-8 and BAe-146 was 0.25 pptv, BAe-146 being higher. Comparing the ICARTT flights to this lab comparison shows different relationships for both the DC-8/WP-3D and DC-8/BAe-146 intercomparisons (see Figures 5 – 6). The average lab comparison level of 533 pptv is much higher than the average level seen during the intercomparison flights which have an average of level of 131 pptv for the DC-8/WP-3D flights and 23 pptv for the DC-8/BAe-146 flight. This difference between intercomparisons does not seem unreasonable, considering that instrument performance can vary depending on calibration and environmental factors, and the time intervals were not the same for all instruments.

4.2 Precision Analysis

A detailed description of the precision assessment is given in Section 3.1 of the introduction. The IEIP precision, expected variability, and adjusted precision could not be calculated for ethyne because of the small number of points and large time gaps between measurements.

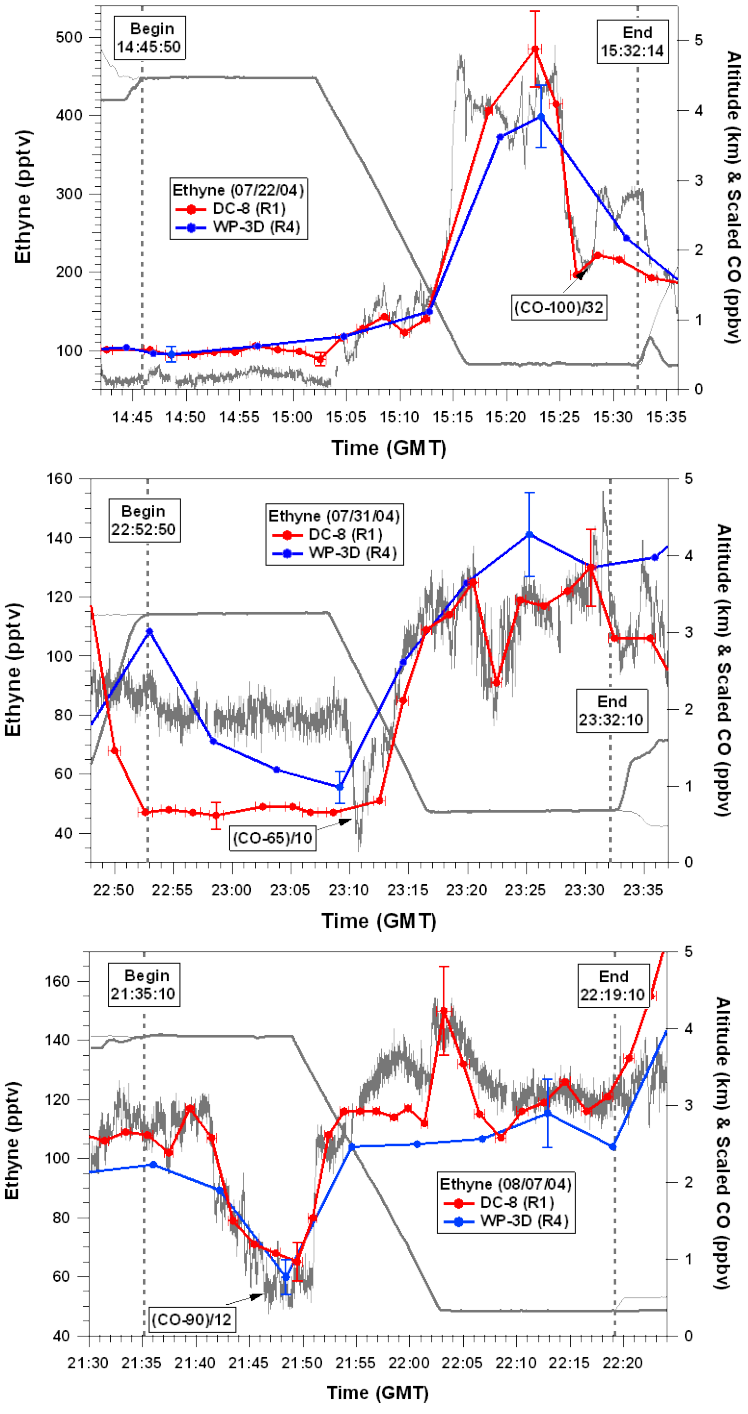

Figure 2. Time series of ethyne measurements and aircraft altitudes from two aircraft on the three intercomparison flights between the NASA DC-8 and the NOAA WP-3D. Error bars represent the PI reported uncertainty. In parenthesis next to the plane is the data version number.

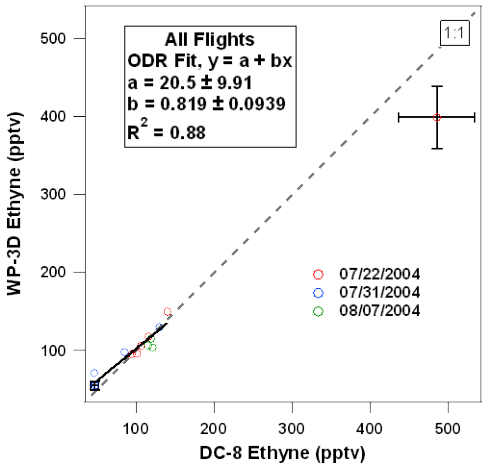

Figure 3. Combined correlation for the ethyne measurements on NASA DC-8 and the NOAA WP-3D for 7/22, 7/31, and 8/07 2004. Error bars represent the PI reported uncertainty. One influential point was not included in the regression analysis.

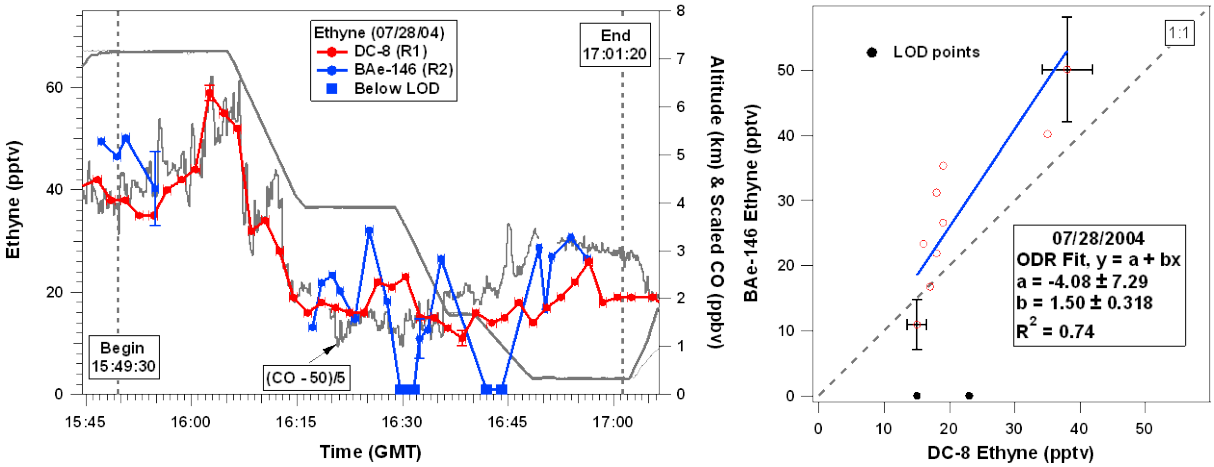

Figure 4. (left panel) Time series of ethyne measurements and aircraft altitudes from the intercomparison flight between the NASA DC-8 and the FAAM BAe-146. In parenthesis next to the plane is the data version number. (right panel) Correlation between the ethyne measurements on the two aircraft. LOD points are not included in calculating the regression equation. Error bars represent the PI reported uncertainty.

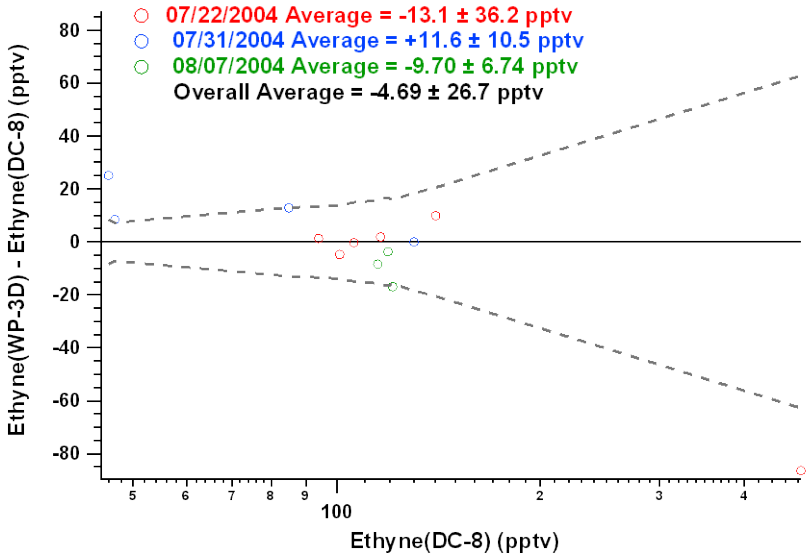

Figure 5. Difference between ethyne measurements from the three DC-8/WP-3D intercomparison flights as a function of the DC-8 ethyne. The dashed lines indicate the range of the results expected from the reported measurement uncertainties.

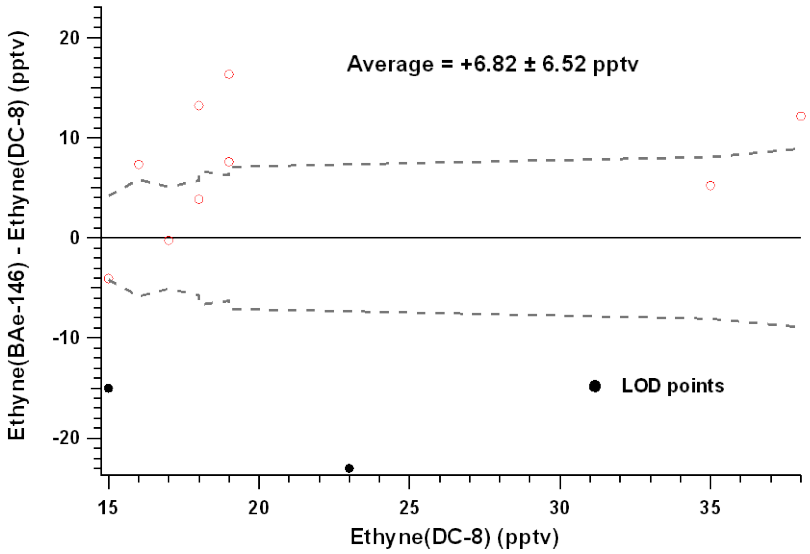

Figure 6. Difference between ethyne measurements from the DC-8/BAe-146 intercomparison flights as a function of the DC-8 ethyne. The LOD points are not included in the average. The dashed lines indicate the range of the results expected from the reported measurement uncertainties.

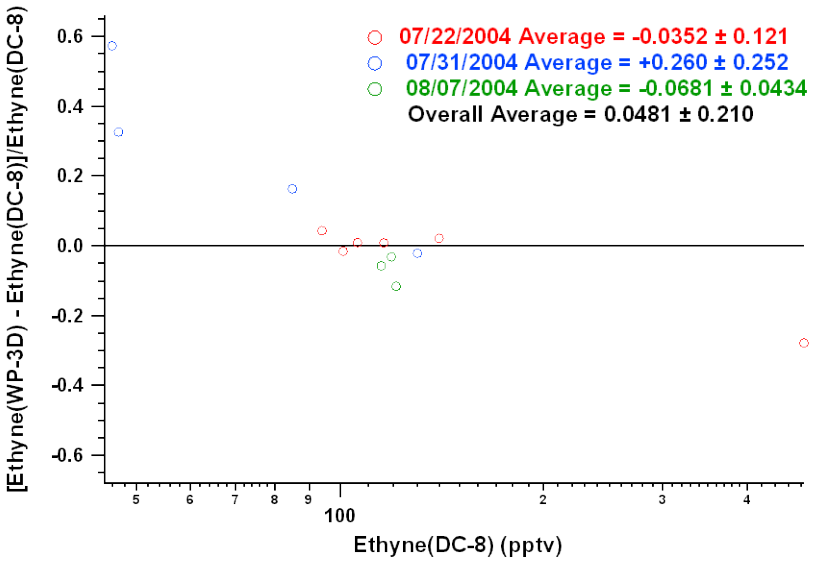

Figure 7. Relative difference between ethyne measurements from the three DC-8/WP-3D intercomparison flights as a function of DC-8 ethyne. A correction was made to account for bias.

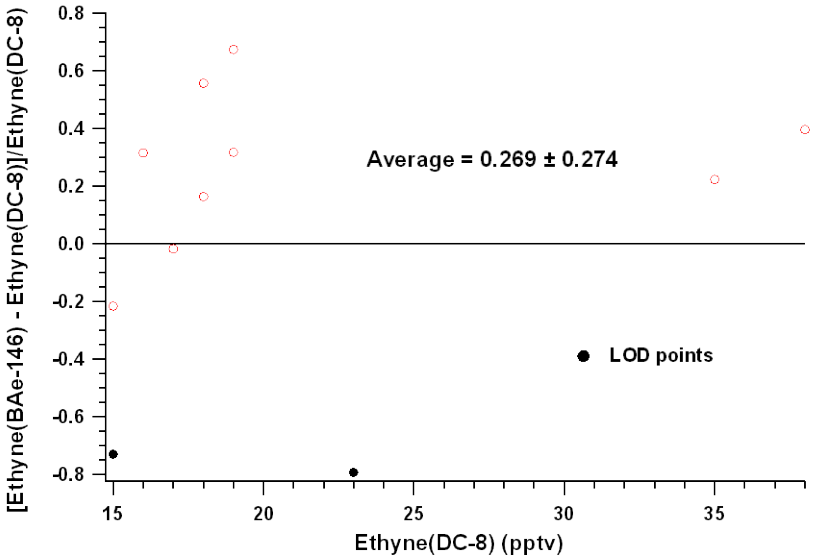

Figure 8. Relative difference between ethyne measurements from the DC-8/BAe-146 intercomparison flight as a function of DC-8 ethyne. The LOD points are not included in the average. A correction was made to account for bias.

References

Colman, J.J., et al. (2001), Description of the analysis of a wide range of volatile organic compounds in whole air samples collected during PEM-Tropics A and B, *Anal. Chem* ., 73, 3723-3731.

Fehsenfeld, F. C., et al. (2006), International Consortium for Atmospheric Research on Transport and Transformation (ICARTT): North America to Europe—Overview of the 2004 summer field study, *J. Geophys. Res., 111*, D23S01, doi:10.1029/2006JD007829.

Hopkins, J. R., K. A. Read, and A. C. Lewis. (2003), A Column Method For Long-term Monitoring Of Non-Methane Hydrocarbons (NMHCs) and Oxygenated Volatile Organic Compounds, *Journal of Environmental Monitoring*, 5 (1), 8-13.

Singh, H. B., et al. (2006), Overview of the summer 2004 Intercontinental Chemical Transport Experiment-North America (INTEX-A), *J. Geophys. Res., 111*, D24S01, doi:10.1029/2006JD007905.

Appendix A

TAbMEP Participants

Participants	Contributions	Affiliation	E-mail
Bruce Anderson	Aerosol Measurements	NASA LaRC	bruce.e.anderson@nasa.gov
Eric Apel	Trace Gas Measurements	NCAR	apel@ucar.edu
Steve Arnold	Modeling	Univ. of Leeds	s.arnold@see.leeds.ac.uk
Melody Avery	Trace Gas Measurements	NASA LaRC	melody.a.avery@nasa.gov
Huisheng Bian	Modeling	UMBC	Huisheng.bian-1@nasa.gov
Don Blake	Trace Gas Measurements	Univ. of CA, Irvine	drblake@uci.edu
Nicola Blake	Trace gas Measurements	Univ. of CA, Irvine	nblake@uci.edu
Chuck Brock	Aerosol Measurements	NOAA/ESRL	charles.a.brock@noaa.gov
Greg Carmichael	Reg. Model: Trace Gas & Aerosol	Univ. of IA	gcarmich@engineering.uiowa.edu
Gao Chen	Organizer, data analysis	NASA LaRC	gao.chen@nasa.gov
Mian Chin	Global Model: Aerosols	NASA GSFC	mian.chin-1@nasa.gov
Mike Cubison	Aerosol Composition	Univ. of CO	michael.cubison@colorado.edu
Jack Dibb	Trace Gas Measurements, Aerosol Measurements	Univ. of NH	jack.dibb@unh.edu
Glenn Diskin	Trace Gas Measurements	NASA LaRC	glenn.s.diskin@nasa.gov
Louisa Emmons	Global Model: Trace Gas	NCAR	emmons@ucar.edu
Mat Evans	Global & Reg. Model: Trace Gas	Univ. of Leeds	mat@env.leeds.ac.uk
Arlene Fiore	Global Model: Trace Gas	NOAA/GFDL	Arlene.Fiore@noaa.gov
Frank Flocke	Trace Gas Measurements	NCAR	ffl@ucar.edu
Greg Huey	Trace Gas Measurements	GA Tech	greg.huey@eas.gatech.edu
Jose Jimenez	Aerosol Measurements	Univ. of CO	jose.jimenez@colorado.edu
Terry Keating	HTAP & EPA Representive	EPA	keating.terry@epa.gov
Mary Kleb	Organizer, data analysis	NASA LaRC	mary.m.kleb@nasa.gov
Dan Lack	Aerosol Measurements	NOAA	daniel.lack@noaa.gov
Qing Liang	Global Model: Trace Gas	NASA GSFC	qing.liang-1@nasa.gov
David McCabe	EPA Representive	AAAS/EPA	McCabe.David@epa.gov
Pete Parker	Statistican	NASA LaRC	peter.a.parker@nasa.gov
David Parrish	Trace Gas Measurements	NOAA/ESRL	David.D.Parrish@noaa.gov
Margaret Pippin	Organizer, data analysis	NASA LaRC	m.pippin@nasa.gov
Trish Quinn	Aerosol Measurements	NOAA/PMEL	patricia.k.quinn@noaa.gov
Tom Ryerson	Trace Gas Measurements	NOAA/ESRL	thomas.b.ryerson@noaa.gov
Hans Schlager	Airborne Measurements	DLR	hans.schlager@dlr.de
Michael Schulz	Global Model: Aerosols	LSCE	michael.schulz@cea.fr
Ariel Stien	Aerosol Modeling	NOAA	Ariel.Stein@NOAA.gov
Jian Wang	Aerosol Measurements	DOE/BNL	jian@bnl.gov